STRINGQFT

String-Theoretic Construction
of Quantum Field Theory

VOLUME XV

F-Theory: Six-Dimensional Theories, SCFTs and Little String Theory

Xingyang Yu

StringQFT v1.0 / Source build candidate

Drafted with AI assistance under the supervision of the author.
Manuscript free to read. All rights reserved.

Contents

XV.1 Six-dimensional gauge theories from elliptic Calabi–Yau threefolds **1**

XV.1.1 A curve configuration in an elliptic threefold 1
XV.1.2 The split Tate model 3
XV.1.3 Gauge and flavor divisors 7
XV.1.4 Matter at intersections 9
XV.1.5 Multiplets and the local limit 13
XV.1.6 A single-node comparison 16
XV.1.7 Exercises 20

XV.2 Tensor branches, string charges and couplings **23**

XV.2.1 The tensor scalars as areas 23
XV.2.2 Wrapped D3 strings 27
XV.2.3 The integral charge pairing 29
XV.2.4 Gauge couplings along the branch 31
XV.2.5 Dynamical tensors and background parameters 35
XV.2.6 Changing areas without declaring a fixed point 39

XV.3 Anomaly polynomials and Green–Schwarz cancellation **45**

XV.3.1 Which anomalies constrain the construction 45
XV.3.2 Trace identities from weights 47
XV.3.3 A single gauge node 50
XV.3.4 Two nodes and their common hypermultiplet 53
XV.3.5 The Green–Schwarz matrix 55
XV.3.6 Changed ranks and uncancelled anomalies 58
XV.3.7 Compact gravitational constraints 62
XV.3.8 Exercises 66

XV.4 Non-Higgsable clusters and gauge tuning **69**

XV.4.1 Sections restricted to a negative curve 69
XV.4.2 A forced type-IV sector 71
XV.4.3 A non-split comparison 74
XV.4.4 An allowed gauge tuning 79
XV.4.5 When the proposed tuning fails 81
XV.4.6 Returning to the two-node construction 84

XV.4.7 Exercises . . . 88

XV.5 Contraction limits and six-dimensional SCFTs 92
XV.5.1 Resolving a non-minimal point . . . 92
XV.5.2 The complete compact curve lattice . . . 96
XV.5.3 Contraction and gravity decoupling . . . 99
XV.5.4 A gauge-free ADE configuration . . . 102
XV.5.5 Tensor-branch theory and its UV interpretation . . . 105
XV.5.6 A changed configuration that fails . . . 109

XV.6 E-strings, conformal matter and exceptional constructions 116
XV.6.1 The geometric E-string . . . 116
XV.6.2 Resolving an E6 collision . . . 120
XV.6.3 Resolving an E7 collision . . . 123
XV.6.4 Gauge matter on the tensor branch . . . 126
XV.6.5 Anomaly contributions of the interacting sector . . . 130
XV.6.6 Partial contraction and retained spectators . . . 135

XV.7 Organization of SCFTs and RG flows 143
XV.7.1 Organizing the constructions already obtained . . . 143
XV.7.2 Gauging and compatibility . . . 145
XV.7.3 A tensor branch deformation . . . 148
XV.7.4 A Higgs branch deformation . . . 150
XV.7.5 Tracking sectors and anomalies . . . 153
XV.7.6 The scope of the classification . . . 156
XV.7.7 Exercises . . . 159

XV.8 Geometric little string limits and the string scale 163
XV.8.1 A finite string scale after gravity decouples . . . 163
XV.8.2 From a negative-definite to a semidefinite pairing . . . 166
XV.8.3 The null charge and its wrapped string . . . 169
XV.8.4 Dynamical and nondynamical tensor directions . . . 171
XV.8.5 Comparing an SCFT limit with an LST limit . . . 173
XV.8.6 Geometric existence beyond the lattice . . . 176
XV.8.7 Exercises . . . 181

XV.9 Worked little string constructions and SCFT subsectors 184
XV.9.1 A loop of actual curves . . . 184
XV.9.2 A split elliptic fiber over the loop . . . 186
XV.9.3 The two ends of an interval . . . 190
XV.9.4 Gauge anomaly without an inverse . . . 194
XV.9.5 Taking a limit on a proper subchain . . . 197
XV.9.6 Changing a tuning and testing it . . . 201
XV.9.7 Exercises . . . 204

XV.10 Circle compactification and little string duality 207

XV.10.1 Two elliptic projections of one geometry 207
XV.10.2 Momentum and winding on a circle 210
XV.10.3 The M-theory description 213
XV.10.4 Two six-dimensional readings of the product 215
XV.10.5 Matching charges and finite scales 218
XV.10.6 The five-dimensional gauge theory 221
XV.10.7 A birational comparison from Appendix F 226

XV.11 Six-dimensional construction atlas 231
XV.11.1 Gauge theories on finite tensor branches 231
XV.11.2 Surface contractions and tensor limits 235
XV.11.3 Conformal matter and source transfer 237
XV.11.4 Affine fibers and the heterotic interval 239
XV.11.5 Charge lattices and retained scales 242
XV.11.6 Circle comparison and inverse selection 244

Chapter XV.1

Six-dimensional gauge theories from elliptic Calabi–Yau threefolds

XV.1.1 A curve configuration in an elliptic threefold

A seven-brane in a six-dimensional compactification fills spacetime and wraps a complex curve. Which parts of the resulting field theory can we calculate from the base surface and the elliptic equation? The curve area measured in the normalized Einstein-frame Kähler class $j = J_E/\sqrt{J_E^2}$ probes a compact tensor scalar. The overall base volume belongs to the hypermultiplet sector. The generic fiber over the curve determines the gauge algebra. Special fibers over points can supply charged hypermultiplets. We will compute these three pieces in a model with two intersecting curves, and then repeat the calculation for a single curve with a different self-intersection.

We use the elliptic-fiber dictionary of XIV.1, and the transverse Kodaira classification of Volume IV, Chapter 8. The four-dimensional construction in XIV.2, is useful for comparison but is not required. Here the gauge divisors are curves, and their mutual intersections are points. The ordinary sectioned F-theory frame with no frozen sector has six-dimensional $\mathcal{N} = (1, 0)$ supersymmetry, with eight real supercharges.

Let $\mathbb{F}_n$ be the ruled surface over $\mathbb{P}^1$ with section S of square $-n$. Write F for the class of a fiber. Fibers at different base points are disjoint, and each meets the section once. Thus

$$S^2 = -n, \qquad S \cdot F = 1, \qquad F^2 = 0. \tag{XV.1.1}$$

Both curves are rational. Adjunction says $(K_B + D) \cdot D = -2$ for each such smooth curve D. This gives two independent equations for the coefficients of K_B:

$$K_{\mathbb{F}_n} \cdot F = -2, \qquad K_{\mathbb{F}_n} \cdot S = n - 2, \tag{XV.1.2}$$

$$K_{\mathbb{F}_n} = -2S - (n + 2)F. \tag{XV.1.3}$$

The fiber pairing fixes the coefficient of S. The section pairing then fixes the coefficient of F.

Start with $\mathbb{F}_2$. Use w along the ruling base and z along the fibers in an affine chart with $S = \{z = 0\}$. Blow up the two points $(z, w) = (1, 0), (2, 0)$. We write S, F also for the pullback classes and E_1, E_2 for the exceptional curves. A pullback pairs to zero with each exceptional curve, and each exceptional curve has normal bundle $\mathcal{O}_{\mathbb{P}^1}(-1)$. The centers are distinct, so the E_i are disjoint. In this ordered basis the intersection matrix and canonical class are

$$M_B = \begin{pmatrix} -2 & 1 & 0 & 0 \\ 1 & 0 & 0 & 0 \\ 0 & 0 & -1 & 0 \\ 0 & 0 & 0 & -1 \end{pmatrix}, \qquad K_B = -2S - 4F + E_1 + E_2. \tag{XV.1.4}$$

The positive exceptional coefficient in K_B is the order of the Jacobian. For instance, at $z = p$, set $z = p + \xi,\ w = \xi t$. Then

$$dz \wedge dw = \xi \, d\xi \wedge dt. \tag{XV.1.5}$$

The pullback of a locally nonzero canonical form therefore has one zero on the new exceptional curve.

The strict transform of $w = 0$ is the closure of the old fiber with the two centers removed. Its class is the total transform less the two exceptional components. The section misses the centers, so its strict and pullback classes agree:

$$C_1 = S, \qquad C_2 = F - E_1 - E_2, \qquad F = C_2 + E_1 + E_2. \tag{XV.1.6}$$

For example, $C_2^2 = F^2 + E_1^2 + E_2^2 = -2$, whereas a generic fiber in the class F still has square zero. The class relation also accounts for every intersection with the total fiber:

$$F \cdot C_2 = (-2) + 1 + 1 = 0, \qquad F \cdot E_i = 1 - 1 = 0. \tag{XV.1.7}$$

The three effective components of the relation $F = C_2 + E_1 + E_2$ have positive areas if we stay in the Kähler cone. This identity will later explain how the total fiber grows while C_2 remains finite.

The blowups do not change the neighborhood of $z = w = 0$, where the two curves meet transversely. Near each center the strict fiber has one point on the exceptional curve, given by its tangent direction. The two strict curves are still smooth copies of $\mathbb{P}^1$. Using (XV.1.4),

$$(C_i \cdot C_j) = \begin{pmatrix} -2 & 1 \\ 1 & -2 \end{pmatrix}, \qquad K_B \cdot C_1 = K_B \cdot C_2 = 0. \tag{XV.1.8}$$

The canonical pairings also follow from adjunction on the two -2 curves. This is the base of the model we call CHAIN45. The numbers will label the two split multiplicative fibers.

Figure XV.1.1 distinguishes the strict fiber from its class before subtracting the exceptional curves. The placement of the centers also matters. Move the first center to $S \cap F_0$ and leave the second off S on the same fiber F_0. Then

$$C_1' = S - E_1, \quad C_2' = F - E_1 - E_2, \qquad (C_1')^2 = -3, \quad C_1' \cdot C_2' = 1 - 1 = 0. \tag{XV.1.9}$$

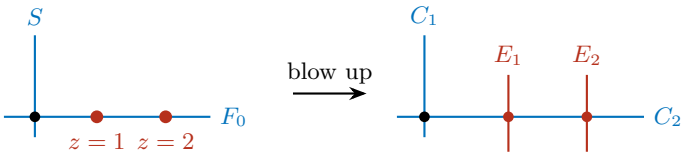


Figure XV.1.1: The selected fiber of $\mathbb{F}_2$ and its total transform. Blowing up the two marked points leaves S unchanged. The strict fiber C_2 meets each exceptional curve once. Its meeting with C_1 is the old intersection $z = w = 0$.

The strict curves now meet the first exceptional curve in different tangent directions. The same number of blowups can give different gauge-curve incidence, even before specifying the elliptic fibration.

To build that fibration, take a line bundle L on the new base. In the affine fiber chart use x in L^2, y in L^3 and sections a_i of L^i. Each term of the cubic lies in L^6. With u the homogeneous coordinate used to recover the affine chart $u = 1$, the equation is

$$y^2u + a_1xyu + a_3yu^2 = x^3 + a_2x^2u + a_4xu^2 + a_6u^3. \tag{XV.1.10}$$

There is a section $[u : x : y] = [0 : 0 : 1]$, where the derivative of the difference of the two sides with respect to u is 1 in the chart $y = 1$. The point is regular, including over singular fibers.

To find the canonical line, take the relative residue in the affine chart. If the local frame of L changes by $e' = \lambda e$, the coefficient of a section of L^i changes by λ^{-i}. Relative differentials are taken with the base fixed. Hence

$$x' = \lambda^{-2}x, \qquad y' = \lambda^{-3}y, \qquad a_i' = \lambda^{-i}a_i, \tag{XV.1.11}$$

$$\omega'_{\mathrm{rel}} = \frac{d_{\mathrm{rel}}x'}{2y' + a_1'x' + a_3'} = \lambda\frac{d_{\mathrm{rel}}x}{2y + a_1x + a_3}. \tag{XV.1.12}$$

Wedge the residue with a base two-form. The gluing is that of $\pi^*(K_B \otimes L)$, where π denotes the projection to B. Hypersurface adjunction interprets this line as the dualizing sheaf across singular fibers as well. Thus our canonical choice is

$$L = K_B^{-1}, \qquad \omega_{\mathrm{dual}} \simeq \mathcal{O}. \tag{XV.1.13}$$

When the discriminant is not identically zero, the smooth genus-one generic fiber and the section make this an elliptic Weierstrass model. Triviality of its dualizing line does not by itself construct a smooth global crepant resolution. The next step is to produce actual coefficient sections on the blown-up base.

XV.1.2 The split Tate model

Can one set of coefficients realize the two tunings at once? Write $z = Z/W$, $w = U/V$. Here $[U : V]$ are homogeneous ruling coordinates, Z cuts out S, and W has class $S + nF$.

A section of $AS + BF$ on $\mathbb{F}_n$, for $A \geq 0$, is built from the terms

$$Z^j W^{A-j} p_j(U,V), \qquad 0 \leq j \leq A, \qquad \deg p_j = B - n(A-j). \tag{XV.1.14}$$

Indeed the fiber-coordinate factor contributes $AS + n(A-j)F$, and a homogeneous ruling polynomial of degree d adds dF. A negative required degree contributes no term. In the affine chart, a monomial $z^j w^k$ is allowed precisely when

$$0 \leq j \leq A, \qquad 0 \leq k \leq B - n(A-j). \tag{XV.1.15}$$

Restricting to S keeps only $j = 0$, of degree $B - nA$ in the ruling coordinate. Restricting to a fixed fiber gives a section of degree A in the fiber coordinate.

For the five Tate indices $i = (1, 2, 3, 4, 6)$, use the split I_4 and I_5 ansätze with exponents

$$(u_i) = (0, 1, 2, 2, 4), \qquad (v_i) = (0, 1, 2, 3, 5). \tag{XV.1.16}$$

The intended factorization on the blown-up base divides a_i by the indicated powers of the sections of C_1, C_2. It reads $a_i = z^{u_i} w^{v_i} \beta_i$ near their meeting, and the residual section has class

$$-iK_B - u_i C_1 - v_i C_2 = (2i - u_i)S + (4i - v_i)F - (i - v_i)(E_1 + E_2). \tag{XV.1.17}$$

In each row $i - v_i = 1$. Put $A = 2i - u_i$, $B = 4i - v_i$ in the Cox formula. The new strict-fiber degree is $A - 2$, since the downstairs section has a zero at each center before the exceptional factors are removed. The section degree is $B - 2A$, since neither center lies on S.

i	(u_i, v_i)	(A, B)	$\deg \beta_i\|_{C_1}$	$\deg \beta_i\|_{C_2}$
1	(0,0)	(2,4)	0	0
2	(1,1)	(3,7)	1	1
3	(2,2)	(4,10)	2	2
4	(2,3)	(6,13)	1	4
6	(4,5)	(8,19)	3	6

Here is a lift that works for every compatible pair of restrictions in the table. Let $P(w)$ have degree at most $B - 2A$ and $Q(z)$ degree at most $A - 2$. The common value at the corner must be the same in the local frames used there. Set

$$D(z) = \frac{(z-1)(z-2)}{2}, \qquad D(0) = 1, \tag{XV.1.18}$$

$$\widehat{\beta}(z,w) = P(w) + D(z)Q(z) - P(0), \qquad P(0) = Q(0). \tag{XV.1.19}$$

The w-dependent terms obey (XV.1.15) at $j = 0$. The product DQ has degree at most A in z, so every term of that product satisfies the bound at $k = 0$. Thus $\widehat{\beta}$ homogenizes. Along $z = 0$ it equals P. Along $w = 0$ it equals DQ, so it vanishes at the two centers. After the blowup, the pullback divided by the exceptional sections is

a section of $AS + BF - E_1 - E_2$. On the strict fiber, removing the two marked zeros identifies this restriction with Q as a section of $\mathcal{O}(A-2)$. The normalization $D(0) = 1$ preserves the frame match at the corner.

For $i = 6$, the choices $P = 2 + w^3$, $Q = 2 + z^6$ give

$$\widehat{\beta}_6 = w^3 + D(z)(2 + z^6). \tag{XV.1.20}$$

If we replace Q by $3 + z^6$ while leaving P fixed, the two degree bounds still hold, but their corner values are 2 and 3. No section can realize this pair in the stated frames. Degree bounds on the two curves solve separate extension problems. Agreement at the corner is what joins them.

A downstairs section with the required first-order zeros gives a quotient in each exceptional chart. At either $p = 1$ or 2, the two charts of the point blowup are

$$(z, w) = (p + \xi, \xi t), \qquad E = \{\xi = 0\}, \qquad C_2 = \{t = 0\}, \tag{XV.1.21}$$

$$(z, w) = (p + \eta h, \eta), \qquad E = \{\eta = 0\}. \tag{XV.1.22}$$

The strict fiber appears in the first chart. In the second it would require a direction with $w = 0$, which is at $h = \infty$. Define the local representatives of the residual by

$$\beta^{(\xi)}(\xi, t) = \frac{\widehat{\beta}(p + \xi, \xi t)}{\xi}, \qquad \beta^{(\xi)}(0, t) = \widehat{\beta}_z(p, 0) + t\widehat{\beta}_w(p, 0), \tag{XV.1.23}$$

$$\beta^{(\eta)}(\eta, h) = \frac{\widehat{\beta}(p + \eta h, \eta)}{\eta}, \qquad \beta^{(\eta)}(0, h) = h\widehat{\beta}_z(p, 0) + \widehat{\beta}_w(p, 0). \tag{XV.1.24}$$

The numerator vanishes to first order or higher, so these expressions are regular. In the overlap $\eta = \xi t$, $h = 1/t$, they satisfy $\beta^{(\xi)} = t\beta^{(\eta)}$. This factor is a frame change for the same line bundle. For example, (XV.1.20) gives $\widehat{\beta}_{6,w}(p, 0) = 0$ and $\widehat{\beta}_{6,z}(p, 0) = D'(p)(2 + p^6)$. The exceptional value is nonzero at $t = 0$ but vanishes in the direction $h = 0$.

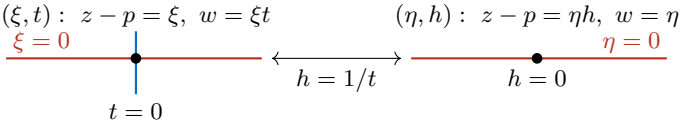


Figure XV.1.2: Two affine charts on the same exceptional $\mathbb{P}^1$. The point $t = 0$ is the strict-fiber direction and belongs to the ξ chart; $h = 0$ is the direction omitted by that chart. The exceptional value of the divided coefficient is the first jet evaluated in the indicated direction.

The division required for the Tate coefficient itself uses the new canonical bundle. Downstairs the expression is $z^{u_i} w^{v_i} \widehat{\beta}_i$. Divide its pullback by the i-th exceptional power, as dictated by L^i and (XV.1.5). Since $v_i + 1 = i$, the new expressions are

$$a_i^{(\xi)} = (p + \xi)^{u_i} t^{v_i} \beta_i^{(\xi)}, \tag{XV.1.25}$$

$$a_i^{(\eta)} = (p + \eta h)^{u_i} \beta_i^{(\eta)}, \qquad a_i^{(\xi)} = t^i a_i^{(\eta)}. \tag{XV.1.26}$$

This calculation uses a blowup of the base and a change of the fiber-coordinate bundles. In the first chart, $x_{\rm old} = \xi^2 x_{\rm new}$ and $y_{\rm old} = \xi^3 y_{\rm new}$. All terms of the old cubic then carry ξ^6. In the short Weierstrass form this reads

$$f_{\rm old} = \xi^4 f_{\rm new}, \qquad g_{\rm old} = \xi^6 g_{\rm new}, \qquad \Delta_{\rm old} = \xi^{12}\Delta_{\rm new}. \tag{XV.1.27}$$

The second chart has the corresponding powers of η. These are proper coefficient transforms on the new base. Dividing out a common factor without changing the base would be a different construction.

For the constant restrictions 1 of $\beta_1, \beta_2, \beta_3, \beta_4$ and the choice (XV.1.20), the five downstairs coefficients take the explicit form

$$(\widehat{a}_1, \widehat{a}_2, \widehat{a}_3) = D(z)(1, zw, z^2w^2), \tag{XV.1.28}$$

$$(\widehat{a}_4, \widehat{a}_6) = \big(z^2w^3 D(z),\ z^4w^5[w^3 + D(z)(2 + z^6)]\big). \tag{XV.1.29}$$

To see how a single example passes through both charts, define $d_p(\ell) = D(p+\ell)/\ell = D'(p) + \ell/2$. The two local representatives of a_6 are

$$a_6^{(\xi)} = (p+\xi)^4 t^5 [\,\xi^2 t^3 + d_p(\xi)(2 + (p+\xi)^6)\,], \tag{XV.1.30}$$

$$a_6^{(\eta)} = (p+\eta h)^4 [\,\eta^2 + h d_p(\eta h)(2 + (p+\eta h)^6)\,]. \tag{XV.1.31}$$

Each expression is polynomial. In the overlap the bracket on the left is t times the bracket on the right, so the coefficients differ by t^6, as required for L^6. The factor t^5 in the first chart describes the strict gauge fiber, and the missing factor in the second is consistent with that chart omitting the strict-fiber direction.

For the singular-fiber calculation, first complete the square with $Y = y + (a_1x + a_3)/2$. Define

$$B_2 = a_1^2 + 4a_2, \qquad B_4 = a_1a_3 + 2a_4, \quad B_6 = a_3^2 + 4a_6, \tag{XV.1.32}$$

$$Y^2 = x^3 + \tfrac{1}{4}B_2x^2 + \tfrac{1}{2}B_4x + \tfrac{1}{4}B_6. \tag{XV.1.33}$$

The shift $x = X - B_2/12$ removes the quadratic term. Collecting the linear and constant coefficients gives

$$f = -\frac{B_2^2}{48} + \frac{B_4}{2}, \qquad g = \frac{B_2^3}{864} - \frac{B_2B_4}{24} + \frac{B_6}{4}. \tag{XV.1.34}$$

In $4f^3 + 27g^2$, the terms proportional to B_2^6 and $B_2^4B_4$ cancel. The remaining terms proportional to $B_2^3B_6$ and $B_2^2B_4^2$ combine because

$$B_8 = \tfrac{1}{4}(B_2B_6 - B_4^2) = a_1^2a_6 + 4a_2a_6 - a_1a_3a_4 + a_2a_3^2 - a_4^2, \tag{XV.1.35}$$

$$\Delta = 4f^3 + 27g^2 = \tfrac{1}{16}\left(B_2^2B_8 + 8B_4^3 + 27B_6^2 - 9B_2B_4B_6\right). \tag{XV.1.36}$$

The standard elliptic discriminant is -16Δ; it has the same zero orders. Keeping B_8 in factored coefficient form makes the parity difference between the two tunings visible in the matter calculation.

Along either gauge curve the generic affine cubic reduces to $y^2 + a_1xy = x^3$. The tangent cone at the node is

$$y(y + a_1x) = 0. \tag{XV.1.37}$$

For $a_1 \neq 0$ it has distinct lines over the function field of the gauge curve, which is the split test. This test is independent of the order of Δ. For example, the leading coefficient along C_1 involves $-a_4^2$ in B_8, of order four, while that term has order six along C_2 and cannot contribute at order five. The restrictions calculated below give nonzero leading coefficients at generic points, with f, g units. The regular relatively minimal transverse surface models therefore have split I_4, I_5 there. No global Tate normal form for every Weierstrass model is needed: we have chosen an ansatz and realized it in actual coefficient bundles.

XV.1.3 Gauge and flavor divisors

Which curves support their own nonabelian vectors? The ordinary split-fiber dictionary assigns $\mathfrak{su}(n)$ to a split I_n curve. In our compact parent both tuned curves have finite area, so both are gauge curves. To see what other curves the equation generically supplies, we have to examine the coefficient systems away from the tuning. Counting the number of factors removed along C_1, C_2 does not establish the multiplicities of the remaining discriminant components.

Consider $AS + BF - E_1 - E_2$ with $A \geq 2$, $B \geq 2A$, which includes every residual bundle in the table. Its sections generate the fiber at each base point. On C_1 or C_2, use (XV.1.19). The restrictions are complete systems $\mathcal{O}(B - 2A)$ and $\mathcal{O}(A - 2)$ on projective lines. Their degrees are nonnegative. At the common point take nonzero matching values. At infinity take a section with nonzero top homogeneous coefficient in the relevant coordinate. Away from S and the total transform of F_0, a section of the form

$$Z^A U\, q(U, V), \qquad \deg q = B - 1, \tag{XV.1.38}$$

vanishes at the centers and can be chosen nonzero at the desired point. The factor U cuts out F_0 downstairs and is a unit at the point in question.

On each exceptional $\mathbb{P}^1$, use two allowed sections with affine expressions $D(z)$ and wz. The first has z-degree two and the second obeys the bound $1 \leq B - 2(A - 1)$. Their first jets at a center p are

$$dD|_{(p,0)} = D'(p)\, dz, \qquad d(wz)|_{(p,0)} = p\, dw. \tag{XV.1.39}$$

Here $D'(1) = -1/2$, $D'(2) = 1/2$. For instance, at $p = 1$ the two divided sections restrict to $(-1/2, t)$ in the first chart and $(-h/2, 1)$ in the second. At $p = 2$ the corresponding pairs are $(1/2, 2t)$ and $(h/2, 2)$. At least one is nonzero in every direction. Testing only the t chart would leave the direction $h = 0$ untested. This completes the pointwise generation argument, including the exceptional curves.

Now let $\mathcal{P}$ be the product of all five complex coefficient spaces, and let $B^\circ = B \setminus (C_1 \cup C_2)$. Over B° the prescribed tuning factors are units. The independent

sections β_4, β_6 give independent value variations $\delta a_4, \delta a_6$ at any chosen point. In a local frame, (XV.1.34) gives

$$\frac{\partial(f,g)}{\partial(a_4,a_6)} = \begin{pmatrix} 1 & 0 \\ -B_2/12 & 1 \end{pmatrix}. \tag{XV.1.40}$$

For example, varying a_4 changes B_4 by twice that variation. Varying a_6 changes only B_6, by four times the variation. The determinant is one, so the universal section can move in both fiber directions independently.

There are two relevant strata in the two-dimensional space of values. The singular point of the discriminant is $(f,g) = (0,0)$. Away from it the curve $4f^3 + 27g^2 = 0$ has gradient

$$d\Delta = 12f^2\, df + 54g\, dg. \tag{XV.1.41}$$

It is smooth at every nonzero value on that curve. Pull back the point stratum and this smooth curve stratum separately to $\mathcal{P} \times B^\circ$ using the rank calculation. The incidences are smooth of codimensions two and one, respectively. Generic smoothness over $\mathbb{C}$, applied to their projections to $\mathcal{P}$, then gives the expected smooth intersections on a dense open of the coefficients. A nondominating incidence has empty generic fiber. Thus on this open, any common zeros have independent df, dg. Other discriminant zeros are smooth and reduced in B°. In particular, there is no off-gauge $(4,6)$ point and there is no other multiple discriminant component.

For clarity, the two generic base tests have different linearizations. At a common zero the map of base tangent spaces is $v \mapsto (df(v), dg(v))$, which must have rank two. At a zero in the smooth-value stratum the single equation requires a nonzero covector $d\Delta$. In particular, at a nonzero discriminant value in the second stratum, $g \neq 0$, and the universal variation alone can move the value across that stratum:

$$\left.\frac{\partial \Delta}{\partial a_6}\right|_f = 54g \neq 0. \tag{XV.1.42}$$

This calculation is in coefficient space. The assertion about the derivative along the base, for a fixed generic coefficient choice, uses the smooth incidence projection. At a common zero, $d\Delta = 0$ even when df, dg are independent, so reducedness and smoothness of the nonzero-value locus must not be applied there.

There is a separate smoothness check for the total space. In the affine fiber chart let $\mathcal{F}$ denote the left side minus the right side of the Tate equation. At any point over B°, a section variation with $\delta a_6 = 1$ gives

$$\delta \mathcal{F} = -1. \tag{XV.1.43}$$

The universal hypersurface there is smooth. Generic smoothness of its projection to $\mathcal{P}$ gives smoothness of the affine Weierstrass total space off the tuned curves for generic choices. The section at infinity is already regular. These are statements about an open set in the full coefficient systems. A sparse choice of restrictions is enough to show that a desired intersection pattern is achievable, but that calculation does not by itself test every stratum of the sparse model. Neither argument constructs a resolution over the gauge curves or determines the group of sections.

The ordinary gauge assignment and the geometric multiplicity statement may therefore be summarized at generic points of the components:

$$\operatorname{ord}_{C_1}\Delta = 4, \qquad \operatorname{ord}_{C_2}\Delta = 5, \qquad \operatorname{ord}_{D}\Delta = 1 \quad (D \text{ a reduced residual component}). \tag{XV.1.44}$$

The first two orders still require their split test (XV.1.37); neither is inferred from generic smoothness away from the tuning.

A reduced residual component over the nonzero value stratum has generic fiber I_1. Its node has no nonabelian root algebra, even if the component meets a gauge curve at several points. To read off a flavor background from a noncompact seven-brane, first specify a gauge singularity on the noncompact curve. In the unwarped kinetic approximation, the putative constant gauge mode on a curve D has coefficient of the form

$$\frac{1}{g_{6,D}^2} = \mathcal{K}_7 \int_D \operatorname{vol}_{D,E}, \tag{XV.1.45}$$

with $\mathcal{K}_7$ the fixed microscopic factor in this reduction. A finite-area compact curve gives a finite coefficient. If the kinetic norm of the constant mode diverges on a noncompact curve under the chosen boundary conditions, this mode is not a dynamical six-dimensional field. The fixed boundary gauge field is then a flavor background for the compact sector.

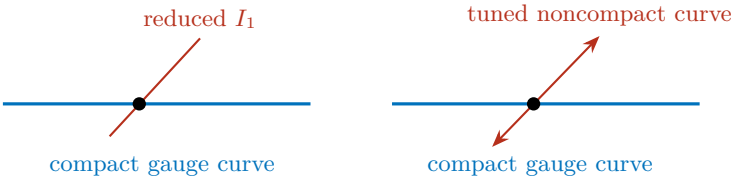


Figure XV.1.3: A generic reduced residual branch meeting a compact gauge curve, and a separate local model with a specified gauge singularity on a noncompact curve. In the first panel the meeting can give localized charged matter without a second nonabelian divisor algebra. In the second panel a divergent constant-mode kinetic norm leaves the noncompact field as a background.

The right panel of Figure XV.1.3 describes a different tuning from the generic reduced residual in the left panel. In the gauge and hypermultiplet description, rotations of identical fundamentals can also be used as background subgroups, for example $SU(3)$ and $SU(6)$ for the external fundamentals counted below. That choice does not assemble the residual intersections into geometric $SU(3)$ or $SU(6)$ stacks. It also leaves the full quantum flavor symmetry and global form unspecified. To tell which localized fields we have, we must restrict the actual residual discriminant to the gauge curves.

XV.1.4 Matter at intersections

When does a discriminant zero on a gauge curve support an ordinary charged hypermultiplet? We need three facts: the residual meets the curve at a specific point, the

enhancement has the right local analytic form, and that form is in the domain of the ordinary matter dictionary. The first two are calculations in the elliptic model. The third is a physical input.

Near $C_1 \cap C_2$, write $\Delta = z^4 w^5 \mathcal{R}$. The product divides the discriminant, as follows by computing its leading orders separately in z, w. For the ordered terms $a_1^2 a_6, 4a_2 a_6, -a_1 a_3 a_4, a_2 a_3^2, -a_4^2$ of B_8, the two exponent lists are

	$a_1^2 a_6$	$4a_2 a_6$	$-a_1 a_3 a_4$	$a_2 a_3^2$	$-a_4^2$
z	4	5	4	5	4
w	5	6	5	5	6

(XV.1.46)

The lowest exponents of B_4, B_6 are $(2,4)$ in z and $(2,4)$ in w. Hence the other three terms in (XV.1.36) have z- and w-orders at least six, eight and six, respectively. At the two lowest orders only $B_2^2 B_8$ contributes, with $B_2|_{C_i} = \beta_1^2$. Using the compatible frames of (XV.1.19),

$$16\mathcal{R}|_{C_1} = \beta_1^4 R_1, \qquad R_1 = \beta_1^2\beta_6 - \beta_1\beta_3\beta_4 - w\beta_4^2, \tag{XV.1.47}$$

$$16\mathcal{R}|_{C_2} = \beta_1^4 R_2, \qquad R_2 = \beta_1^2\beta_6 - \beta_1\beta_3\beta_4 + z\beta_2\beta_3^2. \tag{XV.1.48}$$

The frame on C_2 in this formula removes the two marked zeros in each residual coefficient. We will check the discriminant's change of frame explicitly at those points. At the corner both expressions equal $\beta_1^5(\beta_1\beta_6 - \beta_3\beta_4)$ after multiplication by β_1^4. In particular one cannot use the odd-node expression R_2 in place of the even-node expression R_1 along the rest of C_1.

The residual line bundle follows from $\Delta \in H^0(B, L^{12})$. Subtracting the two tuning divisors gives

$$[\mathcal{R}] = -12K_B - 4C_1 - 5C_2, \tag{XV.1.49}$$

$$[\mathcal{R}]\cdot C_1 = -4(-2) - 5 = 3, \qquad [\mathcal{R}]\cdot C_2 = -4 - 5(-2) = 6. \tag{XV.1.50}$$

The degrees of the polynomial terms in (XV.1.48) agree with this result. Along C_1 the term $w\beta_4^2$ has degree at most $1+2=3$. Along C_2, the term $z\beta_2\beta_3^2$ has degree at most $1+1+4=6$. The class tells us the total intersection with each compact curve. Simplicity and location of the roots still have to be checked.

Choose $\beta_1, \ldots, \beta_4$, with indices $1,2,3,4$, to have constant restriction 1 on both curves. Use (XV.1.20) for β_6. The residual factors are

$$R_1 = 1 - w + w^3, \qquad R_2 = 1 + z + z^6. \tag{XV.1.51}$$

To test the first polynomial, suppose $R_1' = 3w^2 - 1 = 0$. Then $R_1 = 1 - 2w/3$, which could vanish only at $w = 3/2$, incompatible with $w^2 = 1/3$. If $R_2' = 1 + 6z^5 = 0$, then $R_2 = 1 + 5z/6$. Its candidate $z = -6/5$ does not have $z^5 = -1/6$. Hence both polynomials are squarefree. Their top coefficients are nonzero and they have no roots at infinity. Their corner values are both 1, and on C_2

$$R_2(1) = 3, \qquad R_2(2) = 67. \tag{XV.1.52}$$

Thus the external points miss both exceptional meetings. The nonvanishing of these marked values and of the polynomial discriminants is open in the coefficient spaces. So is $\beta_1 \neq 0$ along either curve, since the restrictions have degree zero. The lift provides a witness to all these conditions together. The resulting nonempty open and the off-gauge open of the previous section have nonempty intersection in the irreducible full coefficient space.

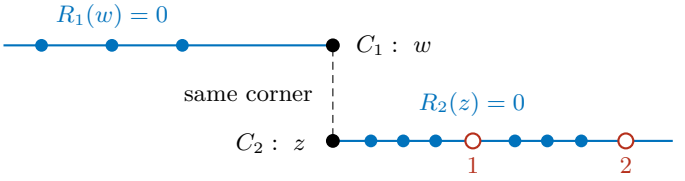


Figure XV.1.4: Marked points of the strict gauge curves. Each dot labeled by a residual polynomial represents one simple zero. Their positions are schematic: the roots are on complex projective lines. The circles on C_2 mark the exceptional meetings $z = 1, 2$, where the residual is nonzero. The shared corner is separate from all nine external points.

Why would the calculation on the original fiber give a different answer? For this choice, every $\widehat{\beta}_i(z, 0)$ is divisible by $D(z)$. All contributing terms in B_8 at order w^5 have three factors of D. The prefactor B_2^2 adds four more. With the downstairs coordinates and the old canonical line,

$$\left.\frac{16\Delta_{\text{old}}}{z^4 w^5}\right|_{w=0} = D(z)^7 R_2(z). \tag{XV.1.53}$$

Its polynomial degree is twenty. At $z = p + \xi,\ w = \xi t$, dividing the discriminant by ξ^{12} and removing t^5 gives

$$\left.\frac{16\Delta_{\text{new}}}{t^5}\right|_{t=0} = (p+\xi)^4 \left(\frac{D(p+\xi)}{\xi}\right)^7 R_2(p+\xi). \tag{XV.1.54}$$

Since $D'(p) \neq 0$, the right-hand side is nonzero at $\xi = 0$ for each center. The strict residual loses seven powers at each exceptional meeting. Those powers were part of the transformation of the discriminant line and its tuned fiber component. They were not fourteen additional matter points.

For the same witness, the linear term in $\widehat{\beta}_1$ along $t = 0$ is $D'(p)\xi$. Hence $a_1^{(\xi)} = D'(p)$ at the meeting. There $f_{\text{new}} = -a_1^4/48$ and $g_{\text{new}} = a_1^6/864$ are units. Equation (XV.1.54) also shows that the discriminant has no exceptional divisor component: the quotient after removing t^5 is nonzero near the meeting, including on the adjacent open part of E_i with $t \neq 0$. Downstairs the point orders were $(4, 6, 12)$. The division (XV.1.27) shows the lower bounds on the orders, and the corresponding new coefficients are nonzero at generic directions on the exceptional line, giving equality. This is why the base blowups were part of the construction.

Next take a point on one of the tuned curves where f, g are nonzero. Choose the stationary root r of the cubic that is the double root at the point. Since $r \neq 0$, a local analytic branch satisfies $f = -3r^2$. In the short Weierstrass coordinate $x = r + X$ the cubic becomes

$$x^3 + fx + g = (g - 2r^3) + X^2(3r + X), \tag{XV.1.55}$$

$$\Delta = 27(g - 2r^3)(g + 2r^3). \tag{XV.1.56}$$

At the double root $g = 2r^3$, the second discriminant factor is nonzero. Choose a local square root of $3r + X$. The two fiber coordinates

$$U_* = y - X\sqrt{3r + X}, \qquad V_* = y + X\sqrt{3r + X} \tag{XV.1.57}$$

give an invertible analytic change near the node. Their product is $g - 2r^3$. Absorbing the discriminant unit into a coordinate gives the exact local form

$$U_* V_* = \Delta. \tag{XV.1.58}$$

At the corner, $\mathcal{R}$ is a unit, so the threefold germ is $U_* V_* = z^4 w^5$ after another unit change. A generic disk through the corner meets each axis to first order. Its surface germ is $U_* V_* = \tau^9$, which has type A_8. This is an enhancement on a transverse surface. The two generic divisor algebras remain $\mathfrak{su}(4) \oplus \mathfrak{su}(5)$.

The order nine is tied to the choice of disk. For example, $z = \tau,\ w = \tau$ yields order nine, while $z = \tau,\ w = \tau^2$ yields

$$\operatorname{ord}_\tau\left(z^4 w^5\right) = 4 + 2 \cdot 5 = 14. \tag{XV.1.59}$$

The second disk is tangent to C_2 at the corner. Its higher order does not change the threefold germ or give a different ordinary transverse matter rule at that point.

At an external residual zero, take σ normal to the gauge curve and let s be the residual itself in a local frame. Simplicity of the restricted zero makes (σ, s) local coordinates. Thus

$$U_* V_* = \sigma^n s \quad \xrightarrow{\text{transverse disk}} \quad U_* V_* = \tau^{n+1}, \qquad n = 4, 5, \tag{XV.1.60}$$

where a unit is again absorbed. The surface has type A_n, and the ordinary relatively minimal transverse fiber is I_{n+1}. The disk diagnoses the local enhancement; it does not count the intersections of the two branches. For that count we used the restricted derivative.

Two changes to β_6 isolate the needed hypotheses. On C_1, replace its restriction by $2 - w^2 + w^3$. The degree bound and compatibility at the corner still hold, but

$$R_1 = 1 - w - w^2 + w^3 = (1 - w)^2(1 + w). \tag{XV.1.61}$$

There are two distinct roots with total multiplicity three. The squarefree point calculation no longer applies. Alternatively subtract 1 from both restrictions of β_6 in the original witness. The resulting R_1 starts with $-w$ and R_2 starts with z at the corner. The common residual has zero constant term and a nonzero linear term. Thus

$$\operatorname{ord}_{(0,0)} \Delta = 4 + 5 + 1 = 10 \tag{XV.1.62}$$

instead of nine. Compatibility alone did not ensure a unit residual there.

We can now apply the ordinary isolated matter rule to the simple-root example. In a transverse split A-type enhancement the charged root blocks identify the representations. For the corner, decompose the defining space of $\mathfrak{sl}_9$ as $\mathbb{C}^4 \oplus \mathbb{C}^5$. A block mapping $\mathbb{C}^5$ to $\mathbb{C}^4$ transforms as a fundamental on the left and an antifundamental on the right. Thus, under $\mathfrak{sl}_4 \oplus \mathfrak{sl}_5$,

$$\mathfrak{sl}_9 = (\mathfrak{sl}_4, \mathbf{1}) \oplus (\mathbf{1}, \mathfrak{sl}_5) \oplus \mathbf{1} \oplus (\mathbf{4}, \overline{\mathbf{5}}) \oplus (\overline{\mathbf{4}}, \mathbf{5}). \tag{XV.1.63}$$

The block dimensions sum to $15+24+1+20+20 = 80$. The two off-diagonal blocks are conjugates. In the ordinary local matter dictionary they supply one full hypermultiplet, with the conjugate components paired by the quaternionic reality condition. They do not count as two full hypers. Changing the orientation of the edge amounts to conjugating one gauge-factor convention. At a simple external enhancement, the same block argument with $\mathbb{C}^{n+1} = \mathbb{C}^n \oplus \mathbb{C}$ gives one fundamental block and its conjugate, hence one full fundamental by the same physical rule.

	$\mathbb{C}^4$	$\mathbb{C}^5$
$\mathbb{C}^4$	4×4	$(\mathbf{4}, \overline{\mathbf{5}})$
$\mathbb{C}^5$	$(\overline{\mathbf{4}}, \mathbf{5})$	5×5

Figure XV.1.5: Matrix blocks for the A_8 enhancement at the corner. The off-diagonal spaces are dual under the two gauge algebras and give the conjugate components of one full bifundamental in the ordinary local matter dictionary. The traceless condition is on the entire matrix.

On the displayed simple-root domain, the two rational curves give no bulk adjoint hypers by the smooth-curve genus rule. The charged sector we have obtained is

$$3(\mathbf{4}, \mathbf{1}) \ \oplus \ 6(\mathbf{1}, \mathbf{5}) \ \oplus \ (\mathbf{4}, \overline{\mathbf{5}}) \tag{XV.1.64}$$

in full hypermultiplets. The $\mathfrak{su}$ labels describe the nonabelian algebras and representation types. They do not fix the global form of the compact gauge group. Neither neutral hypers nor abelian vectors are counted here. The anomaly chapter will use the dimensions of these representations as inputs, without inferring the matter from an anomaly equation in reverse.

XV.1.5 Multiplets and the local limit

What can be made large while keeping the two gauge curves at finite area? Before taking a limit, separate the different roles of the base. In the ordinary compactification, the tensor scalars describe Kähler shape: the normalized class is $j = J_E/\sqrt{J_E^2}$, with $j \cdot C_i$ its normalized curve areas. The overall volume $J_E^2/2$ belongs to the hypermultiplet sector. For the scaling at fixed microscopic units we use the unnormalized areas A_i. A

two-form comes from reducing the IIB four-form in the corresponding dual curve sector. Schematically, with ω_i a two-form used in this reduction,

$$C_4 \supset B_2^i \wedge \omega_i, \qquad A_i = \int_{C_i} J_E. \tag{XV.1.65}$$

The basis for B_2^i and the tensor kinetic terms will be developed in the next chapter. A D3-brane wrapped on C_i is extended in two spacetime dimensions and is electrically charged as a string. The vector multiplet instead comes from the generic split fiber, and the charged hypers in (XV.1.64) from its isolated enhancements.

In the ordinary finite local reference, one normalizable tensor per retained independent compact curve gives two tensor multiplets for the chain. The geometric string pairing in the chosen sign is

$$\Omega_{ij} = -C_i \cdot C_j = \begin{pmatrix} 2 & -1 \\ -1 & 2 \end{pmatrix}. \tag{XV.1.66}$$

Its eigenvalues are $1, 3$. Positivity of this pairing does not compute a physical kinetic metric or establish normalizability. In the ordinary compact supergravity description, the base supplies a lattice of signature $(1, T)$. The positive direction belongs to the gravity multiplet's self-dual tensor, and

$$h^{1,1}(B) = 4, \qquad T_{\text{compact}} = h^{1,1}(B) - 1 = 3. \tag{XV.1.67}$$

Here the two point blowups each add one class to the rank-two ruled-surface lattice. The compact T is therefore different from the count in the retained local sector. The exceptional curves are part of the compact lattice but are not additional tuned gauge curves.

The charge-sector dimensions give two other counts. Let H_{ch} be the sum of the complex dimensions of the displayed charged representations, counted once per full hyper. Let V_{nonab} count the vector generators of the displayed nonabelian algebra. Then

$$H_{\text{ch}} = 3 \cdot 4 + 6 \cdot 5 + 4 \cdot 5 = 62, \tag{XV.1.68}$$

$$V_{\text{nonab}} = (4^2 - 1) + (5^2 - 1) = 39. \tag{XV.1.69}$$

A charged representation of dimension twenty contributes twenty here, even though it is one full bifundamental. These numbers leave the compact neutral hypers and any abelian gauge sector undetermined.

For the geometric limit, take $J = J_E$ in fixed microscopic units. Specify positive areas A_1, A_2 for C_1, C_2 and a parameter ρ for a generic fiber. Write $J = \rho S + bF - e_1 E_1 - e_2 E_2$ in the real divisor basis, identified with its cohomology classes. Pairing with S, F, C_2, E_i gives

$$J \cdot S = b - 2\rho, \qquad J \cdot F = \rho, \tag{XV.1.70}$$

$$J \cdot C_2 = \rho - e_1 - e_2, \qquad J \cdot E_i = e_i. \tag{XV.1.71}$$

Solving with $e_1 = e_2$ yields

$$J = \rho S + (2\rho + A_1)F - \frac{\rho - A_2}{2}(E_1 + E_2), \qquad \rho > A_2 > 0, \quad A_1 > 0. \tag{XV.1.72}$$

The generic fiber grows but its strict transform remains fixed. The growing area lies in the two exceptional curves in the total transform.

To verify that J is Kähler, we need to test the actual cone of effective curves. An irreducible curve on the blown-up surface is exceptional, a strict fiber, the section, or the strict transform of a different non-fiber curve. For the last case, let the downstairs class be $dS + b'F$ with multiplicities m_1, m_2 at the centers. Intersection with S gives $b' \geq 2d$, while intersection with the selected fiber gives $m_1 + m_2 \leq d$. The latter inequality follows because the local intersection multiplicity with the smooth fiber is at least m_i at each center. In the basis of effective generators the strict class is

$$dS + b'C_2 + (b' - m_1)E_1 + (b' - m_2)E_2. \tag{XV.1.73}$$

All coefficients are nonnegative. A different fiber has class $F = C_2 + E_1 + E_2$. Thus S, C_2, E_1, E_2 generate the closed effective curve cone. The path pairs strictly positively with these generators. Its self-intersection is positive, as is also seen from the following volume calculation. The surface Kähler criterion now applies.

For the symmetric path,

$$\begin{aligned} \mathrm{Vol}_E(B) = \tfrac{1}{2}J^2 &= \rho^2 + \rho A_1 - \tfrac{1}{4}(\rho - A_2)^2 && \text{(XV.1.74)} \\ &= \tfrac{3}{4}\rho^2 + \rho(A_1 + A_2/2) - \tfrac{1}{4}A_2^2. && \text{(XV.1.75)} \end{aligned}$$

Because $0 < \rho - A_2 < \rho$, the negative term in the first line is less in magnitude than $\rho^2/4$. There is also an asymmetric path at the same retained areas. Replace J by $J_\epsilon = J - \epsilon E_1 + \epsilon E_2$. Then

$$J_\epsilon \cdot E_{1,2} = (\rho - A_2)/2 \ \pm \epsilon, \qquad \mathrm{Vol}_E(B; J_\epsilon) = \mathrm{Vol}_E(B; J) - \epsilon^2. \tag{XV.1.76}$$

For $|\epsilon| < (\rho - A_2)/2$ all cone pairings stay positive, and the volume remains positive. At fixed ϵ, the quadratic growth coefficient remains $3/4$. In contrast, multiplying the whole original J by a large number would scale both A_i by that number. It would not be a limit at the same gauge-curve areas.

The same symmetric path can be expressed in a basis adapted to the retained tensor curves. This is useful because fixing their areas then amounts to fixing two coordinates. Define $H = 2S + 4F - E_1 - E_2$. The pairings of (XV.1.4) and the inverse of (XV.1.66) give

$$H \cdot C_i = 0, \qquad H^2 = 6, \qquad \Omega^{-1} = \tfrac{1}{3}\begin{pmatrix} 2 & 1 \\ 1 & 2 \end{pmatrix}. \tag{XV.1.77}$$

For the column $A = (A_1, A_2)^{\mathsf{T}}$, take $J = RH - \sum_i C_i(\Omega^{-1}A)_i$. Then

$$J \cdot C_j = A_j, \qquad J \cdot F = 2R - \tfrac{1}{3}(2A_1 + A_2). \tag{XV.1.78}$$

The minus sign in the first line compensates the negative intersection form on the compact curve span. The two exceptional areas are equal because H and both C_i are symmetric under exchanging E_1, E_2. Setting $J \cdot F = \rho$ therefore recovers (XV.1.72).

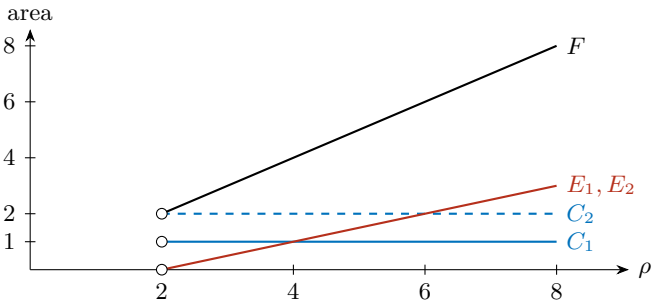


Figure XV.1.6: Area path for $A_1 = 1,\ A_2 = 2$, in fixed units with $\rho > 2$. The selected curve areas are horizontal. Each exceptional area grows with slope $1/2$, and the generic fiber has area ρ. The curves refer to areas, while the base volume in (XV.1.75) has units of area squared.

Orthogonality makes the volume especially simple in this frame:

$$\tfrac{1}{2}J^2 = 3R^2 - \tfrac{1}{2}A^{\mathsf{T}}\Omega^{-1}A. \tag{XV.1.79}$$

The R direction can grow without changing the compact pairings. Substituting $R = \frac{1}{2}[\rho + (2A_1 + A_2)/3]$ into this expression gives the same quadratic and linear terms as (XV.1.75). This is a decomposition of the intersection form. It identifies which geometric direction is growing and which is held fixed. The physical normalization of tensors in that limit is a separate calculation.

In the leading unwarped reduction, insert an external metric independent of the base into the Einstein term. With κ_{10} fixed, the coefficient of $\frac{1}{2}\int d^6x\sqrt{-g_6}\,R_6$ is

$$\kappa_6^{-2} = \kappa_{10}^{-2}\int_B \mathrm{vol}_{B,E} = \kappa_{10}^{-2}\mathrm{Vol}_E(B). \tag{XV.1.80}$$

The area-squared factor converts length dimension -8 of κ_{10}^{-2} to dimension -4 of κ_6^{-2}. Equations (XV.1.45) and (XV.1.75) show why this path is useful: the leading gravity zero-mode coefficient diverges, while the wrapped gauge area factors stay finite. It is a geometric calculation with a leading reduction, not a statement that all excitations outside the finite sector are heavy. Growing directions can have light Kaluza–Klein modes. To establish an isolated theory one must control the metric and boundary limit, the norms of the retained modes, and their couplings to the bulk tower. Nothing in the area and intersection calculations supplies those estimates. Chapter 2 will use these curve areas and classes to derive string tensions and tensor couplings in its stated regime.

XV.1.6 A single-node comparison

What changes if the I_5 tuning wraps a negative section of square -1? Take the unblown base $\mathbb{F}_1$. Its section is again $S = \{z = 0\}$, and $S^2 = -1$, $S \cdot F = 1$. Equation (XV.1.3)

gives $K_B = -2S - 3F$. Use only the I_5 exponents $v_i = (0, 1, 2, 3, 5)$, with $a_i = z^{v_i}\beta_i$ near S. The coefficient class and its degree on S are

$$[\beta_i] = (2i - v_i)S + 3iF, \tag{XV.1.81}$$

$$[\beta_i] \cdot S = i + v_i, \qquad \big(\deg \beta_1, \deg \beta_2, \deg \beta_3, \deg \beta_4, \deg \beta_6\big)|_S = (1, 3, 5, 7, 11). \tag{XV.1.82}$$

In contrast to the chain's degree-zero β_1, the degree-one coefficient has a zero on S.

Every polynomial $P_i(w)$ of the indicated degree lifts. In fact, in (XV.1.14) take $j = 0$ and use

$$\widehat{\beta}_i = W^{2i-v_i} V^{i+v_i} P_i(U/V). \tag{XV.1.83}$$

The base factor is homogeneous of degree $i + v_i$, and the W factor gives the rest of the divisor class. In particular, a coefficient chosen to be 1 in the affine chart is homogenized with the indicated power of V; it need not be nowhere zero on S. The full systems $AS + BF$ used here have $B \geq A$. At a point with $W \neq 0$, use $j = 0$ with a homogeneous ruling polynomial nonzero there. At a point with $Z \neq 0$, use $j = A$ with a nonzero value. This proves pointwise generation, so the full-system generic argument of Section XV.1.3 applies off S. Again it is an open-family statement, not a global smoothness check of the sparse coefficients we choose next.

The odd tuning yields the analogue of R_2, but there is no second tuned curve to remove. The powers of z in B_8 are $5, 6, 5, 5, 6$, so

$$16\,\big(\Delta/z^5\big)\big|_S = \beta_1^4 P, \tag{XV.1.84}$$

$$P = \beta_1^2\beta_6 - \beta_1\beta_3\beta_4 + \beta_2\beta_3^2. \tag{XV.1.85}$$

The term degrees are $2 + 11 = 1 + 5 + 7 = 3 + 2 \cdot 5 = 13$. The residual degree, including the fourth power, also follows directly from the class:

$$(-12K_B - 5S) \cdot S = (19S + 36F) \cdot S = 17 = 4 + 13. \tag{XV.1.86}$$

This total counts intersection multiplicities. We must still determine the nature and location of the intersections.

Choose the five polynomials on S to be

$$(\beta_1, \beta_2, \beta_3, \beta_4, \beta_6) = (w, 1, 1, 0, w^{11}). \tag{XV.1.87}$$

Use (XV.1.83) as a sparse witness for the SU5-F1 germ along S. It has a nonminimal divisor at $W = 0$, disjoint from S. With $Z = V = 1$, its nonzero (a_1, a_2, a_3, a_6) are $(W^2 w, W^3, W^4, W^7 w^{11})$, giving generic orders $(6, 7, 14)$ for (f, g, Δ). On S, $P = 1 + w^{13}$, whose derivative vanishes only at $w = 0$ in the affine chart. That point is not a root. The top homogeneous coefficient is nonzero, so all thirteen roots are simple and finite. This establishes a nonempty open in the full coefficient parameter space: β_1 is a nonzero section with a simple zero, $\beta_2\beta_3$ is a unit there, and the degree-thirteen binary form P is squarefree. The ordinary compact-family interpretation uses the intersection of this restriction open and the full-system open off S. The unit condition forces $P \neq 0$ at the zero of β_1. It does not force squarefreeness elsewhere. At a simple root of P, f, g are

units and the residual meets S transversely. Equation (XV.1.60) with $n = 5$ gives an I_6 fiber on a generic transverse disk.

The point $\beta_1 = 0$ requires a different calculation. Translate it to $w = 0$ and use the maximal ideal $\mathfrak{m} = (z, w)$. Write b_2, b_3 for the nonzero values of β_2, β_3 there. The leading forms, with errors of higher total degree, are

$$B_2 = 4zb_2 + O(\mathfrak{m}^2), \qquad B_4 = O(\mathfrak{m}^3), \tag{XV.1.88}$$

$$B_6 = z^4 b_3^2 + O(\mathfrak{m}^5), \qquad B_8 = z^5 b_2 b_3^2 + O(\mathfrak{m}^6). \tag{XV.1.89}$$

For example, $a_1 a_3$ has total degree at least three, and the first term in B_8 with only one z-power from a_2 and four from a_3^2 is of degree five. Substitution into (XV.1.34) and (XV.1.36) gives

$$f = -\tfrac{1}{3} b_2^2 z^2 + O(\mathfrak{m}^3), \qquad g = \tfrac{2}{27} b_2^3 z^3 + O(\mathfrak{m}^4), \tag{XV.1.90}$$

$$\Delta = b_2^3 b_3^2 z^7 + O(\mathfrak{m}^8). \tag{XV.1.91}$$

The orders on a generic disk transverse to S are $(2, 3, 7)$, giving the D_5 enhancement in the ordinary transverse classification. This point is not a node of the kind studied at $f, g \neq 0$.

To read its representation, use the D_5 roots $\pm e_i \pm e_j$, $1 \leq i < j \leq 5$, in an orthonormal basis. Roots $e_i - e_j$ with $i \neq j$ give the A_4 algebra. Restrict the positive sums to its traceless Cartan subspace. With $\lambda_i = e_i - \frac{1}{5} \sum_k e_k$, those weights and their negatives are

$$\{ \pm(\lambda_i + \lambda_j) : i < j \}. \tag{XV.1.92}$$

They are the weights of $\bigwedge^2 \mathbf{5} = \mathbf{10}$ and its conjugate, with ten weights in each. The ordinary localized D_5 to A_4 matter rule assigns one full antisymmetric hyper at this point. The factor β_1^4 instead records a fourth-order residual intersection with the gauge curve. It is not a multiplicity of four fundamentals.

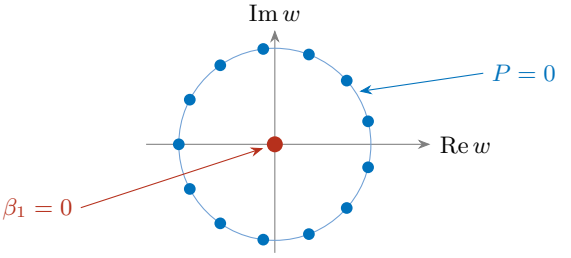


Figure XV.1.7: In the affine w-plane for (XV.1.87), the thirteen roots of $1 + w^{13}$ lie on the unit circle. The point at the origin is the separate zero of β_1. It has residual weight four and ordinary D_5 type. There is no root at infinity.

Two admissible changes distinguish the tests for the ordinary spectrum. First replace $\beta_2 = 1$ by $\beta_2 = w$ in the same bundle. Now $P = w + w^{13}$, and the simple root at the

origin coincides with $\beta_1 = 0$. With the other polynomials unchanged, $B_2 = w^2 + 4zw$ and $B_4 = wz^2$ have total orders two and three. The leading terms of f, g, Δ are

$$\tfrac{1}{2}wz^2, \qquad \tfrac{1}{4}z^4, \qquad \tfrac{27}{16}z^8. \tag{XV.1.93}$$

Indeed B_6 starts at order four and B_8 now starts at order six. Thus $27B_6^2$ is the only term of order eight in the discriminant. The new orders $(3, 4, 8)$ differ from (XV.1.91), and the ordinary separated calculation cannot be used there.

For a second change, keep $\beta_2 = \beta_3 = 1$ and alter only β_6 to

$$L_6(w) = -\tfrac{13}{11} + \tfrac{2}{11}w^{11}. \tag{XV.1.94}$$

This is a legal lift of the same degree. It leaves the D_5 calculation at the origin unchanged since $b_2 = b_3 = 1$. Now

$$P = 1 - \tfrac{13}{11}w^2 + \tfrac{2}{11}w^{13}, \qquad (P(1), P'(1), P''(1)) = (0, 0, 26). \tag{XV.1.95}$$

The degrees thirteen and seventeen are unchanged, but $w = 1$ has multiplicity two. The transverse coefficient tells us what happened to the residual curve itself. Set $Q_* = \Delta/z^5$ in the affine frame. With $B_2 = w^2 + 4z,\ B_4 = wz^2,\ B_6 = z^4 + 4z^5L_6$, the two leading z-coefficients are

$$B_8 = z^5(1 + w^2L_6) + 4z^6L_6, \tag{XV.1.96}$$

$$Q_* = \frac{w^4(1 + w^2L_6)}{16} + \frac{z}{16}\left(12w^4L_6 + 8w^2 - w^3\right) + O(z^2). \tag{XV.1.97}$$

For the linear coefficient, the $B_2^2B_8$ contribution is $12w^4L_6 + 8w^2$, and the $8B_4^3$ and $-9B_2B_4B_6$ terms sum to $-w^3$. Since $L_6(1) = -1$, the gradient of Q_* at $(0, 1)$ is $(-5/16, 0)$ in (z, w). The residual is smooth there and tangent to S. Its intersection with S has multiplicity two, since the restriction starts at quadratic order in $w - 1$. On the disk $z = \tau,\ w = 1 + 2\tau$, f, g are units and Δ starts at $-5\tau^6/16$, so an I_6 disk still occurs at the tangent point. The disk does not split that tangency into two points. We assign no new matter spectrum at this tuning.

The leading graph of the residual makes the distinction visible. Put $q = w - 1$. The restriction of Q_* to $z = 0$ starts with $13q^2/16$, while its derivative in z is $-5/16$. Solving $Q_* = 0$ for z by the implicit function theorem gives

$$z = \frac{13}{5}q^2 + O(q^3). \tag{XV.1.98}$$

The local intersection multiplicity comes from contact of this graph with $z = 0$, not from a singular residual branch. Figure XV.1.8 compares the graph and a disk that cuts across both curves.

For (XV.1.87), or the nonempty open with thirteen simple residual zeros and $\beta_2\beta_3 \neq 0$ at the β_1 zero, the ordinary charged sector is one full **10** and thirteen full **5**s. The smooth rational section gives no bulk adjoint. Hence the selected dimensions are

$$H_{\mathrm{ch}} = 10 + 13 \cdot 5 = 75, \qquad V_{\mathrm{nonab}} = 5^2 - 1 = 24. \tag{XV.1.99}$$

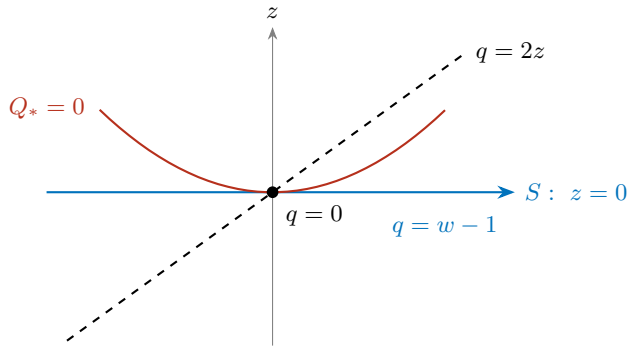


Figure XV.1.8: Real-coordinate slice of the complex germ at the repeated root. The blue line is S, and the solid red curve is the quadratic approximation $z = 13q^2/5$ to the smooth residual. The dashed line is the disk $q = 2z$. Its nonzero transverse slope tests the fiber order without resolving the quadratic contact into separate intersections.

The two changes demonstrate why degree, or even degree together with the persistence of the D_5 point, does not imply that spectrum.

The one-node example also permits a fixed-area path. On $\mathbb{F}_1$, S, F generate the effective curve cone: for any other non-fiber irreducible curve $dS + bF$, its intersections with F, S give $d \geq 0$, $b \geq d$. Thus the class

$$J = \rho S + (\rho + A)F, \qquad J \cdot S = A, \qquad J \cdot F = \rho, \tag{XV.1.100}$$

$$\mathrm{Vol}_E(B) = \tfrac{1}{2}\rho^2 + \rho A, \qquad A, \rho > 0 \tag{XV.1.101}$$

is Kähler. The same leading Einstein calculation applies with this base volume. In the compact reference $T = 2 - 1 = 1$, while the ordinary finite local reference has one tensor associated to the retained section, conditional on its normalizable sector. Equality of these two numbers does not identify the compact signature-$(1, 1)$ lattice with the selected local curve lattice. Chapters 2 and 3 will use the local pairing, compact tensor count, and charged dimensions for separate purposes.

XV.1.7 Exercises

1. **Change a center and test compatibility.** On $\mathbb{F}_2$ move the first center onto $S \cap F_0$, leaving the second at $z = 2$ on F_0. Give both strict classes and their ordered intersection matrix. Separately, on the original base take $i = 4$. Give the bounds for P, Q and decide whether $P = 3 + 2w$, $Q = 3 + z^2 + 2z^4$ lift together. What changes if the constant of Q is 4? Explain why moving the center changes the class computation but the restriction question uses the original base.

2. **Even and odd residuals.** On the original chain set the first four restricted coefficients $(\beta_1, \beta_2, \beta_3, \beta_4) = (1, 3, 1, 2)$ on both curves. Take $P_6 = 3+3w-w^2+w^3$, $Q_6 = 3 + 2z^6$. Compute both residual factors R_1, R_2 without the prefactor in

(XV.1.48). For each factor, give its degree, the number of distinct roots, and the number of roots of multiplicity one over $\mathbb{C}$. Explain which parity term distinguishes the factors.

3. **Change the corner.** Take the first four restricted coefficients $(1, 2, 2, 3)$ on both curves and take $P_6 = 6 + w^3$, $Q_6 = 6 + z^6$. Give the constant and linear coefficients of $\mathcal{R} = \Delta/(z^4 w^5)$ at the corner in the compatible frame (XV.1.48), in the order $1, z, w$. Give the point order of Δ. Explain why the ordinary unit-residual argument cannot be repeated with these inputs.

4. **Redistribute exceptional areas.** Keep $A_1 = 2$, $A_2 = 3$ and assign one third of the excess fiber area to E_1 and two thirds to E_2. At $\rho = 12$ give $J \cdot (C_1, C_2, E_1, E_2)$ and $\mathrm{Vol}_E(B)$. Find the leading coefficient of ρ^2 at large ρ and the allowed range of ρ. Explain why a uniform rescaling of J does not do the same job.

5. **Separate weighted degree from matter.** On $\mathbb{F}_1$ take $(\beta_1, \beta_2, \beta_3, \beta_4, \beta_6) = (w, 2, 1, 0, 2w^{11})$ in the same affine extension. Give the degree of $\beta_1^4 P$, the number of simple P-roots, and the ordinary matter multiplicities on S, giving the anti-symmetric and fundamental separately. Then replace β_2 by $2w$. Compute the new point orders of f, g, Δ at the origin and state whether the ordinary separated argument applies there.

6. **What remains to be established?** A proposed local limit keeps the area of a compact gauge curve finite and sends the base volume to infinity. What further information would determine whether the retained tensor and gauge modes define an isolated theory? Which parts of the complete compact massless spectrum are missing from the calculations of this chapter?

Use `benchmark/tasks.json` for the JSON fields and `benchmark/PROTOCOL.md` for submission. Written explanations, including the last exercise, are assessed by a reader.

Status and sources

§1. The base and the canonical choice. The lattice and dualizing-line computations are [MATH]. The ordinary sectioned frame uses the sectioned and adiabatic hypotheses of XIV.1. For the ruled-surface intersection and compact base conventions see Kumar et al. (2010), arXiv:1008.1062v1, §5.1, eqs. (5.1)–(5.5). The point blowups and relative residue are computed here. A smooth global crepant resolution, including flatness of any proposed resolution, has not been established.

§2. The Tate construction. The residual bundles, lift, charts, normalization and split transverse type are [MATH]. The selected split order rows are from Katz, Morrison, et al. (2011), arXiv:1106.3854v1, Appendix A, eq. (A.1) and Table 2, PDF pp. 22–23. See also Morrison and Taylor (2012), arXiv:1106.3563v3, eqs. (3.58),(3.61). The orders are used as ansätze; the chapter constructs their global sections on the chosen bases. The Kodaira interpretation uses the Weierstrass convention $\Delta_{\mathrm{book}} = 4f^3 + 27g^2$ and the stated ordinary transverse hypotheses.

§3. Gauge and background fields. The ordinary split-fiber Lie algebra is [GEO-X]. Pointwise generation and full-system generic smoothness off the tuned curves are [MATH]. The noncompact seven-brane background interpretation is [GEO-E], conditional on the boundary conditions and divergent gauge kinetic norm. See Ohmori et al. (2014), arXiv:1408.5572v2, §3.3.1, eqs. (3.26)–(3.31), and Kumar et al. (2010), §§5.1–5.2, PDF pp. 20,23–25. The norm of a specific noncompact metric has not been computed.

§4. Chain matter. The residual, strict transform and analytic germs are [MATH]. The local hypermultiplets and absence of genus matter are [GEO-E], using the ordinary isolated A-type and smooth-curve rules. See Katz and Vafa (1997), arXiv:hep-th/9606086v1, §2 and eq. (2.1), §4.1 and eq. (4.1), and Morrison and Taylor (2012), PDF pp. 15–17 and 24–26, eqs. (2.26),(3.21)–(3.28). The representation branching does not independently establish the localized zero-mode rule.

§5. Multiplets and area scaling. The fixed-area path and selected dimensions are [MATH]. The compact and conditional local tensor readings are [GEO-E]; see Kumar et al. (2010), §§5.1–5.2, Ohmori et al. (2014), §3.3.1, and Heckman et al. (2015), arXiv:1502.05405v3, §§2.2–3, eqs. (2.13),(3.1),(3.2), for the wrapped string and base pairing. The leading unwarped reduction is [SUGRA]. The existence of an isolated interacting local limit remains a [DEC] premise beyond the scaling test.

§6. The single curve. The weighted residual, jets and two controls, selected dimensions, and $\mathbb{F}_1$ area path are [MATH]. The ordinary simple-open matter assignment is [GEO-E]. See Katz and Vafa (1997), §4.2(ii), and Morrison and Taylor (2012), eq. (3.28) and the following SU(5) discussion. The I_6 order on the transverse disk is computed here; the printed A5 discriminant order in that discussion is inconsistent with the calculation. The simple-root hypothesis is separate from the weighted class and no matter multiplicity is assigned at the tuned tangency.

References

Heckman, J. J. et al. (2015). "Atomic classification of 6D SCFTs". In: *Fortsch. Phys.* 63, pp. 468–530. arXiv: 1502.05405 [hep-th].

Katz, S., D. R. Morrison, et al. (2011). "Tate's algorithm and F-theory". In: *JHEP* 08, p. 094. arXiv: 1106.3854 [hep-th].

Katz, S. and C. Vafa (1997). "Matter from geometry". In: *Nucl. Phys. B* 497, pp. 146–154. arXiv: hep-th/9606086.

Kumar, V., D. R. Morrison, and W. Taylor (2010). "Global aspects of the space of 6D N=1 supergravities". In: *JHEP* 11, p. 118. arXiv: 1008.1062 [hep-th].

Morrison, D. R. and W. Taylor (2012). "Matter and singularities in F-theory models". In: *JHEP* 01, p. 022. arXiv: 1106.3563 [hep-th].

Ohmori, K. et al. (2014). "Anomaly polynomial of general 6D SCFTs". In: *PTEP* 2014, 103B07. arXiv: 1408.5572 [hep-th].

Chapter XV.2

Tensor branches, string charges and couplings

XV.2.1 The tensor scalars as areas

Can we change the coupling on one seven-brane curve without changing the coupling on its neighbor? We will answer by constructing a Kähler class whose evaluations on the two curves can be specified independently. The same evaluations give the tensions of strings that wrap the curves. The calculation starts with the base of Chapter 1. We use the quadratic brane actions of Volume III, Chapter 3, and the calibrated-area calculation of Volume IV, Chapter 6.

Let J be the Einstein-frame Kähler class of a compact base B and let $V = J^2/2$ be its volume. A period here means the integral of a two-form over a curve. We write a_i for the area period of a holomorphic curve C_i, and j for the normalized Kähler class:

$$a_i = \int_{C_i} J = J \cdot C_i, \qquad j = \frac{J}{\sqrt{2V}}, \qquad j^2 = 1, \qquad j \cdot C_i = \frac{a_i}{\sqrt{2V}}. \tag{XV.2.1}$$

In the compact two-derivative reduction it is the variations of j on the unit-norm slice that describe tensor multiplet scalars. The overall volume belongs to a hypermultiplet. We will work with the dimensionful periods a_i to keep track of tensions and kinetic coefficients. A change in a_i at fixed V can therefore be a tensor scalar variation; scaling the whole class at fixed j cannot.

Start with the ruled surface $\mathbb{F}_2$ and choose a fiber F_0 of the ruling. The class F of a generic fiber has square zero, because two distinct fibers do not meet. The negative section S has square -2 and meets each fiber once. Blow up two distinct smooth points of F_0 away from S. For example, if z is the affine fiber coordinate with $S = \{z = 0\}$, and w is the ruling coordinate with $F_0 = \{w = 0\}$, take $(z, w) = (1, 0), (2, 0)$. Write S, F also for their pullback classes. The exceptional curves E_i are disjoint, have square -1, and pair to zero with pullbacks. In the ordered basis (S, F, E_1, E_2), the intersection

matrix M and canonical class are

$$M = \begin{pmatrix} -2 & 1 & 0 & 0 \\ 1 & 0 & 0 & 0 \\ 0 & 0 & -1 & 0 \\ 0 & 0 & 0 & -1 \end{pmatrix}, \qquad K_B = -2S - 4F + E_1 + E_2. \tag{XV.2.2}$$

The canonical class downstairs follows from adjunction on S, F. At a blowup the canonical bundle acquires one exceptional divisor: in a chart $z - z_0 = \xi,\ w = \xi u$, the pullback of $dz \wedge dw$ is $\xi\, d\xi \wedge du$.

The strict transform of the chosen fiber is what remains after subtracting the two exceptional components of the total transform. The section does not pass through either blowup center. Thus

$$C_1 = S, \qquad C_2 = F - E_1 - E_2, \qquad C_1^2 = C_2^2 = -2, \qquad C_1 \cdot C_2 = 1. \tag{XV.2.3}$$

Figure XV.2.1 shows why the two blowups change the fiber square and leave the crossing with the section intact. Using (XV.2.2), $K_B \cdot C_1 = K_B \cdot C_2 = 0$. Hence $2g(C_i) - 2 = (K_B + C_i) \cdot C_i = -2$, in agreement with the strict transforms being smooth rational curves. If the second blowup were on another fiber, the chosen strict fiber would be $F - E_1$ and would have square -1. The number of blowups alone does not fix the pairing.

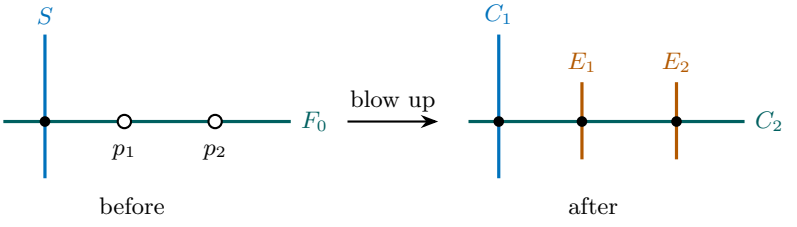


Figure XV.2.1: The chosen fiber before and after the two blowups. Both centers are away from the crossing with the section. On the right, the total fiber has three components. Its class is still F, while the horizontal component is the strict transform C_2.

To vary the two areas we must check the whole Kähler chamber of this parent, since a third curve can reach zero area first. On this base the cone of effective curve classes is generated by C_1, C_2, E_1, E_2. To see this, first consider a vertical irreducible curve, meaning one that maps to a point under the ruling. It lies in an ordinary fiber of class $F = C_2 + E_1 + E_2$ or is a component of the distinguished fiber. The section is itself one of the proposed generators. For any other irreducible horizontal curve, write the class of its image downstairs as $dS + bF$ and the multiplicities at the two centers as m_1, m_2. Intersecting with a generic fiber gives $d > 0$. Intersection with S gives $b - 2d \geq 0$; intersection with the distinct curve F_0 gives $m_1 + m_2 \leq d$, since a local intersection with the smooth fiber is at least the multiplicity at the point. The strict class is then

$$dS + bF - m_1E_1 - m_2E_2 = dC_1 + bC_2 + (b - m_1)E_1 + (b - m_2)E_2. \tag{XV.2.4}$$

Every coefficient on the right is nonnegative, and each generator is effective. This proves the cone assertion, including the exceptional directions.

Put $C = (C_1, C_2)$ for the matrix of the two class columns, using the same notation for their Poincaré duals. Let $\Omega = -C^T M C$; the sign makes the local string pairing positive. Two classes orthogonal to both C_i, and to each other, are

$$H = 2S + 4F - E_1 - E_2, \qquad H^2 = 6, \tag{XV.2.5}$$

$$W = E_1 - E_2, \qquad W^2 = -2. \tag{XV.2.6}$$

To prescribe $a = (a_1, a_2)^T$, solve for the curve-span component Cc of J. Since $C^T M(Cc) = -\Omega c = a$, the solution and the full class are

$$\Omega = \begin{pmatrix} 2 & -1 \\ -1 & 2 \end{pmatrix}, \qquad D = -C\Omega^{-1}, \qquad J = RH + Da + sW. \tag{XV.2.7}$$

Here D is a matrix of real class columns with $C^T M D = \mathbf{1}$. Its coefficients may be negative or fractional. The test for a Kähler class is its evaluation on curves, not positivity of its coefficients in a divisor basis.

For example, $C^T M E_1 = (0, 1)^T$, so $Da \cdot E_1 = -(\Omega^{-1}a)_2$; the same equation holds for E_2. In contrast, $W \cdot E_1 = -1$ and $W \cdot E_2 = +1$. With $v = (a_1 + 2a_2)/3$, the four evaluations and the volume are

$$(J \cdot C_1, J \cdot C_2, J \cdot E_1, J \cdot E_2) = (a_1, a_2, R - v - s, R - v + s), \tag{XV.2.8}$$

$$V = 3R^2 - \tfrac{1}{2} a^T \Omega^{-1} a - s^2. \tag{XV.2.9}$$

For these classes positivity on the four generating curves already implies $V > 0$. Indeed, $R > v + |s|$ in the interior, and

$$3(v + |s|)^2 - \tfrac{1}{2} a^T \Omega^{-1} a - s^2 = a_2(a_1 + a_2) + 6v|s| + 2s^2 > 0. \tag{XV.2.10}$$

The surface Kähler cone criterion, positivity of the square and of the curve evaluations in the Kähler component, now gives precisely this chamber. One can also locate the classes in that component by using the strict positive evaluations on the finitely generated curve cone.

At $a = (2, 5)^T$ and $R = 5$ in common area units, $v = 4$. Keeping the two selected periods fixed and changing s gives

s	$(a_1, a_2, J \cdot E_1, J \cdot E_2)$	V
0	$(2, 5, 1, 1)$	62
$\frac{1}{2}$	$(2, 5, \frac{1}{2}, \frac{3}{2})$	$\frac{247}{4}$
1	$(2, 5, 0, 2)$	61

(XV.2.11)

The last row is nef and lies on a wall. A test that kept only a_1, a_2, V would have missed it. On the symmetric slice $s = 0$ a second useful coordinate is the generic fiber period $r = J \cdot F = a_2 + 2(R - v) = 2R - (2a_1 + a_2)/3$. Expanding the class and replacing R in the volume yields

$$J = rS + (2r + a_1)F + \tfrac{a_2 - r}{2}(E_1 + E_2), \tag{XV.2.12}$$

$$V = r^2 + ra_1 - \tfrac{1}{4}(r - a_2)^2. \tag{XV.2.13}$$

In the first row of (XV.2.11), $r = 7$, and the two exceptional areas are each $(7-5)/2 = 1$.

For comparison take $\mathbb{F}_1$ and select its negative section S. The ruling has $S^2 = -1$, $S \cdot F = 1$, $F^2 = 0$ and $K_B = -2S - 3F$. Adjunction again gives $g(S) = 0$, now with $K_B \cdot S = -1$. A horizontal curve other than S has class $dS + bF$ with $d > 0$ and $b \geq d$ by intersection with S; the vertical generator is F. Thus the Kähler condition is positivity on S, F together with positive square. Writing the area on S as a_S, one obtains

$$J = L(S+F) - a_S S, \qquad (J \cdot S, J \cdot F) = (a_S, L - a_S), \qquad V = \tfrac{1}{2}(L^2 - a_S^2). \tag{XV.2.14}$$

Here $L > a_S > 0$ gives the chamber. The two terms in the class are orthogonal: $S \cdot (S + F) = 0$. This is the one-curve version of (XV.2.7) and makes it easy to increase L at fixed a_S.

The elliptic tuning labels the gauge sectors; the areas do not determine that tuning. Recall that the i-th Tate coefficient is a section of $-iK_B$, for $i = 1, 2, 3, 4, 6$. Write the exponents along C_1, C_2 as u_i, v_i. Removing those powers leaves the class

$$-iK_B - u_i C_1 - v_i C_2 = (2i - u_i)S + (4i - v_i)F - (i - v_i)(E_1 + E_2). \tag{XV.2.15}$$

For the split I_4, I_5 model, called CHAIN45, take $u = (0, 1, 2, 2, 4)$, $v = (0, 1, 2, 3, 5)$. Changing to $v = (0, 1, 3, 3, 6)$ gives split I_4, I_6 on the same base, CHAIN46. The changes are possible because the coefficient degrees also change. For instance the residual sixth coefficient on C_2 has degree $12 - 4 - 2(6 - 5) = 6$ in the first model and $12 - 4 - 2(6 - 6) = 8$ in the second. In the changed model the coefficient downstairs no longer has to vanish at either blowup point for this row. The section degree changes from $4(6) - 5 - 2(12 - 4) = 3$ to 2.

The mixed discriminant term tells us where this change enters. Near the crossing use local equations $z = 0$ for C_1 and $w = 0$ for C_2, and write the Tate sections as $A_i = z^{u_i} w^{v_i} \beta_i$ to distinguish them from the areas a_i. Define the Tate combinations

$$b_2 = A_1^2 + 4A_2, \quad b_4 = A_1 A_3 + 2A_4, \quad b_6 = A_3^2 + 4A_6, \tag{XV.2.16}$$

$$b_8 = \tfrac{1}{4}(b_2 b_6 - b_4^2) \tag{XV.2.17}$$

$$= A_1^2 A_6 - A_1 A_3 A_4 - A_4^2 + 4A_2 A_6 + A_2 A_3^2. \tag{XV.2.18}$$

The term $b_2^2 b_8/16$ in $4f^3 + 27g^2$ supplies the leading mixed order: the other terms $b_4^3, b_6^2, b_2 b_4 b_6$ have larger exponents of both z and w. The powers in the first three terms of b_8 are

	$A_1^2 A_6$	$-A_1 A_3 A_4$	$-A_4^2$
I_4, I_5	$(4, 5)$	$(4, 5)$	$(4, 6)$
I_4, I_6	$(4, 6)$	$(4, 6)$	$(4, 6)$

(XV.2.19)

The last two terms of b_8 have at least five powers of z and at least five or seven powers of w, respectively for the first and second tuning. Thus at a generic crossing the leading mixed term changes from $z^4 w^5$ to $z^4 w^6$. In the second tuning the A_4^2 term contributes at that order as well. The base pairing calculation has no input from any of these coefficients.

The allowed sections lift compatible restrictions from the two meeting curves; the details are recalled at the end of the chapter. With generic nonzero leading terms the

two distinct nodal tangents give the split fibers. The resulting gauge algebras in the ordinary local description are $\mathfrak{su}(4) \oplus \mathfrak{su}(5)$ and $\mathfrak{su}(4) \oplus \mathfrak{su}(6)$, respectively. On $\mathbb{F}_1$ the split I_5 exponents on S leave degree $i + v_i$, from $((2i - v_i)S + 3iF) \cdot S$. The same split-fiber interpretation gives the single $\mathfrak{su}(5)$ sector of SU5-F1. Chapter 1 develops the tuning and ordinary matter dictionary. For the wrapped-string calculation here, what matters is that (XV.2.3) and (XV.2.8) apply to either tuning of the two-curve base. Changing a Kähler period within one tuning changes no Tate exponent.

XV.2.2 Wrapped D3 strings

What remains of the D3 worldvolume after it wraps a base curve? A D3 along $\Sigma_2 \times C$, where C is a compact holomorphic curve and Σ_2 a timelike sheet in six-dimensional spacetime, has two external dimensions left. An observer in six dimensions measures the energy per unit length on Σ_2. The Dirac–Born–Infeld action measures a four-volume. In an unwarped reference, with fixed embedding and no internal-external metric mixing, the worldvolume determinant factors into the determinants on Σ_2 and C. Figure XV.2.2 distinguishes this base curve from the elliptic fiber.

Write $g_s^{\text{met}} = e^{\Phi/2} g_E$ for the string-frame metric, Φ for the unshifted dilaton, and $\lambda = 2\pi\alpha'$ with $[\alpha'] = \text{length}^2$. Here $P[B]$ pulls back the NS two-form. Use a D3 reference with

$$\mathcal{F}_{\text{bg}} = P[B] + \lambda F_{\text{bg}} = 0, \qquad \mu_3 = \frac{1}{(2\pi)^3 \alpha'^2} \equiv \frac{1}{k_3}. \tag{XV.2.20}$$

The zero refers to the combination that enters the determinant. Setting the field strength alone to zero is insufficient if the pulled-back two-form is nonzero. For example a nonzero magnetic component $f\, e^1 \wedge e^2$ of $\mathcal{F}_{\text{bg}}$ in a string-frame orthonormal coframe on C multiplies the internal area density by $\sqrt{1 + f^2}$.

Under the frame change the D3 volume element acquires $e^{4\Phi/4} = e^{\Phi}$, which cancels the DBI dilaton factor at this reference background. In a holomorphic orientation the Kähler form restricts to the area form: for a unit tangent u on C, $J(u, Iu) = 1$ with I the complex structure. Integrating gives

$$\begin{aligned} S_{\text{DBI}} &= -\mu_3 \int_{\Sigma_2 \times C} e^{-\Phi} \sqrt{-\det P[g_s^{\text{met}}]}\, d^4\xi \\ &= -\mu_3 \int_{\Sigma_2} \sqrt{-\det P[g_E]_{\Sigma_2}}\, d^2\sigma \int_C J, \end{aligned} \tag{XV.2.21}$$

$$t_i = \frac{a_i}{k_3}, \qquad T(q) = \frac{q^T a}{k_3} = q^T t. \tag{XV.2.22}$$

Here q is the integer column of wrapping numbers in the chosen basis. For an effective calibrated sum of curves the area contributions add, including when the configuration is reducible. The calibration identifies the area of the holomorphic configuration with the closed-form period; it does not furnish a connected stable string for every effective class. In particular, one cannot take a signed lattice column, contract it with a, and conclude that a BPS string with that tension exists.

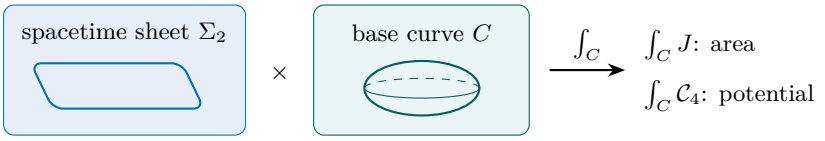


Figure XV.2.2: A D3 on the product of a spacetime sheet and a curve in the base. The area integral on C leaves a tension on Σ_2; integrating the two internal legs of the RR four-form leaves a two-form coupling on the same sheet.

Take $q = (2,1)^T$, realized in the area calculation by two copies of C_1 and one of C_2. The periods in (XV.2.11) give area 9 in the chosen units. Exchanging the periods while keeping the same curves and charge gives

$$q^T(2,5)^T = 9, \qquad q^T(5,2)^T = 12. \tag{XV.2.23}$$

The second point remains inside the Kähler cone at $R = 5, s = 0$: $v = 3$ and both exceptional areas are 2. Here the tension changes because the heavier wrapping number multiplies the larger area. Exchanging two coordinate labels would instead transform q as well and leave the tension invariant. A tension has dimension mass^2, since a_i is an area and k_3 is a length to the fourth power. The inverse squared six-dimensional gauge coupling has the same dimension. Its coefficient must be derived separately.

A string also has an electric coupling to a spacetime two-form. With the D3 orientation chosen above, the part of the Wess–Zumino action that contains the RR four-form is $+\mu_3 \int_{\Sigma_2 \times C} P[C_4]$. Define $\mathcal{C}_4 = \mu_3 C_4/(2\pi)$, and let $\mathcal{B}^i = \int_{C_i} \mathcal{C}_4$ be the spacetime two-forms obtained from its two-internal-leg part. The orientation used to integrate on C_i is the same one used in its period. Then

$$S_{\rm el} = 2\pi \int_{\Sigma_2} \int_{\sum_i q_i C_i} \mathcal{C}_4 = 2\pi \int_{\Sigma_2} q^T \mathcal{B}. \tag{XV.2.24}$$

In a reduction that retains these two-form modes the formula describes their electric sources. More generally it computes the period of the potential against the curve source, without proving that every such potential has a dynamical mode in a noncompact limit. Reversing the wrapped orientation reverses this coupling. The area contribution of the reverse orientation is positive and is not computed by treating a negative period as a calibrated holomorphic area.

The distinction between a period and a charge can already be seen in the worldsheet coupling. At the same point in spacetime, compare two configurations with $q = (2,1)^T$ and $q = (1,2)^T$. Their area difference is $a_1 - a_2$. If the two periods are equal, their leading tensions agree. Yet the difference in the electric coupling is

$$S_{\rm el}(2,1) - S_{\rm el}(1,2) = 2\pi \int_{\Sigma_2} (\mathcal{B}^1 - \mathcal{B}^2). \tag{XV.2.25}$$

Equality of the two tensions is a statement about the chosen Kähler class; the two strings still represent different wrapped charges. A common variation of the periods would keep their tensions equal, while a variation in the relative period separates them.

On the selected span, write D^i for the columns of $D = -C\Omega^{-1}$, so $\int_{C_j} D^i = \delta^i_j$. The same class can be expanded in these unit-period forms or the Poincaré duals of the C_i, with coefficients $\mathcal{B}_{\mathrm{PD}}$ in the latter basis:

$$\mathcal{C}_4 \;\sim\; \sum_i \mathcal{B}^i \wedge D^i = \sum_i \mathcal{B}^i_{\mathrm{PD}} \wedge \mathrm{PD}(C_i), \tag{XV.2.26}$$

$$\mathcal{B} = -\Omega\, \mathcal{B}_{\mathrm{PD}}. \tag{XV.2.27}$$

Indeed, integrating the second expansion over C_j inserts the intersection $C_i \cdot C_j = -\Omega_{ij}$. This minus sign is a consequence of the geometric evaluation; it is not a choice of six-dimensional tensor chirality. In a compact parent the expansions refer to the selected part of the two-form data, not the entire compact mode space. The calculation gives two uses of a charge column: pairing with an area for a tension, and pairing with a potential for an electric coupling. To compare two string charges we now need a pairing on the charge lattice itself.

XV.2.3 The integral charge pairing

How can the components of a string charge change while its physical pairings remain the same? The integral lattice Λ considered here is generated by the two compact curve classes. In the six-dimensional tensor-string dictionary its positive pairing on these negative curves is minus their intersection. For example, for $q = (2,1)^T$ and $r = (1,-1)^T$ we have

$$\langle q, r\rangle = q^T \Omega r = (2,1) \begin{pmatrix} 2 & -1 \\ -1 & 2 \end{pmatrix} \begin{pmatrix} 1 \\ -1 \end{pmatrix} = 3. \tag{XV.2.28}$$

The signed vector r is an integral lattice test. In the effective cone generated by C_1, C_2 it is not a holomorphic wrap. This calculation uses the selected local sublattice; the compact parent has other curve classes and an intersection form of mixed signature.

To make an internal two-form with specified periods on C_1, C_2, first restrict to their real span. If $D^1 = xC_1 + yC_2$ is the class with period 1 on C_1 and 0 on C_2, then

$$-2x + y = 1, \qquad x - 2y = 0 \quad \Longrightarrow \quad D^1 = -\frac{2C_1 + C_2}{3}. \tag{XV.2.29}$$

Interchanging the two columns gives $D^2 = -(C_1 + 2C_2)/3$, so the matrix of solutions is the D of (XV.2.7). These classes are unique within the selected real span because $\det \Omega = 3$. In the compact parent one can add a class in the orthogonal complement without changing either period. This real period dual is not required to be a globally integral divisor. For instance D^1 has nonintegral coordinates even in the parent basis. The integral class F has period vector $(1,0)^T$ but has components outside the selected span.

Now change the integral generators to $C' = CU$ with U unimodular. Solving $Cq = C'q'$ gives the new charge components. Evaluating J on C' gives the new periods,

and evaluating intersections on both columns gives the new matrix:

$$q' = U^{-1}q, \qquad a' = U^T a, \qquad \Omega' = U^T \Omega U, \tag{XV.2.30}$$

$$D' = -CU(U^T\Omega U)^{-1} = DU^{-T}, \qquad \mathcal{B}' = U^T\mathcal{B}. \tag{XV.2.31}$$

The opposite transformations of q and a cancel in the area contraction. They also cancel in the electric coupling, while the two factors of U in Ω' cancel the transformations of both charges:

$$q'^T a' = q^T a, \qquad q'^T\mathcal{B}' = q^T\mathcal{B}, \qquad q'^T\Omega' r' = q^T\Omega r. \tag{XV.2.32}$$

Thus if a is held fixed and only q is relabeled, the resulting contraction does not in general represent the same geometry.

Take the shear $C_1' = C_1,\ C_2' = C_1 + C_2$. On the example q, r, a of (XV.2.23) and (XV.2.28), it gives

$$U = \begin{pmatrix} 1 & 1 \\ 0 & 1 \end{pmatrix}, \quad q' = \begin{pmatrix} 1 \\ 1 \end{pmatrix}, \quad r' = \begin{pmatrix} 2 \\ -1 \end{pmatrix}, \quad a' = \begin{pmatrix} 2 \\ 7 \end{pmatrix}, \quad \Omega' = \begin{pmatrix} 2 & 1 \\ 1 & 2 \end{pmatrix}. \tag{XV.2.33}$$

The contraction for the area is $2 + 7 = 9$. Also $\Omega' r' = (3, 0)^T$, so the pairing remains 3. The sign of the off-diagonal matrix entry changes. Its meaning is now the pairing of C_1 with $C_1 + C_2$, not the pairing of the two irreducible curves.

The selected effective cone has to be carried through the shear as well. If $q' = (x, y)^T$, then $q = Uq' = (x + y, y)^T$. In the new coordinates the cone and its positive area condition are

$$y \geq 0, \quad x + y \geq 0; \qquad a_1' > 0, \quad a_2' - a_1' > 0. \tag{XV.2.34}$$

Figure XV.2.3 shows both descriptions of the charge cone. The original curve C_2 has $q' = (-1, 1)^T$; its area at the displayed point is $-2 + 7 = 5$. Conversely, $(a_1', a_2') = (3, 2)$ has positive entries but evaluates negatively on C_2. The full parent cone still includes the two exceptional conditions. Neither the new coordinate quadrant nor the sign pattern of Ω' replaces the geometric cone.

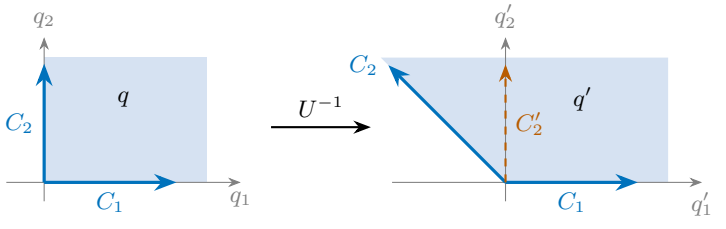


Figure XV.2.3: The selected effective cone in the two charge coordinate systems. The right-hand slanted ray has coordinates $(-1, 1)$ and is still C_2. The dashed ray is $C_2' = C_1 + C_2$, which lies inside the cone.

The shear also gives a quick way to check the real period forms directly. The inverse transpose in (XV.2.31) gives

$$D'^1 = D^1 - D^2, \qquad D'^2 = D^2, \qquad (C_1' \cdot D'^1, C_2' \cdot D'^1) = (1, 1-1) = (1, 0). \tag{XV.2.35}$$

Thus the first new unit period is achieved by increasing the old period on C_1 while decreasing the one on C_2 by the same amount. For example, a small change $\delta a' = (\delta, 0)^T$ around the displayed point gives $\delta a = (\delta, -\delta)^T$. It changes the two original tensions in opposite directions, and the tension of $C_2' = C_1 + C_2$ stays fixed. The D'^1 class was obtained by evaluating against both curves, not by dividing the class C_1' by its own self-intersection. Using $-C_1'/2$ would also give period 1 on C_1', but it gives period $1/2$ on C_2'.

The abstract positive-pairing dual lattice is a third object. Its elements pair integrally with every integral charge:

$$\Lambda^* = \{x \in \mathbb{Q}^2 : \Omega x \in \mathbb{Z}^2\} = \Omega^{-1}\mathbb{Z}^2, \qquad \Omega^{-1} = \frac{1}{3}\begin{pmatrix} 2 & 1 \\ 1 & 2 \end{pmatrix}. \tag{XV.2.36}$$

Here the first dual generator $x = (2,1)^T/3$ has pairing $+1$ with the first charge and 0 with the second. The geometric form giving the same evaluation by intersection is $-Cx$, because the geometric form uses M instead of the positive pairing. Twice x differs from the second abstract dual generator by $(1,0)^T$, and $3x = (2,1)^T$ is integral. Thus x generates a quotient of order three. In Smith reduction, swapping the columns of Ω, then negating the first row, gives $\left(\begin{smallmatrix} 1 & -2 \\ 2 & -1 \end{smallmatrix}\right)$. Subtract twice the first row from the second and add twice the first column to the second. The result is $\mathrm{diag}(1,3)$. Equivalently,

$$\Lambda^*/\Lambda \simeq \mathbb{Z}^2/\Omega\mathbb{Z}^2 \simeq \mathbb{Z}/3\mathbb{Z}. \tag{XV.2.37}$$

For the $\mathbb{F}_1$ section, the one-curve pairing is (1), the geometric period dual is $-S$, and the abstract dual lattice has trivial quotient by the original lattice. The change from order three to one is controlled by the base intersections. It does not determine a gauge-group global form or supply fractional elementary strings. We can already see this separation on the two-curve base: the changed I_4, I_6 model keeps the same quotient, while changing the second gauge algebra. Next we compute how the gauge sector depends on the periods that appeared in the string tension.

XV.2.4 Gauge couplings along the branch

Why does a six-dimensional gauge instanton carry the charge of a wrapped D3? A seven-brane on C_i fills all of six-dimensional spacetime. A gauge field concentrated in four of its spatial directions can leave a string along the other spatial direction. We will compare this configuration with the wrapped D3 in two independent ways: its energy per unit length, and its source for the RR four-form. Both comparisons require fixing the gauge trace before reducing the action.

Work at quadratic order in the weak D7 reference description with a product metric, no warping, and constant internal gauge zero mode. On the D7 reference background require $P[B] + \lambda F_{\mathrm{bg}} = 0$ on the worldvolume, just as for the D3 on its own reference. We take the no-internal-flux reference for the RR increment below. Let F in the determinant now denote the fluctuating field strength in the six external directions. For the matrix $A = \lambda(g_s^{\mathrm{met}})^{-1}F$ on worldvolume tangent indices, antisymmetry gives

$\mathrm{tr}_{\mathrm{wv}}\, A = 0$, and raising indices with g_s^{met} gives $\mathrm{tr}_{\mathrm{wv}}\, A^2 = -\lambda^2 F_{ab} F_s^{ab}$. Expanding the logarithm gives

$$\tfrac{1}{2}\,\mathrm{tr}_{\mathrm{wv}} \log(1+A) = -\tfrac{1}{4}\,\mathrm{tr}_{\mathrm{wv}}\, A^2 + \cdots , \tag{XV.2.38}$$

$$\sqrt{\det(1+A)} = 1 + \tfrac{\lambda^2}{4} F_{ab} F_s^{ab} + \cdots . \tag{XV.2.39}$$

Here the determinant expansion is for one abelian component. At order F^2 on a stack it gives the fundamental trace tr_f on the two gauge factors. This use of the quadratic term does not require an all-order nonabelian determinant. If the DBI background combination were nonzero, the expansion would be around $P[g_s^{\mathrm{met}}] + \mathcal{F}_{\mathrm{bg}}$; already for an internal magnetic component the magnetic area prefactor discussed after (XV.2.20) would survive.

In string frame the quadratic action is

$$S_7^{(2)} = -\frac{\mu_7 \lambda^2}{4} \int d^8\xi\, e^{-\Phi} \sqrt{-g_s^{\mathrm{met}}}\; \mathrm{tr}_f(F_{ab} F_s^{ab}), \qquad \mu_7 = (2\pi)^{-7} \alpha'^{-4}. \tag{XV.2.40}$$

The eight-volume contributes $e^{2\Phi}$ and the two inverse metrics in F^2 contribute $e^{-\Phi}$. Together with the DBI dilaton they give $e^{-\Phi} e^{2\Phi} e^{-\Phi} = 1$. This is a cancellation in the gauge term; the eight-dimensional volume term alone has a different Weyl weight. Match the resulting action to $-\,\mathrm{tr}_f\, F^2/(2g_{8,E}^2)$, with Hermitian generators $\mathrm{tr}_f(T_a T_b) = \delta_{ab}/2$:

$$\frac{1}{2g_{8,E}^2} = \frac{\mu_7 \lambda^2}{4}, \qquad k_8 \equiv g_{8,E}^2 = 2(2\pi)^5 \alpha'^2. \tag{XV.2.41}$$

For a single normalized $SU(N)$ generator the component action is $-F^a_{\mu\nu} F^{a\,\mu\nu}/(4g^2)$. The trace in the stack action is part of this matching.

For comparison, take $F = f P_1$ with $P_1 = \mathrm{diag}(1, 0, \ldots, 0)$. A particle of unit charge on that entry couples to f's gauge potential without a generator rescaling. Alternatively take $F = f\mathbf{1}_N$, so the same component field acts with unit charge on all entries. In the component action $-f^2/(4g^2)$ these give

generator of f	$\mathrm{tr}_f(F_{ab}F^{ab})$	$g_{8,E}^2$ for f
P_1	$f_{ab} f^{ab}$	$k_8/2$
$\mathbf{1}_N$	$N f_{ab} f^{ab}$	$k_8/(2N)$

(XV.2.42)

A single D7 uses the first line. The two lines agree only for $N = 1$. For example, on the second curve of CHAIN45 the full identity coefficient is $k_8/10$; changing the tuning to CHAIN46 changes it to $k_8/12$. These are comparisons of local trace normalizations, not statements about a massless diagonal $U(1)$ in either compactification.

Integrating the constant $SU(N)$ mode over C_i multiplies the eight-dimensional kinetic coefficient by a_i. Combining (XV.2.41) and (XV.2.22) gives

$$\phi_i \equiv g_{6,i}^{-2} = \frac{a_i}{k_8}, \qquad t_i = \frac{k_8}{k_3}\phi_i = 8\pi^2 \phi_i. \tag{XV.2.43}$$

The coupling itself grows as the period decreases. If one used the unit-charge single-entry coupling in this ratio, one would obtain $4\pi^2$, the ratio to a different inverse squared

coupling. Also, if the calculation is performed at constant $g_s = e^{\Phi}$ in string frame, the inverse coefficients contain $e^{-\Phi}$ and the area must be measured in the same frame. The comparison here uses Einstein-frame areas and keeps the microscopic α' fixed.

Use the first row of (XV.2.11) as a reference and now increase a_1 from 2 to 3 while holding $a_2 = 5, R = 5, s = 0$. This is allowed since the exceptional areas change from 1 to 2/3, both still positive. The change multiplies ϕ_1 and t_1 by 3/2 and leaves ϕ_2, t_2 fixed. Table XV.2.1 records the common area dependence; the inverse coupling and tension columns use different units.

Table XV.2.1: Changing one area on the two-curve branch. An area unit ℓ^2 is used for all entries, so $k_8\phi_i/\ell^2$ and $k_3 t_i/\ell^2$ report the same numbers.

a/ℓ^2	i	$k_8\phi_i/\ell^2$	$k_3 t_i/\ell^2$
$(2,5)$	1	2	2
$(2,5)$	2	5	5
$(3,5)$	1	3	3
$(3,5)$	2	5	5

To see the same coefficient from a gauge configuration, choose four oriented Euclidean directions transverse to a static string. Assume the scalar ϕ_i is constant and consider a smooth finite-action $SU(N)$ field in the ordinary instanton sector there. We use the Hermitian F convention with a positive instanton self-dual. In exterior-form notation the energy per unit length and the topological charge are

$$\mathcal{E} = \phi_i \int_{\mathbb{R}^4} \mathrm{tr}_f\, F \wedge *_4 F, \qquad k = \frac{1}{8\pi^2} \int_{\mathbb{R}^4} \mathrm{tr}_f\, F \wedge F. \tag{XV.2.44}$$

The factor from $\int F \wedge *_4 F = \frac{1}{2}\int F_{mn}F^{mn} d^4x$ agrees with the action above. With $\epsilon = \mathrm{sgn}(k)$ for $k \neq 0$, expand the squared norm of $F - \epsilon *_4 F$:

$$\mathcal{E} = \frac{\phi_i}{2} \int \mathrm{tr}_f (F - \epsilon *_4 F) \wedge *_4 (F - \epsilon *_4 F) + 8\pi^2 \phi_i |k|. \tag{XV.2.45}$$

The cross terms reconstruct the instanton density because $*_4^2 = 1$ on two-forms. The first term is nonnegative and vanishes for $F = \epsilon *_4 F$. For $k = 0$ the energy is nonnegative directly from (XV.2.44). At positive $k = 1$ on C_2 at $a = (3,5)$, the saturated energy is $5\ell^2/k_3$. At $k = -2$ on C_1 it is $6\ell^2/k_3$; the sign of k will appear in the RR charge, not the energy.

Figure XV.2.4 gives the integration order for the charge calculation. The field strength has both its legs in the transverse four-plane, so $F \wedge F$ saturates the plane. The surviving component of C_4 has its four legs on $\Sigma_2 \times C_i$, exactly the worldvolume used in (XV.2.24). This identifies the tensor source with the same base curve whose area occurs in ϕ_i.

For the charge, retain the term in the D7 Wess–Zumino action with two powers of F. At fixed background and fixed curvature contributions, and with the D3 and D7

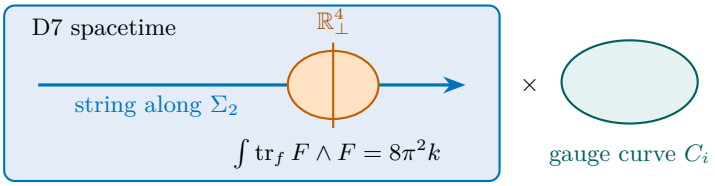


Figure XV.2.4: The six-dimensional spacetime of the D7, times the gauge curve C_i. Integrating the instanton density in the oriented four-plane transverse to Σ_2 leaves the coupling on $\Sigma_2 \times C_i$.

RR orientations aligned as above, it gives the increment

$$\delta S_{\mathrm{WZ}} = \mu_7 \frac{\lambda^2}{2!} \int_{\Sigma_2 \times C_i} C_4 \int_{\mathbb{R}^4} \mathrm{tr}_f\, F \wedge F,$$
$$\mu_7 \frac{\lambda^2}{2!} (8\pi^2 k) = k(2\pi)^4 \alpha'^2 \mu_7 = k\mu_3. \tag{XV.2.46}$$

The 1/2! comes from the second power of the WZ exponential. Dropping it doubles the electric charge even though the Yang–Mills calculation of the energy would be unchanged. For the $k = -2$ example the source is $-2\mu_3$ on C_1. The calculation compares the leading fixed-scalar soliton and wrapped-string couplings. It does not identify all quantum strings with smooth Yang–Mills instantons or extend the weak action to a zero-area endpoint.

The energy and charge checks respond differently to a change in period. For the instanton on C_1, increasing a_1 from $2\ell^2$ to $3\ell^2$ at fixed $k = -2$ changes the saturated energy by $2\ell^2/k_3$ and changes the RR source by zero. At fixed area, reversing the sign of k reverses the RR increment and leaves the saturated energy fixed:

$$\mathcal{E}_{\mathrm{sat}}(-k) = \mathcal{E}_{\mathrm{sat}}(k), \qquad \delta S_{\mathrm{WZ}}(-k) = -\delta S_{\mathrm{WZ}}(k). \tag{XV.2.47}$$

Both statements assume the constant-scalar leading action. The distinction is useful when the brane area is a field: it appears directly in the gauge kinetic term, whereas the coefficient multiplying the topological source is fixed by the charge units.

The same base divisor also enters a tensor Bianchi identity in the anomaly calculation. For clarity, switch to the anomaly convention here only. Write $F_O = -iF_{\mathrm{phys}}/(2\pi)$ for the source curvature in terms of the Hermitian field, $\mathrm{Tr}_O = 2\,\mathrm{tr}_f$ on the gauge factor, and X for the four-form column dH in the compact-curve Poincaré dual basis. In this convention the ten-dimensional five-form is taken anti-self-dual and the selected six-dimensional three-forms self-dual. The gauge-only ten-dimensional source has internal two-form $\mathrm{PD}(C_i)$ for the contribution of the i-th gauge factor. Integrating its wedge product with $\mathrm{PD}(C_j)$ inserts $-\Omega_{ji}$. The Bianchi projection includes a minus sign on that integral, giving

$$Y_j = (\Omega X)_j = \frac{1}{4} \sum_i \Omega_{ji}\, \mathrm{Tr}_O\, F_{O,i}^2, \qquad X_i = \frac{1}{4}\, \mathrm{Tr}_O\, F_{O,i}^2. \tag{XV.2.48}$$

The geometric periods would instead be $-\Omega X$, as in (XV.2.27). The PD coefficients and negatively signed projections give $I_{\rm GS} = X^T\Omega X/2 = Y^T\Omega^{-1}Y/2$, with wedge products understood. This gauge piece includes only the two selected curves; Chapter 3 uses the full four-forms. The projection does not set the Hermitian instanton sign in (XV.2.46). To decide which fields propagate, we need an internal kinetic norm.

XV.2.5 Dynamical tensors and background parameters

When does a period describe a field that can fluctuate in six dimensions? The period on a compact curve measures a two-form only on that curve. In a kinetic term one integrates the squared norm of the form over the entire internal space. We first calculate this norm on the compact parent, where the harmonic representatives exist. Then we compare it with a noncompact example in which the period stays finite and the kinetic norm diverges.

Let ω_x be the harmonic $(1,1)$ representative of a real class x on the compact Kähler surface, and use its complex orientation. The normalized Kähler form j is self-dual. In an oriented orthonormal coframe its unnormalized direction is $e^1\wedge e^2 + e^3\wedge e^4$; the star exchanges the two summands. The primitive $(1,1)$ subspace, defined pointwise by wedging to zero with j, is anti-self-dual. For example $e^1\wedge e^2 - e^3\wedge e^4$ is one primitive direction. The off-diagonal real $(1,1)$ directions have the same star eigenvalue. On a compact Kähler surface contraction with the Kähler form commutes with the Laplacian, so the contraction of ω_x is a harmonic function and is constant. The decomposition into the Kähler direction and the primitive part is therefore

$$\omega_x = (j^T M x) j + \omega_{x,\rm prim}, \tag{XV.2.49}$$

$$*\omega_x = (j^T M x) j - \omega_{x,\rm prim}. \tag{XV.2.50}$$

In this notation $j^T M x = \int_B j\wedge\omega_x$, with the denominator equal to one because $j^2 = 1$. Integrating the star against a second form gives

$$\int_B \omega_y \wedge *\omega_x = 2(y^T M j)(j^T M x) - y^T M x, \qquad G = 2(Mj)(Mj)^T - M. \tag{XV.2.51}$$

The positive G is a norm on form classes. On primitive classes the intersection is negative, and the star turns it into a positive norm. Along j, G assigns unit squared norm. Thus even in the compact theory the intersection matrix and the Hodge norm serve different purposes.

There is a further distinction between the norm of a form and the norm of a variation of the tensor scalars. Differentiating $j^T M j = 1$ gives $j^T M\, dj = 0$. At fixed V, $dj = dJ/\sqrt{2V}$ and $J\cdot dJ = 0$, so the variation of J is primitive. In the two-curve coordinates at $s=0$ with $ds = 0$, the derivative of (XV.2.9) gives

$$0 = 6R\, dR - a^T\Omega^{-1} da, \tag{XV.2.52}$$

$$dJ = H\,\frac{a^T\Omega^{-1}da}{6R} + D\, da. \tag{XV.2.53}$$

Varying the areas within this slice generally requires changing R. Since $H^2 = 6$, $H \cdot D^i = 0$, and $D^T M D = -\Omega^{-1}$, the fixed-volume squared norm is

$$\|dJ\|^2_{\text{fixed V}} = -dJ^T M\, dJ = da^T \Omega^{-1} da - 6(dR)^2, \tag{XV.2.54}$$

$$K_{\text{fixed V}} = \Omega^{-1} - \frac{(\Omega^{-1}a)(\Omega^{-1}a)^T}{6R^2}. \tag{XV.2.55}$$

The subtraction comes from the positive square of the compensating H component. It leaves a positive norm because the tangent is orthogonal to the positive Kähler direction.

What if we evaluate just the harmonic form $D\,da$ at the same point? Holding R, s fixed produces that form, but it generally changes V. Indeed $J \cdot (D\,da) = -a^T \Omega^{-1} da$. The norm now has a contribution from the component along j:

$$K_{\text{form, fixed R}} = D^T G D = \Omega^{-1} + \frac{(\Omega^{-1}a)(\Omega^{-1}a)^T}{V}. \tag{XV.2.56}$$

The positive correction belongs to the form norm. Substituting it for (XV.2.55) would describe a variation that has left the fixed-volume slice. The two formulas agree for a period tangent orthogonal to $\Omega^{-1}a$.

At $a = (2,5)^T,\ R = 5,\ s = 0$, $V = 62$ and $\Omega^{-1}a = (3,4)^T$. For $da = (1,0)^T$ in the same area units, the compact scalar variation has $dR = 1/10$. The two norms give

$$\|dJ\|^2_{\text{fixed V}} = \frac{2}{3} - \frac{9}{150} = \frac{91}{150}, \qquad \|D\,da\|^2 = \frac{2}{3} + \frac{9}{62} = \frac{151}{186}. \tag{XV.2.57}$$

At fixed R the volume derivative would instead be -3 in the corresponding volume units. On $\mathbb{F}_1$, varying the section period a_S of (XV.2.14) at fixed V similarly requires $dL = (a_S/L)\, da_S$, since $dV = L\, dL - a_S\, da_S$. The primitive norm is $(1 - a_S^2/L^2)(da_S)^2$. The one-curve subtraction is the same compensation, now for the positive class $S + F$.

We can realize the first variation as a curve through the Kähler cone, rather than only as a formal differential. Write $a = (2 + h, 5)^T$, keeping $s = 0$. Its quadratic area term in (XV.2.9) is $13 + 3h + h^2/3$. To stay at $V = 62$ take the positive solution

$$R(h) = \sqrt{25 + h + \tfrac{1}{9}h^2}, \qquad R'(0) = \tfrac{1}{10}. \tag{XV.2.58}$$

For sufficiently small h all four periods remain positive by continuity. Along the fixed-R path the volume is $62 - 3h - h^2/3$ instead. Figure XV.2.5 compares their tangent directions. This distinction disappears for some nonzero period tangents even at finite R. For example $da = (4,-3)^T$ is orthogonal to $(3,4)^T = \Omega^{-1}a$. In that direction $dR = 0$ at fixed volume and both formulas give $da^T \Omega^{-1} da = 26/3$. A fixed-$R$ path in this direction can still leave the volume slice at second order.

The dimensionful kinetic coefficient follows from the compact Einstein reference. Let $\kappa_{10}^2 = (2\pi)^7 \alpha'^4/2$ in the unshifted Einstein convention. Reducing the Einstein term with no warping gives $M_6^4 = V/\kappa_{10}^2$. In the compact two-derivative scalar term, restore

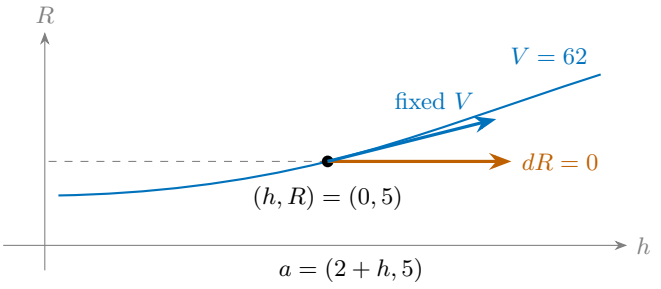


Figure XV.2.5: Schematic paths in the (h, R) slice, with the second period fixed. At the marked point the fixed-volume path has $dR/dh = 1/10$, whereas the horizontal path has $dR/dh = 0$. The slopes are exaggerated for readability.

M_6^4 in front of the dimensionless j kinetic coefficient:

$$S_{\text{scal}} = -\frac{M_6^4}{2} \int G_{\alpha\beta}\, dj^\alpha \wedge *_6 dj^\beta, \tag{XV.2.59}$$

$$S_{\text{scal}}\big|_{\text{fixed V}} = -\frac{1}{2} \int \frac{G_{\alpha\beta}}{2\kappa_{10}^2}\, dJ^\alpha \wedge *_6 dJ^\beta. \tag{XV.2.60}$$

Here d acts on the spacetime dependence of the class coordinates. The forms in (XV.2.50) instead live on the internal surface. This is the scalar kinetic term; the six-dimensional chiral two-forms require their separate duality condition. In particular the term does not supply a covariant action for unconstrained two-form fields.

At fixed a, with $s = 0$ and $R \to \infty$, the corrections in (XV.2.55) and (XV.2.56) vanish. The limiting norm for the compact tangent uses Ω^{-1}. To see the two independent directions, compare a common period shift $(1, 1)$ with a relative shift $(1, -1)$. Their squared norms from Ω^{-1} are 2 and $2/3$; replacing Ω^{-1} by Ω would leave the first unchanged but give 6 for the second. Restoring the prefactor and changing variables from a to t or ϕ gives the limiting compact reference coefficients

$$K^{\text{kin}}_{a,\infty} = \frac{\Omega^{-1}}{2\kappa_{10}^2}, \qquad K^{\text{kin}}_{t,\infty} = \frac{k_3^2\Omega^{-1}}{2\kappa_{10}^2} = \frac{\Omega^{-1}}{2\pi}, \tag{XV.2.61}$$

$$K^{\text{kin}}_{\phi,\infty} = \frac{k_8^2\Omega^{-1}}{2\kappa_{10}^2} = 4(2\pi)^3\Omega^{-1}. \tag{XV.2.62}$$

The coefficients multiply a term written with an overall $-1/2$. The fields t and ϕ carry mass dimension two, as six-dimensional scalars with this kinetic normalization should, but their kinetic matrices are not the identity.

To see how the two kinetic matrices approach the same value, keep $a = (2, 5)^T$ and move R from five to ten. The linear function $a^T\Omega^{-1}da$ evaluates to 7 on the common tangent and -1 on the relative tangent. Thus

da	$\|dJ\|^2_{\text{fixed V}}$	$\|D\,da\|^2_{\text{fixed R}}$
$(1, 1)^T$	$2 - 49/(6R^2)$	$2 + 49/V$
$(1, -1)^T$	$2/3 - 1/(6R^2)$	$2/3 + 1/V$

(XV.2.63)

Quadrupling R^2 reduces either tangent correction by four, while the form correction follows the full volume $3R^2 - 13$. The physical scalar kinetic comparison at each point uses the middle column. The final column asks a question about the same internal forms at that point, without compensating the area variation.

The limit of this compact matrix does not identify the local spectrum. The compact class $W = E_1 - E_2$ has zero period on both selected curves. On the symmetric slice it is orthogonal to J, and hence has squared compact norm $-W^2 = 2$ for every R. Yet $J \cdot E_i = R - v$ grows without bound. A finite compact norm can persist in a direction invisible to the selected periods. To decide whether a harmonic form has a nonzero square-integrable limit, one would have to control its profile on the growing geometry. A matrix of compact inner products at a sequence of Kähler classes gives no such profile.

A product surface shows a different failure of period data. Give $\mathbb{P}^1 \times \mathbb{C}$ a fixed product metric, with sphere area A and flat metric on the plane. Let ω be a smooth closed two-form, and suppose its period on one sphere slice is $p \neq 0$. The slices over the endpoints of any path in the plane are homologous by the product of that path with $\mathbb{P}^1$. Stokes' theorem makes the period p the same on every slice. Write the restriction to the sphere at z as $f_z\, dA$. The product metric makes components with different numbers of legs along the sphere orthogonal. Hence

$$p^2 = \left(\int_{\mathbb{P}^1} f_z \, dA \right)^2 \leq A \int_{\mathbb{P}^1} f_z^2 \, dA \leq A \int_{\mathbb{P}^1} |\omega|^2 \, dA. \tag{XV.2.64}$$

Even if the form has additional legs on the plane, their contribution to the squared norm cannot offset this lower bound. Integrating over the disk D_L of radius L gives

$$\|\omega\|^2_{\mathbb{P}^1 \times D_L} \geq \frac{\pi L^2 p^2}{A}. \tag{XV.2.65}$$

Equality is attained by the pullback of $(p/A)dA$. For $A = 2, p = 3$, disks of radii two and four give lower bounds 18π and 72π. Figure XV.2.6 shows why no radial decay of the sphere period is available to make the norm finite: every sphere carries the same period. This is an actual noncompact example with a finite period and no L^2 closed representative of that nonzero period. It is not a model for the asymptotic metric of CHAIN45.

There is a conditional positive test for a local sector. Suppose the selected image of compactly supported cohomology in ordinary cohomology is realized, for the chosen metric and boundary conditions, by square-integrable primitive harmonic forms ω_i with the stipulated pairing $\int \omega_i \wedge \omega_j = C_i \cdot C_j = -\Omega_{ij}$. Suppose these forms represent the indicated curve duals, so their evaluations on the selected curves agree with the intersection matrix. Then $*\omega_i = -\omega_i$, and in the curve-dual and period-dual coordinates the norms are respectively

$$\left(\int \omega_i \wedge *\omega_j \right)_{ij} = \Omega, \qquad (-\Omega^{-1})^T \, \Omega \, (-\Omega^{-1}) = \Omega^{-1}. \tag{XV.2.66}$$

The second identity changes to unit-period forms. It explains how the compact tangent limit can agree with a genuine local norm if those modes and that pairing are established.

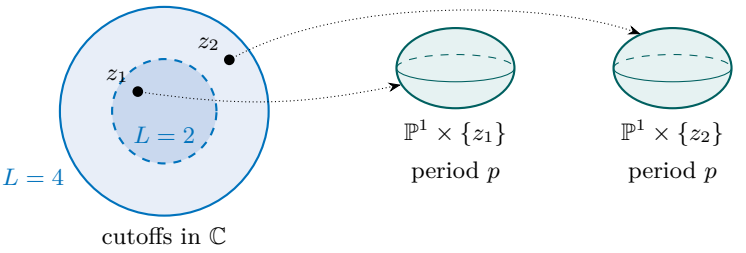


Figure XV.2.6: On the product surface, every point of the plane supports a sphere of area A with period p. The radius-four cutoff covers four times the area of the radius-two cutoff, so the lower bound on the squared norm grows by the same factor.

It does not prove the existence of the representatives for the local limit of the two-curve base or classify other normalizable modes. A finite externally prescribed period can instead enter as background data. The same test matters for a gauge field: a constant internal profile on a seven-brane curve of infinite area gives a divergent bare kinetic integral, whereas a decaying profile requires its own analysis. We can nevertheless study how the finite wrapped-string and gauge coefficients change along the compact paths, before making any claim about the limiting field content.

XV.2.6 Changing areas without declaring a fixed point

What can we conclude when a string becomes tensionless? There are two operations to distinguish. We can lower the area of a selected curve while staying in a compact parent of finite volume. We can also make the parent volume large while holding the selected periods fixed. The first operation changes the tension of a wrapped string. The second suppresses the coupling of the compact gravitational zero mode. Neither calculation by itself supplies the spectrum of the limiting theory.

Take a path to a single wall on the two-curve base:

$$a_1 = \varepsilon, \qquad a_2 = b > 0, \qquad s = 0, \qquad R > \frac{\varepsilon + 2b}{3}. \tag{XV.2.67}$$

For a fixed $R > 2b/3$ this inequality holds for all sufficiently small positive ε, so the exceptional curves stay positive up to the limit. The wall belongs to the closure of the chamber. The leading string tensions and gauge kinetic coefficients along the interior path are

$$T(q) = (q_1\varepsilon + q_2 b)/k_3 \;\longrightarrow\; q_2 b/k_3, \qquad q_1, q_2 \geq 0, \tag{XV.2.68}$$

$$(\phi_1, \phi_2) = (\varepsilon, b)/k_8 \;\longrightarrow\; (0, b/k_8). \tag{XV.2.69}$$

Within the selected effective cone, a nonzero charge loses all its tension only on the first ray. For the two elementary charges e_1, e_2 and their sum, this gives the ordered limit

$$k_3\big(T(e_1), T(e_2), T(e_1 + e_2)\big) \;\longrightarrow\; (0, b, b). \tag{XV.2.70}$$

A class with an exceptional component also pays the corresponding positive exceptional area; its contribution does not vanish just because C_1 collapses. For a concrete compact path take $b = 5$, $R = 5$. At the wall both exceptional areas are $5/3$, and $V \to 75 - 25/3 = 200/3$ in the chosen units. The parent volume does not go to zero.

Now set $a = (\varepsilon, \eta\varepsilon)^T$ with fixed $\eta > 0$ and fixed $R > 0, s = 0$. This is again an interior path for small positive ε, but the endpoint is the origin in the period plane. The tension now satisfies

$$T(q) = \varepsilon(q_1 + \eta q_2)/k_3, \qquad V = 3R^2 - \tfrac{\varepsilon^2}{3}(1 + \eta + \eta^2). \tag{XV.2.71}$$

Both elementary charges become tensionless, as does any fixed nonnegative combination. Figure XV.2.7 distinguishes the zero sets of the tension on the two paths. In each case the word tensionless refers to the limit of the calibrated area calculation. The scale $\sqrt{T}$ of a wrapped string is no longer large compared with a fixed low-energy scale when $T \to 0$; an effective description that integrated out the string cannot be justified uniformly along the path. Also $g_{6,1}^{-2} \to 0$ in (XV.2.69), so the leading gauge term does not yield a weak description of the endpoint.

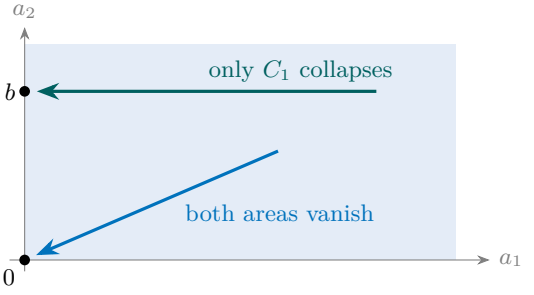


Figure XV.2.7: The selected period plane. The horizontal approach at $a_2 = b$ leaves nonzero tension for charges with $q_2 > 0$. The diagonal approach at $a_2 = \eta a_1$ sends both periods to zero. The paths are drawn near their endpoints, where the exceptional areas are positive for the indicated choice of R.

To vary the gravitational scale instead, hold the two periods at fixed positive values, set $s = 0$, and increase R. In the unwarped reduction the external Ricci scalar is independent of the internal coordinates, and its coefficient in the Einstein action is

$$\frac{1}{2\kappa_{10}^2}\int_B \frac{J^2}{2}\int d^6x\,\sqrt{-g_6}\,\mathcal{R}_6 = \frac{M_6^4}{2}\int d^6x\,\sqrt{-g_6}\,\mathcal{R}_6, \qquad M_6^4 = \frac{V}{\kappa_{10}^2}. \tag{XV.2.72}$$

The assumption here is that κ_{10} stays fixed. As $R \to \infty$ the volume grows as $3R^2$, hence M_6^4 diverges, while every $T(q)$ for fixed q in the selected span and every ϕ_i stays fixed. For example at $a = (2, 5)$ the volumes at $R = 5$ and 10 are 62 and 287. The two exceptional periods increase from 1 to 6, whereas the charge $q = (2, 1)$ still has area 9. This path moves in the parent Kähler cone at one point of the selected period plane. In the one-curve model (XV.2.14), $L \to \infty$ with a_S fixed gives $V \sim L^2/2$ and fixed

tension a_S/k_3. In both cases a normalized compact zero mode couples with a factor proportional to M_6^{-2}. The calculation does not bound the coupling to the rest of the bulk spectrum or demonstrate a Kaluza–Klein gap.

The two changes can also be made on a single path. For example take $a = (\varepsilon, 5)^T$, $s = 0$, and $R = 5/\varepsilon$, with $0 < \varepsilon \le 1$ in the chosen area units. The exceptional periods are positive because $R \ge 5$ while $v \le 11/3$. The limiting data are

$$V(\varepsilon) = \frac{75}{\varepsilon^2} - \frac{\varepsilon^2 + 5\varepsilon + 25}{3}, \tag{XV.2.73}$$

$$(k_3T(e_1), k_3T(e_2), k_3T(e_1+e_2)) = (\varepsilon, 5, 5+\varepsilon). \tag{XV.2.74}$$

The first string loses its tension and the gravitational zero mode is suppressed along this path. These statements use different terms in the reduction. In particular, suppressing the gravitational coupling does not lower the tension of the second string. Nor does the calculation show that the first is isolated from other modes as the geometry grows.

The same single-wall test on $\mathbb{F}_1$ has only one selected generator. In (XV.2.14) let $a_S \to 0$ at fixed $L > 0$. Then the fiber still has area L and the compact volume tends to $L^2/2$. For instance, choosing $L = 4\ell^2$ and decreasing a_S from ℓ^2 to zero gives

$$J \cdot F : \ 3\ell^2 \ \longrightarrow \ 4\ell^2, \qquad V : \ \tfrac{15}{2}\ell^4 \ \longrightarrow \ 8\ell^4, \qquad T(S) : \ \ell^2/k_3 \ \longrightarrow \ 0. \tag{XV.2.75}$$

The base curve S has square -1, unlike the two -2 curves above, but its calibrated tension still goes to zero by the same area rule. The fiber area illustrates why one cannot infer collapse of other effective classes from a wall of the selected cone.

These results separate the inputs needed for further constructions. Curve areas tell us which calibrated configurations become tensionless. Negative intersection data, expressed in the positive local pairing, constrain which collections can enter a point contraction, but do not establish that a given elliptic model has the required contraction and consistent local physics. Likewise, if an intersection presentation has a null direction, the inversion used to make D in (XV.2.7) is no longer available on the whole span. A null direction alone does not produce an intrinsic little string scale: one still needs a geometric limit and a finite tension for the appropriate wrapped cycle. Chapter 3 uses the lattice and gauge divisors to compute anomalies. Chapter 5 studies contraction and the conditions for the superconformal interpretation, and Chapter 8 constructs limits with a finite little string scale.

Exercises

Use exact area units in these exercises. For the numerical fields, write exact rational numbers as integers or fraction strings. Use `benchmark/tasks.json` for the JSON fields and `benchmark/PROTOCOL.md` for submission. Explanations in all six exercises are for human assessment.

1. On the two-curve parent, take $(a_1, a_2, R, s) = (4, 3, 6, \frac{1}{3})$. Compute the ordered areas of C_1, C_2, E_1, E_2 and the volume. Is the class in the Kähler cone? Explain why keeping only the first two periods does not suffice to answer the last question.

2. Use $C_1' = C_1$ and $C_2' = 2C_1 + C_2$. Find q', r', a', and Ω' for $q = (3,2)^T$, $r = (1,-2)^T$, $a = (4,3)^T$. Compute the invariant pairing and tension area. In the primed basis give the charge column of C_2, the other generating ray of the effective cone.

3. In CHAIN46 take the second gauge curve to have area $7\ell^2$, with a duality-saturating configuration of instanton number -3. Find $k_8\phi/\ell^2$, the positive energy per length in units of ℓ^2/k_3, and the signed RR increment in units of μ_3. Give $t_i/(\pi^2\phi_i)$ and the ratio of the full identity component coupling squared to k_8. Why does the signed RR increment not equal the positive energy in these units?

4. At $a = (4,3)^T$, $R = 6$, $s = 0$ take $da = (1,-2)^T$ in the indicated area units. Find dR at fixed V, the fixed-volume squared norm of dJ, and the squared norm of $D\,da$. Give form norms before the common kinetic prefactor.

5. Change the product example to sphere area $A = 5/2$ and period $p = 4$. Find the lower bound, divided by π, on the norm squared over a radius-three disk. Explain why the same estimate cannot decide whether W yields a local mode in the two-curve model. What additional analytic data would be needed?

6. Approach the wall by $a = (2\varepsilon, 7)^T$ at $R = 6, s = 0$. Find $k_3 T(q)$ in the limit for $q = (3,0)^T$ and $q = (1,2)^T$, in that order. Explain what these two numbers tell you about the interior path and what additional geometric or physical conditions would be needed to identify its endpoint as a local fixed point.

Status and sources

§1. Base curves, periods and split tunings. The intersections, effective cone, classes and Tate coefficients are [MATH]. The ordinary local gauge-algebra assignment is [GEO-E]; see Morrison and Taylor (2012), arXiv:1106.3563v3, §2.3.2 eq. (2.26), §3 eqs. (3.28), (3.58), (3.61), and Chapter 1 for the parent models. The upstream Chapter 1 results for CHAIN45 and SU5-F1 apply under the split, transverse and simple-root hypotheses stated there. This chapter uses no global resolution or matter multiplicity from CHAIN46. In this discriminant convention, $\Delta_{\text{book}} = 4f^3 + 27g^2$. For the two tunings, the mixed leading coefficients of Δ_{book} after removing the divisor factors are, with β_i the residual Tate coefficients,

$$\frac{\beta_1^5(\beta_1\beta_6 - \beta_3\beta_4)}{16}, \qquad \frac{\beta_1^4(\beta_1^2\beta_6 - \beta_1\beta_3\beta_4 - \beta_4^2)}{16}.$$

At $\beta_1 \neq 0$, the nodal tangent cone $Y(Y + \beta_1 X)$ splits, and $f = -\beta_1^4/48$, $g = \beta_1^6/864$ at the crossing. The discriminant residual degrees on the curves are $(3,6)$, $(2,8)$, and 17 on the $\mathbb{F}_1$ section. For the lifts in (XV.2.15), write the downstairs residual bundle as $\mathcal{O}(dS + bF)$. The kernel of restriction to $S \cup F_0$ is $\mathcal{O}((d-1)S + (b-1)F)$; its ruling pushforward is the sum of $\mathcal{O}(b-1-2j)$, $0 \le j \le d-1$, and has zero H^1 for these rows. One lifts restrictions agreeing at the crossing, with a zero at each blowup center in the multiplicity-one rows, then divides by the exceptional factors. The multiplicity-zero rows require no such zeros. On $\mathbb{F}_1$ the residual bundles are globally generated.

§2. Wrapped string. The wrapped-D3 tension and electric interpretation are [GEO-E] in the calibrated unwarped reference. See Myers (1999), hep-th/9910053v2, eqs. (1), (3), (5), (6), and (21)–(24), with the unshifted-field translation in the wrapped D3 action above. For the geometric identification see Heckman et al. (2015), arXiv:1502.05405v3, §§2.2, 3, and Lee et al. (2018), JHEP 10 (2018) 164, eq. (2.46) and App. A. The reference determinant requires the vanishing worldvolume combination in (XV.2.20). Additivity concerns the calibrated area of the stated configuration.

§3. Lattice and period bases. The positive local string-pairing identification is [GEO-E]; see Shimizu and Tachikawa (2016), JHEP 11 (2016) 165, §2.1 eqs. (2.1)–(2.2), (2.6)–(2.7), and Ohmori et al. (2014), arXiv:1408.5572v2, eq. (3.28). The basis changes and discriminant computation are [MATH]. The real duals need not be integral divisors, and the quotient in (XV.2.37) uses only the selected string lattice.

§4. Gauge and RR couplings. The weak-reference action coefficient and instanton WZ match are [GEO-E]. The fixed-scalar Yang–Mills square completion is [MATH]. Use Myers (1999), eqs. (1), (24), (35), (47),. Compare Lee et al. (2018), §2.1 eqs. (2.11)–(2.12) and App. A eqs. (A.1)–(A.7), distinguishing the single-field and $SU(N)$ trace conventions. The unit-charge single-entry comparison and the N-dependent full identity trace are distinct, as computed in (XV.2.42). The Bianchi projection is [GEO-E] in the anomaly source frame of Ohmori et al. (2014), §3.3 eqs. (3.26)–(3.32) and footnote 6, in its integral anomaly normalization. No sign is transferred between the two curvature conventions in these applications.

§5. Norms and localization. The compact Hodge and tangent identities and the product bound are [MATH]. The compact two-derivative action normalization is [SUGRA]; see Lee et al. (2019), Nucl. Phys. B 938 (2019) 321–350, §3.1 eqs. (3.1)–(3.10), including note 7, and Lee et al. (2018), App. A. The local kinetic interpretation is conditional [DEC]. Equation (XV.2.66) is a norm computation assuming the given L^2 primitive representatives, boundary conditions and pairing, with no existence or classification assertion.

§6. Limits. The restricted area limits are [MATH]; their use as tensions uses the leading wrapped-string dictionary of §2. The gravitational zero-mode scaling is [SUGRA] with fixed microscopic parameters and unwarped Einstein reduction. The endpoint interpretation requires further [DEC] premises; see Heckman et al. (2015), §3, and Bhardwaj et al. (2016), arXiv:1511.05565v3, §2 and opening of §3. The compact limits supply no bulk isolation, UV completion or all-strata resolution.

References

Bhardwaj, L. et al. (2016). "F-theory and the Classification of Little Strings". In: *Phys. Rev. Lett.* 116, p. 161601. DOI: 10.1103/PhysRevLett.116.161601. arXiv: 1511.05565 [hep-th].

Heckman, J. J. et al. (2015). "Atomic classification of 6D SCFTs". In: *Fortsch. Phys.* 63, pp. 468–530. arXiv: 1502.05405 [hep-th].

Lee, S.-J., W. Lerche, and T. Weigand (2018). "Tensionless Strings and the Weak Gravity Conjecture". In: *JHEP* 10, p. 164. arXiv: 1808.05958 [hep-th].

Lee, S.-J., W. Lerche, and T. Weigand (2019). "A Stringy Test of the Scalar Weak Gravity Conjecture". In: *Nucl. Phys. B* 938, pp. 321–350. arXiv: 1810.05169 [hep-th].

Morrison, D. R. and W. Taylor (2012). "Matter and singularities in F-theory models". In: *JHEP* 01, p. 022. arXiv: 1106.3563 [hep-th].

Myers, R. C. (1999). "Dielectric-branes". In: *JHEP* 12, p. 022. DOI: 10.1088/1126-6708/1999/12/022. arXiv: hep-th/9910053.

Ohmori, K. et al. (2014). "Anomaly polynomial of general 6D SCFTs". In: *PTEP* 2014, 103B07. arXiv: 1408.5572 [hep-th].

Shimizu, H. and Y. Tachikawa (2016). "Anomaly of strings of 6d $\mathcal{N} = (1, 0)$ theories". In: *JHEP* 11, p. 165. arXiv: 1608.05894 [hep-th].

Chapter XV.3

Anomaly polynomials and Green–Schwarz cancellation

XV.3.1 Which anomalies constrain the construction

In Chapter B.1 we read the gauge algebra and the ordinary charged matter from the elliptic fiber. In Chapter B.2 we found the pairing of strings wrapped on the gauge curves and the coupling of their two-forms to gauge instantons. Why do we need both results to define a chiral gauge theory? The fermion measure can transform under a gauge transformation. A transformation of the tensor potentials can compensate that variation. We will compute the two contributions separately and compare them, first on a negative section of $\mathbb{F}_1$ and then on two intersecting curves. The comparison requires the anomaly descent and six-dimensional multiplets of Volume I, Chapter 8. We recall the index factors as we use them.

We work at a weakly described generic point of the tensor branch. The vector fields for the indicated simple gauge algebras are dynamical. We use nondynamical curvatures for the R symmetry, selected rotations of identical external hypers, and gravity. This distinction determines what must vanish. In the descent convention used here, on a local extension of spacetime the invariant eight-form I_8 obeys

$$I_8 = dI_7^{(0)}, \qquad \delta I_7^{(0)} = dI_6^{(1)}, \qquad \delta \log Z = 2\pi i \int I_6^{(1)}. \tag{XV.3.1}$$

If a term mixes a dynamical gauge curvature with a background curvature, we must account for it even though the background does not fluctuate. A pure background term instead describes a possible transformation of the generating functional for external sources. Here we test the local polynomial, which does not detect global anomalies.

Write F_i for the rescaled anti-Hermitian curvature, $F_i = -iF_{\mathrm{phys},i}/(2\pi)$, with F_{phys} Hermitian. The traces below are ordinary defining traces unless a representation is

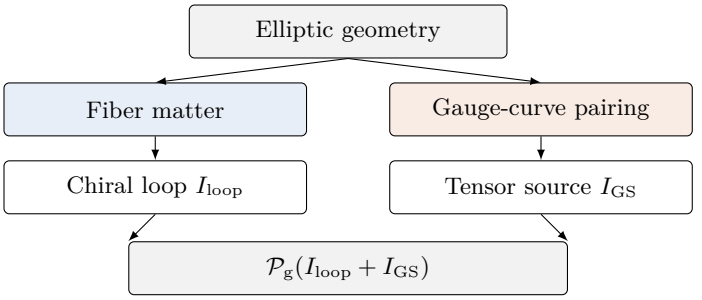


Figure XV.3.1: Two inputs from the same elliptic construction. Matter from the discriminant gives a chiral index. The intersections of the gauge curves pair the four-form tensor sources. The gauge projection tests their sum.

indicated. Our four-forms and independent degree-eight gauge invariants are

$$\begin{aligned} s_i &= \operatorname{tr}_{\text{f}} F_i^2, \quad & q_i &= \operatorname{tr}_{\text{f}} F_i^4, \\ t_i &= \operatorname{tr}_{\text{f}} F_{\text{fl},i}^2, \quad & \ell_i &= \operatorname{tr}_{\text{f}} F_{\text{fl},i}^4, \\ p &= p_1(T), \quad & c &= c_2(R), \quad & p_2 &= p_2(T). \end{aligned} \tag{XV.3.2}$$

Here T in a Pontryagin class denotes the spacetime tangent bundle. Later T in a multiplet count will denote the number of tensor multiplets. Products of forms are wedge products. Neither q_i nor t_i is a string charge or a tension. The use of distinct variables q_i and s_i^2 for the gauge algebras in this chapter will be justified directly by their weights.

Define $\mathcal{P}_{\text{g}}$ to remove the part independent of all dynamical gauge curvatures. For example, consider a polynomial on a single $\mathfrak{su}(5)$ node and switch off the other probes except gravity:

$$I_8 = \alpha q + \beta s^2 + \gamma ps + \delta p^2 + \epsilon p_2, \tag{XV.3.3}$$

$$\mathcal{P}_{\text{g}} I_8 = I_8 - I_8\big|_{s=q=0} = \alpha q + \beta s^2 + \gamma ps. \tag{XV.3.4}$$

The ps term is part of the gauge test. To see it directly, let $\omega_3^{(0)}$ be the gauge Chern–Simons form with $d\omega_3^{(0)} = s$ and variation $d\omega_2^{(1)}$. Since $dp = 0$ and p has even degree, its product with this form gives

$$d(p\omega_3^{(0)}) = ps, \qquad \delta(p\omega_3^{(0)}) = d(p\omega_2^{(1)}). \tag{XV.3.5}$$

The descended variation is nonzero in general when the background p is present. The p_2 term does not participate in this test, but becomes an independent condition when gravity is made dynamical.

A Green–Schwarz contribution is quadratic in four-forms. On this single node with just the gravity probe, a single source $X = us + vp$ produces

$$\frac{1}{2}X^2 = \frac{u^2}{2}s^2 + uv\, ps + \frac{v^2}{2}p^2. \tag{XV.3.6}$$

Adding more such sources can change these coefficients. It cannot produce the independent invariant q, because the only available quadratic gauge invariant is s. Thus $\alpha = 0$ is a prerequisite for cancellation. Also, removing only the pure gauge terms before turning on a probe could miss a nonzero γ. We will keep the mixed terms in the same calculation.

Figure XV.3.1 fixes the order of operations. We will count the charged hypers before asking which coefficients the tensor sources can cancel. Solving a quartic constraint for an unknown multiplicity may be useful as a necessary condition. It gives no section of a line bundle and no information about whether its roots lie at ordinary points. To implement the loop calculation, we start with a single weight of a representation.

XV.3.2 Trace identities from weights

How can two representations with the same dimension give different gauge anomalies? The gravitational term of an uncharged fermion depends on how many components it has. The gauge terms also depend on their charges. Take a formal traceless diagonal curvature with entries x_i, $i = 1, \dots, N$. We evaluate polynomial identities on this Cartan. The entries may be manipulated as formal commuting variables. Numerical substitutions into these identities need not be physical curvatures or quantized fluxes. Define

$$\sum_i x_i = 0, \qquad s = \sum_i x_i^2, \qquad q = \sum_i x_i^4, \qquad \operatorname{tr}_\rho F^j = \sum_{\mu \in \rho} \mu(x)^j. \tag{XV.3.7}$$

Each weight in the last sum is included with its multiplicity. The adjoint is the traceless part of the endomorphisms of the defining representation. The basis matrix e_{ij} has weight $x_i - x_j$. Removing the identity leaves $N - 1$ zero weights in the diagonal sector. Hence

$$\dim \mathrm{adj} = N(N-1) + (N-1) = N^2 - 1. \tag{XV.3.8}$$

For positive moments we may sum over all i, j since the diagonal terms vanish. In the quadratic moment the cross term is $-2(\sum_i x_i)^2$. In the fourth moment the $x_i^3 x_j$ and $x_i x_j^3$ terms vanish for the same tracelessness reason, leaving

$$\sum_{i,j} (x_i - x_j)^2 = 2Ns, \tag{XV.3.9}$$

$$\sum_{i,j} (x_i - x_j)^4 = 2Nq + 6 \sum_{i,j} x_i^2 x_j^2 = 2Nq + 6s^2. \tag{XV.3.10}$$

This derivation explains why dropping Cartan weights would go undetected in a gauge trace test and still corrupt the gravitational index.

The exterior square has the weights $x_i + x_j$ for $i < j$. The corresponding ordered double sum has the same even moments as the ordered difference sum: the only changed signs multiply terms with $\sum_i x_i = 0$. The diagonal terms are now $2x_i$ and must be removed before dividing by two. This gives

$$\operatorname{tr}_{\Lambda^2} F^2 = \tfrac{1}{2}(2Ns - 4s) = (N-2)s, \tag{XV.3.11}$$

$$\operatorname{tr}_{\Lambda^2} F^4 = \tfrac{1}{2}(2Nq + 6s^2 - 16q) = (N-8)q + 3s^2. \tag{XV.3.12}$$

In particular the $\mathfrak{su}(5)$ antisymmetric has dimension $5 \cdot 4/2 = 10$, with traces $3s$ and $-3q + 3s^2$. A negative coefficient of q here is compatible with summing nonnegative fourth powers of real test weights. For example, with $x = (1, -1, 0, 0, 0)$ the result is $-3 \cdot 2 + 3 \cdot 4 = 6$. It is a coefficient in a two-invariant expansion, not the fourth moment itself.

Next put two independent traceless Cartans x, y on the two factors of $(\mathbf{N}, \overline{\mathbf{M}})$. The matrix entries of this representation have weights $x_i - y_j$. Each x_i occurs in M columns when $y = 0$; the second factor is a spectator in that restriction. The full rectangular sum gives

$$\mathrm{tr}_{N\bar{M}}\, F^2 = M s_x + N s_y, \tag{XV.3.13}$$

$$\mathrm{tr}_{N\bar{M}}\, F^4 = M q_x + N q_y + 6 s_x s_y. \tag{XV.3.14}$$

The cross term comes from $6x_i^2 y_j^2$ in each cell. It survives because the two quadratic sums need not vanish. Odd cross terms again contain a first moment of one of the Cartans and vanish. Conjugating either factor does not affect these even sums. One full complex hyper uses one such trace. Its conjugate is already included by the reality condition in the index convention. Counting the two rectangular blocks as separate hypers would double the single-factor traces and the mixed trace together.

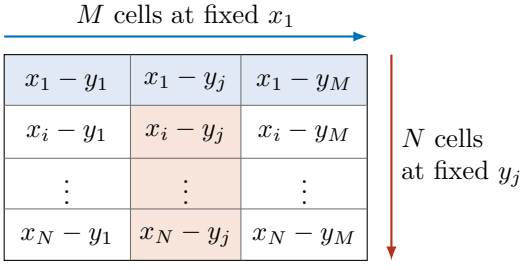


Figure XV.3.2: The weight array for $(\mathbf{N}, \overline{\mathbf{M}})$. The sample entries show which Cartan each index belongs to. Every row has M cells and every column has N, which gives the spectator multiplicities in the one-factor traces.

For a numerical test of Figure XV.3.2, use $x = (2, 1, -1, -2)$ and $y = (3, 1, 0, -1, -3)$. They give $(s_x, q_x) = (10, 34)$ and $(s_y, q_y) = (20, 164)$. Thus

$$\mathrm{tr}_{4\bar{5}}\, F^2 = 50 + 80 = 130, \qquad \mathrm{tr}_{4\bar{5}}\, F^4 = 170 + 656 + 1200 = 2026. \tag{XV.3.15}$$

Appending a zero to y embeds it in a six-dimensional defining representation and preserves both y moments. The product traces increase by 10 and 34, respectively. The mixed term stays 1200 while one spectator multiplicity increases. Alternatively take $y' = (3, 1, 1, -1, -1, -3)$, for which $(s_{y'}, q_{y'}) = (22, 166)$. The traces become $60 + 88 = 148$ and $204 + 664 + 1320 = 2188$. This separates a change in the probe eigenvalues from a change in the dimension of the probe representation.

Before expanding the index, we need to know when q can be regarded as independent of s^2. At $N \geq 4$, use the test weights $x = (1, -1, 0, \ldots)$ and $x = (1, 1, -1, -1, 0, \ldots)$.

The evaluation matrix has nonzero determinant:

$$\det \begin{pmatrix} q(x_{\text{first}}) & s(x_{\text{first}})^2 \\ q(x_{\text{second}}) & s(x_{\text{second}})^2 \end{pmatrix} = \det \begin{pmatrix} 2 & 4 \\ 4 & 16 \end{pmatrix} = 16. \tag{XV.3.16}$$

For $N = 2$, the weights are $a, -a$, so $q = 2a^4 = s^2/2$. For $N = 3$, write $e_2 = x_1x_2 + x_1x_3 + x_2x_3 = -s/2$. Squaring e_2, the cross term is $2x_1x_2x_3(x_1 + x_2 + x_3) = 0$. It follows that

$$s^2 = q + 2\sum_{i<j} x_i^2 x_j^2 = q + 2e_2^2 = q + \frac{s^2}{2}. \tag{XV.3.17}$$

We will apply this relation to two flavor probes. Applying it to the $\mathfrak{su}(4)$ gauge node instead would erase an actual anomaly constraint.

The two-invariant test also gives a way to extract coefficients from a direct list of weights. For the **10** of $\mathfrak{su}(5)$, use $x = (2, 1, 0, -1, -2)$. Its exterior-square weights are $3, 2, 1, 0, 1, 0, -1, -1, -2, -3$. Their fourth powers add to 198. For $x' = (1, 1, -1, -1, 0)$, the weights consist of ± 2 once each, ± 1 twice each, and four zeros. Their fourth powers add to 36. If the fourth trace is $Bq + Cs^2$, these values imply

$$\begin{pmatrix} 34 & 100 \\ 4 & 16 \end{pmatrix} \begin{pmatrix} B \\ C \end{pmatrix} = \begin{pmatrix} 198 \\ 36 \end{pmatrix}, \qquad (B, C) = (-3, 3). \tag{XV.3.18}$$

These two test points distinguish the two terms. On a single test point with $q = s^2/2$, the value would determine only $B/2 + C$, even for $\mathfrak{su}(5)$. For example the pair $(0, 3/2)$ would reproduce the fourth moment of the antisymmetric at $(1, -1, 0, 0, 0)$ and fail both of the points in (XV.3.18). The general weight expansion establishes the form of the identity; the independent evaluations test the numerical coefficients.

We can now convert weights into the polynomial of a chiral multiplet. In the curvature frame of (XV.3.2), take the positive hyperino chirality. The index is the degree-eight part of $\widehat{A}(T)\,\mathrm{ch}_\rho(F)$. The even terms needed for the products are

$$\widehat{A}(T) = 1 - \frac{p}{24} + \frac{7p^2 - 4p_2}{5760} + \cdots, \tag{XV.3.19}$$

$$\mathrm{ch}_\rho(F) = \dim \rho - \frac{\mathrm{tr}_\rho F^2}{2} + \frac{\mathrm{tr}_\rho F^4}{24} + \cdots. \tag{XV.3.20}$$

Here we have suppressed terms of degree two and six, which do not contribute to these products. In particular the product of the two degree-four terms has a positive sign. Put $W_{1/2} = (7p^2 - 4p_2)/5760$. The hyper contributes

$$I_{\mathrm{h}}(\rho) = \frac{\mathrm{tr}_\rho F^4}{24} + \frac{p\ \mathrm{tr}_\rho F^2}{48} + \dim \rho\, W_{1/2}. \tag{XV.3.21}$$

The gaugino has the opposite chirality and is an R doublet with the symplectic reality condition. With Chern roots $r, -r$ and $c = -r^2$, the effective R factor is

$$\frac{1}{2}\,\mathrm{ch}(\mathbf{2}_R) = \frac{e^r + e^{-r}}{2} = 1 - \frac{c}{2} + \frac{c^2}{24} + \cdots. \tag{XV.3.22}$$

The degree-four term of $\widehat{A}\,\mathrm{ch}_{\mathrm{adj}}$ is $-\operatorname{tr}_{\mathrm{adj}} F^2/2 - d_G p/24$, where $d_G = \dim G$ denotes the algebra dimension. Multiplying by $-c/2$, adding the degree-eight R term and reversing the chirality yields

$$I_{\mathrm{v}} = -I_{\mathrm{h}}(\mathrm{adj}) - \frac{c}{4}\operatorname{tr}_{\mathrm{adj}} F^2 - d_G\left(\frac{c^2}{24} + \frac{cp}{48}\right). \tag{XV.3.23}$$

The minus sign multiplies the full index, including the R-gauge term. The factor of one half on the doublet fixes its constant term to one. Omitting it would also double the pure gauge term. A tensor multiplet has no gauge trace in the one-loop calculation. With the compatible chiral two-form and tensorino signs its background term is

$$I_{\mathrm{t}} = \frac{c^2}{24} + \frac{cp}{48} + \frac{23p^2 - 116p_2}{5760}. \tag{XV.3.24}$$

The tensor potential enters a second time through its sourced Bianchi identity, a different mechanism from its one-loop index. We will see both contributions in the same background polynomial. We first need the actual charged representations to which (XV.3.21) applies.

XV.3.3 A single gauge node

How do we turn the zeros of a residual discriminant into a trace computation? Use the negative section S in $\mathbb{F}_1$. Denote the ruling fiber class by F_{b} to distinguish it from curvature. With $S^2 = -1$, $S \cdot F_{\mathrm{b}} = 1$ and $F_{\mathrm{b}}^2 = 0$, the canonical class is $K = -2S - 3F_{\mathrm{b}}$. In particular,

$$(-K)\cdot S = 1, \qquad (-12K - 5S)\cdot S = 17. \tag{XV.3.25}$$

In the Tate equation use $z = 0$ on S and w along S, and write $a_i = z^{v_i}\beta_i$. The index i runs over $1, 2, 3, 4, 6$; the split I_5 row is $v = (0, 1, 2, 3, 5)$. The restricted coefficient degrees are

$$\deg_S(-iK - v_i S) = i + v_i = (1, 3, 5, 7, 11)_i. \tag{XV.3.26}$$

To find what the degree seventeen measures, complete the square and the cube of the Tate equation. In our discriminant convention the intermediate quantities are

$$(B_2, B_4, B_6) = (a_1^2 + 4a_2,\ a_1a_3 + 2a_4,\ a_3^2 + 4a_6), \tag{XV.3.27}$$

$$B_8 = a_1^2a_6 + a_2a_3^2 + 4a_2a_6 - a_1a_3a_4 - a_4^2, \tag{XV.3.28}$$

$$f = -B_2^2/48 + B_4/2, \tag{XV.3.29}$$

$$g = B_2^3/864 - B_2B_4/24 + B_6/4, \tag{XV.3.30}$$

$$16\Delta = B_2^2B_8 + 8B_4^3 + 27B_6^2 - 9B_2B_4B_6. \tag{XV.3.31}$$

Here $\Delta = 4f^3 + 27g^2$; the conventional elliptic discriminant is -16Δ. The identity $B_8 = (B_2B_6 - B_4^2)/4$ removes the leading $a_1^2a_3^2$ term. In the I_5 row the orders of B_4, B_6 are at least two and four. The terms in B_8 of order five are $a_1^2a_6, a_2a_3^2, -a_1a_3a_4$. This gives

$$16\frac{\Delta}{z^5}\bigg|_S = \beta_1^4(\beta_1^2\beta_6 + \beta_2\beta_3^2 - \beta_1\beta_3\beta_4) = w^4(1 + w^{13}) \tag{XV.3.32}$$

for the restricted tuple $(w, 1, 1, 0, w^{11})$. All thirteen roots of $1 + w^{13}$ are simple since they are nonzero and its derivative is $13w^{12}$. The leading coefficient is nonzero, so there is no root at infinity. At those roots a_1 is a unit and the residual meets S transversely. The ordinary nodal enhancement gives a defining hyper at each such point. We derive the node equation explicitly below for the two-curve retuning.

At $w = 0$ the hypothesis that a_1 is a unit fails. For the sparse witness on a generic disk through that point with z and w of order one, B_2 starts with $4z$, B_4 with wz^2, and B_6 with z^4. The leading term of B_8 is z^5. The leading discriminant term is then $16z^7$ in 16Δ, and the orders are

$$(\operatorname{ord} f, \operatorname{ord} g, \operatorname{ord} \Delta) = (2, 3, 7). \tag{XV.3.33}$$

The ordinary transverse fiber enhances to D_5. Under $\mathfrak{su}(5)$, the D_5 roots outside the A_4 system are the pair sums of the five defining weights and their negatives. Restricting to the traceless Cartan gives the Λ^2 weights used in (XV.3.12). The ordinary local matter dictionary assigns one full antisymmetric hyper to the point. The multiplicity four in (XV.3.32) measures intersection with the residual divisor. It does not assign four hypers to the point.

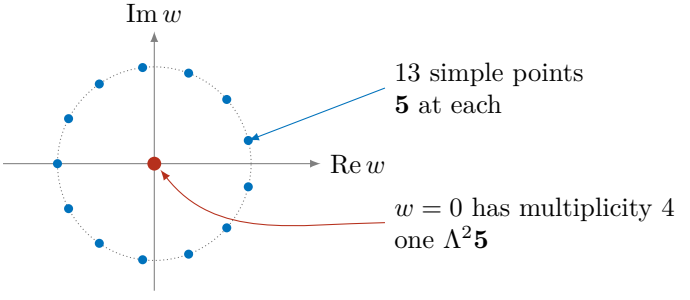


Figure XV.3.3: The zeros on the affine w-plane in SU5-F1. The thirteen simple roots of $w^{13} = -1$ lie on the unit circle. The separate central point has residual multiplicity four and a D_5 transverse enhancement.

These statements describe the witness near S and the open of ordinary restrictions described in B.1. Why is the global coefficient system a separate issue? In the sparse extension of that witness, use $W = 0$ for the other section of the ruling, away from S. Its affine coefficients in the frame with the two other homogeneous coordinates set to one are

$$(a_1, a_2, a_3, a_4, a_6) = (W^2 w,\ W^3,\ W^4,\ 0,\ W^7 w^{11}). \tag{XV.3.34}$$

The leading B_2, B_4, B_6 terms are $4W^3, wW^6, 4w^{11}W^7$, respectively. In f the first two contributions compete at order six, with coefficient $-1/3 + w/2$. In g the B_2^3 and $B_2 B_4$ terms start at order nine, leaving the $B_6/4$ term at order seven. For generic w the g^2 term then sets the discriminant order:

$$\operatorname{ord}_{W=0}(f, g, \Delta) = (6, 7, 14). \tag{XV.3.35}$$

This divisor is nonminimal. It does not touch the ordinary points of Figure XV.3.3, but it excludes this sparse member from the regular compact comparison. The latter uses the open of the full coefficient system and still presupposes the required compact regularity and spectrum.

Use the simple flavor algebra $\mathfrak{su}(13)$ to rotate the thirteen defining hypers. As far as its selected background curvature is concerned, their trace is that of one product $(\mathbf{5}, \overline{\mathbf{13}})$. The antisymmetric is flavor neutral in this choice of probes. The dimensions are

$$H_{\mathrm{ch}} = 5 \cdot 13 + 10 = 75, \qquad V = 5^2 - 1 = 24. \tag{XV.3.36}$$

Here H_{ch} counts charged hyper dimensions, not the number of localized points. There is no genus adjoint on the rational section. Using one retained tensor for the local calculation, the gauge-dependent loop terms can only come from the charged hyperinos and the gaugino. In the order q, s^2, ps their coefficients are

$$[q] I_{\mathrm{loop}} = \frac{-3 + 13 - 10}{24} = 0, \tag{XV.3.37}$$

$$[s^2] I_{\mathrm{loop}} = \frac{3 - 6}{24} = -\frac{1}{8}, \tag{XV.3.38}$$

$$[ps] I_{\mathrm{loop}} = \frac{3 + 13 - 10}{48} = \frac{1}{8}. \tag{XV.3.39}$$

The R term comes from $-c \operatorname{tr}_{\mathrm{adj}} F^2/4$; the mixed flavor term comes from the product fourth moment. Together,

$$\mathcal{P}_{\mathrm{g}} I_{\mathrm{loop}} = -\frac{s^2}{8} + \frac{ps}{8} - \frac{5cs}{2} + \frac{st}{4}. \tag{XV.3.40}$$

Consider changing the ten to two fives with the probes off. Their gravitational dimensions agree, but the new matter traces are $2s, 2q$ in place of $3s, -3q + 3s^2$. The change in the gauge projection is

$$\delta \mathcal{P}_{\mathrm{g}} I_{\mathrm{loop}} = \frac{5q - 3s^2}{24} - \frac{ps}{48}. \tag{XV.3.41}$$

The q term alone obstructs a four-form square. Replacing the whole residual divisor degree by seventeen defining hypers would be a different error: it would even give $H_{\mathrm{ch}} = 85$.

For the actual matter, we can already see the shape of the tensor contribution. The positive local pairing is $-S^2 = 1$. A source $X = s/2 + y$ produces $s^2/8 + sy/2 + y^2/2$. The first term cancels the pure gauge square. The cross term fixes

$$y = 5c - \frac{t}{2} - \frac{p}{4}. \tag{XV.3.42}$$

In particular the sign of the gravitational projection agrees with $-((-K) \cdot S)p/4$. The R and flavor coefficients here come from cancellation in the chosen probe sector. We will derive the matrix version of this step, including what can be learned from the remaining $y^2/2$. Before that, we need a loop term that a single gauge curve could never see.

XV.3.4 Two nodes and their common hypermultiplet

Which term notices that the two gauge curves meet? Start with the chain of B.1 on the blowup of $\mathbb{F}_2$ at two points on the same ruling fiber. Take that fiber to be $w = 0$, and take the centers at $z = 1, 2$, away from the negative section $z = 0$. Use total pullbacks S, F_{b} and exceptional classes E_1, E_2. In this basis the nonzero intersections are $S^2 = -2$, $S \cdot F_{\mathrm{b}} = 1$, $E_a^2 = -1$. In particular the exceptional classes are orthogonal to the total pullbacks. The actual gauge curves are the strict transforms with classes

$$C_1 = S, \quad C_2 = F_{\mathrm{b}} - E_1 - E_2, \qquad K = -2S - 4F_{\mathrm{b}} + E_1 + E_2. \tag{XV.3.43}$$

Their self-intersections are both -2 and $C_1 \cdot C_2 = 1$. Since $K \cdot C_i = 0$, adjunction gives $2g(C_i) - 2 = -2$. There are no genus adjoints. The intersection at $(0, 0)$ is untouched by the blowups.

First tune the split I_4, I_5 rows, with respective orders

$$k = (0, 1, 2, 2, 4), \qquad j = (0, 1, 2, 3, 5), \qquad L_i = -iK - k_i C_1 - j_i C_2. \tag{XV.3.44}$$

The residual Tate coefficient β_i is a section in L_i. Its two restriction degrees are $2k_i - j_i$ and $2j_i - k_i$ because $K \cdot C_i = 0$. They give $(0, 1, 2, 1, 3)$ and $(0, 1, 2, 4, 6)$, respectively. In the ordinary witness, the first four β_i restrict to one in each affine frame. The last restricts to $2 + w^3$ and $2 + z^6$, in that order. For these orders every term of 16Δ other than $B_2^2 B_8$ contains at least $z^6 w^6$ near the corner. In B_8, dividing by $z^4 w^5$ leaves

$$\frac{B_8}{z^4 w^5} = \beta_1^2 \beta_6 - \beta_1 \beta_3 \beta_4 - w\beta_4^2 + z\beta_2 \beta_3^2 + 4zw\beta_2 \beta_6. \tag{XV.3.45}$$

On either axis $B_2 = \beta_1^2$ in the corner patch. Using the actual strict restrictions, the residual numerators are

$$R_1 = 1 - w + w^3, \qquad R_2 = 1 + z + z^6. \tag{XV.3.46}$$

They have degrees three and six. For $R_1 = R_1' = 0$ one would need $w^2 = 1/3$ and $w = 3/2$. For $R_2 = R_2' = 0$ one would need $z^5 = -1/6$ and $z = -6/5$. Neither is possible. The leading terms rule out infinity, the constant terms rule out the corner, and $R_2(1) = 3$, $R_2(2) = 67$ rule out the two exceptional meetings in the strict frame. In B.1 the apparent downstairs zeros at the old centers divide out after the crepant transforms. The even retuning below will make the chart computation explicit.

Here is the nodal calculation that identifies the ordinary loci. At a point where a_1 is a unit on a gauge branch and the higher Tate coefficients vanish, the tangent lines of the affine Tate node are $y(y + a_1 x) = 0$. The leading completed f and g there are $-a_1^4/48$ and $a_1^6/864$, both units. Choose the holomorphic branch of r with $f = -3r^2$ and $g = 2r^3$ at the node. In completed coordinates put $x = r + \xi$. Then

$$y^2 = \xi^2(3r + \xi) + (g - 2r^3), \tag{XV.3.47}$$

$$\Delta = 27(g - 2r^3)(g + 2r^3). \tag{XV.3.48}$$

The second discriminant factor is a unit, and $3r + \xi$ is a unit at the node. A local analytic square root of $3r + \xi$ allows a change to the two factors $U_* = y - \xi\sqrt{3r + \xi}$,

$V_* = y + \xi\sqrt{3r+\xi}$. The Jacobian in the two fiber coordinates is nonzero there. Their product is $g - 2r^3$. Absorbing a further base unit in one factor gives, in the two cases,

$$U_*V_* = \begin{cases} z^4 w^5, & \text{at the corner,} \\ u^N v, & \text{at a simple residual root on an } I_N \text{ branch.} \end{cases} \tag{XV.3.49}$$

In the second line $u = 0$ is the gauge curve and $v = 0$ is the residual. They form coordinates because the derivative of the residual along the gauge curve is nonzero. A disk through the point transverse to both branches gives exponent $N + 1$. A disk transverse to both gauge curves at the corner gives exponent nine. These are fiber enhancements in a surface section, with the two original gauge curves still present in the threefold.

The ordinary matter dictionary now supplies one defining hyper at each simple residual root and one full bifundamental at the transverse split corner. To see the representation at the corner, restrict the enhanced A_8 roots to the two traceless Cartans. The off-diagonal blocks of $\mathfrak{su}(9)$ have weights $x_i - y_j$ and $y_j - x_i$. They are precisely the pair of orientations of the same $(\mathbf{4}, \overline{\mathbf{5}})$ full hyper. At a simple residual enhancement the extra block has one column, which gives the defining weights. This uses the ordinary localized matter rule in addition to the analytic surface calculation. A tangent residual or a nonminimal collision need not obey the same rule.

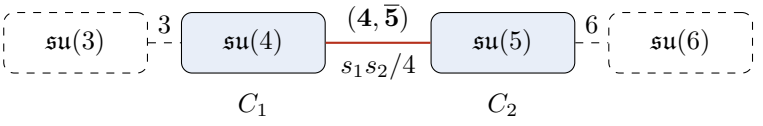


Figure XV.3.4: The ordinary CHAIN45 matter input. The three and six external hypers are supported at distinct simple residual points. The edge denotes one full hyper at the common point of the gauge curves and contributes the mixed term $s_1 s_2/4$. Flavor labels denote selected probes.

The dimensions behind Figure XV.3.4 are $3 \cdot 4,\ 6 \cdot 5$ for the external matter and $4 \cdot 5$ for the shared hyper. Thus

$$H_{\text{ch}} = 12 + 30 + 20 = 62, \qquad V = (4^2 - 1) + (5^2 - 1) = 39. \tag{XV.3.50}$$

Viewed from node one, the shared representation supplies five defining traces; viewed from node two, it supplies four. Write $N = (4, 5)^{\mathsf{T}}$ for the sizes of the defining representations, $m = (3, 6)^{\mathsf{T}}$ for the external multiplicities and $n_{\text{eff}} = (m_1 + N_2, m_2 + N_1)^{\mathsf{T}}$ for the effective defining trace multiplicities. Then

$$\begin{aligned} n_{\text{eff}} &= (8, 10)^{\mathsf{T}}, \\ [q_i] I_{\text{loop}} &= \frac{n_{\text{eff},i} - 2N_i}{24} = 0, \qquad [ps_i] I_{\text{loop}} = \frac{n_{\text{eff},i} - 2N_i}{48} = 0. \end{aligned} \tag{XV.3.51}$$

Each adjoint contributes $-s_i^2/4$ and $-N_i c s_i/2$. For the external hypers we keep $\mathfrak{su}(3) \oplus \mathfrak{su}(6)$ flavor probes, with $s_i t_i/4$ from each product. Using the mixed moment of

the one shared hyper yields the full gauge projection

$$\mathcal{P}_{\mathrm{g}} I_{\mathrm{loop}} = -\frac{s_1^2 + s_2^2}{4} + \frac{s_1 s_2}{4} - \frac{c}{2}(4s_1 + 5s_2) + \frac{s_1 t_1 + s_2 t_2}{4}. \tag{XV.3.52}$$

The term that sees the edge is $s_1 s_2/4$. As a test, replace the shared hyper by five external fundamentals at node one and four at node two, with flavor probes switched off. All the q_i and ps_i terms remain zero. The mixed term disappears because no one fermion carries both charges. The replacement also doubles the twenty shared components in the gravitational count. A node-by-node cancellation would accept the former spectrum test and miss both discrepancies. We now compare the mixed gauge coefficient with the tensor pairing fixed by the actual intersecting curves.

XV.3.5 The Green–Schwarz matrix

How does the pairing of wrapped string charges enter a variation of the path integral? Let M denote the compact intersection matrix and let C be the matrix of coordinate columns for the selected gauge curves. Use $\omega_i = \mathrm{PD}(C_i)$ for their Poincaré duals. On the retained local sector, whose tensor modes are assumed as in B.2, the sign convention for the positive pairing is

$$\Omega = -C^{\mathsf{T}} M C, \qquad \kappa_i = \int_B (-K) \wedge \omega_i = -K \cdot C_i. \tag{XV.3.53}$$

In this integral K denotes the two-form class. The one-node values are $\Omega = (1)$, $\kappa = (1)$. The two-node values are

$$\Omega = \begin{pmatrix} 2 & -1 \\ -1 & 2 \end{pmatrix}, \qquad \Omega^{-1} = \frac{1}{3}\begin{pmatrix} 2 & 1 \\ 1 & 2 \end{pmatrix}, \qquad \kappa = \begin{pmatrix} 0 \\ 0 \end{pmatrix}. \tag{XV.3.54}$$

The two eigenvalues of Ω are $1, 3$; the retained curve span is negative definite in M and has no null direction.

In the source convention for the IIB five-form, expand $F_5 = \sum_i H^i \wedge \omega_i$, and denote its Bianchi source by $\mathcal{Z} = dF_5$. Let $X^i = dH^i$ be its coefficients in the retained curve basis. Projecting onto ω_i gives

$$Y_i = -\int_B \mathcal{Z} \wedge \omega_i = \sum_j \Omega_{ij} X^j. \tag{XV.3.55}$$

This is projection using the intersection form. It does not require interpreting Ω as a kinetic norm for an arbitrary set of noncompact modes. In the source convention the five-form uses the anti-self-dual sign, so that on the negative curve span the six-dimensional fields H^i are self-dual. The sourced tensor contribution to the anomaly is minus half the internal square of the projected six-form source. Equivalently,

$$I_{\mathrm{GS}} = -\frac{1}{2}\int_B \Big(\sum_i X^i \omega_i\Big)^2 = \frac{1}{2} X^{\mathsf{T}} \Omega X = \frac{1}{2} Y^{\mathsf{T}} \Omega^{-1} Y. \tag{XV.3.56}$$

For descent, a local Chern–Simons representative $X = dX_3^{(0)}$ changes by $dX_2^{(1)}$. Defining $H = dB + X_3^{(0)}$ requires $\delta B = -X_2^{(1)}$. The descent representative for (XV.3.56) is $X_3^{(0)\,\mathsf{T}}\Omega X/2$, whose variation descends to $X_2^{(1)\,\mathsf{T}}\Omega X/2$. This is the sourced self-dual tensor normalization: the paired components in Y have not introduced additional tensors. In particular one cannot count the two appearances of a mixed source in the quadratic and omit its overall one half.

The gauge instanton coefficient in $\mathcal{Z}$ is $\mathrm{Tr}_O\, F_i^2/4$ times ω_i, where $\mathrm{Tr}_O = \mathrm{tr}_{\mathrm{adj}}\,/h^\vee$. For $\mathfrak{su}(N)$, $h^\vee = N$ and (XV.3.10) gives $\mathrm{Tr}_O\, F_i^2 = 2s_i$. The gravitational term in $\mathcal{Z}$ is $(-K)p/4$. Thus its contribution to the paired column, with gauge and gravity terms displayed, is

$$Y\big|_{c=t=0} = \frac{\Omega s}{2} - \frac{\kappa p}{4}. \tag{XV.3.57}$$

The tensor carrying the unit charge on the i-th curve is identified by the instanton construction of B.2. The numerical sign of its instanton form depends on the curvature and potential conventions. In fact in our frame

$$\frac{s_i}{2} = -\frac{1}{8\pi^2}\,\mathrm{tr_f}\, F_{\mathrm{phys},i}^2. \tag{XV.3.58}$$

This is minus the positive Hermitian instanton density on the same oriented test cycle. It does not change the positive Wess–Zumino increment for the weak-frame positive instanton. Likewise the geometric period dual of B.2 is $D = -C\Omega^{-1}$, since $C^{\mathsf{T}}MD = 1$; period coefficients of a vector in the curve span are $-\Omega$ times its curve coefficients. Our paired source is $+\Omega X$ by (XV.3.55). The two signs refer to different pairings.

Write $Y = \Omega s/2 + y$, where s and t are columns of the corresponding invariants. Multiplying out the half quadratic gives

$$I_{\mathrm{GS}} = \frac{s^{\mathsf{T}}\Omega s}{8} + \frac{s^{\mathsf{T}}y}{2} + \frac{1}{2}y^{\mathsf{T}}\Omega^{-1}y. \tag{XV.3.59}$$

The first term gives $s^2/8$ for SU5-F1. For CHAIN45 it gives $(s_1^2 + s_2^2 - s_1 s_2)/4$, the negative of the pure gauge block in (XV.3.52). If we erased the edge of Ω while keeping the same hyper, a residual $s_1 s_2/4$ would remain. Turning to the cross term, the ps_i coefficients in (XV.3.40) and (XV.3.52) are $\kappa_i/8$. The opposite term $-s^{\mathsf{T}}\kappa p/8$ is already fixed geometrically. The cs_i and $s_i t_i$ terms require

$$y = Nc - \frac{t}{2} - \frac{\kappa p}{4}, \qquad X = \frac{s}{2} + \Omega^{-1}y. \tag{XV.3.60}$$

This step compares coefficients of independent dynamical s_i. It fixes the R and selected flavor contributions within the retained tensor space. We have not independently obtained those terms by constructing flavor branes or R background geometry. For example, a formal orthogonal tensor direction with pairing $\lambda > 0$, source u depending only on backgrounds, and no gauge component would add $\lambda u^2/2$ and would change none of the gauge tests. This illustrates why the argument requires that the gauge-source directions span the retained tensor space. It does not posit an extra mode in the examples.

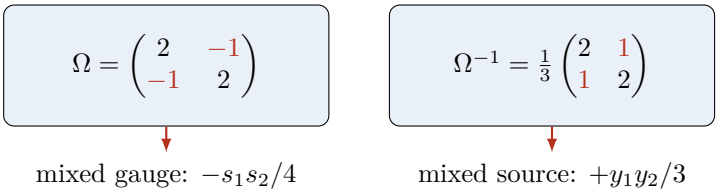


Figure XV.3.5: The edge entry of Ω produces the mixed gauge counterterm. The positive off-diagonal entry of the inverse gives the cross term between the two background source components. The inverse acts on the paired source Y.

We can check that the quadratic in Figure XV.3.5 is basis independent. Make the unimodular change $C' = CU$ with

$$\begin{aligned} U &= \begin{pmatrix} 1 & 1 \\ 0 & 1 \end{pmatrix}, & \Omega' &= U^{\mathsf{T}}\Omega U = \begin{pmatrix} 2 & 1 \\ 1 & 2 \end{pmatrix}, \\ X' &= U^{-1}X = \begin{pmatrix} X_1 - X_2 \\ X_2 \end{pmatrix}, & Y' &= U^{\mathsf{T}}Y = \begin{pmatrix} Y_1 \\ Y_1 + Y_2 \end{pmatrix}. \end{aligned} \tag{XV.3.61}$$

The new curve basis is $C_1, C_1 + C_2$; the gauge couplings no longer have component column $s/2$ in that basis. If $X = (a, b)^{\mathsf{T}}$ for any two four-forms, the quadratic becomes

$$\tfrac{1}{2}X'^{\mathsf{T}}\Omega' X' = (a-b)^2 + (a-b)b + b^2 = a^2 - ab + b^2. \tag{XV.3.62}$$

Keeping the stale components (a, b) instead would change the square by $2ab$. In paired coordinates the same identity uses $\Omega'^{-1} = U^{-1}\Omega^{-1}U^{-\mathsf{T}}$. Even when both matrices exist, applying Ω^{-1} to the curve components in (XV.3.56) would give the wrong polynomial. When the local pairing has a null direction the inverse in this calculation is undefined. The later little-string chapters require a different treatment.

To compare the operations on explicit numbers, take the four-form coefficients $s = (2, 1)^{\mathsf{T}}$ and $c = 1$ along a common formal four-form in the odd chain; set $t = p = 0$. These are coefficient tests of the polynomial and carry no flux interpretation. Then

$$y = \begin{pmatrix} 4 \\ 5 \end{pmatrix}, \qquad Y = \begin{pmatrix} 11/2 \\ 5 \end{pmatrix}, \qquad X = \begin{pmatrix} 16/3 \\ 31/6 \end{pmatrix}. \tag{XV.3.63}$$

The term $s^{\mathsf{T}}\Omega s/8$ has coefficient $3/4$, and $s^{\mathsf{T}}y/2$ has coefficient $13/2$. These sum to $29/4$, the opposite of the coefficient of the gauge projection in (XV.3.52). The background term has coefficient $61/3$. Thus the total square is $331/12$, even though the part needed for gauge cancellation is only $29/4$. Cancelling the gauge variation does not require the entire square to vanish, and the three pieces can be tested separately. In the sheared basis $X' = (1/6, 31/6)^{\mathsf{T}}$; it gives the same total $331/12$, whereas preserving the original components would add $2(16/3)(31/6)$.

What is left after the gauge projection vanishes? We can assemble it with dynamical curvatures set to zero. The pure loop gravity term is $(H_{\mathrm{ch}} - V)W_{1/2}$, plus the p, p_2 part of each retained tensor. The flavor term is $\sum_i N_i(\ell_i/24 + pt_i/48)$; the adjoint R

term uses the full vector dimension V. With n retained tensors this gives

$$\begin{aligned} I_{\rm ret} &= (H_{\rm ch}-V)W_{1/2}+(n-V)\left(\frac{c^2}{24}+\frac{cp}{48}\right)+n\frac{23p^2-116p_2}{5760} \\ &\quad+\sum_i N_i\left(\frac{\ell_i}{24}+\frac{pt_i}{48}\right)+\frac{1}{2}y^{\mathsf T}\Omega^{-1}y. \end{aligned} \tag{XV.3.64}$$

For the single node the flavor algebra is $\mathfrak{su}(13)$, so the two quartic invariants of that probe are independent. In particular the pt term receives $5pt/48$ from the external hyper and $pt/8$ from $(5c-t/2-p/4)^2/2$. The p^2 term gets $380p^2/5760$ from the loops and $p^2/32$ from the square. Expanding all terms gives

$$\begin{aligned} I^{\rm F1}_{\rm ret} &= \frac{277}{24}c^2-\frac{83}{48}cp+\frac{7}{72}p^2-\frac{p_2}{18} \\ &\quad+\frac{t^2}{8}+\frac{5\ell}{24}-\frac{5}{2}ct+\frac{11}{48}pt. \end{aligned} \tag{XV.3.65}$$

There are eight nonzero coefficients in this restricted basis.

For the chain the first probe is $\mathfrak{su}(3)$. Its loop quartic reduces to $4\ell_1/24=t_1^2/12$, by (XV.3.17). Using $y=(4c-t_1/2,\,5c-t_2/2)^{\mathsf T}$, the square is $(y_1^2+y_1y_2+y_2^2)/3$. The t_1t_2 coefficient is $1/12$ from the square alone. The c^2 coefficient is $(16+20+25)/3+(2-39)/24=451/24$. Thus

$$\begin{aligned} I^{45}_{\rm ret} &= \frac{451}{24}c^2-\frac{37}{48}cp+\frac{23}{640}p^2-\frac{9}{160}p_2 \\ &\quad+\frac{t_1^2}{6}+\frac{t_1t_2}{12}+\frac{t_2^2}{12}+\frac{5\ell_2}{24} \\ &\quad-\frac{13}{6}ct_1-\frac{7}{3}ct_2+\frac{pt_1}{12}+\frac{5pt_2}{48}. \end{aligned} \tag{XV.3.66}$$

There are twelve nonzero coefficients. They describe the one restricted branch polynomial in the indicated probes. A direct Cartan evaluation of the original weight sums tests the trace algebra and the coefficient assembly. It does not compare to a second theory. To transfer this polynomial to a UV theory, one would need a UV theory with the same exact symmetries and the specified retained spectrum, including any other sectors needed in the matching. The calculation here contains no independent UV anomaly match. We can, however, change the geometry and rerun all the gauge tests.

XV.3.6 Changed ranks and uncancelled anomalies

Keep the same base and replace the second split I_5 tuning by I_6. What must change before we can repeat the anomaly calculation? The divisor classes of C_1, C_2 and hence the pairing are unchanged. The Tate rows and their coefficient systems change. In the order $i=1,2,3,4,6$, use

$$k=(0,1,2,2,4), \qquad j=(0,1,3,3,6), \tag{XV.3.67}$$

$$\deg_{C_1} L_i = 2k_i-j_i=(0,1,1,1,2)_i, \quad \deg_{C_2} L_i = 2j_i-k_i=(0,1,4,4,8)_i. \tag{XV.3.68}$$

The degree two and eight entries suggest a pair of polynomial restrictions for β_6. We must realize them by actual sections and make sure that the discriminant has ordinary roots.

On $\mathbb{F}_2$, the downstairs numerator β_i belongs to $A_iS + B_iF_{\mathrm{b}}$ with $A_i = 2i - k_i$, $B_i = 4i - j_i$. Its lift to the blown-up base must subtract $m_i = i - j_i$ copies of each exceptional divisor to land in L_i. In the chosen affine coordinates a monomial $z^a w^b$ is allowed in $AS + BF_{\mathrm{b}}$ when

$$0 \le a \le A, \qquad 0 \le b \le B - 2(A - a). \tag{XV.3.69}$$

Indeed the homogeneous monomial with fiber powers $a, A - a$ needs a base coefficient of degree $B - 2(A - a)$; homogenizing w^b in the two ruling coordinates is possible precisely in this range. Here

$$(A_i) = (2, 3, 4, 6, 8), \quad (B_i) = (4, 7, 9, 13, 18), \quad (m_i) = (1, 1, 0, 1, 0). \tag{XV.3.70}$$

The odd tuning instead had $m_i = 1$ for all five indices. Using those same multiplicities for the even tuning would change the restrictions.

Write $D(z) = (z-1)(z-2)/2$, so $D(0) = 1$. Prescribe $P_i(w)$ on C_1 and $Q_i(z)$ on C_2, with $P_i(0) = Q_i(0)$. In the first four entries set both to one. In the last set $P_6 = 4 + w^2$, $Q_6 = 4 + z^8$. The downstairs affine numerators are

$$H_i = P_i(w) + D(z)^{m_i} Q_i(z) - P_i(0), \tag{XV.3.71}$$

$$(H_1, H_2, H_3, H_4, H_6) = (D, D, 1, D, 4 + w^2 + z^8). \tag{XV.3.72}$$

On $z = 0$ the two constant pieces cancel, leaving P_i. On $w = 0$ the numerator is $D^{m_i} Q_i$, so division at the two centers yields Q_i in the strict-fiber frame using D. Each numerator obeys (XV.3.69). For example the w^2 term uses $18 - 2 \cdot 8 = 2$ at $a = 0$, and the z^8 term uses $a = 8$. For the three D's all z powers are at most two, and their w degree is zero. The constant numerator for $i = 3$ has $B_3 - 2A_3 = 1$. This construction realizes full Tate coefficient sections; it does not require any anomaly relation.

To see the crepant transforms locally, fix a center $z = a$, $a = 1, 2$, and use the two charts

$$(z, w) = (a + u, uv), \qquad (z, w) = (a + \tilde{u}\tilde{v}, \tilde{v}), \qquad \tilde{u} = 1/v, \quad \tilde{v} = uv \tag{XV.3.73}$$

on their overlap. In the first chart the exceptional curve is $u = 0$ and the strict fiber is $v = 0$. In the second chart the exceptional curve is $\tilde{v} = 0$, and the meeting point with the strict fiber is outside this chart. The downstairs coefficients are $a_i = z^{k_i} w^{j_i} H_i(z, w)$. Since $K_{\mathrm{up}} = \pi^* K_{\mathrm{down}} + E_a$, the upstairs a_i are obtained by dividing by u^i or $\tilde{v}^i$; the fiber coordinates have the corresponding weights two and three. Explicitly,

$$a_i^{(1)} = (a + u)^{k_i} v^{j_i} \frac{H_i(a + u, uv)}{u^{m_i}}, \tag{XV.3.74}$$

$$a_i^{(2)} = (a + \tilde{u}\tilde{v})^{k_i} \frac{H_i(a + \tilde{u}\tilde{v}, \tilde{v})}{\tilde{v}^{m_i}}. \tag{XV.3.75}$$

For $m_i = 1$ the two quotients are $(2a - 3 + u)/2$ and $\tilde{u}(2a - 3 + \tilde{u}\tilde{v})/2$. For $m_i = 0$ the original numerators are polynomials with no exceptional division. The quotients

transform by v^{m_i} from chart two to chart one on the overlap. Including v^{j_i} gives $a_i^{(1)} = v^i a_i^{(2)}$, as required for the same line bundle. In particular $a_1^{(1)}(0,0) = (2a-3)/2 \neq 0$. No pole or new nodal-tangent degeneration is hidden at the two strict meetings.

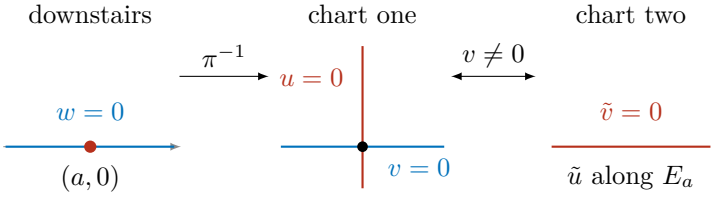


Figure XV.3.6: The charts near either center. In chart one the strict $w = 0$ branch is $v = 0$; it meets the exceptional curve at $u = v = 0$. Chart two covers the other directions of the exceptional line. The overlap has $v \neq 0$ and $\tilde{u} = 1/v$.

Next divide the discriminant near the corner by z^4w^6. Now B_4 is divisible by z^2w^3, and B_6 by z^4w^6. In the analogue of (XV.3.45), the two terms $a_2a_3^2$ and $4a_2a_6$ are above the leading order on both axes, while $-a_4^2$ is of order z^4w^6. The terms other than $B_2^2B_8$ in (XV.3.31) vanish on both axes after division. Thus

$$16\frac{\Delta}{z^4w^6}\bigg|_{\text{either axis}} = \beta_1^4\big(\beta_1^2\beta_6 - \beta_1\beta_3\beta_4 - \beta_4^2\big). \tag{XV.3.76}$$

There is no extra factor of w on the β_4^2 term and no $z\beta_2\beta_3^2$ term on the second axis. For example, copying the odd second-axis expression would give $3 + z + z^8$ rather than the even result $2 + z^8$. Substituting the strict restrictions gives

$$R_1 = 2 + w^2, \qquad R_2 = 2 + z^8, \tag{XV.3.77}$$

$$\big((-12K - 4C_1 - 6C_2)\cdot C_i\big)_{i=1,2} = \big(8-6,\ -4+12\big) = (2, 8). \tag{XV.3.78}$$

The derivatives $2w, 8z^7$ are nonzero at their roots. Both constant terms are nonzero and the leading coefficients exhaust the respective degrees, so the corner and infinity contribute none of these roots.

There is one further excision to check. The downstairs leading quotient along $w = 0$ contains $D^6R_2/16$, since H_1, H_4 each carry one D. In chart one, Δ is divided by u^{12} and w^6 contributes u^6v^6. The residual on $v = 0$ is therefore

$$\frac{\Delta^{(1)}}{v^6}\bigg|_{v=0} = \frac{(a+u)^4}{16}\left(\frac{D(a+u)}{u}\right)^6\big(2 + (a+u)^8\big). \tag{XV.3.79}$$

At $u = 0$ this is nonzero at both centers, since $D(a+u)/u$ tends to $\pm 1/2$ and $R_2(a)$ is 3 or 258. This calculation removes exactly the six spurious downstairs orders at each center. In the disk $u = 0$, $v = \tau$ the leading discriminant coefficients are $3/1024$ and $129/32$, respectively, with order six at each. Together with the unit of the transformed a_1, this excludes extra matter at the strict meetings in the ordinary calculation. It does not examine every stratum away from the selected curves.

At the original corner $a_1 = 1$, and the factor $\Delta/(z^4w^6)$ has value $1/8$. In the analytic construction (XV.3.48), $r = 1/12$ there, $g+2r^3$ and $3r+\xi$ are units, and $g-2r^3$ is a unit times z^4w^6. The analytic factorization therefore gives the node equation $U_*V_* = z^4w^6$ after absorbing a unit. On $z = w = \tau$,

$$\Delta = \frac{\tau^{10}}{8} + O(\tau^{11}), \qquad (\operatorname{ord}_\tau f, \operatorname{ord}_\tau g, \operatorname{ord}_\tau \Delta) = (0, 0, 10). \tag{XV.3.80}$$

At any of the simple residual roots the same unit argument gives $U_*V_* = u^N v$ with v a transverse residual coordinate. The two lines $y(y + \beta_1 x) = 0$ are distinct over the ordinary split gauge branches. Thus the same sourced rule now applies at the new loci. At the corner the enhanced transverse A_9 roots have a 4-by-6 block and its conjugate; these give one full $(\mathbf{4}, \overline{\mathbf{6}})$. The two and eight ordinary one-sheet enhancements give the external defining hypers on the respective branches. These conclusions use the near-curve ordinary strata and the matter dictionary. The diagonal disk and analytic factorization do not give a global resolution theorem.

We can check an actual transverse disk through the first type of simple root. Write $\mathcal{R} = \Delta/(z^4w^6)$ near C_1. The first-order normal term in $B_8/(z^4w^6)$ follows from the $a_2a_3^2$ and $4a_2a_6$ terms:

$$\frac{B_8}{z^4w^6} = D^2(H_6 - 2) + zwD(1 + 4H_6). \tag{XV.3.81}$$

At $z = 0, w = w_*$ with $w_*^2 = -2$, $H_6 = 2$. The first term of (XV.3.81) vanishes there, so the derivative of B_2^2 makes no contribution to the derivative of $\mathcal{R}$. The other discriminant terms have at least two extra powers of z. It follows that $16\partial_z\mathcal{R} = 9w_*$, whereas $16\partial_w\mathcal{R} = 2w_*$. On $z = \tau, w = w_* + \tau$ this gives

$$\Delta = \frac{11w_*^7}{16}\tau^5 + O(\tau^6). \tag{XV.3.82}$$

The coefficient is nonzero. The disk meets both branches to first order. A disk tangent to the residual could give a higher order without adding a second matter point. The count uses the simple intersections on the gauge curves, rather than the largest order achievable by a choice of disk.

There is a legal deformation that shows why the root test was needed. Replace P_6 by $4 + w^2 + 2\sqrt{2}w$ and leave Q_6 fixed. This adds an allowed monomial to H_6 and does not alter the corner value. The restricted residual is now $(w + \sqrt{2})^2$, of the same degree and with a repeated root. We cannot assign two separated ordinary hypers by the preceding argument. A different legal change replaces the matched constant 4 by 2 on both axes. This kills the residual unit at the corner and invalidates the ordinary corner calculation there. Indeed with $H_6 = 2 + w^2 + z^8$, the first two terms of (XV.3.81) start with $w^2 + 9zw$ at the corner. On $z = w = \tau$ the discriminant starts at order twelve, not ten. The residual no longer supplies a unit multiplying the old normal form. Both examples preserve the base intersections. Neither is a license to use the old charged spectrum.

For the actual ordinary even witness the effective defining multiplicities, total charged dimension and vector dimension are

$$(2+6,\ 8+4) = (8, 12), \qquad H_{\mathrm{ch}} = 8+48+24 = 80, \qquad V = 15+35 = 50. \tag{XV.3.83}$$

The q_i and ps_i coefficients vanish by the same formula as in (XV.3.51). The one shared hyper still gives $s_1 s_2/4$, regardless of the rectangular block sizes. The pure gauge loop terms are thus unchanged, but the mixed R block is now $-c(4s_1 + 6s_2)/2$. Keeping $\mathfrak{su}(2) \oplus \mathfrak{su}(8)$ flavor probes yields

$$\mathcal{P}_{\mathrm{g}} I^{46}_{\mathrm{loop}} = -\frac{s_1^2 + s_2^2 - s_1 s_2}{4} - \frac{c}{2}(4s_1 + 6s_2) + \frac{s_1 t_1 + s_2 t_2}{4}. \tag{XV.3.84}$$

It is cancelled by (XV.3.59) with the same Ω, zero κ, and $y = (4c - t_1/2, 6c - t_2/2)^{\mathsf{T}}$. The $\mathfrak{su}(2)$ probe also has $\ell_1 = t_1^2/2$, so the t_1^2 coefficient stays $1/6$ after adding the square. The term linear in ct_2 changes to $-(4 + 12)/6 = -8/3$. Using the updated dimensions in (XV.3.64), the twelve coefficients are

$$\begin{aligned} I^{46}_{\mathrm{ret}} = {} & \frac{70}{3}c^2 - cp + \frac{2}{45}p^2 - \frac{11}{180}p_2 \\ & + \frac{t_1^2}{6} + \frac{t_1 t_2}{12} + \frac{t_2^2}{12} + \frac{\ell_2}{4} \\ & - \frac{7}{3}ct_1 - \frac{8}{3}ct_2 + \frac{pt_1}{12} + \frac{pt_2}{8}. \end{aligned} \tag{XV.3.85}$$

The polynomials (XV.3.65), (XV.3.66) and (XV.3.85) have eight, twelve and twelve retained coefficients, respectively. Each is an identity for a specified branch and probe choice. None is an independent match to an externally computed UV polynomial.

Finally take the new ranks and the old external multiplicities $(3, 6)$, with flavor probes off. The effective multiplicities are $(9, 10)$, so their excess relative to $(8, 12)$ is $(1, -2)$. The R, shared, and pure squared terms are unchanged from (XV.3.84); the correct square for the new ranks still cancels them. The uncancelled gauge projection is

$$\frac{q_1}{24} - \frac{q_2}{12} + \frac{ps_1}{48} - \frac{ps_2}{24}. \tag{XV.3.86}$$

No change to a quadratic of four-forms can remove q_1, q_2. Conversely the equations $m_1 = 2N_1 - N_2,\ m_2 = 2N_2 - N_1$ are necessary quartic tests for this two-node matter ansatz. They do not construct the coefficients in (XV.3.72) or decide whether any of the roots are simple. We obtained the necessary multiplicities from the geometry before using them in the index. The last comparison asks what additional condition arises when the same curve data are placed in a compact gravitational theory.

XV.3.7 Compact gravitational constraints

What additional anomaly constraint applies if gravity itself fluctuates? For this comparison turn off the R and flavor backgrounds. Take a compact gravitational parent with one gravity multiplet and T tensor multiplets in addition to it. The full pairing M has signature $(1, T)$. It includes the gravity two-form direction and any tensor directions outside the gauge curves. The local count of retained tensors cannot substitute for T.

We first compute the gravity multiplet's chiral polynomial in the same signs used for the loops. For a positive chiral spin-3/2 field the index is $\widehat{A}(T)$ times the complex

tangent character with one spinor subtracted for the net ghost contribution. To see the needed character, take formal tangent roots $\pm x_a$, $a = 1, 2, 3$. With $p = \sum_a x_a^2$, $p_2 = \sum_{a<b} x_a^2 x_b^2$, the expansion is

$$\mathrm{ch}(T_{\mathbb{C}}) = \sum_{a=1}^{3} (e^{x_a} + e^{-x_a}) = 6 + p + \frac{p^2 - 2p_2}{12} + \cdots . \tag{XV.3.87}$$

Multiplying by $\widehat{A}$ after subtracting one gives

$$I^{+}_{3/2} = 5W_{1/2} - \frac{p^2}{24} + \frac{p^2 - 2p_2}{12} = \frac{275p^2 - 980p_2}{5760}. \tag{XV.3.88}$$

The tensorino in (XV.3.24) contributes $W_{1/2}$ at $c = 0$. The real chiral two-form in that multiplet thus contributes $(16p^2 - 112p_2)/5760$, the degree-eight signature index with the corresponding sign and the real field normalization. The gravity multiplet has the opposite two-form and gravitino chiralities in this convention. Its polynomial is

$$I_{\mathrm{grav}} = -I^{+}_{3/2} - \frac{16p^2 - 112p_2}{5760} = \frac{-291p^2 + 1092p_2}{5760}. \tag{XV.3.89}$$

The graviton does not add a chiral index. These signs let us combine the gravity contribution with the previously calculated charged gauge terms rather than translating a compact condition in different curvature units.

Let H include all charged dimensions and all neutral hypers, and let V count vector multiplets, including the dimension of any extra abelian algebra if present. The background gravity part of the complete loop polynomial is

$$I^{\mathrm{grav}}_{\mathrm{loop}} = (H - V)W_{1/2} + T\frac{23p^2 - 116p_2}{5760} + I_{\mathrm{grav}}, \tag{XV.3.90}$$

$$[p_2] I^{\mathrm{grav}}_{\mathrm{loop}} = -\frac{H - V + 29T - 273}{1440}. \tag{XV.3.91}$$

A quadratic in four-form invariants cannot cancel the independent p_2. Its coefficient must vanish, giving $H - V = 273 - 29T$. Substituting this value into the coefficient of p^2 leaves

$$\frac{7(273 - 29T) + 23T - 291}{5760} = \frac{9 - T}{32}. \tag{XV.3.92}$$

This substitution determines a necessary dimension count. It gives no information about which neutral fields exist in an elliptic model.

For the reducible compact anomaly the source lives in the full base lattice. The compensation, with the sign of M itself rather than the positive local pairing, is

$$Z = \frac{Cs}{2} - \frac{Kp}{4}, \tag{XV.3.93}$$

$$I^{\mathrm{comp}}_{\mathrm{GS}} = -\frac{1}{2} Z^{\mathsf{T}} M Z \tag{XV.3.94}$$

$$= -\frac{s^{\mathsf{T}}(C^{\mathsf{T}} M C)s}{8} + \frac{p\, s^{\mathsf{T}} C^{\mathsf{T}} M K}{8} - \frac{p^2 K^{\mathsf{T}} M K}{32}. \tag{XV.3.95}$$

On the gauge span the first term agrees with the positive local half square. The middle term gives $-ps/8$ for $\mathbb{F}_1$, where $K\cdot S=-1$, and zero on the chains. The last term instead sees the full canonical class. On $\mathbb{F}_1$ the pairing in (S,F_{b}) has determinant -1; it has one positive and one negative direction. The square $K^2=(-2S-3F_{\mathrm{b}})^2=-4+12=8$ cancels (XV.3.92) at $T=1$. On $\mathbb{F}_2$ the square is $-8+16=8$, and adding the two orthogonal exceptional components reduces it to 6, with $T=3$. This agrees with $9-T$ for both chains. The three terms in (XV.3.95) therefore cancel the corresponding loop terms once the dimension requirement is imposed.

The full basis is especially useful on $\mathbb{F}_1$, where the local gravitational projection is nonzero. In (S,F_{b}), one has $Z=(s/2+p/2,3p/4)^{\mathsf{T}}$. Using $S^2=-1$ and $S\cdot F_{\mathrm{b}}=1$, the compact counterterm becomes

$$-\tfrac{1}{2}Z^{\mathsf{T}}MZ=\tfrac{1}{2}(s/2+p/2)^2-(s/2+p/2)(3p/4)=\frac{s^2}{8}-\frac{ps}{8}-\frac{p^2}{4}. \qquad \text{(XV.3.96)}$$

The first two coefficients agree with the local gauge terms, while the purely gravitational coefficient is negative. Reversing the sign of Kp in Z would preserve the p^2 term but leave $ps/4$ in the total. A comparison of the two diagonal squares alone would not detect the error. On the chains the gravitational direction is orthogonal to both gauge curves, so the mixed gravity coefficient is absent in either choice of sign.

There is an independent comparison of the geometric input to the group contractions. Write $\mathrm{tr}_\rho F^2=A_\rho s$, $\mathrm{tr}_\rho F^4=B_\rho q+C_\rho s^2$; the subscript on C_ρ distinguishes a trace coefficient from a curve column. For the SU factors, expanding the compact factorization in intersection units gives

$$K\cdot C_i=\frac{A_{\mathrm{adj}}-\sum_\rho A_\rho}{6}, \qquad C_i^2=\frac{\sum_\rho C_\rho-C_{\mathrm{adj}}}{3}, \qquad C_1\cdot C_2=\sum_{\rho,\sigma}A_\rho A_\sigma. \quad \text{(XV.3.97)}$$

The sums are over the hypers, including spectator dimensions for a single node, and over shared hypers for the mixed equation. At the single node the three relevant inputs are $A_{\mathrm{adj}}=10$, $\sum A_\rho=16$, $\sum C_\rho=3$. They give $-1,-1$ in the first two equations. At each chain node the total A equals $2N_i$ and the total C_ρ is zero. This gives $0,-2$. The one shared defining product gives 1 in the third equation. All agree with the curve intersections computed before using the spectrum. This checks the curve data against the contractions that occur in the anomaly constraints; the two expressions still concern the same branch.

The decomposition can be exhibited in classes. On $\mathbb{F}_1$, $S+F_{\mathrm{b}}$ is orthogonal to S and has square 1. On the blown-up base K is orthogonal to both gauge curves, and E_1-E_2 is orthogonal to both curves and to K. The complement is two-dimensional, with these two directions of nonzero square:

Base	Complement generators over $\mathbb{R}$	Pairing on the complement
$\mathbb{F}_1$	$S+F_{\mathrm{b}}$	(1)
$\mathrm{Bl}_2\,\mathbb{F}_2$	$K,\ E_1-E_2$	$\mathrm{diag}(6,-2)$.

(XV.3.98)

These are real-span calculations and do not claim the combined generators form an integral basis of the full compact lattice. The second row has an extra negative direction

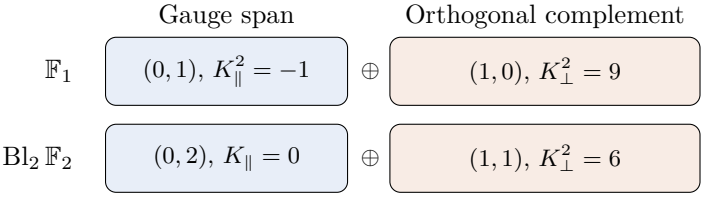


Figure XV.3.7: Gauge-curve subspaces and their orthogonal complements in the compact lattices. The two chains have the same decomposition of the base pairing. In each example the compact gravitational square uses the full K, including its component outside the gauge span.

besides the two retained tensors, as well as a positive direction. It accounts for why the compact tensor-multiplet count on this base is three rather than two.

In Figure XV.3.7, the projection $K_\parallel$ onto the local curve span satisfies $K_\parallel^2 = -\kappa^{\mathsf{T}}\Omega^{-1}\kappa$. For example $K_\parallel = S$ on $\mathbb{F}_1$; then $(K-S)^2 = 9$. On the chains $K_\parallel = 0$. Reusing the local square, even with the p part of (XV.3.60), would leave

$$\frac{p^2}{32}\big(K^2 + \kappa^{\mathsf{T}}\Omega^{-1}\kappa\big) = \begin{cases} 9p^2/32, & \mathbb{F}_1, \\ 3p^2/16, & \mathrm{Bl}_2\,\mathbb{F}_2. \end{cases} \tag{XV.3.99}$$

In particular equal numbers of local and compact tensor multiplets on the single-node example do not make the two pairings interchangeable: the gravity multiplet has its own tensor.

If there are no additional charged or abelian sectors, write $H = H_{\mathrm{ch}} + H_0$ with H_0 the neutral count. The necessary value is $H_0^{\mathrm{req}} = 273 - 29T + V - H_{\mathrm{ch}}$. Inserting the computed charged and vector dimensions gives

Input	T	H_{ch}	V	H_0^{req}
SU5-F1	1	75	24	193
CHAIN45	3	62	39	163
CHAIN46	3	80	50	156

(XV.3.100)

For instance at the last entry the allowed total $H-V$ is 186, so $H_0^{\mathrm{req}} = 186+50-80 = 156$. If the actual theory had one more neutral hyper and no other changes, the residual would be $W_{1/2}$ including $-p_2/1440$. A wrong choice of lattice at the required neutral count gives instead the purely reducible residual (XV.3.99). These diagnose two different omissions. More generally, using the full pairing but leaving H_0 unknown gives

$$I_8^{\mathrm{comp}} = (H_0 - H_0^{\mathrm{req}})W_{1/2} \tag{XV.3.101}$$

for this conditional compact spectrum. None of the three required numbers is an independently determined neutral spectrum. For SU5-F1 the sparse member used to read the near-section matter is excluded from the regular compact comparison by its $W = 0$ nonminimal divisor. It is the full coefficient-system open that supplies the

setting for that comparison; global resolution and the complete field content remain separate requirements.

The rigid branch calculation also has a distinct scope. It assumes the specified retained tensor modes and tests the polynomial in the indicated backgrounds. It does not establish the full noncompact spectrum, a global gauge group, an isolated limit or a UV fixed point. The next chapter returns to the geometric constraints on tunings. Later chapters take up contraction and the change of pairing in the little-string setting, where the inverse in (XV.3.56) cannot be used on a null direction.

XV.3.8 Exercises

1. **Transfer the moment calculation.** Use the Cartans

$$x = (3, 0, -1, -2), \qquad y = (4, 1, 0, -1, -1, -3).$$

Compute the defining quadratic and quartic moments, the $\mathfrak{su}(4)$ adjoint weight count and moments, the exterior-square moments and dimension, and the product moments and dimension. Give the three separate quartic product contributions. Explain why replacing the sum by a sum over only nonzero adjoint weights changes the dimension test.

2. **Detect coalescing roots.** In the even witness change the first residual to $w^2 + bw + d$ with $d \neq 0$; match the constant on the second axis by taking its residual to be $z^8 + d$. Try $(b, d) = (3, 1), (4, 4)$. Give the degree, the number of distinct roots, the quadratic discriminant and the decision whether the ordinary simple-root count applies. Explain why a fixed intersection degree does not settle that decision.

3. **Perturb one external count.** With flavor curvatures off, keep ranks $(4, 6)$, the shared full hyper, and the same pairing. Change the external counts to $(2, 9)$. Give every coefficient in the gauge projection before and after adding the correctly normalized square with $y = (4, 6)^{\mathsf{T}} c$. Identify what an attempted change in y cannot repair.

4. **Change the source basis.** Use $U = \left(\begin{smallmatrix} 1 & 0 \\ 2 & 1 \end{smallmatrix}\right)$, Ω from (XV.3.54), and source coefficients $X = (3/2, -2/3)^{\mathsf{T}}$ along a common formal four-form. Give Ω', X', Y', and the old and new scalar coefficients of the square of that form. Explain the different transformation rules for the two source columns.

5. **Change a compact count.** Use the CHAIN46 compact comparison. Hypothetically add one abelian vector and five charged hyper components, keeping T and the old required neutral count fixed. Give the old required neutral count, the p_2 residual and the neutral shift required to remove it. Explain why this is only an irreducible gravity test of hypothetical data.

6. **Remove the common hyper.** Compare the $(4, 5)$ chain with a shared full hyper to the model where external fundamentals replace its spectator traces at

each node. Keep the same lattice and switch off the flavor probes. Give both quartic coefficient columns, both one-loop $s_1 s_2$ coefficients and both coefficients after adding the same square. Explain what additional input would be needed to compare background anomalies to a UV theory.

Use `benchmark/tasks.json` for the JSON fields and `benchmark/PROTOCOL.md` for submission. Written explanations are assessed by a reader.

Status and sources

§1. Local polynomial and projection. The descent and gauge test are [ANOM], in the integral differential-form descent convention of Ohmori et al. (2014), arXiv:1408.5572v2, §2.1. The background-only polynomial is restricted to the indicated probes.

§2. Weight sums and the multiplet index. The adjoint, antisymmetric, product and low-rank trace identities are [MATH]. The multiplet polynomials are [ANOM], with the full-hyper and chiral tensor conventions of Ohmori et al. (2014), Appendix A, eqs. (A.1)–(A.4). The weight calculation uses their anti-Hermitian curvature frame.

§3. Negative section. The residual and intersection calculations are [MATH], using the Weierstrass convention $\Delta_{\text{book}} = 4f^3 + 27g^2$ and the near-curve input of Chapter 1. The ordinary localized spectrum is [GEO-E]; see Morrison and Taylor (2012), arXiv:1106.3563v3, §3.2, eqs. (3.23),(3.28) and the following SU(5) discussion. The transverse I_6 orders use the actual germ calculation. The loop coefficients are [ANOM] with this spectrum. The sparse witness is not a regular compact member.

§4. The shared hyper. The ordinary branch matter input of B.1 is [GEO-E]; see Morrison and Taylor (2012), §2.3, eq. (2.26) and §3.3, eqs. (3.58),(3.61). The loop including mixed gauge terms is [ANOM]. Split tangents, simple residual points and a transverse corner enter the ordinary matter rule.

§5. Source pairing and retained coefficients. The geometric tensor and source dictionary is [GEO-E], assuming the retained modes of B.2. See Ohmori et al. (2014), §3.3.1, eqs. (3.26)–(3.33) and footnote 6 for the five-form sign. The gauge and background identities are [ANOM], with §2.1 and §3.1, eqs. (3.1)–(3.5); the basis calculations are [MATH]. Solving mixed coefficients does not establish independent background geometry or UV matching.

§6. The even retuning. The Cox lifts, crepant charts, residuals and node calculation are [MATH]. The ordinary matter inference is [GEO-E], with the same hypotheses and physical source as §4. Cancellation and the stale-spectrum obstruction are [ANOM]. The near-curve calculation uses no assertion of a resolution away from the selected strata.

§7. Compact conditions. The gravity index, compact count and full-signature cancellation are [ANOM]. See Alvarez-Gaumé and Witten (1984), §7 and §12, eqs. (114),(116),(118), and Kumar et al. (2010), arXiv:1008.1062v1, §2.1, eqs. (2.1)–(2.13) and §5.1, eqs. (5.1)–(5.5). The geometric intersection comparison is [MATH] in the indicated SU normalization. The compact factorized polynomial in the latter source is the loop term. The neutral requirements assume the stated charged content and compact tensor and gravity multiplets; no separate neutral count is given.

References

Alvarez-Gaumé, L. and E. Witten (1984). "Gravitational anomalies". In: *Nucl. Phys. B* 234, pp. 269–330. DOI: 10.1016/0550-3213(84)90066-X.

Kumar, V., D. R. Morrison, and W. Taylor (2010). "Global aspects of the space of 6D N=1 supergravities". In: *JHEP* 11, p. 118. arXiv: 1008.1062 [hep-th].

Morrison, D. R. and W. Taylor (2012). "Matter and singularities in F-theory models". In: *JHEP* 01, p. 022. arXiv: 1106.3563 [hep-th].

Ohmori, K. et al. (2014). "Anomaly polynomial of general 6D SCFTs". In: *PTEP* 2014, 103B07. arXiv: 1408.5572 [hep-th].

Chapter XV.4

Non-Higgsable clusters and gauge tuning

XV.4.1 Sections restricted to a negative curve

How can a seven-brane gauge sector be compulsory when the coefficients of the elliptic equation are still free? The freedom to choose a polynomial in one coordinate patch can overstate the freedom to choose a section on the base. Along a negative curve the leading coefficient can have negative degree. It must then vanish, so the fiber degenerates on the whole curve. We will first compute this restriction and then lift the coefficients on a ruled surface. After that we can ask two separate questions: which components can be labeled consistently along the curve, and whether the proposed tuning creates points at which the original base must be changed. We use the local fiber dictionary of IV.8, the two-curve construction of B.1, and the anomaly conventions of B.3.

Let B be a smooth complex surface and $L = \mathcal{O}_B(-K_B)$ the anticanonical line bundle. We use the short Weierstrass equation and the following discriminant convention:

$$y^2 = x^3 + fx + g, \qquad f \in H^0(B, L^4), \quad g \in H^0(B, L^6), \qquad \Delta = 4f^3 + 27g^2. \tag{XV.4.1}$$

The elliptic discriminant is -16Δ; the discriminant of the monic polynomial $X^3 + fX + g$ is $-\Delta$. We distinguish two orders. The order along C counts the power of a local normal equation $z = 0$ at the generic point. At a closed point p in coordinates z, w centered at p, the order is the smallest total degree in the two variables. In particular, a unit along the generic curve can still vanish at p.

$$\nu_C(z^a h) = a \quad (h|_C \not\equiv 0), \qquad \nu_p\Big(\sum h_{ij} z^i w^j\Big) = \min_{h_{ij} \neq 0} (i + j). \tag{XV.4.2}$$

Suppose $C \simeq \mathbb{P}^1$ and $C^2 = -n$. Adjunction gives

$$(K_B + C) \cdot C = -2, \qquad K_B \cdot C = n - 2. \tag{XV.4.3}$$

For a section of $-kK_B$ divisible by z^a, dividing in a local frame leaves a section of $-kK_B - aC$. Restrict that section to C. If the restriction vanishes, it has another factor z. Globally this is the kernel statement in

$$0 \longrightarrow \mathcal{O}_B(-kK_B - (a+1)C) \longrightarrow \mathcal{O}_B(-kK_B - aC) \longrightarrow \mathcal{O}_C(-kK_B - aC) \longrightarrow 0. \tag{XV.4.4}$$

The line on the right has degree

$$d_{k,a} = (-kK_B - aC) \cdot C = k(2-n) + na. \tag{XV.4.5}$$

A negative degree line on $\mathbb{P}^1$ has no nonzero section: the zero divisor of such a section would have negative degree. Hence the first candidate for a nonzero residue is

$$a \;\geq\; \max\{0, \lceil k(n-2)/n \rceil\} \qquad (n > 0). \tag{XV.4.6}$$

In divisor language, the residual effective divisor with C removed has nonnegative intersection with C. The two arguments give the same bound. Nonnegative degree by itself does not make the restriction map on global sections surjective. Also, the bound for $k = 12$ concerns a section of that class; a Weierstrass discriminant is constrained by (XV.4.1).

For actual lifts use the ruled surface $\mathbb{F}_n$. The section S has square $-n$; a ruling fiber F_{b} has square zero and meets S once. Adjunction on these two rational curves fixes the canonical class. Write $[U : V]$ for the base of the ruling and Z, W for homogeneous fiber coordinates:

$$K_B = -2S - (n+2)F_{\mathrm{b}}, \tag{XV.4.7}$$

$$[U] = [V] = F_{\mathrm{b}}, \qquad [Z] = S, \qquad [W] = S + nF_{\mathrm{b}}, \tag{XV.4.8}$$

$$S = \{Z = 0\}. \tag{XV.4.9}$$

The two Cox scalings encode these classes. For a homogeneous polynomial $p_a(U, V)$ of degree $d_{k,a}$, its lift and its class are

$$\sigma_{k,a} = Z^a W^{2k-a} p_a(U, V), \tag{XV.4.10}$$

$$[\sigma_{k,a}] = 2kS + [n(2k-a) + d_{k,a}]F_{\mathrm{b}} = -kK_B. \tag{XV.4.11}$$

Here $0 \leq a \leq 2k$. Conversely every monomial of class $-kK_B$ has these exponents and that degree. For example, at $n = 2$ the term with $a = 0$ is W^{2k} times a constant. At $n = 3$ the $a = 1$ term of f would require degree -1, while $a = 2$ permits every quadratic. At $a = 2$ the g residue has degree zero. Evaluating the ceiling for $k = 4, 6, 12$ gives

n	2	3	12
(a_4, a_6, a_{12})	$(0, 0, 0)$	$(2, 2, 4)$	$(4, 5, 10)$

(XV.4.12)

These lifts explain why it is meaningful to ask whether the first possible residue actually survives.

The same lift also tells us how to compute at infinity. In the frame $V = W = 1$ write $z = Z/W, w = U/V$, understood as the normalized affine coordinates. In the

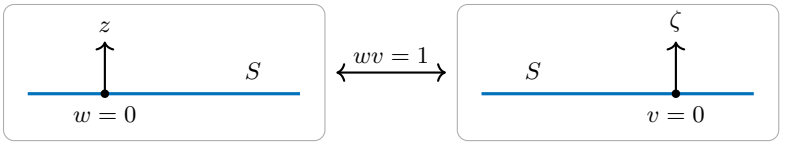


Figure XV.4.1: Two frames near the negative section S. The normal coordinate vanishes along S. The ruling coordinates overlap away from $0, \infty$; the coefficient frames on S differ by $v^{d_{k,a}}$. The point $V = 0$ is visible at $v = 0$ in the right frame.

frame $U = W = 1$ write ζ, v. On the overlap the base scaling takes $(U, V) = (w, 1)$ to $(1, v)$. It rescales W by v^n; restoring $W = 1$ gives $\zeta = v^{-n} z$. Thus, in the two frames,

$$w = v^{-1}, \qquad z = v^n \zeta, \tag{XV.4.13}$$

$$\sigma_k^{(U)}(\zeta, v) = v^{k(2-n)} \sigma_k^{(V)}(v^n \zeta, v^{-1}), \tag{XV.4.14}$$

$$p_a^{(U)}(v) = v^{d_{k,a}} p_a^{(V)}(v^{-1}). \tag{XV.4.15}$$

The last identity follows term by term from (XV.4.11); it removes the apparent pole of every allowed polynomial. For example on $\mathbb{F}_3$ the f_2 lift with $p_2 = U^2$ becomes ζ^2 in the second chart. The choice $p_2 = V^2$ would become $\zeta^2 v^2$ there. Both have degree two on S, but their doubled zeros lie in different charts. Figure XV.4.1 records the frame change used below. In particular the degree of a dehomogenized polynomial need not equal the total degree of its zero divisor on S.

There is a complementary chart check away from S. The two scalings of the homogeneous coordinates, with parameters α, β, act as

$$(U, V, Z, W) \longmapsto (\beta U, \beta V, \alpha Z, \alpha \beta^n W). \tag{XV.4.16}$$

They let us set $Z = 1$ away from S, in addition to $V = 1$ or $U = 1$. In the $V = 1$ base frame, the change from $W = 1$ to $Z = 1$ rescales by $\alpha = z^{-1}$. It sends z to the reciprocal coordinate $q = W/Z$ and the section is multiplied by q^{2k}:

$$\sigma_k^{(V,Z)}(q, w) = q^{2k} \sigma_k^{(V,W)}(1/q, w) = \sum_a q^{2k-a} p_a(w, 1). \tag{XV.4.17}$$

Here the first equality holds on the overlap and the right side is regular at $q = 0$. In the $U = 1$ base frame one obtains the same sum with $p_a(1, v)$. The limiting coefficient at $q = 0$ is therefore p_{2k} evaluated in the corresponding base frame. This gives an elementary way to test whether a model that works near S fails at the other section $W = 0$. We will see both outcomes.

XV.4.2 A forced type-IV sector

What actually survives at the first allowed order on the isolated negative section of $\mathbb{F}_3$? The degree computation gives $f_2 \in H^0(S, \mathcal{O}(2))$ and $g_2 \in H^0(S, \mathcal{O})$. The latter can be

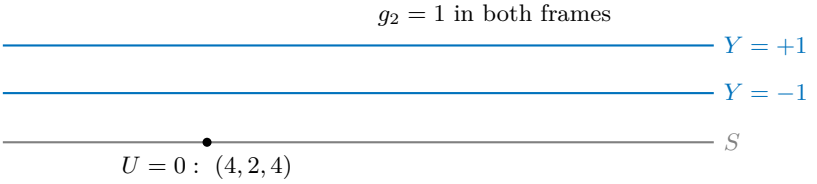


Figure XV.4.2: The forced IV section of (XV.4.18). The point $U = 0$ changes the order of f, but the residual discriminant has no zero anywhere on S. The separate horizontal lines indicate the two globally labeled sheets of the constant cover.

a unit everywhere on S, as realized by the exact model

$$f = Z^2W^6U^2 + Z^8(U^{20} + 2V^{20}), \qquad g = Z^2W^{10}. \tag{XV.4.18}$$

In the full coefficient space, $g_2 \neq 0$ is a nonempty open condition because the displayed section realizes it. The generic orders are $(2, 2, 4)$ on the subopen with $f_2 \neq 0$. More explicitly, if $f = z^2\widehat{f}$, $g = z^2\widehat{g}$, the discriminant residual is

$$z^{-4}\Delta = 4z^2\widehat{f}^{\,3} + 27\widehat{g}^{\,2}, \qquad (z^{-4}\Delta)|_S = 27g_2^2. \tag{XV.4.19}$$

The coefficient line of this last expression has degree $d_{12,4} = 0$. There is no collision with a residual discriminant along S. At $U = 0$, by contrast, the leading coefficient of f has a double zero. In the $V = W = 1$ chart the first terms are $z^2w^2, z^2, 27z^4$ for f, g, Δ. Therefore at the point

$$(\nu_p(f), \nu_p(g), \nu_p(\Delta)) = (4, 2, 4). \tag{XV.4.20}$$

The extra vanishing of f alone has no effect on the discriminant order.

Now divide the fiber equation by z^2 after setting $x = zX, y = zY$. Its leading equation is

$$Y^2 = zX^3 + z\widehat{f}X + \widehat{g}, \qquad Y^2|_{z=0} = g_2. \tag{XV.4.21}$$

The component labels are the two roots over the field $\mathbb{C}(S)$ of rational functions on S. The residue lies in the square of the root line, $(-3K_B - S)|_S$; its degree is zero here. A change of frame rescales g_2 by a square. In one global frame g_2 is a nonzero complex constant and has a complex square root. The conclusion is unchanged if we replace 1 in (XV.4.18) by 2: splitting is over $\mathbb{C}(S)$, even when the constant is not a square over $\mathbb{Q}$. The two roots remain distinct and can be labeled consistently. This transport of component labels along the curve is different from transverse elliptic monodromy on one-cycles.

It helps to compare the coefficient lines of the three leading terms. They have degrees $2, 0, 0$ for f, g, Δ. Thus a nonzero f_2 must have zeros, whereas g_2 and the leading discriminant can be units. Indeed the order of f along S can be raised further by setting the entire f_2 to zero:

$$f_2 = 0, \quad g_2 \neq 0 \quad \Longrightarrow \quad \nu_S(f) \geq 3, \quad \nu_S(g) = 2, \quad \nu_S(\Delta) = 4. \tag{XV.4.22}$$

The z^0 equation of the cover in (XV.4.21) does not change. The forced degeneracy is a property of the available sections. It does not depend on restricting attention to the member with a particular f_2.

The local algebra dictionary assigns split IV to $\mathfrak{su}(3)$ under the ordinary minimal F-theory hypotheses. The isolated-cluster matter rule gives no localized charged hypers on this S: there are no residual intersections and the genus is zero. The pure gauge description applies to the specified sector. Neither statement determines the global form of the gauge group or all sectors of a compact model. A separate check on the displayed coefficients shows that no point away from S has orders $(4, 6)$ or worse. This check will also be useful for the later ruled examples.

On $Z \neq 0$ use $q = W/Z$ in either normalized base frame. The examples with $f = f_a Z^a W^{8-a} + f_8 Z^8$ have

$$f = Aq^{8-a} + B_8, \qquad \partial_q f = (8-a)Aq^{7-a}. \tag{XV.4.23}$$

For (XV.4.18), $A = U^2, B_8 = U^{20} + 2V^{20}$ are evaluated in the relevant frame and have no shared projective zero. If $q \neq 0$ and $f = 0$, then $A \neq 0$ and the derivative is nonzero. If $q = 0$ and $f = 0$, use a base derivative of B_8. In the $V = 1$ frame its roots solve $w^{20} = -2$ and have $20w^{19} \neq 0$. In the $U = 1$ frame it takes value 1 at $v = 0$. Thus f has order at most one at every zero off S. For the $\mathbb{F}_2$ examples the power 20 is replaced by 16; the same argument checks simplicity. The additional requirement that A, B_8 have disjoint zeros will be checked for the actual choices. This is a point-order calculation; it does not give a smooth resolved threefold.

We can compare the isolated sector to the mixed-gauge and gauge-square conditions of B.3. Use formal traceless Cartan eigenvalues x_i, $i = 1, 2, 3$, and $s = \sum_i x_i^2$. With $x_3 = -x_1 - x_2$ the fourth moment is $\sum_i x_i^4 = s^2/2$. The positive moments of the adjoint are sums over $x_i - x_j$, and the terms with a single power on one side vanish by tracelessness. Thus

$$\mathrm{tr}_{\mathrm{adj}}\, F^2 = 6s, \tag{XV.4.24}$$

$$\mathrm{tr}_{\mathrm{adj}}\, F^4 = 6\sum_i x_i^4 + 6s^2 = 9s^2. \tag{XV.4.25}$$

The low-rank relation used here can also be obtained without choosing a basis for the Cartan. Since $x_1 + x_2 + x_3 = 0$, $\sum_{i<j} x_i x_j = -s/2$. Squaring this last sum gives $\sum_{i<j} x_i^2 x_j^2$, because the cross terms are proportional to $x_1 x_2 x_3 (x_1 + x_2 + x_3)$. Hence

$$\sum_{i<j} x_i^2 x_j^2 = s^2/4, \qquad \sum_i x_i^4 = s^2 - 2\sum_{i<j} x_i^2 x_j^2 = s^2/2. \tag{XV.4.26}$$

There is only the square invariant in this comparison. The absence of an independent quartic here is a weight identity; it does not mean the adjoint makes no fourth-order contribution.

For the defining reference trace the factor λ is one. In the convention $a = K_B, b = S$, the pure-sector conditions compare these traces to

$$K_B \cdot S = \frac{6}{6} = 1, \qquad S^2 = -\frac{9}{3} = -3. \tag{XV.4.27}$$

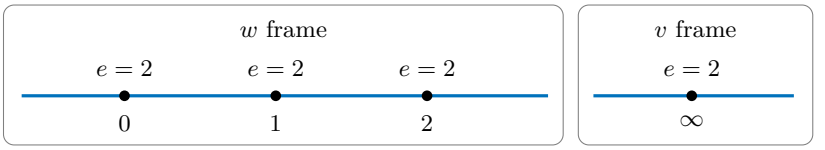


Figure XV.4.3: Branch divisor of the normalized double cover in (XV.4.29). The points $0, 1, 2$ are in the w-chart, and the fourth zero is at $v = 0$. Each mark has index two. The line indicates the base of the cover, not an embedding of its genus-one total space.

They agree with (XV.4.3) and the self-intersection. In this comparison the spectrum came from the isolated geometry and the local matter rule. Solving these two equations cannot produce the unit in (XV.4.19). We next change the residue line so that a nonzero section need not be a unit.

XV.4.3 A non-split comparison

How can the same divisorial orders give different algebras, and how can a neighboring curve constrain the very existence of a split tuning? We first vary a double cover while keeping the base fixed. Then we change the base and derive the leading cubic from simultaneous constraints. In both cases the relevant field is the function field of the gauge curve.

The $\mathbb{F}_2$ section has no forced vanishing. For instance take $f = W^8 + Z^8(U^{16} + 2V^{16})$, $g = W^{12}$; on S the discriminant is 31 in the constant frame and the generic fiber is I_0. To tune IV, suppress the earlier coefficients and take the lifts

$$f_2 = U^4 + 2V^4, \quad f_8 = U^{16} + 2V^{16}, \qquad g_2 = UV(U - V)(U - 2V). \tag{XV.4.28}$$

Coefficients not written are zero. These are sections of the degrees required by (XV.4.5). The equations in the two frames for the double cover are

$$Y^2 = w(w - 1)(w - 2), \qquad \widetilde{Y}^{\,2} = v(1 - v)(1 - 2v), \qquad \widetilde{Y} = v^2 Y. \tag{XV.4.29}$$

The right frame accounts for the fourth simple zero at $V = 0$. At a simple zero the valuation is odd, while the valuation of a square of any rational function is even. This proves generic irreducibility and explains why a local choice of complex square root away from the zeros cannot label the components globally. Near a simple zero the equation is $Y^2 = u$ times a unit, for a local coordinate u; extracting the unit's analytic square root gives ramification index two. The function-field cover is connected, and on its normalization

$$2g_{\mathrm{cov}} - 2 = 2(-2) + 4(2 - 1) = 0. \tag{XV.4.30}$$

Thus the genus of this cover is one. It is not the genus of the gauge curve.

The point-order computation on the surface uses z as well. At each branch point f_2 is a unit, with values $2, 3, 18, 1$ in the indicated finite and infinite frames. With local parameter u along S, the leading forms of f and g are proportional to z^2 and $z^2 u$. The

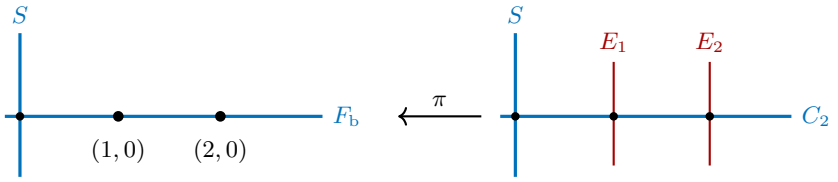


Figure XV.4.4: The blowups producing the retained $(-3,-2)$ pair. Both centers lie on the original ruling fiber away from the corner. After the blowups, C_2 meets the exceptional curves at distinct points; S still meets C_2 at $z = w = 0$.

two terms of Δ have degree six but different monomials, z^6 and z^4u^2, so they do not cancel:

$$(\nu_p(f), \nu_p(g), \nu_p(\Delta)) = (2, 3, 6). \tag{XV.4.31}$$

Now replace g_2 by $(U^2 + V^2)^2$. The generic orders remain $(2, 2, 4)$. In the two frames the roots are $\pm(w^2 + 1)$ and $\pm(1 + v^2)$. At $w = \pm i$, $f_2 = 3$ and g_2 has a double zero. The leading z^2u^2 term of g now gives order four, while f^3 still gives order six. The normalized cover has separate sheets even though they meet in the displayed polynomial model at the double zeros. Both models pass the off-section f test of (XV.4.23): a zero of $U^4 + 2V^4$ in $V = 1$ has $w^{16} = 16$, hence $B_8 = 18$; at $V = 0$ both are units. The control with $f_0 = 1$ has no common zero either. The ordinary IV dictionary gives $\mathfrak{sp}(1) \cong \mathfrak{su}(2)$ for the connected cover and $\mathfrak{su}(3)$ for the split cover. For the former the defining quadratic trace has weights $x, -x$, giving $2x^2$ in either description, with $\lambda = 1$. Branch count alone has supplied no charged multiplicities.

We can see the distinction between the split and nonsplit zeros directly in a small neighborhood of a point of the curve. Let u be a local parameter on S. After rescaling Y by a square root of a unit, a simple zero gives $Y^2 = u$. A double zero of the square gives $Y^2 = u^2$. In the second case the normalization is obtained by taking the two branches separately. Their maps to S are the identity in the coordinate u. Explicitly,

$$Y^2 = u: \qquad u = Y^2, \quad e = 2, \tag{XV.4.32}$$

$$Y^2 = u^2: \qquad (Y, u) = (u, u), (-u, u), \quad e = 1, 1. \tag{XV.4.33}$$

The two raw roots agree at $u = 0$ in both equations. This agreement cannot by itself tell us whether the sheets exchange. The cubic example will require the same distinction, with three generic labels instead of two.

To obtain a coupled example, blow up $\mathbb{F}_3$ at $(z, w) = (1, 0), (2, 0)$, away from S. If E_1, E_2 are the exceptional curves, the strict fiber is $C_2 = F_b - E_1 - E_2$. Here and below classes S, F_b on the blowup denote pullbacks. They have zero intersection with E_j; $E_i \cdot E_j = -\delta_{ij}$. The retained intersections are

$$S^2 = -3, \quad C_2^2 = -2, \quad S \cdot C_2 = 1, \qquad K_B \cdot S = 1, \quad K_B \cdot C_2 = 0. \tag{XV.4.34}$$

For a section of $-kK_B$ with exact multiplicities a, b on the two curves, remove those

curves. Nonnegative residual intersections with both require

$$(-kK_B - aS - bC_2)\cdot S = 3a - b - k \geq 0, \qquad (-kK_B - aS - bC_2)\cdot C_2 = 2b - a \geq 0. \tag{XV.4.35}$$

In particular $b \geq \lceil a/2 \rceil$. For $k = 4$, $a \leq 1$ cannot satisfy the first inequality and $(a, b) = (2, 1)$ satisfies both. For $k = 6$, $a = 2$ gives $3a - b \leq 5$; at $a = 3$, $b \geq 2$ and $b = 2$ works. For $k = 12$, $a = 4$ gives at most 10 and $a = 5, b = 3$ works. Smaller a give still smaller $3a - \lceil a/2 \rceil$, and the lower bounds on b are monotone. These are the componentwise least lattice pairs. Now use the actual discriminant: f^3 has at least the pair $(6, 3)$, g^2 at least $(6, 4)$. The effective-class candidate $(5, 3)$ is therefore impossible for the discriminant of this pair.

We can attain the strengthened orders near the two curves. Put $D(z) = (z-1)(z-2)/2$ and take

$$f = z^2 w D(z)^3, \qquad g = z^3 w^2 D(z)^4, \tag{XV.4.36}$$

$$\Delta = z^6 w^3 D(z)^8 [4D(z) + 27w]. \tag{XV.4.37}$$

These are affine expressions for actual homogeneous sections downstairs: the f exponents of z run from 2 to 8 with base power w^1 allowed by $d_{4,a} = 3a - 4 \geq 2$. The g exponents run from 3 to 11 with w^2 allowed by $d_{6,a} = 3a - 6 \geq 3$. At either center $z = c \in \{1, 2\}$ let $h = z - c$ and $D(c + h) = h d_c(h)$, where $d_c(0) = (2c-3)/2 \neq 0$. The orders there are $4, 6$. By $K_{\text{new}} = \pi^* K_{\text{old}} + E$, the new coefficients divide the pullbacks by the exceptional coordinate to powers $4, 6$. In the two blowup charts the quotients are

$$(h, w) = (e, et): \qquad (f', g') = ((c+e)^2 t d_c(e)^3,\ (c+e)^3 t^2 d_c(e)^4), \tag{XV.4.38}$$

$$(h, w) = (es, e): \qquad (f', g') = ((c+es)^2 s^3 d_c(es)^3,\ (c+es)^3 s^4 d_c(es)^4). \tag{XV.4.39}$$

The exceptional coordinates in the two rows are related by $e_w = t e_h$ and $s = 1/t$; the second quotients are t^{-4}, t^{-6} times the first. In the first chart the strict fiber is $t = 0$. At its meeting with E the orders are $(1, 2, 3)$ because $c, d_c(0) \neq 0$. This also shows that f'/t is a unit there. Away from the centers and S, the residual coefficient $z^{-2} f/w = D^3$ is a unit on the finite strict fiber; at its fiber-coordinate infinity $q = 1/z = 0$, the regular coefficient of f/w is

$$q^8 z^2 D(z)^3\big|_{z=1/q} = \tfrac{1}{8}(1-q)^3(1-2q)^3. \tag{XV.4.40}$$

It is also a unit there.

Along S, the generic orders from (XV.4.37) are $(2, 3, 6)$, while on C_2 they are $(1, 2, 3)$. At the corner $z = w = 0$, $D(0) = 1$ and the orders are $(3, 5, 9)$. At $w = -4/27$ the bracket has a simple zero along S and both leading Weierstrass coefficients are units after dividing out the powers of z. Thus the point has orders $(2, 3, 7)$. In the $U = W = 1$ frame, (XV.4.15) gives

$$f = \zeta^2 v D(v^3\zeta)^3, \qquad g = \zeta^3 v D(v^3\zeta)^4. \tag{XV.4.41}$$

At $zeta = v = 0$ this gives $(3, 4, 8)$, since the square term of the discriminant leads. Every point of the retained union passes the $(4, 6)$ test, so the open complement of the closed bad locus contains that union.

There is an actual failure away from the union. In the chart $U = Z = 1$, put $v = V/U$ and use $q = W$ in that frame. The $z^a w^b$ monomial becomes $q^{2k-a} v^{d_{k,a}-b}$. For f the lowest total degree term comes from $a = 2, b = 1$, giving $q^6 v$; for g it comes from $a = 3, b = 2$, giving $q^9 v$. Both have coefficient one. Increasing a by one raises the total degree by two. The remote point $q = v = 0$ consequently has orders

$$(\nu_p(f), \nu_p(g), \nu_p(\Delta)) = (7, 10, 20), \tag{XV.4.42}$$

with g^2 of lower order than f^3. Our sparse witness is useful near the retained pair and fails as a globally minimal compact model.

What components are transported along S? The leading I_0^* cubic has root coordinate X in the frame of $(-2K_B - S)|_S$. Its coefficients are the restrictions of $f/z^2, g/z^3$ in (XV.4.37):

$$R(X) = X^3 + wX + w^2, \qquad \operatorname{disc}_X R = -w^3(4 + 27w). \tag{XV.4.43}$$

If a root lies in $\mathbb{C}(w)$, write it p/q with relatively prime polynomials. Clearing denominators in the monic equation gives $q \mid p^3$, so q is a unit. A polynomial root of degree $d \geq 2$ would have $3d > \max(d + 1, 2)$, which leaves its highest term uncanceled. Its constant term must vanish at $w = 0$; the only candidates are $X = hw$. Substitution gives

$$R(hw) = w^2[(h + 1) + h^3 w]. \tag{XV.4.44}$$

The two coefficients cannot vanish together. More generally the leading polynomials have the allowed shapes $w(A + Bw), w^2(C + Dw)$, now with A, B, C, D constants. The same argument bounds the root degree since the coefficient degrees are at most two and three. For $A \neq 0$ the root test is

$$Ah + C = 0, \qquad h^3 + Bh + D = 0. \tag{XV.4.45}$$

Eliminating $h = -C/A$ gives a closed condition inside $A \neq 0$. Our coefficients lie outside it, so irreducibility is realized on a nonempty open of the actual leading family.

The permitted coefficient variations really occur on the surface. Starting with (XV.4.37), replace the factor w in f by $w(A + Bw)$ and w^2 in g by $w^2(C + Dw)$. The largest new powers of w are 2 and 3, at or below the minimum degrees $d_{4,2} = 2$ and $d_{6,3} = 3$. At the blowup centers the same factors h^3, h^4 remain in the powers of $D(z)$, so the chart division is still regular. For example $A = C = 1, B = 0, D = 1$ gives slope $h = -1$ with vanishing remaining coefficient, whereas $A = C = 1, B = D = 0$ gives the remaining coefficient -1. The cover type can change within the realized coefficients without a new negative-curve degree calculation.

The raw discriminant vanishes to order three at $w = 0$. To find the true ramification, set $t = X/w$ at generic $w \neq 0$, then solve the resulting linear equation for w:

$$w = -\frac{t + 1}{t^3}, \qquad X = -\frac{t + 1}{t^2}, \qquad \frac{dw}{dt} = \frac{2t + 3}{t^4}. \tag{XV.4.46}$$

This is a rational parameter of the function field, hence the normalization is $\mathbb{P}^1_t$. At $t = -1$ the zero of w is simple; at $t = \infty$, $w = -(1 + s)s^2$ with $s = 1/t$, so its zero is

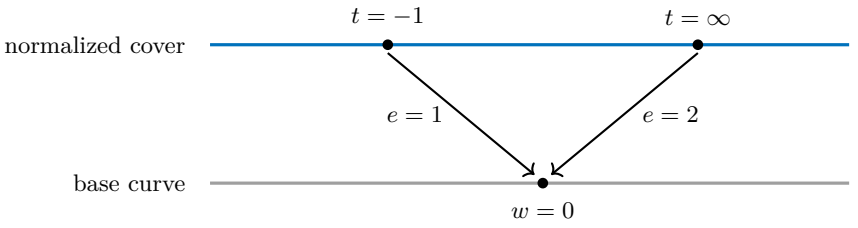


Figure XV.4.5: The two normalized points above $w=0$ under (XV.4.46). The point $t=-1$ supplies one unramified sheet. Near $t=\infty$ the two sheets have parameter $s=1/t$ and exchange around $w=0$. Both points are sent to the same root $X=0$ in the raw polynomial model.

double. The derivative has a simple zero at $t=-3/2$, mapping to $w=-4/27$. Finally $t=0$ is a pole of order three. The contributions $e-1$ above $w=0,-4/27,\infty$ are respectively $1,1,2$, summing to 4 as required for a degree-three map between rational curves.

We can also recover the order-three discriminant zero from the root differences. The sheet near $t=-1$ has $X=wt=-w+O(w^2)$. At the other point, $X=-s(1+s)$ while $w=-s^2(1+s)$. In a sector with a chosen $\sqrt{-w}$, the three roots therefore start as

$$X_0=-w+O(w^2),\qquad X_\pm=\pm\sqrt{-w}+O(w). \tag{XV.4.47}$$

All three pairwise differences start at order $w^{1/2}$, so their squared product has order three. A loop about $w=0$ only exchanges X_+ and X_-. The difference calculation remembers that even the unramified sheet collides in the raw polynomial model, whereas the normalized points in Figure XV.4.5 are separate. Thus the discriminant multiplicity is not a count of ramified points. Neither calculation is a localized matter computation.

For an actual partial splitting change g to $(1+w)g$. The extra power of w remains within the Cox degrees and preserves the center divisibilities. The new cubic factors as

$$(X+w)(X^2-wX+w+w^2),\qquad \operatorname{disc}_X(X^2-wX+w+w^2)=-w(4+3w). \tag{XV.4.48}$$

The quadratic has no rational root, by the odd valuation of its discriminant at zero. At the corner the factor $1+w$ is a unit and the orders remain $(3,5,9)$. The ordinary minimal dictionary gives $\mathfrak{g}_2$ on S for the original irreducible cubic and $\mathfrak{su}(2)$ on its type-III neighbor. It gives $\mathfrak{so}(7)$ on the generic curve in the semisplit case where the same local dictionary applies. No entire family of global completions or localized matter assignments follows from this comparison.

To split completely, one can try multiplying both f,g of (XV.4.37) by w. The cubic is $w^3(t^3+t+1)$ after $X=wt$; the three constant roots are distinct. The corner now has $(4,6,12)$, and the generic neighbor also changes to $(2,3,6)$. There is a separate obstruction that does not require changing the generic neighbor. In any split attempt with the original obligatory factors z^2w,z^3w^2, use the discrete valuation ring of $w=0$ on S. Each rational root of the monic cubic is regular there by integrality. Modulo w all roots are zero because the reduced polynomial is X^3. The elementary symmetric

functions therefore satisfy

$$X_j \in w\mathcal{O}_{S,0} \quad \Longrightarrow \quad f_2 \in (w^2), \qquad g_3 \in (w^3). \tag{XV.4.49}$$

Terms one order higher in z still carry at least w in f and w^2 in g. They cannot reduce the corner orders below $4, 6$. The split dictionary label $\mathfrak{so}(8)$ at the generic point would not pass the fixed-base point test. We now use that point test to compare two exceptional tunings on a single curve.

XV.4.4 An allowed gauge tuning

How far can we enhance the isolated split IV sector on the same $\mathbb{F}_3$? A choice of higher powers of Z is only the first step. We must make the leading cover square if we want the split algebra, and then inspect every zero of its leading coefficient. We keep the base fixed, including its two projective charts.

To impose generic IV^*, take the f coefficients to start at order three and the g coefficients at order four. In the lift (XV.4.11) choose

$$f_3 = U^5, \qquad f_8 = U^{20} + 2V^{20}, \tag{XV.4.50}$$

$$g_4 = P^2, \qquad g_5 = U^9, \qquad P = V(U - V)(U - 2V). \tag{XV.4.51}$$

The residue degrees $5, 20, 6, 9$ follow from (XV.4.5). The root line $(-3K_B - 2S)|_S$ has degree three, so a cubic P gives a square in the correct line. With hats denoting the coefficients after removing z^3, z^4, respectively, we obtain

$$f = z^3\widehat{f}, \qquad g = z^4\widehat{g}, \qquad z^{-8}\Delta = 4z\widehat{f}^{\,3} + 27\widehat{g}^{\,2}. \tag{XV.4.52}$$

The orders $(3, 4, 8)$ are exact generically. In the leading fiber equation set $x = z^2X, y = z^2Y$; after division by z^4, the terms involving X are $z^2X^3 + z\widehat{f}X$. Thus the two branches at $z = 0$ have equation

$$Y^2 = g_4 = P^2. \tag{XV.4.53}$$

This determines the splitting; it has not yet tested minimality at the zeros.

In $V = W = 1$, the leading square root is $(w - 1)(w - 2)$ and the other residues are w^5, w^9. In $U = W = 1$, the square root is $v(1 - v)(1 - 2v)$, and the other residues are both 1. The three roots $w = 1, 2$ and $v = 0$ are simple roots of P, and both other residues are units at each root. Near one of them put $u = 0$ on the base of the ruling and write $P = uA(u)$ with $A(0) \neq 0$. Then

$$f = z^3(f_3(u) + O(z^5)), \qquad g = z^4u^2A(u)^2 + z^5g_5(u). \tag{XV.4.54}$$

The z^5 term is the first one in total degree in g, while f^3 has degree nine and is of lower order than g^2. This gives $(3, 5, 9)$ at all three points. Elsewhere on S, g_4 is nonzero. At $U = 0$, where f_3 and g_5 do vanish, $g_4 = 4$ in $V = 1$ and g has order four. Thus a zero of f_3 does not create a nonminimal point there. The off-S test (XV.4.23) works since $A = U^5$ vanishes only at $U = 0$, where $B_8 \neq 0$. This proves that these

Weierstrass coefficients have no $(4,6)$ point on the original base. With the ordinary minimal dictionary the split IV^* gives $\mathfrak{e}_6$.

To separate the two tests, first preserve the orders and change the cover. Replace g_4 by

$$g_4 = V\prod_{j=1}^{5}(U - jV). \tag{XV.4.55}$$

It has degree six again, but now five simple finite zeros and one at infinity. Its odd valuations rule out a square. The algebra given by the ordinary dictionary is $\mathfrak{f}_4$. The same f_3, g_5 are units at each root. The local leading terms are now z^3 in f, and two distinct degree-five terms z^4u and z^5 in g. The exact orders are again $(3,5,9)$ at all six points. All six pass the point test, and the off-S proof is unchanged because f did not change. The split and nonsplit choices illustrate how the same triple of generic orders and even the same local triple at each residual root can coexist with different generic algebras.

There is a related discriminant calculation on the curve. Divide out z^8 and then restrict to S. For the square choice the restriction is $27P^4$, whereas for the nonsquare choice it is $27g_4^2$. At any root in either model the full residual in the surface has normal derivative

$$\partial_z\big(\Delta/z^8\big)\big|_{z=u=0} = 4f_3(0)^3. \tag{XV.4.56}$$

The derivative of the square term vanishes there because $g_4(0) = 0$. The residual is therefore smooth at those roots, even though its restriction to S vanishes to order four in the split example and two in the nonsplit example. The residual divisor class has degree $d_{12,8} = 12$; the two distributions give $3 \cdot 4 = 6 \cdot 2 = 12$. This counts intersections with multiplicity. It neither counts branch points of the cover nor labels particles. In particular it gives the same total for the two different algebras.

For example at $w = 1$ in the square model, put $u = w - 1$ and write $P = u(-1 + u)$. Along $z = 0$ the residual is $27u^4(-1 + u)^4$, and its normal derivative at the origin is 4. The implicit function theorem therefore gives its equation as a unit times $z - \phi(u)$, with $\phi(u)$ of order four. In the nonsquare model the same root at $w = 1$ has

$$g_4 = u(u-1)(u-2)(u-3)(u-4), \qquad (\Delta/z^8)|_S = 27(24u)^2 + O(u^3). \tag{XV.4.57}$$

The normal derivative is again 4, so the new graph has order two. Figure XV.4.6 compares these two smooth germs. In each case, even high contact of the residual with S is compatible with a unit in the leading coefficient of f/z^3. The point-order test measures the latter as well as the discriminant.

Next preserve the cover and change the higher point orders. Retain the square P^2, replace f_3 by $U^4(U - V)$, and compare two choices of g_5 at $w = 1$. Put $u = w - 1$. The order of f is four because f_3 has a simple zero. If $g_5 = U^9$, its unit at the point still gives order five in g. If $g_5 = U^8(U - V)$, the first terms of g instead have forms z^4u^2, z^5u. Both are of degree six and neither cancels the other. The results are

g_5	$(\nu_S(f), \nu_S(g), \nu_S(\Delta))$	$(\nu_p(f), \nu_p(g), \nu_p(\Delta))$
U^9	$(3,4,8)$	$(4,5,10)$
$U^8(U-V)$	$(3,4,8)$	$(4,6,12)$

(XV.4.58)



square: order 4 nonsquare: order 2

Figure XV.4.6: The residual discriminant after removing z^8 at $w = 1$. Both curves are smooth by their nonzero normal derivative. Their contact with S, drawn in a real schematic slice, has order four for $g_4 = P^2$ and two for the nonsquare choice.

In the second row f^3 contributes z^9u^3, while g^2 has monomials $z^8u^4, z^9u^3, z^{10}u^2$. In particular the z^8u^4 term has a nonzero coefficient and ensures that the discriminant order is exactly twelve. Changing only the square condition probes component transport, while changing f_3, g_5 at a square root probes the Weierstrass orders in the surface. Neither test supplies the matter content at these exceptional fibers.

We can isolate the change in the local ideal. At a simple zero of P, the term z^4P^2 is already in the sixth power of the point ideal. Thus a unit in g_5 is the only degree-five contribution to g in these examples. If $f_3(0)$ is nonzero, its z^3 term alone prevents nonminimality even when g_5 vanishes. If $f_3(0) = 0$, the decision instead rests on $g_5(0)$. This reasoning does not depend on the signs of the two roots $\pm P$. The coefficient g_5 does not occur in the generic cover at all.

These protections can be phrased as conditions on coefficients instead of individual roots. In the split family a cubic P with simple projective zeros and a quintic f_3 with no common zero with P suffice on S, regardless of g_5. At a common zero of P, f_3, the additional requirement is that g_5 be a unit. In terms of projective zero sets, the dangerous set for the displayed split ansatz is

$$\{P = 0\} \cap \{f_3 = 0\} \cap \{g_5 = 0\} \ \subset S. \tag{XV.4.59}$$

The root-counting conditions are imposed in the coefficient lines; they can be tested in both frames using (XV.4.15). For example at infinity the split $P = V(U - V)(U - 2V)$ vanishes in the $U = 1$ frame, but f_3, g_5 do not. Looking only at their common finite zeros would miss this part of the test. Separately one still needs the off-S check, which holds for the original choices by (XV.4.23).

The failure in (XV.4.58) came from a choice of coincident zeros. It can be avoided in the IV^* tuning. For the next tuning, the prescribed divisorial orders remove both ways to protect a zero of the leading g coefficient.

XV.4.5 When the proposed tuning fails

Can one tune II^* on the same $\mathbb{F}_3$ while keeping the base? The generic Weierstrass orders for this tuning require f to be divisible by Z^4, g by Z^5, with nonzero g_5 on S.

At these candidate orders the residual classes of f, g, Δ have degrees

$$(d_{4,4}, d_{6,5}, d_{12,10}) = (8, 9, 18). \tag{XV.4.60}$$

Thus there is no obstruction from negative residual degree. But g_5 is a section of degree nine, so it has nine zeros counted with multiplicity. At each zero, $\nu_p(f) \geq 4$ already, and $g = z^5(g_5 + zg_6 + \cdots)$ has $\nu_p(g) \geq 6$. The discriminant has order at least twelve. If g_5 vanishes identically, the generic divisor already has orders at least $(4, 6)$. In particular neither positivity of the residual degrees nor the generic algebra label is a fixed-base minimality test.

The exact coefficients make the zero count geometric:

$$f_4 = U^8 + 2V^8, \qquad f_8 = U^{20} + 2V^{20}, \qquad g_5 = V(U^8 - V^8). \tag{XV.4.61}$$

On $V = 1$, the roots $w^8 = 1$ are simple because $8w^7 \neq 0$. There $f_4 = 3$. In $U = 1$, $g_5 = v(1 - v^8)$ has a simple zero at $v = 0$ and $f_4 = 1$. There are nine distinct points, including infinity. At each point, with u the centered coordinate along S, the initial forms are

$$f = Az^4 + \cdots, \qquad g = Bz^5u + \cdots, \qquad \mathrm{in}(\Delta) = 4A^3z^{12} + 27B^2z^{10}u^2, \quad AB \neq 0. \tag{XV.4.62}$$

The two distinct monomials establish exact $(4, 6, 12)$ at all nine points. Off S we can apply (XV.4.23). A common finite zero of f_4, f_8 would require $w^8 = w^{20} = -2$, hence $w^4 = -2/4 = -1/2$, incompatible with $w^8 = -2$; at infinity both coefficients are nonzero. The nine points are therefore all the $(4, 6)$ points of this displayed ruled model before any blowup. On $\mathbb{F}_{12}$, $d_{6,5} = 0$ and a nonzero g_5 need not vanish anywhere on S. The forced-zero argument is specific to the positive degree on the chosen curve.

Now blow up only the infinity point. In the $U = W = 1$ frame rename ζ, v as z, w, centered at the point. The two functions are

$$f = z^4(1 + 2w^8) + z^8(1 + 2w^{20}), \qquad g = z^5w(1 - w^8). \tag{XV.4.63}$$

If π denotes this blowup and E the exceptional divisor, then $K_{B'} = \pi^*K_B + E$. With a local equation e for E, the new coefficients and discriminant are

$$f' = e^{-4}\pi^*f, \quad g' = e^{-6}\pi^*g, \qquad \Delta' = e^{-12}\pi^*\Delta. \tag{XV.4.64}$$

Indeed $x = e^2x', y = e^3y'$ removes an overall e^6 from the Weierstrass equation. Orders at least $4, 6$ give regular quotients in both charts. For (XV.4.63) the exact quotients are

$$(z, w) = (e_z, e_zt): \quad f'_z = 1 + 2e_z^8t^8 + e_z^4(1 + 2e_z^{20}t^{20}), \qquad g'_z = t(1 - e_z^8t^8), \tag{XV.4.65}$$

$$(z, w) = (e_ws, e_w): \quad f'_w = s^4[1 + 2e_w^8 + e_w^4s^4(1 + 2e_w^{20})], \qquad g'_w = s^5(1 - e_w^8). \tag{XV.4.66}$$

Here $e_w = te_z$ and $s = 1/t$ on the overlap. The quotients differ by the prescribed powers t^{-4}, t^{-6}. Their restrictions are

$$(f'_z, g'_z)|_E = (1, t), \qquad (f'_w, g'_w)|_E = (s^4, s^5). \tag{XV.4.67}$$

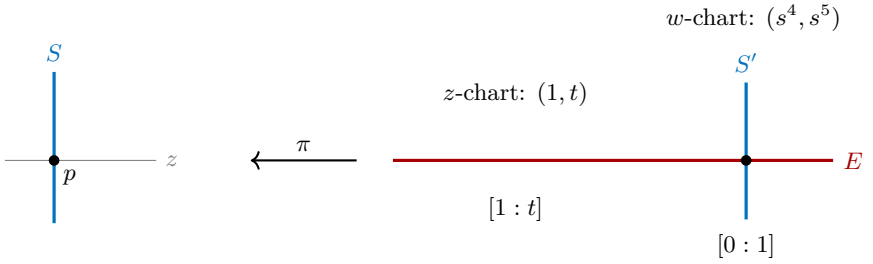


Figure XV.4.7: Blowing up $z = w = 0$ replaces the point by E. A point of E remembers the direction $[z : w]$. In the z-chart its coordinate is $t = w/z$, while the strict transform S' meets E at $s = z/w = 0$ in the w-chart. The indicated pairs are the actual coefficients on E.

In the first chart the exceptional discriminant is $4 + 27t^2$, so E is generically I_0. Its two roots are simple and f'_z is a unit there. In the second chart the restriction is $s^{10}(4s^2 + 27)$, the same section under the transition. The power s^{10} corresponds to the strict transform S', which is $s = 0$ and meets E at $e_w = 0$. At their meeting the leading coefficients of s^4, s^5 are units. The orders there are $(4, 5, 10)$; in particular this direction does not carry a new $(4, 6)$ point. This accounts for every direction on E in Figure XV.4.7. The new geometry contains one new curve and has $(S')^2 = S^2 - 1 = -4$. The other eight bad points are unchanged by this one blowup. No claim of a resolved total space, complete tensor branch or gravity-decoupled fixed point follows from the single operation.

The total and strict transforms express the same change in divisor classes. The section is smooth at the blowup center and has multiplicity one there, so $\pi^* S = S' + E$. At a generic point of E, the orders of the total transforms of f, g, Δ are $4, 6, 12$ by (XV.4.62); these are precisely the orders removed. To see where the remaining discriminant meets E, subtract the contribution $10S'$ as well. The restriction of that residual has degree two on E:

$$(-12K_{B'} - 10S') \cdot E = 12 - 10 = 2. \tag{XV.4.68}$$

Here $E^2 = -1$, $S' \cdot E = 1$, and $K_{B'} \cdot E = -1$. The two zeros of $4+27t^2$ give exactly those intersections. At $s = 0$ the residual after removing s^{10} has value 27, so the remaining meeting there is entirely the strict gauge curve. The point test and the intersection count describe the same local change from different coordinates. In the tensor description of B.2 an extra compact curve changes the available geometric string charges. Assigning a dynamical tensor to a specified limit still requires the retained-mode assumptions of that description.

The generic II^* dictionary assigns $\mathfrak{e}_8$; it does not remove the point obstruction. There is also a useful normalization check if an $\mathfrak{e}_8$ algebra enters an anomaly comparison. Restrict its adjoint to the $\mathfrak{su}(9)$ Lie subalgebra. The three summands have weights of

$\mathrm{adj}_9, \Lambda^3\mathbf{9}, \overline{\Lambda^3\mathbf{9}}$. For traceless x_i, $s_9 = \sum_i x_i^2$, the exterior cube contributes

$$\sum_{i<j<k} (x_i + x_j + x_k)^2 = \binom{8}{2} s_9 + 2\binom{7}{1} \sum_{i<j} x_i x_j = 21 s_9, \tag{XV.4.69}$$

$$\mathrm{tr}_{\mathrm{adj}_{\mathfrak{e}_8}} F^2\big|_{\mathfrak{su}(9)} = (18 + 2 \cdot 21) s_9 = 60 s_9. \tag{XV.4.70}$$

The adjoint factor 18 comes from squaring differences of the nine defining eigenvalues on the eight-dimensional $\mathfrak{su}(9)$ Cartan. The restriction uses only a Lie algebra. In the instanton-source convention of B.3, with $h^\vee = 30$ and the adjoint reference trace for $\mathfrak{e}_8$,

$$\frac{1}{4}\,\mathrm{Tr}_{\mathrm{O}}\, F^2 = \frac{1}{4h^\vee}\,\mathrm{tr}_{\mathrm{adj}}\, F^2 = \frac{1}{2\lambda}\,\mathrm{tr}_{\mathrm{ref}}\, F^2, \qquad \lambda = 60. \tag{XV.4.71}$$

The normalization belongs to the curvature trace, while the blowup changes the intersection pairing. A statement about one cannot replace a calculation of the other. Chapter B.5 takes up the geometry of shrinking curves; here we finish by revisiting the distinct two-node model for which a charged matter comparison is available.

XV.4.6 Returning to the two-node construction

Why does a quiver with consistent gauge anomalies still leave a tuning problem? The CHAIN45 example of B.1 provides enough data to test this directly. We will lift compatible Tate coefficients, divide by the correct exceptional factors, and inspect their roots. Then we change one coefficient without changing the divisor classes. This keeps the formal trace test with the old spectrum available and changes the local geometry to which that spectrum was assigned.

Use $B = \mathrm{Bl}_2\,\mathbb{F}_2$ at $(1,0), (2,0)$ in the same affine coordinates. The notation $C_2 = F_{\mathrm{b}} - E_1 - E_2$ still denotes the strict fiber, but now both retained curves have square -2 and $K_B \cdot S = K_B \cdot C_2 = 0$. For split I_4, I_5 take raw Tate powers k_i, ℓ_i of z, w, in the order $i = 1, 2, 3, 4, 6$:

$$k = (0, 1, 2, 2, 4), \qquad \ell = (0, 1, 2, 3, 5), \qquad M_i = -iK_B - k_i S - \ell_i C_2. \tag{XV.4.72}$$

These powers describe the chosen ansatz before any coefficient is suppressed by local coordinate changes. Intersecting M_i with the two curves gives $(2k_i - \ell_i, 2\ell_i - k_i)$, namely $(0,0), (1,1), (2,2), (1,4), (3,6)$. These numbers give the available degrees for the strict restrictions, not independently chosen functions at the common point.

Let $D(z) = (z-1)(z-2)/2$ and set

$$P(w) = (1, 1, 1, 1, 2 + w^3), \qquad Q(z) = (1, 1, 1, 1, 2 + z^6), \tag{XV.4.73}$$

$$H_i(z, w) = P_i(w) + D(z) Q_i(z) - P_i(0), \qquad a_i = z^{k_i} w^{\ell_i} H_i(z, w). \tag{XV.4.74}$$

At $z = 0$, $D = 1$ and $P_i(0) = Q_i(0)$, so $H_i = P_i(w)$. At $w = 0$, $H_i = DQ_i(z)$. The powers z^{k_i}, w^{ℓ_i} can be attached to these two restrictions simultaneously. In fact the displayed expressions homogenize on $\mathbb{F}_2$. For a term with exponents a, b in a_i, the Cox criterion is $0 \le a \le 2i$, $b \le d_{i,a} = 2a$. In the DQ_i terms $a \le k_i + 2 + \deg Q_i \le 2i$, and

$b = \ell_i \le 2k_i$. In $P_i(w) - P_i(0)$ the only surviving component is $i = 6$, with $a = 4, b = 8$, saturating the base bound. This gives actual simultaneous sections downstairs.

At $z = c = 1, 2$, write $h = z - c$, $D(c + h) = hd_c(h)$. The terms $P_i(w) - P_i(0)$ vanish at least once in w, so $H_i \in (h, w)$ and $a_i \in (h, w)^{\ell_i+1} = (h, w)^i$. In the charts $(h, w) = (e, et), (es, e)$, respectively, the transformed Tate coefficients are

$$a'_{i,h} = (c + e)^{k_i} t^{\ell_i} \frac{H_i(c + e, et)}{e}, \qquad a'_{i,w} = (c + es)^{k_i} \frac{H_i(c + es, e)}{e}. \tag{XV.4.75}$$

They are regular and differ by the required t^{-i} under the change of exceptional coordinate. In the first chart C_2 is $t = 0$; after removing t^{ℓ_i} the restriction is $(c+e)^{k_i} d_c(e) Q_i(c+e)$. This explicitly removes the center zero in D. It also shows why the common factor D downstairs does not represent another intersection on the strict fiber.

We still need to compute the discriminant. For the Tate equation $y^2 + a_1xy + a_3y = x^3 + a_2x^2 + a_4x + a_6$, write

$$b_2 = a_1^2 + 4a_2, \qquad b_4 = a_1a_3 + 2a_4, \qquad b_6 = a_3^2 + 4a_6, \tag{XV.4.76}$$

$$4b_8 = b_2b_6 - b_4^2. \tag{XV.4.77}$$

Complete the square first. The new left coordinate is $Y = y + (a_1x + a_3)/2$, and the cubic is

$$Y^2 = x^3 + \frac{b_2}{4}x^2 + \frac{b_4}{2}x + \frac{b_6}{4}. \tag{XV.4.78}$$

The shift $x = X - b_2/12$ removes the quadratic term, giving

$$f = -\frac{b_2^2 - 24b_4}{48}, \qquad g = \frac{b_2^3 - 36b_2b_4 + 216b_6}{864}, \tag{XV.4.79}$$

$$16\Delta = b_2^2b_8 + 8b_4^3 + 27b_6^2 - 9b_2b_4b_6. \tag{XV.4.80}$$

On either axis of (XV.4.74) only a_1 survives generically. Thus f, g are generically units and the nodal tangent lines are $y = 0$, $y = -a_1x$, distinct over the respective function fields. They also remain distinct at the corner, where $a_1 = 1$. To compute the leading residual, note that b_4, b_6 are divisible by z^2w^2, z^4w^4. The last three terms of 16Δ in (XV.4.80) vanish after division by z^4w^5 and restriction to either axis. Expanding b_8 gives

$$b_8 = a_1^2a_6 + 4a_2a_6 - a_1a_3a_4 + a_2a_3^2 - a_4^2. \tag{XV.4.81}$$

After division by z^4w^5, the terms $4a_2a_6, a_2a_3^2$ still have factors zw, z, respectively. The second vanishes on $z = 0$, but contributes on $w = 0$. The surviving restrictions of $16\Delta/(z^4w^5)$ downstairs are

$$R_S(w) = P_1^4(P_1^2P_6 - P_1P_3P_4 - wP_4^2) = 1 - w + w^3, \tag{XV.4.82}$$

$$\left.\frac{16\Delta}{z^4w^5}\right|_{w=0} = D^7Q_1^4(Q_1^2Q_6 - Q_1Q_3Q_4 + zQ_2Q_3^2) = D^7(1 + z + z^6). \tag{XV.4.83}$$

At the corner the residual is one. Thus $(0, 0, 4), (0, 0, 5)$ are the generic divisorial orders with split tangents, and the point orders are $(0, 0, 9)$. In the fiber-infinity frame the

leading coefficient of $a_1|_{w=0} = D(z)$ is $q^2 D(1/q)$, with value $1/2$ at $q = 0$. Thus the tangent lines there remain distinct as well. Away from the corner the ordinary residual roots must be found on the strict curves.

For the strict fiber take the first chart of (XV.4.75). The transform divides Δ by e^{12}; $w^5 = e^5 t^5$ has already provided five powers. In particular the restriction of the transformed $16\Delta'/t^5$ is

$$(c+e)^4 d_c(e)^7 R_2(c+e), \qquad R_2(z) = 1 + z + z^6. \tag{XV.4.84}$$

At $e = 0$ it is nonzero because $c \neq 0$, $d_c(0) \neq 0$, and $R_2(1) = 3, R_2(2) = 67$. Moreover $a_1' = d_c(0)$ is a unit at the meeting, so f', g' there are units. The factor D^7 on the original fiber is exactly removed by this calculation. Geometrically the residual class on the blowup is $-12K_B - 4S - 5C_2$, with degrees $3, 6$. The strict polynomials have those degrees, so there is no residual root hidden at either projective infinity.

To see why the local geometry at the remaining roots matters, put the completed cubic into an analytic node chart. Wherever a_1 is a unit on an axis and the other a_i vanish there, the double root in the short equation is $X_c = a_1^2/12$. It is nonzero, so the critical equation $3X_c^2 + f = 0$ admits a unique local analytic continuation of this choice. Write $v_0 = g - 2X_c^3$ and $X = X_c + \xi$; then

$$X^3 + fX + g = v_0 + \xi^2(3X_c + \xi), \tag{XV.4.85}$$

$$\Delta = 27(g - 2X_c^3)(g + 2X_c^3). \tag{XV.4.86}$$

The second factor in Δ is a unit near the node. An analytic square root of $3X_c + \xi$ exists on a sufficiently small neighborhood. Set $T = \xi\sqrt{3X_c + \xi}$; the left variables $Y - T, Y + T$ give the product equation $(Y - T)(Y + T) = v_0$. Thus Δ, up to a unit, is the smoothing parameter of the node in these local coordinates. At the transverse corner the parameter is a unit times $z^4 w^5$. At a simple residual root on S it is a unit times $z^4 u$, where u can be taken as a local coordinate independent of z because the residual has a simple zero along S. At a simple residual root on C_2 the same calculation gives $w^5 u$ in local coordinates on that part of the strict base. This is the local input for the ordinary matter rule; it says nothing about a root for which u would fail to be independent of the gauge equation.

Both strict residuals are squarefree. A root shared by R_S, R_S' would obey $w^2 = 1/3$; then $R_S = 1 - 2w/3$ would force $w = 3/2$, incompatible with that square. For R_2, a common root with its derivative would obey $z^5 = -1/6$; then $R_2 = 1 + 5z/6$ forces $z = -6/5$, which does not have that fifth power. Neither residual vanishes at zero. The ordinary minimal split construction of B.1 now supplies the matter on these strata: one full $(\mathbf{4}, \overline{\mathbf{5}})$ at the transverse corner, and three and six external fundamental hypers at the simple residual points. The algebra assignment uses the split tangents, and the ordinary matter comparison uses the simple roots. The argument does not assign fields at unspecified compact strata.

With those multiplicities as inputs, check the gauge conditions of B.3. A full bifundamental contributes five defining traces at the first node and four at the second, and has a mixed quadratic trace product. Write $N_i = (4, 5)_i$ for the dimensions of the defining representations and $n_i = (3 + 5, 6 + 4)_i$ for the effective fundamental counts.

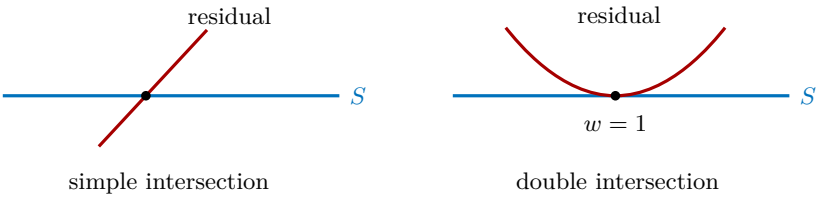


Figure XV.4.8: The residual near S before and after changing P_6. The left diagram depicts the transverse germ at an ordinary simple root in a real schematic slice; the right diagram depicts the smooth residual tangent to S at $w = 1$. The orders count holomorphic intersection multiplicity, independent of that slice.

The mixed-gauge, quartic and gauge-square equations compare

$$K_B \cdot C_i = (2N_i - n_i)/6 = 0, \tag{XV.4.87}$$

$$B_{\mathrm{adj}} - \sum_R x_R B_R = 2N_i - n_i = 0, \tag{XV.4.88}$$

$$C_i^2 = -6/3 = -2, \tag{XV.4.89}$$

$$S \cdot C_2 = 1, \tag{XV.4.90}$$

where $C_1 = S$, both defining-trace factors are one, and the last equality uses the single bifundamental with defining quadratic coefficient one at each node. In the third equality the adjoint has square coefficient 6 and the fundamental has zero, in the basis of independent quartics for these two algebras. The string pairing is minus the intersection matrix, with diagonal 2 and off-diagonal -1. This comparison imposes the matter counts from the geometry; it does not derive them anew from a local polynomial.

Change only P_6 to $2 - w^2 + w^3$. The changed term has legal Cox degrees, vanishes at $w = 0$ after subtracting $P_6(0)$, and has the same restriction on the strict fiber and at the corner. The leading discriminant computation gives

$$R_S^{\mathrm{new}} = 1 - w - w^2 + w^3 = (w - 1)^2(w + 1). \tag{XV.4.91}$$

The class still has degree three on S. The residual is tangent to S at $w = 1$: for example the derivative of $16\Delta/(z^4w^5)$ in the z direction there is nonzero. To see the relevant first-order term, the numerator contributions $b_4^3, b_6^2, b_2b_4b_6$ start at least two powers higher in z than z^4. At $w = 1$, $H_6 = D(2 + z^6)$, so the reduced b_8 has terms $D^3 - D^2 + 9zD^2 + O(z^2)$. Its constant vanishes, so the first-order variation of b_2^2 does not enter. Since $D = 1 - 3z/2 + O(z^2)$, the normal derivative of the residual is $-3/2 + 9 = 15/2$. In particular the new point orders are $(0, 0, 5)$, because z^4 multiplies a residual with a nonzero linear normal term. This is not a $(4, 6)$ failure. It is a failure of the simple-root premise used for the ordinary matter comparison.

In fact, near the double root write $u = w - 1$ and $R = 16\Delta/(z^4w^5)$. Its restriction is $R(0, 1 + u) = u^2(2 + u)$. Since $\partial_z R \neq 0$, the implicit function theorem writes R as a unit times $z - \psi(u)$, with $\psi(u)$ vanishing to order two. The same node construction

now gives

$$(Y - T)(Y + T) = \text{unit} \cdot z^4\big(z - \psi(u)\big), \qquad \nu_u(\psi) = 2. \tag{XV.4.92}$$

The residual itself is smooth, but one cannot use its equation together with z as two independent coordinates at the meeting. The failure is transversality, not an order-$(4, 6)$ obstruction. An assignment of matter at this germ would require new geometric input.

The distinction is visible in Figure XV.4.8. Keeping the old hypermultiplets as formal inputs gives exactly the same polynomial equations (XV.4.90). Those equations know neither the normal derivative at the double root nor the failure of simple intersection. This is a concrete limit on the use of anomaly cancellation to certify a tuning. We have not computed the charged spectrum of the altered geometry. The next step in a different direction is to study the contraction of a given curve configuration; that requires the geometric pairing and control of the base, not just a consistent quiver.

XV.4.7 Exercises

1. **Move the coefficient to another ruled surface.** Take $n = 5, k = 6$. Find the first allowed a, the residue degrees at $a - 1, a$, and all four exponents of the Cox lift with residue $U^j V^{d-j}$, $j = 1$. Give the exponents in $z^a w^j$ and $\zeta^a v^{d-j}$. Explain why the preceding residue is zero even though a function with poles could be written locally.

2. **A zero of f is not a residual zero.** On $\mathbb{F}_3$ take $f_2 = (U - 3V)^2$, keep f_8 as in (XV.4.18), and use $g_2 = 3$. Give the generic orders, the orders at $w = 3$, the constant residual value, and the splitting decision over $\mathbb{C}(S)$. Explain why treating 3 as nonsquare over $\mathbb{Q}$ answers a different question.

3. **Change both terms of the cubic.** Keep the centers and $D(z)$ from (XV.4.37), and use $f = z^2 w(2 + w)D^3$, $g = z^3 w^2(2 + 2w)D^4$. Give the candidate slope h, the remaining coefficient in the slope test, and the quadratic factor if present. Give the generic splitting type and the corner orders. Explain what would be missing from a matter inference based only on this calculation.

4. **Protect two different IV^* points.** Use $P = V(U - 2V)(U - 3V)$, $f_3 = U^4(U - 2V)$, $g_5 = U^8(U - 3V)$, and the same f_8 as in (XV.4.51). Compute the point orders at $w = 2, 3$ and at infinity, and the generic splitting. Determine whether any of the three roots fails the point test. Explain which unit, if any, is used at each root.

5. **Blow up a changed simple point.** In the local frame take $f = z^4(2 + u) + z^8$, $g = z^5 u(3 + u)$. Give the point orders, the exceptional powers removed for f, g, Δ, the two transformed coefficient pairs restricted to E, and the orders where E meets strict S. Give the trace conversion factor λ for the adjoint $\mathfrak{e}_8$ reference. Explain why a point blowup changes the base even when E is generically I_0.

6. **Move the tangency.** Keep Q and the other P_i in (XV.4.74); use $P_6 = 2 + w - 3w^2 - 2w^3$. Compute the two strict residual degrees, the roots of the first residual

with multiplicities, and the orders at its double root. Give the old formal external counts and decide separately whether their gauge equations pass and whether the ordinary simple-root matter inference applies. Explain why these two decisions differ.

Use `benchmark/tasks.json` for the bounded fields and `benchmark/PROTOCOL.md` for submission. Written explanations are assessed by a reader.

Status and sources

§1. Coefficient restrictions and lifts. The degree bound, exact sequence, Cox lifts and chart changes are [MATH]. For the effective-divisor argument and adjunction see Morrison and Taylor (2012a), arXiv:1201.1943v3, PDF pp. 5–6, eqs. (2.5)–(2.6). For the restriction sequence see Morrison and Taylor (2015), arXiv:1412.6112v4, §3.1, eqs. (3.3)–(3.6). The discriminant frame uses the Weierstrass convention $\Delta_{\text{book}} = 4f^3 + 27g^2$.

§2. The isolated section. The forced orders, discriminant, point tests and cover splitting are [MATH]. The ordinary algebra and no localized enhancement matter on the isolated rational section are [GEO-E], using Morrison and Taylor (2012a), §3.1.2 and Table 2, and Katz et al. (2011), arXiv:1106.3854v1, §5, eq. (5.3). The pure gauge comparison is [ANOM] in the trace frame of Kumar et al. (2010), arXiv:1008.1062v1, Table 1 and eqs. (2.11)–(2.13).

§3. Double and cubic covers. The coefficient, cover, chart and order calculations are [MATH]. For the minimal local algebra dictionary, [GEO-E], see Katz et al. (2011), §§5–6, and Morrison and Taylor (2012a), §3.4, eqs. (3.23)–(3.31). The cubic discriminant here is the negative of the Weierstrass convention, and the normalization calculation is for the displayed sparse cubic. No spectrum is assigned from the branch divisor or from the semisplit change.

§4. Exceptional square test. The ruled lifts and changed point orders are [MATH]; the ordinary IV^* algebra labels are [GEO-E]. See Katz et al. (2011), §7, eq. (7.1), and Morrison and Taylor (2015), §§4.2–4.4. Absence of a $(4, 6)$ point is asserted for the specified Weierstrass sections, without a global resolution or matter theorem.

§5. Forced zeros and the point blowup. The degree, exact orders and chart quotients are [MATH]. See Morrison and Taylor (2015), §4.4, and Morrison and Taylor (2012a), PDF p. 6, for the obstruction and base operation, and Katz et al. (2011), §7, eq. (7.3), for the generic II^* label ([GEO-E]). The [ANOM] trace translation uses Kumar et al. (2010), eqs. (2.34)–(2.36) and Table 1, and Ohmori et al. (2014), arXiv:1408.5572v2, p. 3 before §1.1, with the curvature frame of B.3.

§6. Two split multiplicative fibers. The simultaneous Tate lifts, residuals and changed tangency are [MATH]. The raw I_4, I_5 Tate powers follow Katz et al. (2011), arXiv:1106.3854v1, Appendix A, Table 2 (PDF p. 23). Table 3 (PDF p. 25) uses compact forms with selected coefficients suppressed. The ordinary matter, [GEO-E], imports the selected model of B.1 under its split, transverse and simple-root premises; see Morrison and Taylor (2012b), arXiv:1106.3563v3, eqs. (2.26)–(2.29). The polynomial

comparison ([ANOM]) uses B.3 and Kumar et al. (2010), eqs. (2.11)–(2.13). The changed matter is undetermined.

References

Katz, S. et al. (2011). "Tate's algorithm and F-theory". In: *Journal of High Energy Physics* 08, p. 094. arXiv: 1106.3854 [hep-th].

Kumar, V., D. R. Morrison, and W. Taylor (2010). "Global aspects of the space of 6D N=1 supergravities". In: *Journal of High Energy Physics* 11, p. 118. arXiv: 1008.1062 [hep-th].

Morrison, D. R. and W. Taylor (2012a). "Classifying bases for 6D F-theory models". In: *Central European Journal of Physics* 10, pp. 1072–1088. arXiv: 1201.1943 [hep-th].

Morrison, D. R. and W. Taylor (2012b). "Matter and singularities in F-theory models". In: *Journal of High Energy Physics* 01, p. 022. arXiv: 1106.3563 [hep-th].

Morrison, D. R. and W. Taylor (2015). "Non-Higgsable clusters for 4D F-theory models". In: *Journal of High Energy Physics* 05, p. 080. arXiv: 1412.6112 [hep-th].

Ohmori, K. et al. (2014). "Anomaly polynomial of general 6d SCFTs". In: *Progress of Theoretical and Experimental Physics* 2014, 103B07. arXiv: 1408.5572 [hep-th].

Chapter XV.5

Contraction limits and six-dimensional SCFTs

A D3-brane wrapped on a compact base curve gives a string in six dimensions. What happens when several such curves shrink together? A negative intersection matrix tells us when a base surface can develop a point singularity. It does not tell us whether an elliptic Calabi–Yau exists over that base, or what remains in six dimensions when we approach the singularity. The difference matters even for a pair of rational curves with just one intersection.

We will construct an elliptic model for this pair, resolve it, and compute the tensions of strings on the resulting curves. Then we compare two models with the same pairing but different gauge content, and an actual degeneration with a null charge that cannot contract to a point. We use the Weierstrass and Kodaira conventions of Chapter B.1, the D3 area law and tensor pairing of B.2, and the pure gauge anomaly calculation of B.3. The base point blowup and the blowups that resolve the elliptic total space are separate operations.

XV.5.1 Resolving a non-minimal point

Why can two curves with allowed generic fibers force a non-minimal point when they meet? Start with two smooth rational curves C_1, C_2 of self-intersection -3, meeting at exactly one transverse point. We call this the 33 chain. Take $L = -K_B$, the anticanonical line of the smooth base, and write the affine Weierstrass equation and our discriminant as

$$y^2 = x^3 + fx + g, \qquad f \in H^0(B, L^4), \quad g \in H^0(B, L^6), \qquad \Delta = 4f^3 + 27g^2. \tag{XV.5.1}$$

Thus -16Δ is the usual discriminant of the elliptic equation. The question is local on the base, but the line bundles on the full compact curves force the generic vanishing orders.

For a nonzero section of L^k remove its two curve components with multiplicities a_1, a_2. The residual divisor R is effective and contains neither curve, so $R \cdot C_i \geq 0$.

Adjunction gives $K_B \cdot C_i = -2 - C_i^2 = 1$. Applying this to both intersections gives

$$R \sim -kK_B - a_1C_1 - a_2C_2, \qquad 3a_1 - a_2 \geq k, \qquad 3a_2 - a_1 \geq k. \tag{XV.5.2}$$

Each lower bound depends on the other multiplicity. Starting at zero gives a bound on both unknowns, which can be put back into the inequalities. Specifically, the map sends (a, b) to $(\lceil (k + b)/3 \rceil, \lceil (k + a)/3 \rceil)$. It is monotone, and every admissible vector bounds the sequence term by term. Here it reaches

$$k = 4 : \ (0, 0) \to (2, 2), \qquad k = 6 : \ (0, 0) \to (2, 2) \to (3, 3). \tag{XV.5.3}$$

The last vectors satisfy the respective inequalities. If a coefficient vanishes identically its order is infinite, so the same lower bound holds. At the transverse intersection we can use the two curve equations as coordinates u, v. Then f is divisible by u^2v^2 and g by u^3v^3. Orders in the point ideal (u, v) are at least $(4, 6)$. Neither curve by itself needs generic orders $(4, 6)$.

A bound does not yet furnish a coefficient section. To construct one, use a smooth toric base with rays, in their order around the cone,

$$v_0 = (1, 0), \quad v_1 = (0, 1), \quad v_3 = (-1, 3), \quad v_4 = (-3, 8). \tag{XV.5.4}$$

We reserve v_2 for the ray to be inserted. Each adjacent determinant is 1, so the three adjacent pairs give affine planes. The compact curves are the divisors of v_1, v_3. For a character with exponent m, its divisor is $\sum_i \langle m, v_i \rangle D_i$. Since $-K_B = \sum_i D_i$, the section of L^k defined by this character has local exponents $k + \langle m, v_i \rangle$. Choosing

$$\begin{aligned} m_f &= (-4, -2), \quad & m_g &= (-6, -3), \\ a_f &= (0, 2, 2, 0), \quad & a_g &= (0, 3, 3, 0). \end{aligned} \tag{XV.5.5}$$

gives holomorphic sections on the whole toric base. The coordinates (u, v) of each chart are dual to its ordered pair of rays. With unit coefficients the actual local equations therefore have the following coefficient and discriminant functions:

ray pair	f	g	Δ
$(0, 1)$	v^2	v^3	$31v^6$
$(1, 3)$	u^2v^2	u^3v^3	$31u^6v^6$
$(3, 4)$	u^2	u^3	$31u^6$

(XV.5.6)

One can obtain the middle coordinates without guessing a local monomial. The characters dual to v_1, v_3 are $(3, 1)$ and $(-1, 0)$. On any adjacent pair (i, j), let m_σ be the character with pairings $(-k, -k)$ on that pair. It generates the local frame of L^k; the regular function representing our section is $\chi^{m - m_\sigma}$. In the middle chart the two exponents of this difference are its pairings with v_1, v_3. In particular

$$m_{f,\sigma} = (-8, -4), \qquad m_f - m_{f,\sigma} = (4, 2) = 2(3, 1) + 2(-1, 0). \tag{XV.5.7}$$

The g section is obtained by the same calculation with $k = 6$. This construction also shows why the units on a toric overlap do not produce new discriminant zeros. Both

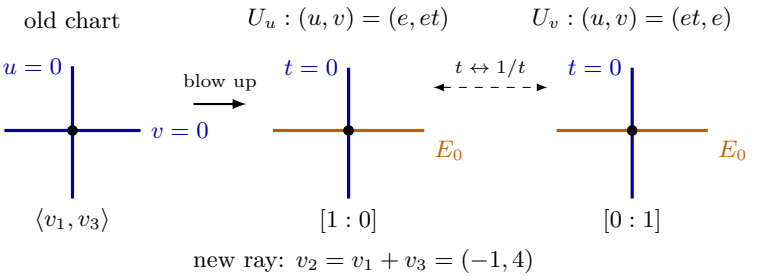


Figure XV.5.1: Blowup of the middle toric chart. The new ray is the sum $v_2 = v_1 + v_3$. The two affine charts on the exceptional curve have reciprocal coordinates on their overlap. Their origins mark two distinct meetings with the strict transforms.

coefficient monomials represent the same global sections in any two frames, and the discriminant, a section of L^{12}, acquires just the twelfth power of the frame factor.

For example, in the middle chart the f-term of the discriminant contributes $4u^6v^6$, and the g-term contributes $27u^6v^6$. There is no cancellation. Thus the middle origin is the unique $(4, 6)$ point, with orders $(4, 6, 12)$. At other points of either compact curve the actual orders are $(2, 3, 6)$; off the curves the discriminant is nonzero.

The blowup of the intersection replaces the point with its projective line of tangent directions. The chart maps, shown in Figure XV.5.1, are

$$U_u : \ (u, v) = (e, et), \qquad U_v : \ (u, v) = (et, e). \tag{XV.5.8}$$

To see which elliptic coefficients should be used, compare three-forms on the complement of the exceptional curve. The base form pulls back to $\pm e\, de \wedge dt$. If $x = e^2X$, $y = e^3Y$, then modulo base differentials $dx/y = e^{-1}dX/Y$, so

$$du \wedge dv \wedge \frac{dx}{y} = \pm de \wedge dt \wedge \frac{dX}{Y}. \tag{XV.5.9}$$

The line bundle statement fixes the rescaling: the new anticanonical line is $\pi^*L \otimes \mathcal{O}(-E_0)$ since $K_{\widetilde{B}} = \pi^*K_B + E_0$, where E_0 is the exceptional base curve. Its fourth and sixth powers require division by e^4, e^6, respectively. Merely pulling back f, g would give the old vanishing at every point of the exceptional curve and would not use the new anticanonical bundle. In the two charts we obtain

$$\widetilde{f} = \pi^*f/e^4 = t^2, \qquad \widetilde{g} = \pi^*g/e^6 = t^3, \qquad \widetilde{\Delta} = \pi^*\Delta/e^{12} = 31t^6. \tag{XV.5.10}$$

The strict transform of $v = 0$ is $t = 0$ in U_u; the strict transform of $u = 0$ is $t = 0$ in U_v. Along the exceptional curve these are the directions $[1 : 0]$ and $[0 : 1]$. At a generic point of E_0 we have $t \neq 0$, so the elliptic fiber is smooth. We gained a compact area even though we did not gain a generic gauge degeneration on that curve.

To match the blowup to the fan, work in the old character basis for the two coordinates. The weights of u, v on $v_2 = v_1 + v_3$ are $(1, 1)$. In U_u the characters $e = u$ and $t = v/u$ have valuations $1, 0$ on v_2 and $0, 1$ on v_3, respectively. Thus (e, t) are the

coordinates of the $(2,3)$ chart. In U_v the ordered coordinates are $(u/v, v) = (t, e)$ on $(1,2)$. In the intersection where both direction coordinates are nonzero, writing the second chart as $(\widehat{e}, \widehat{t})$ gives

$$\widehat{e} = et, \qquad \widehat{t} = t^{-1}, \qquad (\widehat{f}, \widehat{g}) = (t^{-4}\widetilde{f}, t^{-6}\widetilde{g}). \tag{XV.5.11}$$

For example $t^{-4}t^2 = (1/t)^2$, so the proper coefficients agree after the frame change. The overlap excludes both marked direction origins. This is why the diagram has two distinct intersections with E_0, rather than three curves meeting at one point.

The two old outer charts are unchanged. Equivalently, insert $v_2 = (-1, 4)$, for which $k + \langle m, v_2\rangle = 0$ for both choices in (XV.5.5). In the four new ordered toric charts, the full list of coefficients is

ray pair	$\widetilde{f}$	$\widetilde{g}$	$\widetilde{\Delta}$
$(0,1)$	v^2	v^3	$31v^6$
$(1,2)$	u^2	u^3	$31u^6$
$(2,3)$	v^2	v^3	$31v^6$
$(3,4)$	u^2	u^3	$31u^6$

(XV.5.12)

The base is smooth and every chart passes the point-order test, including the two strict-transform meetings with E_0.

There is one more test even at a generic point of a remaining discriminant curve. Write $w = 0$ for that curve, s for a parameter along it, and divide f, g by w^2, w^3 in the cover polynomial. Over $\mathbb{C}(s)$ the I_0^* test gives

$$P(\psi) = \psi^3 + \psi + 1, \qquad \operatorname{disc} P = -31. \tag{XV.5.13}$$

The roots are three distinct complex constants. Thus the cover is split; in the ordinary, unfrozen dictionary it gives $\mathfrak{so}(8)$ on each end. There is no need for rational roots over $\mathbb{Q}$.

The cover of the end curve that tests permutation of these roots must be distinguished from the monodromy of the elliptic curve around that end. The transverse double cover $w = \eta^2$ makes the smooth elliptic family away from $w = 0$ a product in coordinates $x = \eta^2 X,\ y = \eta^3 Y$. In these coordinates,

$$Y^2 = X^3 + X + 1, \qquad (\eta, X, Y) \longmapsto (-\eta, X, -Y). \tag{XV.5.14}$$

The involution on the elliptic factor is inversion. In this equation the origin of the elliptic group law is the section at infinity, and negating Y fixes it. The normalized cubic invariant and the differential on the cover are

$$j = 1728\,\frac{4f^3}{4f^3 + 27g^2} = \frac{6912}{31}, \qquad \frac{dx}{y} \equiv \eta^{-1}\frac{dX}{Y} \pmod{d\eta}. \tag{XV.5.15}$$

Although the product differential dX/Y is odd under inversion, the finite-chart relative form has the compensating odd factor η^{-1}. Thus gluing a relative form does not imply trivial transport of the individual elliptic cycles. In the product with $\eta \neq 0$, a loop around $w = 0$ lifts to a path from η to $-\eta$ and closes only after the deck transformation. The j invariant is constant off the discriminant, but the two elliptic one-cycle periods transform by -1 around the puncture. Constant j does not make the original family a product. We will compare it with a genuine product after computing the compact curve pairing.

XV.5.2 The complete compact curve lattice

Which compact curves can carry strings on the blown-up base? The three visible toric curves give candidates. To see that there are no others, use the morphism from the subdivided fan to the affine toric surface B_0 of the cone $\sigma = \langle v_0, v_4 \rangle$. The refinement has the same support, which gives properness. Along each boundary ray the fans coincide, and the torus is unchanged. Thus the map is an isomorphism off the cone vertex and its exceptional fiber consists of the interior-ray divisors. Every complete irreducible curve maps to a point in the affine surface, since its regular functions are constant. A curve cannot lie over a point where the map is an isomorphism. This proves completeness of the compact *base* curve list; it does not count elliptic fibral components.

A character whose pairings with two adjacent rays are $1, 0$ gives the first local coordinate. For three successive rays the relation is $v_{i-1} + v_{i+1} = n_i v_i$, and the transition of the normal coordinate has power n_i. The two adjacent charts show that the middle ray curve has normal bundle $\mathcal{O}(-n_i)$. Consecutive curves meet at one origin with multiplicity one; separated ones do not meet. In the original fan the two relations have $n_i = 3$. In the refinement the three relations give

$$v_0 + v_2 = 4v_1, \qquad v_1 + v_3 = v_2, \qquad v_2 + v_4 = 4v_3. \tag{XV.5.16}$$

For clarity, use the central relation to read the degree directly. On $\langle v_1, v_2 \rangle$ write (u, v); on $\langle v_2, v_3 \rangle$ the coordinates are (uv, u^{-1}). Along the middle curve the tangent parameter changes from u to $1/u$, while its normal coordinate changes from v to uv. A normal vector has coordinate coefficients with this same factor u on the overlap, as for the tautological line $\mathcal{O}(-1)$. Replacing the middle relation by either end relation gives a factor u^4. The degree is a statement about the normal bundle of a *base* curve and does not use the type of the elliptic fiber above it.

This is the 414 chain, ordered (L, E_0, R) for the two strict transforms and exceptional curve. In the tensor convention $\Omega_{ij} = -C_i \cdot C_j$, the two configurations give

$$\Omega_{33} = \begin{pmatrix} 3 & -1 \\ -1 & 3 \end{pmatrix}, \qquad \Omega_{414} = \begin{pmatrix} 4 & -1 & 0 \\ -1 & 1 & -1 \\ 0 & -1 & 4 \end{pmatrix}, \tag{XV.5.17}$$
$$D_1 = 4, \qquad D_2 = 3, \qquad D_3 = 8.$$

The leading minors D_i imply positive definiteness by Sylvester's criterion. Figure XV.5.2 tracks what changed. In particular, removing the middle entry on account of its smooth generic elliptic fiber would lose a primitive base charge.

For a charge $q = (q_L, q_E, q_R)^{\mathsf{T}}$, completing the square gives an integral version of the geometric basis change:

$$q^{\mathsf{T}} \Omega_{414} q = (q_E - q_L - q_R)^2 + 3q_L^2 - 2q_L q_R + 3q_R^2. \tag{XV.5.18}$$

The new coordinate of E_0 in this expression is integral with integral inverse. Geometrically the basis is $(L + E_0, R + E_0, E_0)$. For instance $(L + E_0) \cdot E_0 = 1 - 1 = 0$, and $(L + E_0) \cdot (R + E_0) = 0 + 1 + 1 - 1 = 1$. The matrix is therefore integrally congruent to

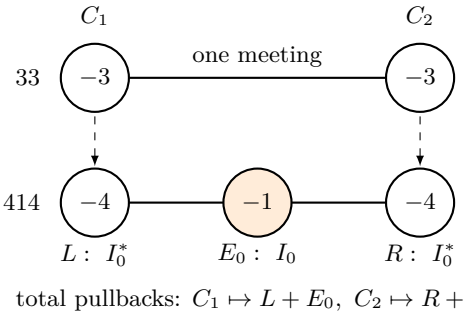


Figure XV.5.2: The base configurations over the same affine vertex. The strict transforms L, R are disjoint. A total pullback of either original curve includes E_0; the two total pullbacks still have intersection number one.

$\Omega_{33} \oplus [1]$. There are three different matrix operations one might have meant by looking only at the ends:

$$\begin{aligned} \Omega_{\text{end classes}} &= \operatorname{diag}(4,4), \\ \Omega_{\text{after blowing down } E_0} &= \operatorname{diag}(4,4) - \begin{pmatrix} -1 \\ -1 \end{pmatrix}(-1,-1) = \Omega_{33}, \\ \Omega_{414}^{-1} &= \tfrac{1}{8}\begin{pmatrix} 3 & 4 & 1 \\ 4 & 16 & 4 \\ 1 & 4 & 3 \end{pmatrix}. \end{aligned} \tag{XV.5.19}$$

The first line is restriction to the actual end classes. To derive the second operation without guessing the off-diagonal correction, consider an end vector q_{end} with fixed coordinates (q_L, q_R) and an undetermined middle coefficient. The pairing with E_0 vanishes exactly if $q_E = q_L + q_R$, as is also apparent from (XV.5.18). Thus the norm before restriction, the norm on end classes and the norm of their orthogonal lifts obey

$$\begin{aligned} q_{\text{strict}}^{\mathsf{T}} \Omega_{414} q_{\text{strict}} &= 4q_L^2 + 4q_R^2, \quad q_{\text{strict}} = (q_L, 0, q_R), \\ q_{\text{pull}}^{\mathsf{T}} \Omega_{414} q_{\text{pull}} &= 4q_L^2 + 4q_R^2 - (q_L + q_R)^2, \quad q_{\text{pull}} = (q_L, q_L + q_R, q_R). \end{aligned} \tag{XV.5.20}$$

For $q_L = q_R = 1$ the two norms are 8 and 4, although the end entries in the charge vector did not change. This is why one cannot replace restriction by orthogonal projection simply because one is only following two of the periods. The second is a Schur complement: it computes the pairing of the orthogonal total pullbacks under the actual blowdown of the -1 curve. For the last line one can use the same basis change, invert the 33 block using its determinant 8, and return to the strict-transform basis. For example the middle column comes from writing $L = (L + E_0) - E_0$ and $R = (R + E_0) - E_0$ when returning to the strict basis. Its off-diagonal entries record that solving for an area-dual class can involve curves other than the one whose area is prescribed. As a simple tension check, at areas $(1, 2, 3)$ in common units, the effective charges $(1, 0, 1)$ and $(1, 1, 1)$ have tensions in ratio $4 : 6$ by linearity of area. A smooth elliptic fiber over E_0 does not remove its contribution.

An area-dual class is another useful distinction. If D^E is dual to the period on E_0, requiring $D^E \cdot C_j = \delta_{Ej}$ gives the negative of the middle column of Ω_{414}^{-1}:

$$D^E = -\tfrac{1}{2}L - 2E_0 - \tfrac{1}{2}R, \qquad D^E \cdot (L, E_0, R) = (0, 1, 0). \tag{XV.5.21}$$

To reproduce the dual class in the pullback basis, its required periods on $L + E_0, R + E_0, E_0$ are $(1, 1, 1)$, not $(0, 0, 1)$. In that basis the two blocks invert separately:

$$\begin{pmatrix} d_{L+E_0} \\ d_{R+E_0} \end{pmatrix} = -\frac{1}{8}\begin{pmatrix} 3 & 1 \\ 1 & 3 \end{pmatrix}\begin{pmatrix} 1 \\ 1 \end{pmatrix} = -\begin{pmatrix} 1/2 \\ 1/2 \end{pmatrix}, \qquad d_{E_0} = -1. \tag{XV.5.22}$$

Adding the two pullbacks' exceptional coefficients to d_{E_0} gives the -2 in (XV.5.21). For instance the middle intersection is $-1/2 + 2 - 1/2 = 1$; each end intersection is $2 - 2 = 0$. The unit *charge* on E_0, by contrast, is the integral curve E_0, not this rational class. The period-dual basis solves a linear system in divisor space; a wrapped charge is specified before that system is solved.

To identify the singular point, use v_0, v_4 as a basis of the sublattice $N' \subset \mathbb{Z}^2$ that they generate. It has index 8. The cone in N' is the ordinary quadrant. The vector $(0, 1)$ in the original lattice has coordinates $(3/8, 1/8)$ in this quadrant basis. Equivalently a monomial with exponents (a, b) on the covering plane descends precisely if

$$(3a + b)/8 \in \mathbb{Z}, \qquad B_0 = \mathbb{C}^2/\tfrac{1}{8}(1, 3), \qquad \frac{8}{3} = 3 - \frac{1}{3}. \tag{XV.5.23}$$

The quotient notation interchanges the two covering coordinates. The cyclic action has determinant character of weight $1 + 3 = 4 \bmod 8$; it is not an $SU(2)$ action. The negative continued fraction agrees with the original two self-intersections. Independently, the Smith group of the lattice is $\mathbb{Z}/8$: the rank-two matrix Ω_{33} has entries of greatest common divisor 1 and determinant 8; the orthogonal [1] adds no discriminant group. One can track the generator without taking the Smith normal form. In the quotient by the image of the 33 pairing, the two column relations on the dual generators are $3e_1 - e_2 = 0$ and $3e_2 - e_1 = 0$. The first eliminates e_2, and the second becomes $8e_1 = 0$. The same computation can be performed on the strict basis by elementary integer row and column operations: use the middle diagonal 1 to eliminate both adjacent entries, giving the 33 block and a unit. Using an entry of magnitude one in that block leaves one last diagonal entry of magnitude 8:

$$\mathrm{Smith}(\Omega_{414}) = \mathrm{diag}(1, 1, 8), \qquad \mathrm{coker}(\Omega_{414}) = \mathbb{Z}/8. \tag{XV.5.24}$$

The unit entries are why the discriminant group has only one generator despite the presence of three compact charges. These are relations on dual charges modulo integral curve charges; they do not identify the quotient action on coordinates of the base. The agreement of the two group orders is useful here, but it is the character congruence that identifies the actual quotient weights.

The explicit toric morphism realizes an algebraic contraction. There is also a criterion that needs no fan: a reduced connected compact curve configuration on a smooth complex surface can be contracted analytically to one point, in a neighborhood of the curves, precisely if its intersection matrix is negative definite. Grauert's theorem

concerns a proper analytic contraction that is an isomorphism off the curves. The configurations here are compact and connected, the toric charts give smoothness, and (XV.5.17) verifies the required sign. The matrix calculation has a useful local converse check. A nonzero vector in the kernel would have zero norm and prevent the inverse period calculation. A vector of zero norm by itself already rules out definiteness, even if the matrix is invertible. For this chain the normalized pivots of a leading elimination are

$$(D_1,\ D_2/D_1,\ D_3/D_2) = (4,\ 3/4,\ 8/3). \tag{XV.5.25}$$

All are positive. The difference between a zero pivot and a nonzero negative one matters in other models, but neither supplies a negative-definite exceptional intersection. Even the original 33 configuration contracts on the base. Yet the elliptic coefficients before the base blowup do not describe an ordinary tensor branch near its intersection. The theorem tests neither Weierstrass minimality nor the existence of a limit of a six-dimensional field theory. Our next task is to realize a shrinking sequence of positive areas.

XV.5.3 Contraction and gravity decoupling

Can the string tensions go to zero without keeping the six-dimensional Einstein coefficient finite? First we construct a Kähler class path on the local 414 base. Then we use a different, compact base to compute the two scales independently. Compact volumes of that example are not volumes of the local base.

Write $a_i = J \cdot C_i$ for physical areas in a Kähler class J. In the real compact divisor span the period equation and its solution are

$$J_{\mathrm{rel}} = \sum_i d_i C_i, \qquad a = -\Omega_{414} d, \qquad a = \varepsilon(1,1,1)^{\mathsf{T}} \implies d = -\varepsilon(1,3,1)^{\mathsf{T}}. \tag{XV.5.26}$$

Solving a linear equation in cohomology alone does not show that a positive representative exists. Here we can test relative ampleness directly. For the integral divisor with ray coefficients $(0,-8,-24,-8,0)$, use the polyhedron $\langle m, v_i\rangle \geq -d_i$ in the character lattice. The vertices for adjacent pairs are determined by taking equality at those two rays:

pair	m	$(\langle m, v_i\rangle + d_i)_{i=0}^{4}$
$(0,1)$	$(0,8)$	$(0,0,8,16,64)$
$(1,2)$	$(8,8)$	$(8,0,0,8,40)$
$(2,3)$	$(40,16)$	$(40,8,0,0,8)$
$(3,4)$	$(64,24)$	$(64,16,8,0,0)$

(XV.5.27)

For example the $(1,2)$ vertex solves $m_y = 8$ and $-m_x + 4m_y = 24$. Strictness on all other rays gives strict convexity of the support data for this subdivision, hence an ample line relative to B_0. Its compact areas are $(8,8,8)$. The numerical link between an edge of the support data and one area can be checked directly. At an interior ray v_i, let m_- solve the equalities on its left adjacent cone. The excess on v_{i+1} is

$$\langle m_-, v_{i+1}\rangle + d_{i+1} = -n_i d_i + d_{i-1} + d_{i+1} = J_{\mathrm{rel}} \cdot C_i. \tag{XV.5.28}$$

The first equality uses $v_{i+1} = n_i v_i - v_{i-1}$; the second uses the self-intersection and both adjacency numbers. Thus the strict wall inequalities encode precisely the periods of the compact curves. Showing positivity this way gives a geometric meaning to the matrix solution, and the full vertex test in (XV.5.27) verifies there is no other inequality to impose in this example. A relative projective embedding over the affine cone supplies a representative positive along the exceptional directions. Adding the pullback of an ambient affine Kähler form supplies positivity in the base directions. In this description the scaled relative class plus affine pullback is Kähler for each $\varepsilon > 0$ and has the periods in (XV.5.26); the pullback has zero period on each exceptional curve. This constructs a path of Kähler classes, without constructing Ricci-flat metrics along it.

To compare physical scales we use CHAIN45, the blowup of $\mathbb{F}_2$ at two distinct points on one fiber, away from its negative section. In the total-pullback basis S, F, E_1, E_2, $S^2 = -2,\ S \cdot F = 1,\ F^2 = 0,\ E_i^2 = -1$, and all other pairings with an E_i vanish. The retained pair is $S, C = F - E_1 - E_2$, with $C^2 = -2$ and $S \cdot C = 1$. The compact parent supplies the split I_4, I_5 gauge pair on these curves.

Why check the whole cone rather than the two retained curves? An irreducible curve other than S, C, E_i pushes forward to a curve of class $dS + bF$, with nonnegative d, and has multiplicities $m_i \geq 0$ at the centers. Its intersection with S implies $b \geq 2d$; intersection of its pushforward with the chosen fiber implies $m_1 + m_2 \leq d$. Curves mapped to points are the E_i, and the special fiber strict transform has already been listed. Using $F = C + E_1 + E_2$ gives

$$dS + bF - m_1E_1 - m_2E_2 = dS + bC + (b - m_1)E_1 + (b - m_2)E_2. \tag{XV.5.29}$$

All coefficients on the right are nonnegative. Each displayed generator is effective and the four are independent, so these are precisely the four rays of the closed cone of curves. Positivity on all four characterizes the ample chamber; using only S, C would miss both exceptional walls.

Let $\rho = J \cdot F,\ A = J \cdot S,\ B = J \cdot C$. Solve first for the coefficients of S, F, then allocate the remaining fiber area $\rho - B$ between the two exceptional curves with a fraction $0 < h < 1$. The solution and the exact chamber in these coordinates are

$$J = \rho S + (2\rho + A)F - e_1E_1 - e_2E_2, \tag{XV.5.30}$$

$$e_1 = h(\rho - B), \qquad e_2 = (1 - h)(\rho - B),$$

$$A > 0, \qquad B > 0, \qquad \rho > B, \qquad 0 < h < 1. \tag{XV.5.31}$$

Here $J \cdot E_i = e_i$; the minus sign in the class expression reflects $E_i^2 = -1$. Computing $J^2/2$ in the total-pullback basis yields

$$V = \rho^2 + \rho A - \tfrac{1}{2}\big[h^2 + (1 - h)^2\big](\rho - B)^2. \tag{XV.5.32}$$

At $h = 1/2$, the subtracted coefficient is $1/4$. At $h = 1/3$ and $(A, B) = (\varepsilon, 2\varepsilon)$ it is $5/18$, and the actual chamber is $\rho > 2\varepsilon > 0$. The test value $\rho = \varepsilon$ has positive volume $31\varepsilon^2/18$ and positive retained areas but negative e_1, e_2. It is outside the chamber.

Use ten-dimensional Einstein frame at fixed microscopic string scale α', leading unwarped reduction, and a calibrated D3 with vanishing pulled-back DBI background combination. Integrating the Einstein term gives M_6^4 as the coefficient in the convention

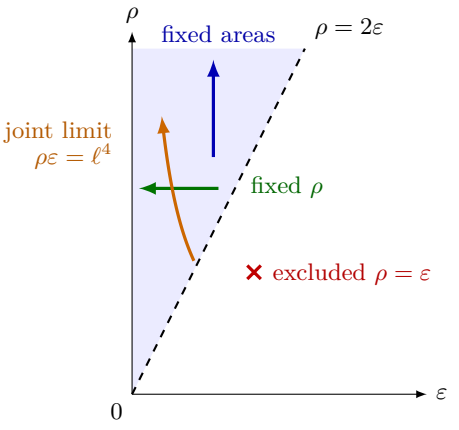


Figure XV.5.3: Three class paths on the CHAIN45 slice $A=\varepsilon,\ B=2\varepsilon,\ h=1/3$. The shaded chamber is $\rho>2\varepsilon>0$. A vertical path increases the bulk area at fixed string areas, a horizontal path shrinks strings at fixed ρ, and the curved path does both. The crossed point at $\rho=\varepsilon$ fails positivity on the exceptional curves.

$M_6^4\int\sqrt{-g_6}R_6/2$. Wrapping the brane on an effective curve class of charge q gives the tension

$$M_6^4=\frac{V}{\kappa_{10}^2},\qquad \kappa_{10}^2=\frac{(2\pi)^7\alpha'^4}{2},\qquad T(q)=\frac{q^{\mathsf T}a}{(2\pi)^3\alpha'^2}. \tag{XV.5.33}$$

The units are useful: $[a]=\text{length}^2$, $[V]=\text{length}^4$, so T has mass dimension two and M_6^4 dimension four. The normalized tensor coordinate $j=J/\sqrt{2V}$ has dimensionless periods and

$$(j\cdot S,j\cdot C)=\frac{(A,B)}{\sqrt{2V}},\qquad (T_S,T_C)=\frac{(A,B)}{(2\pi)^3\alpha'^2}. \tag{XV.5.34}$$

They answer different physical questions. Figure XV.5.3 compares the three possibilities in a single chamber.

First let $\rho\to\infty$ with fixed positive A,B,h. With $c_h=1-\frac12[h^2+(1-h)^2]>0$ we find

$$V=c_h\rho^2+O(\rho),\qquad j\cdot(S,C)\longrightarrow(0,0),\qquad (T_S,T_C)\text{ fixed and nonzero.} \tag{XV.5.35}$$

The Einstein coefficient diverges in microscopic units but the strings do not become tensionless. As an exact check use $h=1/2$ and set the area unit so $A=B=1$. At $\rho=3$, $(e_1,e_2)=(1,1)$ and $V=11$. At $\rho=5$, $(e_1,e_2)=(2,2)$ and $V=26$. Therefore

$$\frac{M_6^4(\rho=5)}{M_6^4(\rho=3)}=\frac{26}{11},\qquad \frac{j(\rho=5)\cdot S}{j(\rho=3)\cdot S}=\sqrt{\frac{11}{26}},\qquad \frac{T_S(\rho=5)}{T_S(\rho=3)}=1. \tag{XV.5.36}$$

Both points satisfy the full chamber. The distinction is already visible at finite parameters; it does not rely on taking a singular limit before measuring tensions. Second, set

$(A, B) = (\varepsilon, 2\varepsilon)$ and send ε to zero at fixed ρ. Then

$$V \to c_h \rho^2 > 0, \qquad T_S, T_C \to 0, \qquad M_6^4 \to c_h \rho^2 / \kappa_{10}^2. \tag{XV.5.37}$$

The strings shrink with finite gravitational coupling. For a joint limit take a reference area $\ell^2 > 0$ and use $\rho = \ell^2 \lambda,\ \varepsilon = \ell^2/\lambda,\ h = 1/3$. Then $\lambda > \sqrt{2}$ is in the chamber, and at large λ

$$V \sim \frac{13}{18} \ell^4 \lambda^2, \qquad (T_S, T_C) = \frac{\ell^2}{(2\pi)^3 \alpha'^2 \lambda} (1, 2), \qquad j \cdot (S, C) = O(\lambda^{-2}). \tag{XV.5.38}$$

A dimensionless tension in Einstein units gives a quantitative check of the distinction. Taking the positive square root of the Einstein coefficient in (XV.5.33), we obtain

$$\frac{T_i}{M_6^2} = \frac{\kappa_{10}}{(2\pi)^3 \alpha'^2} \frac{a_i}{\sqrt{V}} = \frac{\sqrt{2}\, \kappa_{10}}{(2\pi)^3 \alpha'^2}\, j \cdot C_i. \tag{XV.5.39}$$

On the first path this vanishes like ρ^{-1} because M_6^2 grows, not because the physical tension drops. On the second it vanishes like ε while M_6^2 stays finite. In the joint limit it vanishes like λ^{-2} because the two effects multiply. This is why one should state which quantities are fixed before using a normalized tensor coordinate as a test of a decoupling limit. Also e_i grow on the large-ρ paths; these are bulk curve areas, not extra light strings of the retained pair.

All three are paths of classes. The divergence of M_6^4 describes weakening of the gravitational zero mode in the leading reduction. Decompactification can also bring down bulk Kaluza–Klein energies. Equations (XV.5.33)–(XV.5.38) do not establish suppression of the full bulk sector, finite-action normalizable local modes, or physical finite distance to a conformal endpoint. A rigid field theory requires those physical separation and background premises in addition to the geometric area test. To see why even the candidate local field content needs more than an area test, we now keep the 2-curve pairing of S, C and change the elliptic geometry.

XV.5.4 A gauge-free ADE configuration

Why does the same base pairing allow a model with no six-dimensional gauge factors? We need a smooth surface with two (-2)-curves and trivial canonical line. This will let us keep the elliptic fiber smooth and constant everywhere. The surface comes from a quotient in $SU(2)$, unlike the 33 endpoint.

Let a primitive third root of unity ζ act on $(a, b) \in \mathbb{C}^2$ by $(a, b) \mapsto (\zeta a, \zeta^{-1} b)$. The invariant monomials satisfy $i - j = 0 \bmod 3$ for $a^i b^j$. Remove the smaller of i, j in powers of ab; the remaining pure power is a multiple of three. Thus the invariant ring has generators

$$x = a^3, \qquad y = b^3, \qquad z = ab, \qquad \mathbb{C}[a, b]^{\mathbb{Z}_3} = \mathbb{C}[x, y, z]/(xy - z^3). \tag{XV.5.40}$$

The single relation suffices because any monomial can be reduced to one with x or y absent. The reduced monomials have distinct images in $\mathbb{C}[a, b]$ if the pure z monomials

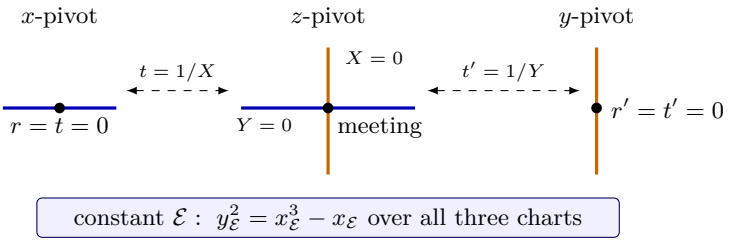


Figure XV.5.4: The two exceptional curves of $xy = z^3$. The middle chart contains their unique meeting; the outer charts add one point to each affine axis. In the product construction every point of these curves, including the meeting, has the same smooth auxiliary elliptic fiber.

are counted only once. This is a surface singularity, not yet an elliptic Weierstrass equation.

Blow up the origin in the three ambient coordinates. If the pivot is x, take $x = r,\ y = rY_x,\ z = rt$, so the strict equation is $Y_x = rt^3$. If the pivot is y, take $y = r',\ x = r'X_y,\ z = r't'$, with $X_y = r't'^3$. For pivot z use $X = x/z,\ Y = y/z$; then $XY = z$. The resulting surface maps are

pivot	surface coordinates	(x, y, z)
x	(r, t)	(r, r^2t^3, rt)
z	(X, Y)	(X^2Y, XY^2, XY)
y	(r', t')	$((r')^2(t')^3, r', r't')$

(XV.5.41)

These are three smooth affine charts. In the middle chart the exceptional fiber is $XY = 0$, two reduced axes crossing transversely. The $Y = 0$ axis is closed by $r = 0$ in the x chart, with $t = 1/X$ on their common open. The $X = 0$ axis is closed by $r' = 0$ in the y chart, with $t' = 1/Y$. Each is a projective line. There are no further compact curves, by properness of the blowup and affineness of the quotient, as in the preceding cone argument.

We can read each normal bundle directly. Along $Y = 0$ the normal coordinate is Y in the middle chart and r in the x chart. Along $X = 0$ it is X in the middle chart and r' in the y chart. Formula (XV.5.41) gives

$$t = X^{-1}, \quad r = X^2Y; \qquad t' = Y^{-1}, \quad r' = Y^2X. \tag{XV.5.42}$$

These are fiber-coordinate transitions for $\mathcal{O}(-2)$. For instance, the tautological line $\mathcal{O}(-1)$ has frames $(1, X)$ and $(t, 1)$ in the two charts, with the first frame equal to X times the second. A section's normal-coordinate coefficients therefore transform with X^2 for the square of the tautological line.

We also need an actual global two-form. On $x \neq 0$, a residue generator of $xy - z^3 = 0$, with a choice of overall sign, is $dx \wedge dz/x$. The substitutions in (XV.5.41) give its expressions in the three charts:

$$\frac{dx \wedge dz}{x} = dr \wedge dt = dX \wedge dY = -dr' \wedge dt'. \tag{XV.5.43}$$

On the original cover the same form pulls back to $3\,da \wedge db$, since $dx = 3a^2 da$ and $dz = b\,da + a\,db$. This checks the $SU(2)$ invariance and explains why the quotient form can extend crepantly. Direct chart calculations are still needed to rule out zeros or poles along the exceptional fiber. For the middle chart the numerator is $X^2 Y\, dX \wedge dY$. In the y chart one can first use $dx \wedge dz/x = -dy \wedge dz/y$, which follows by differentiating the relation. The displayed forms extend without poles or zeros and agree on overlaps. Adjunction gives an independent check of the normal degree. For the smooth rational exceptional curve C_i, the restriction of the canonical line of the surface is trivial, so

$$-2 = \deg K_{C_i} = (K_{S_{A_2}} + C_i) \cdot C_i = C_i^2, \qquad C_1 \cdot C_2 = 1. \tag{XV.5.44}$$

The intersection on the right is the single transverse point of the two axes in the z-pivot; neither outer chart introduces another meeting. The determinant of the positive pairing is 3, distinct from the determinant 8 of the earlier endpoint.

Take the product of this resolved surface S_{A_2} with the smooth projective elliptic curve $\mathcal{E}:\ y_{\mathcal{E}}^2 = x_{\mathcal{E}}^3 - x_{\mathcal{E}}$. The product has the nowhere vanishing three-form obtained by wedging (XV.5.43) with the regular elliptic differential. Its discriminant and string pairing are

$$\Delta_{\mathcal{E}} = -4, \qquad \Omega_{A_2} = \begin{pmatrix} 2 & -1 \\ -1 & 2 \end{pmatrix}. \tag{XV.5.45}$$

In particular the elliptic family has no degeneration along either compact curve, and its period system is trivial on the base. There is no quadratic deck action of the kind in (XV.5.14).

An unequal area ray can be realized, so this comparison does not depend on equal tensions. Solving $a = -\Omega_{A_2} d$ for $a = (\varepsilon, 2\varepsilon)^{\mathsf{T}}$ gives $d = (-4, -5)^{\mathsf{T}}\varepsilon/3$. To check positivity using the construction of Section XV.5.3, use the quotient fan with rays $(1,0), (0,1), (-1,2), (-2,3)$, and coefficients $(0, -4, -5, 0)$. The three support vertices are

$$m_{01} = (0,4), \qquad m_{12} = (3,4), \qquad m_{23} = (15,10). \tag{XV.5.46}$$

Each has equality on its labeled pair and strict inequality on both other rays. For example the middle vertex solves $m_y = 4,\ -m_x + 2m_y = 5$, and its values on the outer rays are 3 and 6. The first and last vertices are also separated from their neighboring walls: at $(0,4)$ the third ray evaluates to $8 > 5$, while at $(15,10)$ the second ray evaluates to $10 > 4$. This verifies actual positive representatives rather than inferring their existence from $\det \Omega_{A_2} > 0$. This fan is the one in (XV.5.41): the valuation vectors of x, y, z on the two compact rays are $(1,2,1)$ and $(2,1,1)$, read from the two coordinate axes in the middle chart. For example, with the displayed rays the characters $m_x = (0,1),\ m_y = (3,2),\ m_z = (1,1)$ obey $m_x + m_y = 3m_z$. Their pairings on the middle pair give the exponents of X^2Y, XY^2, XY with $Y = 0$ corresponding to the first interior ray. On an outer pair they give the monomials of the corresponding outer blowup chart up to exchange of coordinates. Its boundary index is 3, with quotient weights $1, -1$ modulo 3. The ample class, scaled and supplemented by affine pullback as before, yields the claimed area ray.

In this pairing a positive geometric root is a nonnegative integral charge of squared norm two. Since

$$\tfrac{1}{2} q^{\mathsf{T}} \Omega_{A_2} q = q_1^2 - q_1 q_2 + q_2^2 = (q_1 - q_2)^2 + q_1 q_2, \tag{XV.5.47}$$

the only possibilities are $q = (1,0), (0,1), (1,1)$. The enumeration is short: if both coordinates are positive, their product is already at least one, with equality only when both equal one. If one coordinate vanishes, the other coordinate must square to one. Their areas and leading calibrated tensions on this ray are

$$(a_{(1,0)}, a_{(0,1)}, a_{(1,1)}) = \varepsilon(1,2,3), \qquad (T_{(1,0)}, T_{(0,1)}, T_{(1,1)}) = \frac{\varepsilon}{(2\pi)^3 \alpha'^2}(1,2,3). \tag{XV.5.48}$$

Changing the ratio of the two areas leaves the norm-two set fixed but changes the tension ratios. The charge lattice and its periods play different roles. This calculation identifies root charges and periods; it does not enumerate the spectrum of stable bound states.

The quotient and residue calculations do not construct a metric. The physical dictionary uses ordinary Type IIB on the A_2 asymptotically locally Euclidean (ALE) degeneration, in a rigid unshifted background with the relevant periods at the conformal locus. The elliptic curve is auxiliary and encodes the constant axiodilaton. It is not an extra physical two-torus. In this setting the singular limit is the type A_2 $(2,0)$ theory, with two tensor multiplets on its resolved branch. Wrapped D3-branes give chiral strings in six dimensions. Compactifying a spatial direction and wrapping such a string can give a lower-dimensional particle; it does not make a six-dimensional massless gauge vector. In contrast, the two retained curves of CHAIN45 have the same matrix but carry split I_4 and I_5 fibers. The Cartan matrix does not predict the gauge content of a six-dimensional model.

Collapsing the Kähler areas does not tune other background periods by itself. The role of the worldsheet theta angle in the IIB K3 example is a caution about such data, not a derivation of every tuning needed for a local ALE background. We now return to 414, where the Weierstrass fibers really are singular and their full resolution is needed before interpreting a tensor branch.

XV.5.5 Tensor-branch theory and its UV interpretation

The base blowup passed the point-order test. Does its elliptic total space actually have a smooth crepant resolution? We will show this for the exact monomial model, including the gluing of the blowup centers. This is stronger than resolving one surface singularity transverse to a single generic fiber.

Start with coordinates (u, v) on the chart of two successive rays and (u', v') on the next chart. For the relation $v_{i-1} + v_{i+1} = nv_i$, the dual character of u' has coordinates $(n, 1)$ in the old basis: it pairs to $1, 0$ with v_i, v_{i+1}. The character of v' has coordinates $(-1, 0)$. On the common open $u \neq 0$,

$$(u', v') = (u^n v, u^{-1}), \qquad du' \wedge dv' = \mathcal{J}\, du \wedge dv, \qquad \mathcal{J} = u^{n-2}, \qquad n = 4, 1, 4. \tag{XV.5.49}$$

The frame of L dual to the new base form is the old frame divided by $\mathcal{J}$; hence a component of L^k scales by $\mathcal{J}^k$. Use the smooth projective-plane bundle with transitions

$$[x' : y' : z'] = [\mathcal{J}^2 x : \mathcal{J}^3 y : z], \qquad (f', g') = (\mathcal{J}^4 f, \mathcal{J}^6 g). \tag{XV.5.50}$$

The homogeneous cubic $y^2z - x^3 - fxz^2 - gz^3 = 0$ changes by $\mathcal{J}^6$, giving a Cartier hypersurface W. Across either end use $(u, v) = (r, w)$ and $(u', v') = (w', r')$; then $w' = r^4w,\ r' = 1/r,\ x' = r^4x,\ y' = r^6y$ in the affine fiber chart. Across the middle overlap the end coordinates are units, so the discriminant is nonzero. Nonadjacent chart overlaps are in the torus; the same line-bundle law applies.

The only point at $z = 0$ in each projective fiber is $[0 : 1 : 0]$. In the $y = 1$ chart let $\xi = x/y,\ \zeta = z/y$; at infinity

$$H = \zeta - \xi^3 - f\xi\zeta^2 - g\zeta^3 = 0, \qquad H_\zeta|_{\xi=\zeta=0} = 1. \tag{XV.5.51}$$

It is smooth there. In the $z = 1$ chart, at $w \neq 0$ the discriminant $31w^6$ does not vanish, so each such fiber, and the total space over it, is smooth. At $w = 0$ the x, y derivatives vanish simultaneously only at $x = y = 0$; there all derivatives vanish. Thus in the entire projective model the singular locus consists exactly of two disjoint curves, one over each end. The finite-chart equation is integral: the polynomial $x^3 + w^2x + w^3$ has odd degree in x and is not a square in the rational function field, so the quadratic in y is irreducible. There is no additional hypersurface component at infinity, which is only a section. The Cartier hypersurface satisfies Serre's S_2 condition; its singular locus has codimension two in the threefold, so it is regular in codimension one. Thus W is normal.

The ideal (x, y, w) is multiplied generator by generator by units on the end overlap. It defines the first global center, the reduced disjoint union of the two curves, each mapping isomorphically onto the corresponding compact $\mathbb{P}^1$. Blow it up in the ambient projective bundle. This is a projective morphism with a smooth new ambient space. The three affine pivot charts of each transverse blowup give

pivot	$(x_{\text{old}}, y_{\text{old}}, w_{\text{old}})$	strict equation
x	(x, xy, xw)	$y^2 - x(1 + w^2 + w^3) = 0$
y	(yx, y, yw)	$1 - y(x^3 + w^2x + w^3) = 0$
w	(wX, wY, w)	$Y^2 - wP(X) = 0$

(XV.5.52)

Here $P(X) = X^3 + X + 1$. At the center the old equation has multiplicity two, so the proper equations in the table come from division by the square of the pivot. This ordinary scaling of all three transverse ambient coordinates differs from the weighted scaling over the base point blowup.

In the y-pivot the factor multiplying y is a unit on the hypersurface, so the y derivative cannot vanish. The x-pivot can be singular only if $y = 0$ and $1 + w^2 + w^3 = 0$. This requires its ratio $w \neq 0$, so any such point is also in the w-pivot. The w-pivot gradient, in the variables (X, Y, w), is

$$\big(-wP'(X),\, 2Y,\, -P(X)\big), \qquad \operatorname{Sing}(W^{(1)})_{\text{end}}: \quad w = Y = 0, \quad P(X) = 0. \tag{XV.5.53}$$

Indeed P has three simple roots, and at a root the first derivative forces $w = 0$. Conversely all three gradients vanish along each displayed curve. The transformations of the ratio coordinates, obtained by dividing the original transformations, are

$$X' = X, \qquad Y' = r^2Y, \qquad w' = r^4w, \qquad (Y')^2 - w'P(X') = r^4\big(Y^2 - wP(X)\big). \tag{XV.5.54}$$

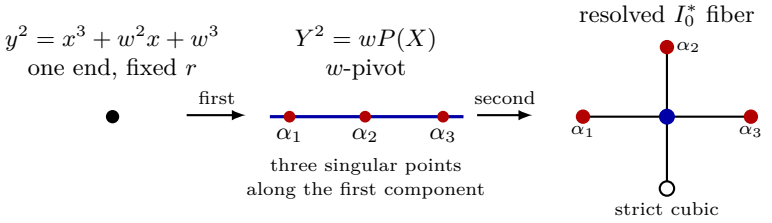


Figure XV.5.5: Transverse resolution over either compact I_0^* end. The first w-pivot exhibits three nodes labeled by the distinct roots of P. Blowing up their reduced global curves produces the three outer exceptional arms. The fourth outer arm is the strict transform of the original cubic fiber; the central component comes from the first blowup.

In particular the residual Y does not glue as an unscaled scalar. The ideal $(w, Y, P(X))$ glues and each root labels one global curve mapping isomorphically to its end $\mathbb{P}^1$. The roots are constant and do not permute. Together the two ends give six disjoint smooth curves, the full reduced singular locus of the first strict transform.

The second blowup uses this reduced union as ambient center. Near each root $U = P(X)$ is an étale coordinate because $P' \neq 0$. This is a local assertion; no global polynomial inverse for P is needed. The equation is $Y^2 = wU$. With each nonpivot coordinate again denoting the ratio to the pivot, the three strict equations are

pivot	U	Y	w
strict equation	$Y^2 - w = 0$	$1 - Uw = 0$	$Y^2 - U = 0.$

(XV.5.55)

In the middle equation U, w are units; the other two equations are linear in one coordinate. The three charts are smooth and cover the second blowup over the center, since smoothness can be tested étale locally. Elsewhere the morphism is an isomorphism. The two successive proper transforms are projective over W, as restrictions of ambient blowups, and the final one is smooth everywhere including infinity.

For crepancy, let G denote the ambient exceptional divisor at a given stage. A blowup of a smooth center of codimension c adds $(c-1)G$ to the pulled-back canonical class. The total transform of a hypersurface of multiplicity m is its proper transform plus mG. Adjunction then gives

$$K_{\text{strict}} = \pi^* K_{\text{old}} + (c - 1 - m)G|_{\text{strict}}, \qquad c = 3, \quad m = 2, \quad c - 1 - m = 0. \tag{XV.5.56}$$

At the first center y^2 is quadratic and the remaining terms are cubic in (x, y, w). At the second, $Y^2 - wU$ is quadratic. Thus this calculation applies at every point of both centers.

Triviality of the original dualizing line also holds globally. In the finite chart use the hypersurface residue of

$$\frac{du \wedge dv \wedge dx \wedge dy}{y^2 - x^3 - fx - g}. \tag{XV.5.57}$$

Under (XV.5.50), the base Jacobian and the two fiber scalings multiply to $\mathcal{J}\mathcal{J}^2\mathcal{J}^3 = \mathcal{J}^6$. Terms in fiber differentials involving base differentials drop out of the numerator. The

denominator scales by the same power. This gives the dualizing generator even on the singular finite chart by Cartier adjunction. In the infinity chart use $x = \xi/\zeta,\ y = 1/\zeta$; the fiber Jacobian is $-\zeta^{-3}$ and the finite equation becomes $\zeta^{-3}H$. The residue therefore agrees up to the indicated sign with the infinity-chart generator, which is nonvanishing there by (XV.5.51). The resolved threefold has trivial canonical line by (XV.5.56). This is an existence result over the stated noncompact base.

The pivot equations also locate the components of a resolved fiber. Away from the roots of P, the first exceptional curve is the line $Y = w = 0$ with coordinate X. Its generic multiplicity in the divisor $w_{\text{old}} = 0$ is two, since $w = Y^2/P(X)$. The x-pivot covers its point at $X = \infty$ and also the meeting with the strict cubic: write the ratio to the x pivot as w_x, so $w_{\text{old}} = xw_x$ and $y^2 = x(1 + w_x^2 + w_x^3)$. Near $y = w_x = 0$ this becomes

$$w_{\text{old}} = \frac{y^2 w_x}{1 + w_x^2 + w_x^3}. \tag{XV.5.58}$$

The two component equations there are $y = 0$ and $w_x = 0$, meeting transversely with multiplicities two and one. At a root use the U-pivot of the second blowup. There $w_{\text{old}} = Uw_{\text{ratio}} = UY_{\text{ratio}}^2$. The new exceptional component $U = 0$ has multiplicity one and meets the first component $Y_{\text{ratio}} = 0$ transversely. This occurs separately at all three roots, away from the strict cubic. Hence there is one central component of multiplicity two and four disjoint outer arms of multiplicity one, as in Figure XV.5.5.

The four outer components around the central I_0^* component give the affine D_4 fiber. The split cover identifies the ordinary end algebras; the middle (-1)-curve has no generic seven-brane gauge factor. In the ordinary interpretation of this branch (Heckman, Morrison, et al. 2014, §4.1), the unpaired tensor is associated with the rank-one E-string sector and the two end algebras gauge subalgebras of its E_8 flavor symmetry. One necessary compatibility check is visible in the integer E_8 roots. With e_i an orthonormal basis, take

$$\{\pm e_i \pm e_j : 1 \le i < j \le 4\} \quad \text{and} \quad \{\pm e_i \pm e_j : 5 \le i < j \le 8\}. \tag{XV.5.59}$$

Each set has $4\binom{4}{2} = 24$ roots and spans a D_4 system; the two sets are orthogonal. This verifies the Lie-algebra embedding needed for that interpretation. It does not calculate the full 414 spectrum, anomaly polynomial or global gauge group.

On a resolved gauged curve of area a_i, dimensional reduction gives the parametric dependence $g_{6,i}^{-2} \propto a_i$ at fixed microscopic normalization. In particular, for the 414 ends we only use this proportionality. At energy $\mathcal{E}_{\text{p}}$ the Yang–Mills expansion parameter scales as

$$g_{6,i}^2 \mathcal{E}_{\text{p}}^{\,2} \ \propto\ \frac{\alpha'^2 \mathcal{E}_{\text{p}}^{\,2}}{a_i}. \tag{XV.5.60}$$

At any fixed nonzero energy it grows as the curves shrink. The weakly coupled tensor-branch Lagrangian therefore cannot calculate the singular endpoint by perturbation theory. An exactly normalized example is the separate CHAIN45 pair: in its defining SU trace convention $g_{6,i}^{-2} = a_i/[2(2\pi)^5\alpha'^2]$. There is no such Yang–Mills term from the smooth generic fiber of E_0.

For the CHAIN45 pure dynamical gauge slice we can see what anomaly cancellation does test. Put the other background curvatures to zero and set $F_i = -iF_{\text{phys},i}/(2\pi)$

and $s_i = \mathrm{tr}_{\mathrm{f}}(F_i^2)$. The actual ordinary CHAIN45 matter recalled from Chapter B.3 consists of three defining hypers on $SU(4)$, six on $SU(5)$, and one shared full $(\mathbf{4}, \overline{\mathbf{5}})$ hyper. Put $q_i = \mathrm{tr}_{\mathrm{f}}(F_i^4)$. The adjoint fourth trace is $2N_i q_i + 6s_i^2$. The shared hyper has fourth trace $5q_1 + 4q_2 + 6s_1 s_2$: terms with one odd single trace vanish by tracelessness, while the coefficient of the product of second traces is $\binom{4}{2} = 6$. Applying the hyper minus vector chirality and the degree-eight index factor $1/24$, the quartic coefficients and the mixed coefficient are

$$[q_1]I_{\mathrm{loop}} = \frac{3+5-8}{24} = 0, \qquad [q_2]I_{\mathrm{loop}} = \frac{6+4-10}{24} = 0, \qquad [s_1 s_2]I_{\mathrm{loop}} = \frac{6}{24}. \tag{XV.5.61}$$

Each adjoint contributes $-6s_i^2/24$ and no other field contributes to the single-factor square. The remaining pure gauge index and tensor source are

$$I_{\mathrm{loop}} = -\tfrac{1}{4}s_1^2 + \tfrac{1}{4}s_1 s_2 - \tfrac{1}{4}s_2^2 = -\tfrac{1}{8}s^{\mathsf{T}}\Omega_{A_2}s, \qquad X = s/2, \qquad Y = \Omega_{A_2}X. \tag{XV.5.62}$$

The Green–Schwarz term with this source sign convention is

$$I_{\mathrm{GS}} = \tfrac{1}{2}Y^{\mathsf{T}}\Omega_{A_2}^{-1}Y = +\tfrac{1}{8}s^{\mathsf{T}}\Omega_{A_2}s. \tag{XV.5.63}$$

The two terms cancel. Reversing the overall sign of the Green–Schwarz *quadratic term* would double the nonzero polynomial, whereas reversing every source Y would leave the square unchanged. This test is for the stated pure gauge slice of CHAIN45. It does not supply an anomaly calculation for the 414 E-string gauging.

In the ordinary rigid F-theory construction the simultaneous contraction of this 414 tensor branch is identified with a $(1,0)$ interacting endpoint. The geometric results specify which base periods collapse, which wrapped strings become light at leading calibrated order, and which elliptic model can be used. The endpoint interpretation additionally assumes an appropriate rigid background and an actual local physical limit with the relevant degrees of freedom retained. Neither the crepant resolution nor the anomaly calculation proves UV existence or bulk isolation. These distinctions give an order of operations in a new example. The negative lattice suggests a candidate point; the coefficient sections and their resolution test whether an ordinary elliptic model can be used over the positive-area branch; calibrated tensions tell us which wrapped strings to track along a proposed path. If the elliptic model fails in the interior there is no branch of the stated type from which to start. If the lattice has a null class, a projective model can exist but the joint point contraction fails. The next examples test these two separate failures.

XV.5.6 A changed configuration that fails

Which part of the construction fails if we change a coefficient or an incidence? First keep the 414 base and the same coefficient orders. Set $f = -3w^2,\ g = 2w^3$ in each of the four charts, using the same line transitions. Then

$$4(-3)^3 + 27(2)^2 = 0, \qquad \Delta \equiv 0, \qquad P(\psi) = (\psi - 1)^2(\psi + 2). \tag{XV.5.64}$$

The point-order test on f, g still passes after the base blowup. Nevertheless the generic cubic is singular: at $w \neq 0$, $(x, y) = (w, 0)$ is a double-root point. This is not an elliptic fibration with smooth generic fiber. The original model depended on the coefficients as well as the fan.

For the second test, change the base itself. We will find two (-2)-curves, as in the A_2 example, but with two meetings instead of one. To construct the base surface take the projective cubic family

$$Y^2Z = X^3 - 3XZ^2 + (2 + t^2)Z^3, \qquad |t| < \delta < 2, \qquad \Delta(t) = 27t^2(t^2 + 4). \tag{XV.5.65}$$

This family supplies the *base* of our comparison, not its auxiliary elliptic fiber. The only singular cubic in the disk is at $t = 0$. At infinity the family is smooth by the derivative test of (XV.5.51). The affine central cubic has its node at $x = 1,\ y = 0$; with $s = x - 1$ the total surface equation is

$$y^2 - 3s^2 - t^2 - s^3 = 0. \tag{XV.5.66}$$

The quadratic term is nondegenerate. Blow up $(s, y, t) = (0, 0, 0)$ in the ambient smooth threefold. Write the ratios to the pivot with the same letters as the original coordinates. The three strict equations are

pivot	strict equation
s	$y^2 - 3 - t^2 - s = 0$
y	$1 - 3s^2 - t^2 - ys^3 = 0$
t	$y^2 - 3s^2 - 1 - ts^3 = 0.$

(XV.5.67)

The first is smooth by its s derivative. In the second, vanishing of the derivatives with respect to the pivot y and ratio t would force $s = t = 0$, contrary to the equation. In the third, the t, y derivatives would force $s = y = 0$, again contrary to the equation. Thus the proper transform is smooth. It remains proper over the disk, since the original cubic is closed in the projective family and the ambient blowup is projective over it.

There are two compact rational curves in its central fiber. The exceptional component is a smooth conic in the direction plane, from the quadratic part of (XV.5.66). The other component is the strict transform of the central cubic. To check its global compact normalization, write $p/q = y/(x - 1)$ where $x \neq 1$; then $x = (p/q)^2 - 2$ and $y = (p/q)((p/q)^2 - 3)$. This gives the map

$$[p : q] \longmapsto [q(p^2 - 2q^2) : p(p^2 - 3q^2) : q^3]. \tag{XV.5.68}$$

It satisfies the homogeneous cubic equation. At $q \neq 0$ the third entry is nonzero, and at $q = 0$ the middle entry is nonzero, giving the point at infinity. The morphism is proper and birational by its inverse on the dense smooth open, so it normalizes the irreducible cubic. Its two preimages of the node have $p/q = \pm\sqrt{3}$. In the s-pivot these branches lift to points with ratio $y = \pm\sqrt{3}$ and ratio $t = 0$, and the strict curve is smooth there. It is therefore the compact $\mathbb{P}^1$ normalization.

In the s-pivot the original base parameter is $t_{\text{old}} = s\,t$. The strict component has $t = 0$, and the conic has $s = 0$. They meet at $y = \pm\sqrt{3}$; these are all meetings, since the two directions with original t-component zero both have nonzero s-component. The

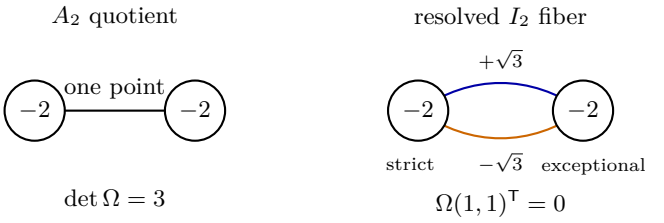


Figure XV.5.6: In the actual I_2 degeneration the strict and exceptional curves meet at both nodal directions $y/s = \pm\sqrt{3}$. Their sum is a principal fiber. The A_2 quotient resolution instead has one transverse meeting and a definite pairing.

y derivative is nonzero at each meeting, so (s, t) are coordinates and both intersections are transverse. Both components occur once in the principal divisor of t_{old}. Calling them $C_{\text{str}}, C_{\text{exc}}$, we get

$$\begin{aligned} F_0 &= \operatorname{div}(t_{\text{old}}) = C_{\text{str}} + C_{\text{exc}}, \qquad F_0 \cdot C_{\text{str}} = F_0 \cdot C_{\text{exc}} = 0, \\ \Omega_{I_2} &= \begin{pmatrix} 2 & -2 \\ -2 & 2 \end{pmatrix}, \qquad\qquad \Omega_{I_2}(1,1)^{\mathsf{T}} = 0. \end{aligned} \tag{XV.5.69}$$

The two meetings give $C_{\text{str}} \cdot C_{\text{exc}} = 2$; principality gives both self-intersections -2. The kernel is generated by the primitive positive charge $(1, 1)$. The class has area $a_{\text{str}} + a_{\text{exc}}$; setting that sum to a fixed positive value does not allow both areas to shrink. By the negative-definiteness criterion the configuration cannot contract to one point. Using this smooth surface as a base and choosing a *separate* constant smooth auxiliary elliptic curve does not change that conclusion. This constraint persists even though the two individual areas can change. For example at total fiber area 6 in fixed units, taking $(a_{\text{str}}, a_{\text{exc}}) = (b, 6 - b)$ with $0 < b < 6$ varies the relative tension without altering the null-charge tension. In this example the normalizations of the two eigenvectors make the distinction transparent:

$$q_- = (1, -1)^{\mathsf{T}}, \quad \Omega_{I_2} q_- = 4q_-, \qquad q_0 = (1, 1)^{\mathsf{T}}, \quad q_0^{\mathsf{T}} a = 6. \tag{XV.5.70}$$

Here q_- is an algebraic difference of curve classes, not an effective wrapped string. A zero norm for q_0 is a statement about the pairing, not a zero value of its area. The null matrix alone neither selects an LST nor supplies its physical scale.

A final transfer uses the same point-blowup method as the 33 example but produces a different chain. Take the pure E_6 collision $f = 0,\ g = u^4 v^4$ on the plane. The original axes are noncompact. Their discriminant orders away from the crossing are eight, with split cover since the residual g is a square there. At the crossing g has order eight, so blow up once. In the chart $(u, v) = (e, et)$ the transformed $g = e^2 t^4$; in the other chart the same formula holds with the axes interchanged. At each of the two new crossings the order is six, hence each requires another blowup. The ray sums and new orders show where the process stops:

$$\begin{aligned} &(1,0), (2,1), (1,1), (1,2), (0,1), \qquad \operatorname{ord}(g) = (4,0,2,0,4), \\ &(1,1) = (1,0) + (0,1), \quad (2,1) = (1,0) + (1,1), \quad (1,2) = (1,1) + (0,1). \end{aligned} \tag{XV.5.71}$$

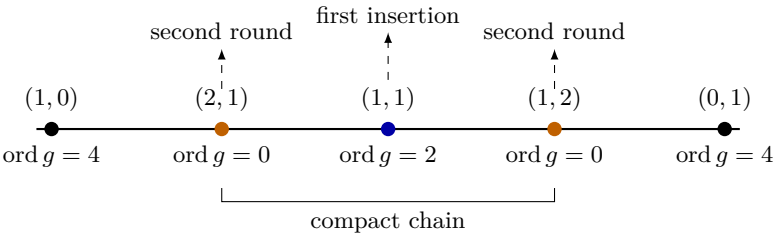


Figure XV.5.7: Insertion order for the pure E_6 collision. The first new ray has residual g-order two. The two remaining adjacent sums reach six and force the last insertions. The final compact chain has normal degrees $-1, -3, -1$. The two boundary rays remain noncompact.

For example, in the chart with $g = e^2t^4$ the second blowup uses $(e, t) = (a, ab)$ and (ab, a). Dividing the pulled-back coefficient by a^6 gives b^4 and b^2, respectively. The other old chart gives the same two equations with the ends interchanged. Thus all four final charts have a genuine nonzero discriminant function, not merely admissible f, g orders. Their g exponents distinguish the proper transform of the first exceptional curve from the new ones. In particular the smooth generic fibers on the new exceptional curves do not remove their compact base charges.

For instance each of the two last exceptional orders is $4 + 2 - 6 = 0$, and the four final adjacent sums are $4, 2, 2, 4$, below six. The two latter centers are disjoint once the first blowup has been performed. The original exceptional curve loses one unit of self-intersection at each of its two ends, so its strict transform is -3; both new ones are -1. The fan relations give the same 131 pairing:

$$\Omega_{131} = \begin{pmatrix} 1 & -1 & 0 \\ -1 & 3 & -1 \\ 0 & -1 & 1 \end{pmatrix}, \qquad a = (L, \varepsilon, R)^{\mathsf{T}}, \qquad d = -\begin{pmatrix} 2L + \varepsilon + R \\ L + \varepsilon + R \\ L + \varepsilon + 2R \end{pmatrix}. \quad \text{(XV.5.72)}$$

Here $L, R > 0$ are end areas. The last column vector is obtained by solving $a = -\Omega_{131}d$. With coefficient zero on the boundary rays the positivity inequalities of the relative support function are just $a_i > 0$: the vertex for an adjacent cone has excess $a_i = n_i(-d_i) + d_{i-1} + d_{i+1}$ on the next ray across v_i. Positive excess at each interior wall gives strict convexity on the subdivided cone. Thus the ray $\varepsilon \to 0^+$ at finite L, R shrinks just the middle curve. The retained middle charge has norm 3. Blowing down the two -1 curves would instead replace its class by its total pullback and give

$$\Omega_{\text{restriction}} = [3], \qquad \Omega_{\text{after two blowdowns}} = [3 - 1 - 1] = [1]. \quad \text{(XV.5.73)}$$

There is a useful test charge for the difference. The middle strict class M has pairing $\Omega_{131}(M, M) = 3$ in the positive convention. The class orthogonal to both ends and projecting to the middle under blowdown is $L_c + M + R_c$, where L_c, R_c denote the end *curves*. Its norm and its period along the partial ray are

$$(1, 1, 1)\Omega_{131}(1, 1, 1)^{\mathsf{T}} = 1, \qquad J \cdot (L_c + M + R_c) = L + \varepsilon + R. \quad \text{(XV.5.74)}$$

Consequently the orthogonal lift is not becoming tensionless in this partial limit; it still includes the two finite end areas. The two answers correspond to different geometry. This collision supplies the bridge to conformal matter: the compact intermediate chain is forced by a collision of noncompact flavor divisors. The detailed conformal matter of that branch is the subject of Chapter B.6. The actual finite-scale construction for LSTs is separate and begins in Chapter B.8.

Exercises

Use `benchmark/tasks.json` for the JSON fields and `benchmark/PROTOCOL.md` for submission. Written explanations, including the choice of hypotheses for physical interpretations, are human assessed.

1. For $f = cu^2v^2,\ g = du^3v^3$ with $(c, d) = (1, 2)$, use the two ordered pivot charts in (XV.5.8). Give their coefficient and discriminant polynomials, the center orders and the generic exceptional orders. Compare $(-3, 2)$, for which the order of the zero discriminant is infinite. Explain which line bundle fixes the exceptional powers.

2. For 414 with areas $(1, 2, 3)$, compute d in the compact divisor span, and the period sums for charges $(1, 0, 1), (1, 1, 1)$. Give the end principal block and the pairing after blowing down E_0, including the two determinants. Explain why a smooth generic elliptic fiber does not make E_0 disappear from the string lattice.

3. For CHAIN45 take $h = 1/4$ and $(\rho, A, B) = (5, 1, 2)$, then $(2, 1, 3)$. Compute e_1, e_2, V, the chamber verdicts and the area ratios $A : B$. On the three paths of Section XV.5.3, give the leading powers of the small parameter in the j-periods, tensions and fourth-power Planck coefficient.

4. Use A_2 with areas $(2, 5)$ and auxiliary cubic $y^2 = x^3 + x + 1$. Compute the three positive root norms and area sums. Compare the discriminant, point-order data and elliptic monodromy with the transverse model $f = w^2,\ g = w^3$. Explain why a Cartan pairing is insufficient to identify a vector multiplet sector.

5. Compare (XV.5.65) with the actual projective cubic having $2+t^3$ in place of $2+t^2$ on the same disk restricted to $|t| < 1$. Near the node take $u = y + s\sqrt{3+s},\ v = y - s\sqrt{3+s}$; the equation becomes $uv = t^3$. In the u-pivot the strict equation is $v' = u(t')^3$; the v-pivot is symmetric, and the t-pivot has $u'v' = t$. Label the strict component first, then the two exceptional components. Use these charts to recover the meeting numbers and null vector. For fixed total area 9 and first two areas $2, 3$, find the remaining positive area, and compare with the two-component case at the same total and first area. Explain why the incidence does not identify a unique physical theory.

6. For the pure E_6 collision take areas $(3, \varepsilon, 5)$. Give the three ray insertions in their partial order, the period coefficients d, and the norm of the retained middle charge. Compare the geometry where the two ends are actually blown down. Why

would simply discarding the finite-area end strings leave the principal restriction instead?

Status and sources

§XV.5.1 [MATH]. The residual-divisor method is in Heckman, Morrison, et al. 2014, Appendix B, (B.1)–(B.3). The $33 \to 414$ example is in Heckman, Morrison, et al. 2014, §4.1, (4.9)–(4.10), Fig. 1; here the characters realize explicit coefficients. The generic-field I_0^* test is in Katz et al. 2011, §6, (6.1)–(6.2); root permutations and transverse elliptic inversion are computed separately above. The calculation uses the Weierstrass convention $\Delta_{\text{book}} = 4f^3 + 27g^2$.

§XV.5.2 [MATH]. The chart intersections, integral change of basis and quotient action are derived in the text. For the continued fraction see Heckman, Morrison, et al. 2014, Appendix D, pp. 42–43. Analytic contractibility is Grauert 1963, Defs. 11–13 and Satz 14, pp. 92, 99; for the necessary intersection sign at a resolved normal point see also Mumford 1961, §I, p. 6.

§XV.5.3 [MATH] [SUGRA] [DEC]. Relative support data and the CHAIN45 chamber are worked above. The calibrated tensions and leading Einstein reduction use the assumptions of Chapter B.2. For the physical decoupling premise and finite-distance discussion see Heckman and Rudelius 2019, §§2.1, 5.1 and Heckman, Morrison, et al. 2014, §§2–3. The comparison constructs no metric or bulk mode analysis.

§XV.5.4 [MATH] [GEO-E]. The quotient charts, residue, product and positive roots are computed above. The auxiliary elliptic dictionary is Vafa 1996, §2; the ordinary local interpretation is Heckman, Morrison, et al. 2014, §3.1, Witten 1995, §1, (1.4)–(1.5), §2, p. 7 and Heckman and Rudelius 2019, §2.1. The K3 theta-angle example warns of other background data.

§XV.5.5 [MATH] [GEO-X] [GEO-E] [ANOM]. The normal cubic, global centers and crepancy are established by the charts and adjunction. For the end algebras and conditional ordinary branch interpretation see Katz et al. 2011, §6 and Heckman, Morrison, et al. 2014, §4.1, with its published erratum Heckman, Morrison, et al. 2015. The selected pure gauge polynomial uses Chapter B.3 and its integral anomaly normalization; it is not a 414 anomaly computation.

§XV.5.6 [MATH]. The zero-discriminant control and the compact I_2 surface are derived above. For the definite versus semidefinite distinction under additional physical hypotheses see Bhardwaj et al. 2016, §2.1, (2.3)–(2.5). The pure E_6 collision and 131 branch use Del Zotto et al. 2015, §2, (2.2), (2.5); the partial-period calculation is geometric.

The geometric examples and scaling comparisons test the stated assumptions in selected cases; some comparisons use different pairings rather than altered geometric models. They do not establish a general classification.

References

Bhardwaj, L. et al. (2016). "F-theory and the Classification of Little Strings". In: *Phys. Rev. D* 93, p. 086002. DOI: 10.1103/PhysRevD.93.086002. arXiv: 1511.05565.

Del Zotto, M. et al. (2015). "6d Conformal Matter". In: *JHEP* 02, p. 054. DOI: 10.1007/JHEP02(2015)054. arXiv: 1407.6359.

Grauert, H. (1963). "Die Bedeutung des Levischen Problems für die analytische und algebraische Geometrie". In: *Proceedings of the International Congress of Mathematicians, Stockholm 1962*, pp. 79–106.

Heckman, J. J., D. R. Morrison, and C. Vafa (2014). "On the Classification of 6D SCFTs and Generalized ADE Orbifolds". In: *JHEP* 05, p. 028. DOI: 10.1007/JHEP05(2014)028. arXiv: 1312.5746.

Heckman, J. J., D. R. Morrison, and C. Vafa (2015). "Erratum to: On the Classification of 6D SCFTs and Generalized ADE Orbifolds". In: *JHEP* 06, p. 017. DOI: 10.1007/JHEP06(2015)017.

Heckman, J. J. and T. Rudelius (2019). "Top Down Approach to 6D SCFTs". In: *J. Phys. A* 52, p. 093001. DOI: 10.1088/1751-8121/aafc81. arXiv: 1805.06467.

Katz, S. et al. (2011). "Tate's Algorithm and F-theory". In: *JHEP* 08, p. 094. DOI: 10.1007/JHEP08(2011)094. arXiv: 1106.3854.

Mumford, D. (1961). "The Topology of Normal Singularities of an Algebraic Surface and a Criterion for Simplicity". In: *Publ. Math. IHES* 9, pp. 5–22. DOI: 10.1007/BF02698717.

Vafa, C. (1996). "Evidence for F-Theory". In: *Nucl. Phys. B* 469, pp. 403–418. DOI: 10.1016/0550-3213(96)00172-1. arXiv: hep-th/9602022.

Witten, E. (1995). "Some Comments on String Dynamics". In: *Future Perspectives in String Theory*, pp. 501–523. arXiv: hep-th/9507121.

Chapter XV.6

E-strings, conformal matter and exceptional constructions

XV.6.1 The geometric E-string

What geometric event creates one tensor without a gauge boson? A codimension-two collision can make the Weierstrass model nonminimal even when each generic codimension-one fiber is allowed. Blowing up the base can replace the collision by a compact curve. The area of that curve controls a wrapped D3 string, whereas its *generic* fiber controls whether it supports gauge bosons. We will follow both tests on the same explicit blowup. We use the local period and anomaly conventions of Chapters B.2 and B.3.

Work over the complex affine plane with coordinates u, v. Use the local frame of $L = -K_B$ induced by $du \wedge dv$ and the short Weierstrass equation

$$\begin{gathered} y^2 = x^3 + fx + g, \qquad f = -3u^4, \quad g = u^5 v, \\ \Delta = 4f^3 + 27g^2 = 27u^{10}(v - 2u)(v + 2u). \end{gathered} \tag{XV.6.1}$$

The usual elliptic discriminant is -16Δ, a constant that will not affect any order. At the generic point of $u = 0$, v is a unit, so the orders are $(4, 5, 10)$, those of a II^* fiber. At a generic point of either residual line $v = \pm 2u$, f, g are units and Δ has a simple zero. These two loci have type I_1. At their common origin the orders are measured in the two-variable maximal ideal, and become

$$(\operatorname{ord}_0 f, \operatorname{ord}_0 g, \operatorname{ord}_0 \Delta) = (4, 6, 12). \tag{XV.6.2}$$

In particular the extra order of g is the simple zero of v along the II^* divisor. It singles out one point at which to blow up.

The blowup records the approach direction $[U : V]$ of (u, v). Its incidence equation and two affine coordinates are

$$uV = vU, \qquad (u, v) = (e, ew), \quad w = V/U; \qquad (u, v) = (br, b), \quad r = U/V. \tag{XV.6.3}$$

The two charts describe a single exceptional $C \simeq \mathbb{P}^1$, with local equations $e = 0$ and $b = 0$. The normal coordinate changes by $b = ew$, which is the transition for $\mathcal{O}(-1)$. Indeed the map $(e, [1 : w]) \mapsto e(1, w)$ realizes the blowup as the total space of the tautological line; the map on the other chart uses $b(r, 1)$. Adjunction on the exceptional zero section then gives

$$N_{C/B'} = \mathcal{O}_C(-1), \qquad C^2 = -1, \qquad (-K_{B'}) \cdot C = 2 + C^2 = 1. \tag{XV.6.4}$$

The canonical base bundle changes under the blowup: $K_{B'} = \pi^* K_B + C$. Thus the proper coefficients in the first chart are the pullbacks divided by e^4, e^6. These are integral powers of the local equation of the exceptional divisor. The powers can also be read directly from the holomorphic residue three-form. In the first chart,

$$\begin{gathered} x = e^2 X, \quad y = e^3 Y, \qquad du \wedge dv = e\, de \wedge dw, \\ \frac{du \wedge dv \wedge dx}{2y} = \frac{de \wedge dw \wedge dX}{2Y}. \end{gathered} \tag{XV.6.5}$$

The term in dx proportional to de wedges to zero. In the other chart $du \wedge dv = b\, dr \wedge db$; using $x = b^2 X', y = b^3 Y'$ cancels the same powers, now in the orientation (r, b). Substitution gives both equations, including their discriminants:

$$(f_U, g_U, \Delta_U) = (-3, w, 27(w^2 - 4)), \tag{XV.6.6}$$

$$(f_V, g_V, \Delta_V) = (-3r^4, r^5, 27r^{10}(1 - 4r^2)). \tag{XV.6.7}$$

In the U-chart f_U is a unit. In the V-chart any candidate point with $f_V = 0$ is on $r = 0$, where g_V has order exactly five. There is no remaining $(4, 6)$ point. This is a test on both charts; a test on C away from the strict transform of $u = 0$ would miss precisely the point at which an extra blowup could be required.

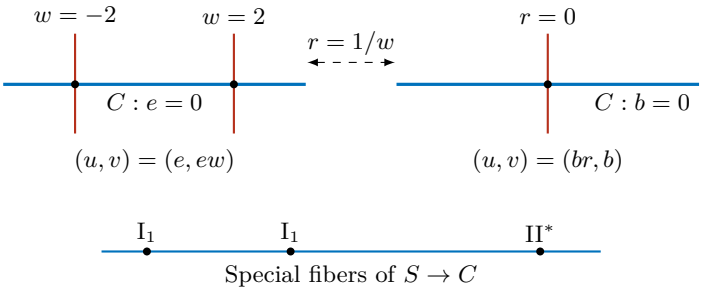


Figure XV.6.1: The two charts of the point blowup describe one compact exceptional curve. The coordinates on that curve are w and $r = 1/w$. The three marked directions give the singular fibers on its elliptic surface. The II^* label refers to the resolved fiber.

Figure XV.6.1 places each strict transform in its chart. The incidence equation also verifies the exceptional multiplicities before we pass to the elliptic surface. In the first

chart the pullbacks of the residual line equations are $e(w-2), e(w+2)$; in the second chart $u = br$. Thus the total transform of the discriminant divisor is

$$\operatorname{div}(\pi^*\Delta) = 12C + 10D + R_+ + R_-, \tag{XV.6.8}$$

where D is the strict transform of $u = 0$, and $R_\pm$ are the strict transforms of the two residual lines. Dividing the coefficients by powers $4, 6$ divides the discriminant by the twelfth exceptional power. In particular the elliptic discriminant of the modified model has no component supported on C. The restrictions of the other components still detect the three directions.

The strict transform of $u = 0$ is $r = 0$ in the second chart. It meets C once, transversely at $(r, b) = (0, 0)$. The strict transforms of the two residual lines meet C at $w = \pm 2$ in the first chart. All three curves remain noncompact. Any complete curve in the blowup maps to a point of the affine plane; the only positive dimensional fiber of the blowup is C. Thus there is just one compact base charge, with positive pairing $\Omega = -[C^2] = [1]$. At a generic point of C, the discriminant in (XV.6.7) is nonzero. The generic fiber is smooth, even though special fibers occur on the curve.

To see the entire compact elliptic surface, use the chart overlap

$$\begin{gathered} r = w^{-1}, \quad b = ew, \quad X' = w^{-2}X, \quad Y' = w^{-3}Y, \\ f_V = w^{-4} f_U, \quad g_V = w^{-6} g_U. \end{gathered} \tag{XV.6.9}$$

The fiber transition depends only on the point of $\mathbb{P}^1$, as do the coefficients. Consequently the modified model is the pullback along $B' \to \mathbb{P}^1$ of a sectioned projective Weierstrass surface W with fundamental line $\mathcal{O}(1)$. Its homogeneous coefficients and discriminant are

$$\begin{gathered} f_C = -3U^4, \qquad g_C = U^5 V, \\ \Delta_C = 27U^{10}(V - 2U)(V + 2U) \in H^0(\mathbb{P}^1, \mathcal{O}(12)). \end{gathered} \tag{XV.6.10}$$

The degree twelve follows from the powers of the fundamental line. All twelve zeros, with multiplicity, are visible: ten at $U = 0$ and one at each of $[1 : \pm 2]$. Projectivizing the cubic adds its section in each fiber. Near the section set the projective coordinate $Y = 1$ and call the other coordinates X, Z. The local equation and its derivative are

$$Z - X^3 - f_C X Z^2 - g_C Z^3 = 0, \qquad \partial_Z (Z - X^3 - f_C X Z^2 - g_C Z^3)\big|_{X=Z=0} = 1. \tag{XV.6.11}$$

Hence the section is in the regular part of the surface.

The cubic is nodal at each simple discriminant root. In the U-chart, with affine fiber coordinates, its two factorizations are

$$X^3 - 3X + w\big|_{w=2} = (X-1)^2(X+2), \qquad X^3 - 3X + w\big|_{w=-2} = (X+1)^2(X-2). \tag{XV.6.12}$$

At the double root, the quadratic terms in the fiber equation give two distinct tangent lines. The derivative of $Y^2 - X^3 + 3X - w$ with respect to w is -1, including at each node. A singular fiber need not give a singular point of its total surface. This distinguishes the two irreducible I_1 fibers from the remaining fiber, where the total surface does have a singularity. At $r = 0$, its only candidate in the affine fiber is

$X' = Y' = 0$, since $\partial_{Y'} = 2Y'$ and $\partial_{X'} = -3X'^2$ at $r = 0$. This is the rational double point of the minimal $(4, 5, 10)$ model. The Weierstrass cubic there is cuspidal. The nine components of the II^* fiber occur on the smooth minimal surface $S \to W$: the eight exceptional components carry the finite E_8 intersection diagram and the additional component completes the affine diagram.

We can check the discrepancy before computing the canonical bundle of S. The Weierstrass surface has invertible dualizing sheaf. If E_j are the exceptional components, write $K_S = \rho^* K_W + \sum_j a_j E_j$ for the resolution ρ. Each E_i is a rational (-2)-curve. Adjunction and the projection formula give

$$0 = K_S \cdot E_i = \sum_j (E_j \cdot E_i) a_j \quad \text{for each } i, \qquad a_j = 0. \tag{XV.6.13}$$

The last step uses the negative definite finite E_8 matrix. For a sectioned Weierstrass surface the canonical bundle in this frame is the pullback of $K_{\mathbb{P}^1} \otimes \mathcal{O}(1)$. For example, the local residues $dw \wedge dX/(2Y)$ and $dr \wedge dX'/(2Y')$ are related by $-w^{-1}$, with the base Jacobian contributing $-w^{-2}$ and the relative residue contributing w. This is the transition of $K_{\mathbb{P}^1} \otimes \mathcal{O}(1)$. By (XV.6.13), the formula also holds on the resolution:

$$K_S = \pi_S^* \mathcal{O}(-1). \tag{XV.6.14}$$

On its dense affine chart, $w = Y^2 - X^3 + 3X$, so its function field is $\mathbb{C}(X, Y)$. In particular S is rational. The line in (XV.6.14) is the same line pulled back from the normal direction to C in the base. The resolved modified threefold and its canonical bundle are therefore

$$\widetilde{X} = S \times_{\mathbb{P}^1} B' = \mathrm{Tot}(M), \qquad M = \pi_S^* \mathcal{O}(-1), \qquad K_{\widetilde{X}} = p_S^*(K_S \otimes M^{-1}) \simeq \mathcal{O}_{\widetilde{X}}. \tag{XV.6.15}$$

The canonical formula uses the vertical tangent line $p_S^* M$ of the total space. The surface resolution pulls back along the line bundle projection, so the map to the modified cubic is proper, birational and crepant. This construction is smooth including above the section and all three special fibers. The affine residue calculation (XV.6.5) explains the coefficient modification; it does not give a global morphism from $\widetilde{X}$ to the original projective cubic.

The distinction between an affine coefficient change and a map on compactified fibers can be checked directly. Off the exceptional base curve the affine change extends by rescaling the two homogeneous fiber coordinates. Formally it sends $[X : Y : Z]$ to $[e^2 X : e^3 Y : Z]$. At the section $[0 : 1 : 0]$ over $e = 0$ all three expressions vanish. In the chart $Y = 1$ one can use the cubic equation to write $Z = X^3$ times a regular unit near the section. The scaling is then represented by

$$[e^2 X : e^3 : X^3(1 + O(X^4))]. \tag{XV.6.16}$$

The three entries have the same order along $X = \lambda e$, but their ratios depend on λ. The raw projective formula alone cannot justify the global map at this locus. The smooth line bundle construction instead resolves the modified Weierstrass model by pullback of a morphism already defined at the section.

Two changes separate features that happen to coexist in the initial model. Keep $g = u^5 v$ and set $f = 0$. On C the first chart becomes $Y^2 = X^3 + w$. The nodal pair merges to one cuspidal fiber at $w = 0$, with $\operatorname{ord}\Delta = 2$ and $\operatorname{ord} g = 1$, hence type II. The derivative in w is still a unit. In the other chart $g_V = r^5$ retains the II* fiber. The compact base curve is unchanged. Instead keep $f = -3u^4$ and use $g = u^5 v^2$. After the first blowup,

$$g_U = ew^2, \qquad g_V = br^5, \qquad \Delta_V = 27r^{10}(b^2 - 4r^2). \tag{XV.6.17}$$

At $(b, r) = (0, 0)$ these coefficients give $(4, 6, 12)$ again. The initial simple zero condition was needed for the one blowup result. If we use $g = u^5$ instead, the putative $g_U = e^{-1}$ has a pole. The original origin in that case was never an allowed center.

In the ordinary unfrozen F-theory interpretation, with noncompact flavor boundary fixed and the local tensor retained, this unpaired (-1) with a noncompact II* neighbor realizes the rank-one E-string on contraction. The generic smooth fiber removes a gauge factor on C, but it does not remove the tensor or its charge. For the calibrated D3 string in the leading local Einstein frame, at vanishing worldvolume background combination and fixed microscopic units,

$$a = \int_C J, \qquad T_q = \frac{qa}{(2\pi)^3 \alpha'^2}, \qquad q \in \mathbb{Z}_{\geq 0}. \tag{XV.6.18}$$

Here a has units of length squared and T_q has units of inverse length squared. The tension of a represented effective wrapped charge goes to zero with the area. This is a local dictionary statement about a calibrated period. It does not determine a normalizable tensor mode or the metric of the shrinking geometry.

XV.6.2 Resolving an E6 collision

How do two exceptional divisors turn a single crossing into three independent compact charges? The first blowup can lower the orders at its generic exceptional point and leave nonminimal *corners* where other divisors meet it. Keeping the whole fan, rather than just the first new curve, tracks those corners and the final self-intersections.

Take the pure model in the same local $L = -K_B$ frame,

$$f = 0, \qquad g = u^4 v^4, \qquad \Delta = 27u^8 v^8. \tag{XV.6.19}$$

We assign infinite order to the identically zero coefficient. The original boundary orders are $(\infty, 4, 8)$ and the origin orders are $(\infty, 8, 16)$. In each smooth toric chart, adjacent ordered rays $a = (a_1, a_2), b = (b_1, b_2)$ have determinant one. Their coordinates (s, t) pull back the original coordinates and residue volume as

$$u = s^{a_1} t^{b_1}, \quad v = s^{a_2} t^{b_2}, \qquad du \wedge dv = s^{|a|-1} t^{|b|-1}\, ds \wedge dt, \qquad |a| = a_1 + a_2. \tag{XV.6.20}$$

The determinant is the coefficient of the Jacobian. The powers of this Jacobian divide the pullbacks of f, g by their fourth and sixth powers, respectively. Thus, for the present g, the proper coefficient in the chart is

$$g_{a,b} = s^{\nu_g(a)} t^{\nu_g(b)}, \qquad \nu_g(a) = 4|a| - 6(|a| - 1) = 6 - 2|a|. \tag{XV.6.21}$$

For the rays retained below, all these exponents are nonnegative.

The sum rule for a new ray can be read from the two local substitutions. For a corner monomial $g = s^i t^j$ the new charts, after dividing by the sixth exceptional power, have

(s,t) in new coordinates	g_{new}	ordered rays
(ST, T)	$S^i T^{i+j-6}$	$(a, a+b)$
(S, ST)	$S^{i+j-6} T^j$	$(a+b, b)$

(XV.6.22)

The fourth-power division for f leaves zero in both charts. The inserted ray first is $m = (1,1)$, with order two. In $(1,0), m$ the coefficient is s^4t^2; in $m, (0,1)$ it is s^2t^4. At the origin of either chart the order of g is six, and the discriminant has order twelve. The calculation itself locates the next centers. Omitting the left blowup, for example, leaves the s^4t^2 corner untouched even if the right corner is treated.

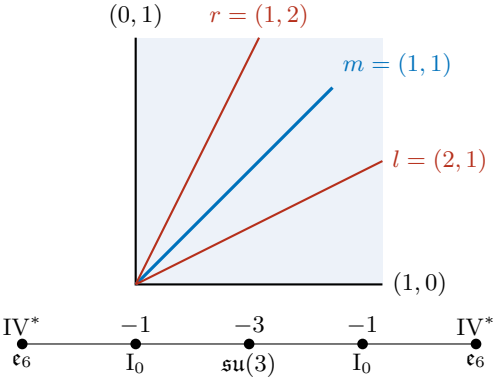


Figure XV.6.2: The pure E_6 fan after all three blowups. The boundary rays are noncompact. The ray m is inserted first, and the two subsequent centers are its corners with the boundary rays. Reading the compact rays in order gives the chain displayed below the fan.

Insert $l = (2,1)$ and $r = (1,2)$ as in Figure XV.6.2. In the final fan, the four coordinate charts read

(a,b)	$((1,0), l)$	(l, m)	(m, r)	$(r, (0,1))$
$g_{a,b}$	s^4	t^2	s^2	t^4

(XV.6.23)

All have $f = 0$. The two recursive transforms of s^4t^2 are S^4 and T^2, in agreement with the first two columns. At each final corner the sum of exponents is at most four. At any point with one coordinate a unit, the order is either a single exponent or zero. These two checks exhaust the charts, so there is no further nonminimal point.

There is a useful direct check on the four chart coefficients. In the (l, m) chart, $u = s^2t$, $v = st$, hence $g_{\text{pull}} = s^{12}t^8$. The determinant of l, m is one, so the residue Jacobian is s^2t. The powers cancel as

$$g_{l,m} = \frac{s^{12}t^8}{(s^2t)^6} = t^2, \qquad \Delta_{l,m} = \frac{27 s^{24} t^{16}}{(s^2t)^{12}} = 27t^4. \tag{XV.6.24}$$

This calculation uses the Jacobian of the composite map, not just the exceptional coordinate of the last blowup. If one divides only by the latter, the old exceptional factor is counted as an additional singular fiber.

For consecutive rays v_{i-1}, v_i, v_{i+1} with smooth adjacent cones, $v_{i-1} + v_{i+1} = b_i v_i$ gives self-intersection $-b_i$. One way to see the sign is to intersect a toric principal divisor $\operatorname{div} \chi^u$ with the compact curve of v_i. Only that curve and its two neighbors contribute; the neighboring intersections are one. Varying the character u yields the ray relation. Here it gives

$$(1,0) + m = l, \qquad l + r = 3m, \qquad m + (0,1) = r, \qquad \Omega_6 = \begin{pmatrix} 1 & -1 & 0 \\ -1 & 3 & -1 \\ 0 & -1 & 1 \end{pmatrix}. \tag{XV.6.25}$$

In particular the first exceptional has changed from square -1 to square -3, once for each point blown up on it. The leading minors of Ω_6 are $1, 2, 1$; the charge pairing is positive definite. The pairing also gives a useful charge check. A class $D = d_l C_l + d_m C_m + d_r C_r$ has periods given by its intersection vector. Suppose the two end periods are A_L, A_R and the middle period is a_m. Solving the two end equations first gives

$$d_l = d_m - A_L, \quad d_r = d_m - A_R, \qquad d_m = -a_m - A_L - A_R. \tag{XV.6.26}$$

This is a direct solution of $-\Omega_6 d = a$; the third equation is the middle intersection after the two substitutions. The minus signs on the d_i refer to a divisor used to encode positive degrees. They are not negative wrapped-string charges. Replacing the center by a (-1) would instead give leading minor $1 \cdot 1 - 1 = 0$ and determinant -1, contradicting the pairing from the actual fan. A chain of three blowups is not in general a chain of three (-1)-curves.

The leading orders of the compact fibers from (XV.6.23) give $\mathrm{I}_0, \mathrm{IV}, \mathrm{I}_0$. The two external fibers are IV^*.

To interpret these Kodaira fibers as ordinary gauge algebras we use generic transverse minimal fibers in the unfrozen theory, with the specified leading coefficients in their $-K$ frames. A type IV fiber can have monodromy: for a local equation $t = 0$ of its divisor, the cover has equation $\psi^2 - g_2 = 0$, where $g_2 = (g/t^2)|_{t=0}$. In the (l, m) chart $g_2 = 1$, but this is a leading section and the frame must be accounted for before interpreting it globally. The (m, r) chart has coordinates (s', t') related by

$$s' = s^3 t, \qquad t' = s^{-1}, \qquad \det \frac{\partial(s', t')}{\partial(s, t)} = s. \tag{XV.6.27}$$

The last equality follows by differentiating $t' = s^{-1}$, so that the off-diagonal product is $-s$. In the primed frame $g' = s^6 g$, and $g'/s'^2 = g/t^2 = 1$ on the overlap. This is consistent with the degree

$$\deg((-6K - 2C_m)|_{C_m}) = 6(2 - 3) - 2(-3) = 0. \tag{XV.6.28}$$

Thus the cover really factors as $(\psi - 1)(\psi + 1)$ over $\mathbb{C}(C_m)$. The leading fourth coefficients on the two external IV^* rays are also unit squares in the indicated charts. The ordinary

split dictionary gives central $\mathfrak{su}(3)$ and external $\mathfrak{e}_6$. Only the compact gauge fields fluctuate in the local model considered here.

For the left end C_l, the coordinate along the curve is $z = s$ in the first chart and $w = t$ in the second, with $w = 1/z$ on the overlap. Restricting the two coefficients gives

$$(f, g)|_{C_l} = (0, z^4) \quad \text{or} \quad (0, w^2), \qquad \Delta|_{C_l} = 27z^8 \quad \text{or} \quad 27w^4. \tag{XV.6.29}$$

The reflection of the fan interchanges the two ends and gives the same calculation. The orders $8 + 4 = 12$ fill the degree of the discriminant on each (-1). These are special fibers on the restricted surface, not gauge factors on the (-1) itself. This restriction also explains why the end strings can couple to flavor on one side and gauge fields on the other.

XV.6.3 Resolving an E7 collision

Why do two further blowups occur for a collision of E_7 divisors? We can use the same fan method, but the first nonzero coefficient is now f, with a different canonical weight. It is also the coefficient that determines how two components of the middle fiber are permuted.

Take the pure model

$$f = u^3v^3, \qquad g = 0, \qquad \Delta = 4u^9v^9. \tag{XV.6.30}$$

The outer orders are $(3, \infty, 9)$ and the origin has $(6, \infty, 18)$. Equation (XV.6.20) gives

$$f_{a,b} = s^{\nu_f(a)}t^{\nu_f(b)}, \qquad \nu_f(a) = 3|a| - 4(|a| - 1) = 4 - |a|. \tag{XV.6.31}$$

The first ray $m = (1, 1)$ therefore has order two. With $a_0 = (1, 0), a_6 = (0, 1)$, the first two chart coefficients are s^3t^2 and s^2t^3; both corners have f-order five. The two blowups insert $l = (2, 1)$ and $r = (1, 2)$. To see what survives, explicitly transform the left corner by the two substitutions:

(s,t)	(ST,T)	(S,ST)
f_{new} from s^3t^2	S^3T	ST^2
rays	(a_0,l)	(l,m)

(XV.6.32)

The right charts are the reflected ones. In the inner chart of (XV.6.32) the sum of orders is three. In the outer chart it is four, so the remaining left blowup occurs next to a_0, and the remaining right blowup next to a_6. The new rays are $L = (3, 1)$ and $R = (1, 3)$. For example the two transforms of s^3t, with division by the fourth exceptional power, are S^3 and T.

Reading Figure XV.6.3 from a_0 to a_6, all six final charts and their coefficients are

(a,b)	(a_0,L)	(L,l)	(l,m)	(m,r)	(r,R)	(R,a_6)
$f_{a,b}$	s^3	t	st^2	s^2t	s	t^3

(XV.6.33)

In every chart $g = 0$, $\Delta = 4f^3$. Any nonminimal point would require f-order at least four. With both coordinates nonzero the order is zero; with just one zero it is its

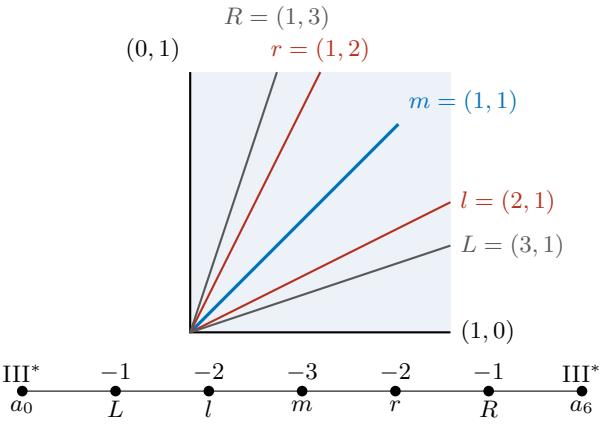


Figure XV.6.3: The pure E_7 fan. The labels m, l, r, and L, R are the first, second and third rounds of insertions. The two neighbors of m control the transition of its cover.

exponent; with both zero it is the sum of exponents. All three tests rule out more centers in the charts. This argument uses the pure monomials. With additional terms, the generic order on a ray alone would not detect possible zeros of a leading coefficient away from a corner.

The third round has an immediate overlap check. In the outermost left cone (a_0, L) the pullback is $u = st^3$, $v = t$; its residue Jacobian is t^3. In the next cone (L, l) the pullback is $u = S^3T^2$, $v = ST$, with residue Jacobian S^3T^2. This gives

$$f_{a_0,L} = \frac{s^3t^{12}}{(t^3)^4} = s^3, \qquad f_{L,l} = \frac{S^{12}T^9}{(S^3T^2)^4} = T. \tag{XV.6.34}$$

On their overlap $S = st$, $T = 1/s$, so restricting to the end gives $z = s$, $w = T = 1/z$. This will account for the two contributions of orders nine and three to the restricted discriminant without counting either as a generic vanishing on the end.

The compact self-intersections follow from the same character calculation as before. On the left and at the center, the relations are $a_0 + l = L$, $L + m = 2l$, and $l + r = 3m$; reflection gives the other two. Therefore

$$\Omega_7 = \begin{pmatrix} 1 & -1 & 0 & 0 & 0 \\ -1 & 2 & -1 & 0 & 0 \\ 0 & -1 & 3 & -1 & 0 \\ 0 & 0 & -1 & 2 & -1 \\ 0 & 0 & 0 & -1 & 1 \end{pmatrix}. \tag{XV.6.35}$$

For a tridiagonal pairing with adjacent entry -1, the leading minors obey $D_i = b_iD_{i-1} - D_{i-2}$ with $D_0 = 1$. Here this gives $1, 1, 2, 3, 1$ for $i = 1, \ldots, 5$. The compact fiber types are $\mathrm{I}_0, \mathrm{III}, \mathrm{I}_0^*, \mathrm{III}, \mathrm{I}_0$. The two noncompact boundary fibers are III*. On the left (-1), restricting to the coordinate along the curve in the first two charts gives

$$(f, g)|_{C_L} = (z^3, 0) \quad \text{or} \quad (w, 0), \qquad \Delta|_{C_L} = 4z^9 \quad \text{or} \quad 4w^3, \qquad w = 1/z. \tag{XV.6.36}$$

The orders $9+3=12$ give III* and III on its restricted surface, and the right end is the reflection. At a generic point of either (-1) the elliptic fiber is smooth.

The middle curve has the same transition (XV.6.27) as in the E_6 example. In the (l,m) chart take $f_2 = f/t^2|_{t=0}$. In the (m,r) chart take $f_2' = f'/s'^2|_{s'=0}$. The two expressions and their overlap law are

$$\begin{aligned} &f_2 = s, \qquad f' = s^4 f, \qquad f_2' = s^{-2} f_2 = t', \\ &\deg((-4K - 2C_m)|_{C_m}) = 4(2-3) + 6 = 2. \end{aligned} \tag{XV.6.37}$$

Thus each III neighbor is a simple zero, one at $s=0$ and the other at $t'=0$. The generic cover is the cubic $\psi^3 + f_2\psi + g_3$, with $g_3 = 0$ here. Over $\mathbb{C}(s)$ it has

$$\psi(\psi^2 + s) = 0, \qquad \operatorname{disc}(\psi^3 + s\psi) = -4s^3 \neq 0, \qquad \operatorname{ord}_{s=0}(-s) = 1. \tag{XV.6.38}$$

The valuation of a rational square at any point is even. Hence $-s$ is not a square in $\mathbb{C}(s)$ and the quadratic factor is irreducible. The argument concerns one function on the curve. Taking a complex square root separately at each smooth point does not supply that function. The primed frame gives the identical test using t', because $\psi' = s^{-1}\psi$ transports the quadratic factor. The linear component is separate at the generic point from the exchanged pair in Figure XV.6.4.

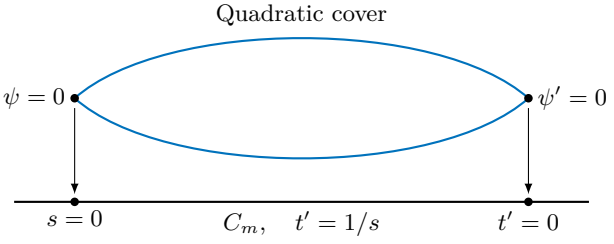


Figure XV.6.4: The quadratic part of the middle I_0^* cover. The two ramification points are detected in different affine frames. The linear component $\psi = 0$ is separate at the generic point.

One can see the exchange directly on the normalized quadratic cover. On the left use the cover coordinate ψ; the projection is $s = -\psi^2$. On the right $\psi' = \psi/s = -1/\psi$, and then

$$t' = -\psi'^2, \qquad \frac{ds}{d\psi} = -2\psi, \qquad \frac{dt'}{d\psi'} = -2\psi'. \tag{XV.6.39}$$

The two simple branch points occur at zero in their respective charts. A loop around either simple zero interchanges the two branches. The two branch points exhaust the ramification of this double cover of the projective line. The third generic root, $\psi = 0$ in the full cubic, is a distinct factor even though it can meet the quadratic part over a special point.

In the ordinary transverse minimal dictionary an I_0^* fiber with exactly this two-factor pattern is semisplit and has algebra $\mathfrak{so}(7)$. The III fibers on l, r support $\mathfrak{su}(2)$, and the

outer III* divisors furnish $\mathfrak{e}_7$ flavor. The curve and cover computations give this generic dictionary input. They are not a full crepant resolution of the collision threefold.

The section frame puts a restriction on any change that preserves these two special points. Write the most general degree-two leading section on C_m as

$$f_2 = a_0 + a_1 s + a_2 s^2, \qquad f_2' = a_2 + a_1 t' + a_0 t'^2. \tag{XV.6.40}$$

A zero at each original intersection requires $a_0 = a_2 = 0$. The coefficient a_1 then gives the simple zeros at both ends whenever it is nonzero. Thus in the $g_3 = 0$ family the two original zeros force the square obstruction. Even a change that keeps a degree-two section may move those zeros. For example $f_2 = s + 2s^2$ has one zero at $s = 0$ and one at $s = -1/2$. In the opposite chart it is $f_2' = 2 + t'$, a unit at $t' = 0$. The quadratic remains irreducible over the function field because its zeros are simple, but the same generic cover factor count does not give the same locations for the two special points. This comparison concerns the leading section on the curve; it does not assert a full retuned threefold.

For a change of the cover, take $f_2 = s^2$ in the first frame and continue to set $g_3 = 0$. Then

$$\psi(\psi^2 + s^2) = \psi(\psi - is)(\psi + is), \qquad f_2' = s^{-2} s^2 = 1. \tag{XV.6.41}$$

The generic cubic splits, but the section now has a double zero at the left and no zero on the right. It no longer has the original two III neighbors in this model. The split cover calculation cannot on its own be used as a retuning with the old curve and matter labels. For the original semisplit cover there is a further question even after the algebra has been fixed: what matter occurs at its two intersections with the III curves?

XV.6.4 Gauge matter on the tensor branch

The cover determines a gauge algebra at a generic point. It does not specify the representation at a special intersection. We use the ordinary matter assignment for the pure collisions just constructed (Del Zotto et al. 2015, eqs. (2.5)–(2.6); Heckman, Morrison, et al. 2015, §6.2). There is a pure $\mathfrak{su}(3)$ vector on the middle (-3) of the E_6 chain. In the E_7 chain there is one half hypermultiplet in $(\mathbf{2}, \mathbf{8}_{\text{spin}})$ at each $\mathfrak{su}(2)$–$\mathfrak{so}(7)$ intersection. The real spinor of $\mathfrak{so}(7)$ tensored with the pseudoreal doublet gives a pseudoreal representation, permitting a half hyper. The vector of $\mathfrak{so}(7)$ is also real, so this argument permits but does not select the spinor. We can test the selected matter by calculating its chiral index before combining it with the tensor sources.

Figure XV.6.5 distinguishes the two matter edges from the unpaired ends. Use the anomaly curvature $F = -iF_{\text{phys}}/(2\pi)$ in the conventions of Chapter B.3. Write $s_i = \operatorname{tr}_{\text{f}} F_i^2$ on the special unitary factors. On the B_3 node write $s_C = \operatorname{tr}_{\mathbf{7}} F_C^2$ and $q_C = \operatorname{tr}_{\mathbf{7}} F_C^4$; this last symbol is a quartic invariant, not a string charge. For $\mathfrak{su}(n)$ the defining weights are x_i with $\sum_i x_i = 0$; the nonzero adjoint weights are $x_i - x_j$, $i \neq j$. The raw adjoint moments follow by summing over i, j:

$$\sum_{i,j} (x_i - x_j)^2 = 2n \sum_i x_i^2, \qquad \sum_{i,j} (x_i - x_j)^4 = 2n \sum_i x_i^4 + 6 \left(\sum_i x_i^2 \right)^2 . \tag{XV.6.42}$$

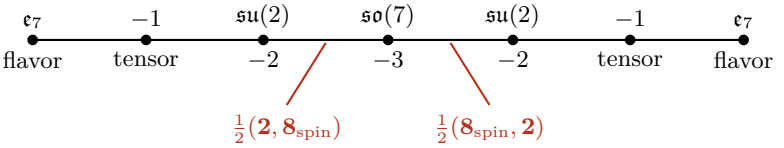


Figure XV.6.5: Gauge and flavor on the E_7 branch. A half product is assigned to each of the two indicated edges. The (-1) curves are compact tensor nodes without gauge vectors.

Terms odd in either factor sum to zero because $\sum_i x_i = 0$. For $n = 2$ the weights are $x, -x$, giving $\sum x_i^4 = s^2/2$. For $n = 3$, $\sum_{i<j} x_i x_j = -s/2$; on squaring, the remaining cross term is $2x_1x_2x_3(x_1 + x_2 + x_3) = 0$. Therefore

$$\sum_{i<j} x_i^2 x_j^2 = s^2/4, \qquad \sum_i x_i^4 = s^2/2 \quad (n = 3). \tag{XV.6.43}$$

The adjoint fourth moments for $n = 2, 3$ are then $8s^2, 9s^2$. There is no independent quartic in these two cases.

For B_3 use Cartan coordinates a, b, d and set $N = a^2 + b^2 + d^2$, $U = a^4 + b^4 + d^4$, $W = a^2b^2 + a^2d^2 + b^2d^2$. The vector has weights $0, \pm a, \pm b, \pm d$, giving $s_C = 2N$ and $q_C = 2U$. The nonzero adjoint weights are the six nonzero vector weights and the twelve signed pairs $\pm a \pm b$, $\pm a \pm d$, $\pm b \pm d$. For a pair of coordinates x, y the four sign choices give

$$\sum_{\sigma,\tau=\pm1} (\sigma x + \tau y)^2 = 4(x^2 + y^2), \qquad \sum_{\sigma,\tau=\pm1} (\sigma x + \tau y)^4 = 4(x^4 + y^4 + 6x^2y^2). \tag{XV.6.44}$$

Each coordinate belongs to two pairs. Adding the six short roots yields $10N$ and $10U + 24W$, respectively. The spinor weights are the eight sign choices of $(\pm a \pm b \pm d)/2$. The sign sum keeps only even powers of each coordinate, so the moments are $8N/4$ and $8(U + 6W)/16$. Expressed in terms of the vector traces, the results are

R	A_R	B_R	C_R	$\dim R$
$\mathbf{7}$	1	1	0	7
$\mathbf{8}_{\text{spin}}$	1	$-1/2$	$3/8$	8
adj	5	-1	3	21

$$\operatorname{tr}_R F_C^2 = A_R s_C, \qquad \operatorname{tr}_R F_C^4 = B_R q_C + C_R s_C^2. \tag{XV.6.45}$$

The three zero adjoint weights matter in $\dim R$ and not in positive moments. The independent quartic can now distinguish the spinor from the vector even though both have $A_R = 1$.

For example, evaluate the two invariants at Cartan inputs $(a, b, d) = (1, 0, 0)$ and $(1/\sqrt{2}, 1/\sqrt{2}, 0)$. They have identical $s_C = 2$ but

$$q_C = 2,\ 1, \qquad \operatorname{tr}_{\mathbf{8}_{\text{spin}}} F_C^4 = 1/2,\ 1, \quad \text{respectively.} \tag{XV.6.46}$$

An expression in s_C^2 alone would be unchanged between these evaluations. This gives a direct way to see why the irreducible quartic remains a separate coefficient test when the Green–Schwarz term is a square of four-forms.

For a product representation with weights $u+v$, one must first sum over both sets of weights. If $a_{k,R}$ is its single-factor trace of power k, and d_R its dimension, the two sums for a full product are

$$a_{2,R\otimes S} = d_S a_{2,R} + d_R a_{2,S}, \tag{XV.6.47}$$

$$a_{4,R\otimes S} = d_S a_{4,R} + d_R a_{4,S} + 6 a_{2,R} a_{2,S}. \tag{XV.6.48}$$

The terms with one linear trace vanish. For each half product we divide the entire answer by two, including its dimension. For a side $i = L, R$, the effective data of one half product are

$$a_2^{(i)} = 4 s_i + s_C, \qquad a_4^{(i)} = 2 s_i^2 - \tfrac{1}{2} q_C + \tfrac{3}{8} s_C^2 + 3 s_i s_C, \qquad d^{(i)} = 8. \tag{XV.6.49}$$

The side sees four doublets; the center sees one spinor from each side. The trace $\operatorname{Tr} F^2$ used for the tensor source is $\operatorname{tr}_{\rm adj} F^2/h^\vee$. Thus $\operatorname{Tr} F^2 = 2 s_i$ for the unitary factors and $\operatorname{Tr} F_C^2 = s_C$ for B_3, with $h^\vee(B_3) = 5$. In a convention that uses reference trace $\lambda^{-1}\operatorname{tr}_{\rm f}$, the three index coefficients become $\lambda A_R, \lambda B_R, \lambda^2 C_R$. For the orthogonal vector $\lambda = 2$; for the unitary doublet $\lambda = 1$. In particular the mixed edge index reads

$$\tfrac{1}{2}(1 \cdot A_{\mathbf{2}})(2 \cdot A_{\mathbf{8}}) = 1, \tag{XV.6.50}$$

equal to the geometric intersection. This equality is the mixed gauge check in normalized traces. It cannot determine the spinor, which has the same quadratic index as the vector.

For the local polynomial use $p = p_1(T)$, $P = p_2(T)$, $c = c_2(R)$, and $G = (7p^2 - 4P)/5760$. From the Weyl index $\widehat{A}(T)\operatorname{tr} e^{iF}$, the factors $-p/24$ and $-a_2/2$ multiply to $+pa_2/48$. A vector has opposite chirality and an R doublet weighted by the reality factor, contributing $1 + c/2 + c^2/24$ in these conventions. The hyper is an R singlet. The tensor includes the chiral two-form index. Thus

$$H(a_2, a_4, d) = a_4/24 + pa_2/48 + dG, \tag{XV.6.51}$$

$$V(a_2, a_4, d) = -a_4/24 - (c/4 + p/48)a_2 - d(c^2/24 + cp/48 + G), \tag{XV.6.52}$$

$$I_T = c^2/24 + cp/48 + (23p^2 - 116P)/5760. \tag{XV.6.53}$$

Here the half product in (XV.6.49) may be inserted directly into H, which is linear in its arguments. Its two quartic terms in q_C cancel the one from the vector:

$$[q_C] I^{(7)}_{\rm loop} = \frac{1}{24} - 2\frac{1}{48} = 0. \tag{XV.6.54}$$

Replacing both half spinors by half vectors instead gives $[q_C] I_{\rm loop} = 1/24 + 2/24 = 1/8$. Doubling the original half products gives $1/24 - 4/48 = -1/24$, a different failure. For the vector replacement the spectator quadratic trace also changes from four to seven halves of a doublet, while the mixed edge term does not change because $A_{\mathbf{7}} = A_{\mathbf{8}}$.

The vector replacement also changes the reducible terms. For one edge its effective trace difference from the spinor half product is

$$\delta a_2 = -s_i/2, \qquad \delta a_4 = -s_i^2/4 + 3q_C/2 - 3s_C^2/8. \tag{XV.6.55}$$

The $s_i s_C$ coefficient is absent from this difference. Adding both differences in H, the gauge residual relative to the spinor assignment is

$$\delta I_g = \frac{q_C}{8} - \frac{s_C^2}{32} - \frac{s_L^2 + s_R^2}{96} - \frac{p(s_L + s_R)}{96}. \tag{XV.6.56}$$

This residual will still be present after adding the unchanged geometry's square. The dimension of the loop also changes by -2, giving the background change $-2G$. The quartic diagnosis does not stand in for that background test.

Before adding the tensors' Green–Schwarz term, the complete gauge-dependent parts of the loop indices are

$$I^{(6)}_{\mathrm{loop},g} = -3s_C^2/8 - (3c/2 + p/8)s_C, \tag{XV.6.57}$$

$$I^{(7)}_{\mathrm{loop},g} = -3s_C^2/32 + s_C(s_L + s_R)/8 - (s_L^2 + s_R^2)/4 - (5c/4 + p/16)s_C - c(s_L + s_R). \tag{XV.6.58}$$

For example each side fourth trace supplies $-8s_i^2/24$ from the adjoint and $+2s_i^2/24$ from the half product. The side ps_i terms cancel because both have quadratic trace $4s_i$. At the center the two hypers supply $2(3s_C^2/8)/24$ against $-3s_C^2/24$ from the vector. The full loop has one tensor for every compact curve, including the two ends. Its background part will enter the next calculation.

To compare the external flavor terms and to reinterpret the ends, we need the normalized exceptional traces in the same frame. This can be done inside one Cartan space of the E_8 root system. In orthonormal coordinates the roots are

$$\{\pm e_i \pm e_j : i < j\} \quad \cup \quad \left\{ \tfrac{1}{2} \sum_i \sigma_i e_i : \sigma_i = \pm 1,\ \prod_i \sigma_i = 1 \right\}. \tag{XV.6.59}$$

They number $112 + 128 = 240$. For the first set each coordinate participates in seven pairs and has second-moment coefficient 28, by (XV.6.44). In the second set parity still allows independent averaging of fewer than eight signs. The contribution is $128\|x\|^2/4 = 32\|x\|^2$. Since $h^\vee(E_8) = 30$, the sum gives

$$\mathrm{tr}_{248}\, F^2 = 60\|x\|^2, \qquad \mathrm{Tr}_{E_8}\, F^2 = 2\|x\|^2. \tag{XV.6.60}$$

Use the differences of the first k coordinates for A_{k-1}, with $k = 3$ or 2. The orthogonal Cartan complement consists of $x = (a, \ldots, a, z_1, \ldots, z_{8-k})$. For $k = 3$, orthogonality to the differences retains the 40 vector roots on the last five coordinates and the 32 spinor roots with the first three signs equal. For $k = 2$, it retains the 60 vector roots on the last six coordinates, the pair $\pm(e_1 + e_2)$ and the 64 spinor roots with equal first two signs. These sets span ranks six and seven and give the regular E_6 and E_7 root systems. Put $N_z = \sum_j z_j^2$, $U_z = \sum_j z_j^4$, and $W_z = \sum_{i<j} z_i^2 z_j^2$. The restricted spinor sums have the first-coordinate contribution $\pm ka/2$; conditional sign parity on the remaining five or six coordinates does not affect any sum of degree at

most four. The moment contributions for the two complements are then

$$M_2^{(6)} = 16N_z + 8(9a^2 + N_z), \tag{XV.6.61}$$

$$M_4^{(6)} = 16U_z + 24W_z + 2(81a^4 + 54a^2N_z + U_z + 6W_z), \tag{XV.6.62}$$

$$M_2^{(7)} = 20N_z + 8a^2 + 16(4a^2 + N_z), \tag{XV.6.63}$$

$$M_4^{(7)} = 20U_z + 24W_z + 32a^4 + 4(16a^4 + 24a^2N_z + U_z + 6W_z). \tag{XV.6.64}$$

The first terms in each line come from the signed pairs of last coordinates. The isolated $8a^2, 32a^4$ come from $\pm(e_1 + e_2)$. Using $N_z^2 = U_z + 2W_z$, these reduce to

	$\mathrm{tr}_{\mathrm{adj}}\, F^2$	$\mathrm{tr}_{\mathrm{adj}}\, F^4$
E_6	$24\|x\|^2$	$18\|x\|^4$
E_7	$36\|x\|^2$	$24\|x\|^4$

(XV.6.65)

Dividing the quadratic moments by $h^\vee = 12, 18$ gives $2\|x\|^2$ in either case. The quartic coefficients in $(\mathrm{Tr}\, F^2)^2$ are $9/2, 6$. The complementary A_{k-1} has $2k\|x\|^2$ by (XV.6.42), so its normalized quadratic trace is also $2\|x\|^2$. The orthogonal decomposition of the Cartan metric proves the index-one restriction

$$h := \mathrm{Tr}_{E_8} F^2 \longmapsto e + 2s, \qquad e = \mathrm{Tr}_{E_{9-k}} F^2. \tag{XV.6.66}$$

Here E_{9-k} is E_6 for $k = 3$ and E_7 for $k = 2$. The statement concerns invariant forms on commuting Lie algebras and fixes no global group quotient. It will let us substitute an exceptional flavor curvature and its neighboring gauge curvature into the same rank-one E-string polynomial.

XV.6.5 Anomaly contributions of the interacting sector

Which coefficients remain when the dynamical gauge dependence cancels? The cancellation is necessary to interpret the branch as a gauge theory. For a comparison to a strongly interacting sector we need more: the coefficients for flavor, R symmetry and gravity after all gauge terms have canceled. We compute them first from the branch, then from the inflow polynomials with the free contributions removed.

Put $x_j = \mathrm{Tr}\, F_j^2/4$ on compact gauge nodes and zero elsewhere. Let $\kappa_i = (-K)\cdot C_i = 2 - \Omega_{ii}$, and use $y_j = h_j^\vee$ for gauge tensors. The unpaired ends have $y_j = 1$ in the local tensor-source prescription (Ohmori, Shimizu, Tachikawa, and Yonekura 2014, eq. (3.42)). This is a separate physical input; it does not follow from the Kodaira order or from gauge cancellation. If e_L, e_R denote the two external $\mathrm{Tr}\, F^2$'s and $\mathbf{e}_i$ are unit node vectors, the paired source and its square are

$$Y = \Omega x + B, \qquad B = -\kappa p/4 + yc - (e_L\mathbf{e}_1 + e_R\mathbf{e}_n)/4, \qquad I_{\mathrm{GS}} = \tfrac{1}{2} Y^t \Omega^{-1} Y. \tag{XV.6.67}$$

The compact-to-external incidence at either end is -1 in $\Omega = -C_i \cdot C_j$, which accounts for the sign of the flavor term. The form Y has a lower node index: the inverse pairing

in I_{GS} raises it. The gauge-dependent and background parts separate as

$$I_{\mathrm{GS}} = \tfrac{1}{2} x^t \Omega x + x^t B + \tfrac{1}{2} B^t \Omega^{-1} B. \tag{XV.6.68}$$

In particular the term linear in x sees only B on gauge nodes. This observation will give a control on which source entries the gauge test can determine. For the exceptional collisions the inflow route uses one M5-brane on the corresponding asymptotically locally Euclidean (ALE) ADE quotient $\mathbb{C}^2/\Gamma$.

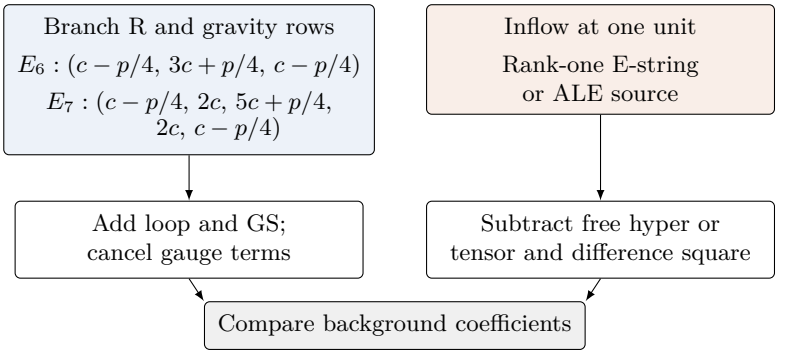


Figure XV.6.6: Inputs and two calculations of the background anomaly. The node rows show the R and gravitational parts of B before any elimination. Flavor enters on the same two rows as the unpaired tensors. The inflow subtraction depends on which source polynomial is used.

Figure XV.6.6 gives the two routes we will compare. On E_6, $x = (0, s_C/2, 0)^t$ and $B_C = 3c + p/4$. The first two terms of (XV.6.68) are

$$I^{(6)}_{\mathrm{GS},g} = \tfrac{3}{8} s_C^2 + \tfrac{1}{2} s_C (3c + p/4). \tag{XV.6.69}$$

On E_7 take $x = (0, s_L/2, s_C/4, s_R/2, 0)^t$. The sides of B on gauge nodes are $2c$, and the center is $5c + p/4$. Multiplying out $x^t \Omega x/2$ gives a negative mixed term for each adjacent pair, hence

$$\begin{aligned} I^{(7)}_{\mathrm{GS},g} = {} & \tfrac{1}{4}(s_L^2 + s_R^2) + \tfrac{3}{32} s_C^2 - \tfrac{1}{8} s_C (s_L + s_R) \\ & + c(s_L + s_R) + (5c/4 + p/16) s_C. \end{aligned} \tag{XV.6.70}$$

These cancel both lines of (XV.6.58), with arbitrary external flavor curvatures. There is no gauge–external flavor term: the flavor part of B is on the ungauged rows. An irreducible quartic could not have been repaired by this square. That is why the trace test (XV.6.54) is necessary before the quadratic source test.

For the one-curve E-string geometry, $\Omega = [1]$, $x = 0$ and there is one flavor neighbor. In the notation of (XV.6.66), the branch polynomial is

$$Y_8 = c - p/4 - h/4, \tag{XV.6.71}$$

$$\begin{aligned} I_{8,\mathrm{int}} &= I_T + \tfrac{1}{2}(c - p/4 - h/4)^2 \\ &= \tfrac{13}{24} c^2 - \tfrac{11}{48} cp + \tfrac{203}{5760} p^2 - \tfrac{29}{1440} P + \tfrac{h^2}{32} - \tfrac{ch}{4} + \tfrac{ph}{16}. \end{aligned} \tag{XV.6.72}$$

The square contains only the tensor's coupling to backgrounds: there is no compact gauge node in this model. Both mixed flavor terms diagnose the sign of h. Reversing that sign preserves the $h^2/32$ coefficient but gives $+ch/4 - ph/16$.

For a separate comparison, the rank-one inflow expression before subtracting its free sector is

$$\begin{aligned} I_{8,\mathrm{all}} &= \chi^2/6 + \chi J_4/2 + J_4^2/2 - J_8, \\ J_4 = (p_N + p + h)/4, \qquad J_8 &= \frac{\chi^2 + P - (p_N - p)^2/4}{48}. \end{aligned} \tag{XV.6.73}$$

Here $p_N = p_1(N)$, $\chi = e(N)$ and $p_2(N) = \chi^2$. Use $\ell = c_2(L)$ for the other normal SU(2), so that $\chi = \ell - c$, $p_N = -2(\ell + c)$. For example, the h-linear part of the first two terms involving J_4 is

$$\frac{(\ell - c)h}{8} + \frac{[-2(\ell + c) + p]h}{16} = -\frac{ch}{4} + \frac{ph}{16}. \tag{XV.6.74}$$

There is no ℓh term. To see what remains in the other coefficients, put $M = \ell + c$, so the $h = 0$ expression is

$$\tfrac{7}{48}(\ell - c)^2 + \tfrac{1}{8}(\ell - c)(p - 2M) + \tfrac{1}{32}(p - 2M)^2 + \tfrac{1}{192}(p + 2M)^2 - \tfrac{P}{48}. \tag{XV.6.75}$$

The ℓc coefficient is $-14/48 + 1/4 + 1/24 = 0$. The ℓ^2 and ℓp terms that remain are $\ell^2/24 + \ell p/48$. The inflow formula includes an E_8-neutral free hyper with this normal-symmetry index. Its polynomial is $G + \ell^2/24 + \ell p/48$. Subtracting it removes both remaining ℓ terms and shifts the two purely gravitational coefficients:

$$\frac{7p^2}{192} - \frac{P}{48} - G = \frac{203p^2}{5760} - \frac{29P}{1440}. \tag{XV.6.76}$$

The c^2, cp coefficients in (XV.6.75) are $13/24, -11/48$. Together with $h^2/32$ and (XV.6.74), this matches all seven coefficients of (XV.6.72). The free hyper is subtracted in the inflow comparison; it was not a charged multiplet to be added to the branch loop.

It is possible to trace the pure R coefficient in the inflow check without ever setting the other normal SU(2) to zero. The c^2 terms of (XV.6.75) sum to

$$\frac{7}{48} + \frac{1}{4} + \frac{1}{8} + \frac{1}{48} = \frac{13}{24}; \qquad [cp]I_{8,\mathrm{all}} = -\frac{1}{8} - \frac{1}{8} + \frac{1}{48} = -\frac{11}{48}. \tag{XV.6.77}$$

The free hyper contains ℓ but no c. Thus the equality of these two coefficients is independent of how the pure gravitational coefficients shift upon its subtraction. The potentially mixed normal term ℓc would have spoiled this separation; its explicit cancellation is part of the comparison.

For the exceptional collisions, first compute the backgrounds directly from the chain. Define $u_j(e) = jc - p/4 - e/4$ and $E = e_L + e_R$. An end pivot of value one in Ω decreases the diagonal of its neighbor by one and adds the end source to that neighbor. This is completion of a square in the inverse pairing; the general identity will be derived in Section XV.6.6. For E_6, the pivot at each end contributes $u_1(e_i)^2/2$. The center starts

at $3c + p/4$ and receives both ends, so it ends at $u_5(E)$ with pivot $3 - 1 - 1 = 1$. For E_7, the end pivots first shift the side sources from $2c$ to $u_3(e_i)$ and their diagonal from two to one. The two shifted side pivots then add their sources to $5c + p/4$ and reduce the central pivot to one. The resulting two background squares are

$$I^{(6)}_{\mathrm{GS},b} = \tfrac{1}{2}\big[u_1(e_L)^2 + u_1(e_R)^2 + u_5(E)^2\big], \tag{XV.6.78}$$

$$I^{(7)}_{\mathrm{GS},b} = \tfrac{1}{2}\big[u_1(e_L)^2 + u_1(e_R)^2 + u_3(e_L)^2 + u_3(e_R)^2 + u_{11}(E)^2\big]. \tag{XV.6.79}$$

The first line's cross term in $e_L e_R$ comes only from the central square and is $1/16$. The second line's mixed ce_i coefficient is $-(1+3+11)/4 = -15/4$. Even though the original ends are disjoint, the inverse pairing couples their external curvatures.

At zero dynamical curvature the loop coefficients can be assembled using dimensions alone, but only after the spectrum has been specified. The E_6 branch has three tensors, eight vector components and no hyper. The E_7 branch has five tensors, $3 + 21 + 3 = 27$ vector components, and two half products with effective dimension eight each. In particular,

$$\begin{aligned} I^{(6)}_{\mathrm{loop},b} &= 3I_T - 8(c^2/24 + cp/48 + G) \\ &= -5c^2/24 - 5cp/48 + (13p^2 - 316P)/5760, \end{aligned} \tag{XV.6.80}$$

$$\begin{aligned} I^{(7)}_{\mathrm{loop},b} &= 5I_T - 27(c^2/24 + cp/48 + G) + 16G \\ &= -22c^2/24 - 22cp/48 + (38p^2 - 536P)/5760. \end{aligned} \tag{XV.6.81}$$

For instance, E_7 has c^2 coefficient $(2+18+121)/2 - 22/24 = 1670/24$, and cp coefficient $-(2+6+11)/4 - 22/48 = -250/48$. Each of its two side-independent flavor squares gets one contribution from each of the three squares in which it appears, $3/32$ in total. These steps use the full source, rather than restricting the background at the outset.

Now specialize the ALE inflow formula to one unit of charge. Let $n_\Gamma = |\Gamma|$, $r_G = \operatorname{rank} G$, $M_G = n_\Gamma(r_G + 1) - 1$, and let $V_G(e) = V(h^\vee e, k_G e^2, d_G)$ use the normalized traces in (XV.6.65). In the present two cases the data are

$$(n_\Gamma, r_G, h^\vee, k_G, d_G) = (24, 6, 12, 9/2, 78) \quad \text{or} \quad (48, 7, 18, 6, 133). \tag{XV.6.82}$$

The one-unit inflow before removing the center terms is

$$I^G_{\mathrm{all}} = \frac{n_\Gamma^2 c^2}{24} - \frac{M_G c(4c+p)}{48} - \frac{n_\Gamma cE}{8} + \frac{cp - P}{48} + \frac{p^2}{192} - \frac{V_G(e_L) + V_G(e_R)}{2}. \tag{XV.6.83}$$

The center sector here is a tensor *and* its square $(e_L - e_R)^2/32$. Subtracting only the tensor would retain an extra difference-flavor term. Subtracting the E-string free hyper instead would also change the gravitational and R symmetry coefficients. Expanding the two vector terms of (XV.6.83) gives $d_G(c^2/24 + cp/48 + G)$, $h^\vee(c/8 + p/96)E$ and $k_G(e_L^2 + e_R^2)/48$. Subtracting the center contributions, the complete comparison formula

becomes

$$I^G_{\mathrm{int}} = \frac{n_\Gamma^2 - 2M_G + d_G - 1}{24}c^2 + \frac{d_G - M_G}{48}cp + \frac{7(d_G+1)}{5760}p^2 - \frac{d_G+1}{1440}P + \left(\frac{k_G}{48} - \frac{1}{32}\right)(e_L^2 + e_R^2) + \frac{e_L e_R}{16} + \left(\frac{h^\vee - n_\Gamma}{8}c + \frac{h^\vee}{96}p\right)E. \tag{XV.6.84}$$

The mixed flavor term $+e_Le_R/16$ now comes wholly from the subtraction, and it has the same sign as the central inverse-pairing term in (XV.6.79). To compare a coefficient sensitive to the number of fields rather than only to the intersection signs, take P. The Green–Schwarz square contains p^2 but no P. On the branch its coefficient therefore counts tensors and the difference of hyper and vector dimensions:

$$[P]I_b^{(6)} = \frac{-3\cdot 116 + 8\cdot 4}{5760}, \qquad [P]I_b^{(7)} = \frac{-5\cdot 116 + (27-16)\cdot 4}{5760}. \tag{XV.6.85}$$

In inflow, it comes from three distinct terms: $-P/48$, $-4d_GP/5760$ from the two external vector terms, and $+116P/5760$ from the center subtraction. Their sum is $-(d_G+1)P/1440$, agreeing with both branch values. This check would change if the two half hypers were accidentally counted as full products.

The curvature coefficient pE on the branch is $2/16$ for E_6 and $3/16$ for E_7, counting squares; in inflow these are $12/96$ and $18/96$. For E_6 take $M_G = 167$; then the inflow c^2 numerator is $576 - 334 + 78 - 1 = 319$. The branch gives $12(2+25) - 5 = 319$ in the same units. For E_7, $M_G = 383$ and inflow gives $2304 - 766 + 133 - 1 = 1670$. The complete values obtained by either route are collected here for comparison:

background structure	E_6	E_7
c^2	$319/24$	$1670/24$
cp	$-89/48$	$-250/48$
p^2	$553/5760$	$938/5760$
P	$-79/1440$	$-134/1440$
$e_L^2 + e_R^2$	$1/16$	$3/32$
e_Le_R	$1/16$	$1/16$
$c(e_L + e_R)$	$-3/2$	$-15/4$
$p(e_L + e_R)$	$1/8$	$3/16$

(XV.6.86)

There are eleven individual monomials, grouped into eight structures by reflection. The matching uses the specified local spectrum, normalization and tensor sources. It does not count a compact neutral sector or check a global anomaly.

A second way to organize the flavor comparison is to turn on just the difference of the two external sources, $e_L = e,\ e_R = -e$. The central background square then has no dependence on e in either chain. In E_6 only the two end squares remain sensitive to e, and in E_7 the two shifted side squares contribute as well. The quadratic flavor coefficients in this specialization are

$$[e^2]I_b^{(6)} = 2/32 = 1/16, \tag{XV.6.87}$$

$$[e^2]I_b^{(7)} = 4/32 = 1/8. \tag{XV.6.88}$$

All terms linear in E disappear. On the inflow side the vector terms give $2k_G/48$, whereas the center square gives $(2e)^2/32 = e^2/8$ before subtraction. Their difference is $3/16 - 1/8 = 1/16$ or $1/4 - 1/8 = 1/8$. The surviving difference-flavor anomaly is therefore not the free difference square itself. Setting $e_L = e_R$ would switch off the free difference square and make it impossible to use that specialization to test this part of the subtraction.

The distinction between this comparison and the gauge test can be seen without changing either gauge algebra. Set the two end entries of y to zero in E_6, leaving all other inputs intact. The x^tB term of (XV.6.68) stays fixed since x vanishes on the ends. In (XV.6.79), however, u_1, u_5 are replaced by u_0, u_3. This changes the c^2 coefficient by $(9-27)/2 = -9$, the cp coefficient by $+1$ and the cE coefficient by $+3/4$. The loop cannot compensate for any of these changes. Gauge consistency alone leaves the R coupling of the unpaired tensors undetermined. In the next section, their full sources are needed even if only some curves are being contracted.

XV.6.6 Partial contraction and retained spectators

What remains coupled when only part of a chain shrinks? There are two distinct operations to compare. We may shrink the unpaired ends and keep all the gauge curves, or shrink the central (-3) and keep its neighbors. In either case we first check which toric contraction the areas approach. The anomaly of the sector on the contracted curves uses a different source square from that of the retained tensors.

The end contractions remove the first and last compact rays. At the left of the E_6 fan, $l = a_0 + m$, where $a_0 = (1, 0)$, so deleting l restores the smooth cone (a_0, m) of determinant one. At the left of the E_7 fan, $L = a_0 + l$, so deleting L restores (a_0, l), also of determinant one. The right contractions are the reflections. Thus the actual ordered ray lists become

$$E_6: \quad a_0, m, a_4; \qquad E_7: \quad a_0, l, m, r, a_6, \qquad a_4 = a_6 = (0, 1) \tag{XV.6.89}$$

where the outer index in each model is its original index. The left restored charts have $g = s^4t^2$ in E_6 and $f = s^3t$ in E_7, by (XV.6.21) and (XV.6.31). The respective point orders are $(\infty, 6, 12)$ and $(4, \infty, 12)$. The reflected right charts have the same point orders. This restores the nonminimal IV*–IV and III*–III collisions. The new base charts are smooth; their elliptic models at the restored corners are nonminimal.

Figure XV.6.7 distinguishes the end coarsenings from the middle coarsenings. To split the sources, put the cut nodes first and write

$$\Omega = \begin{pmatrix} B & C \\ C^t & D \end{pmatrix}, \quad Y = \begin{pmatrix} Z \\ W \end{pmatrix}, \qquad D_* = D - C^tB^{-1}C, \quad W_* = W - C^tB^{-1}Z. \tag{XV.6.90}$$

Here the block B is a pairing, not the background vector in (XV.6.67). Multiplying the pairing and source by the same row elimination, with its transpose on the pairing's right, gives

$$A = \begin{pmatrix} 1 & 0 \\ -C^tB^{-1} & 1 \end{pmatrix}, \quad A\Omega A^t = \begin{pmatrix} B & 0 \\ 0 & D_* \end{pmatrix}, \qquad AY = \begin{pmatrix} Z \\ W_* \end{pmatrix}. \tag{XV.6.91}$$

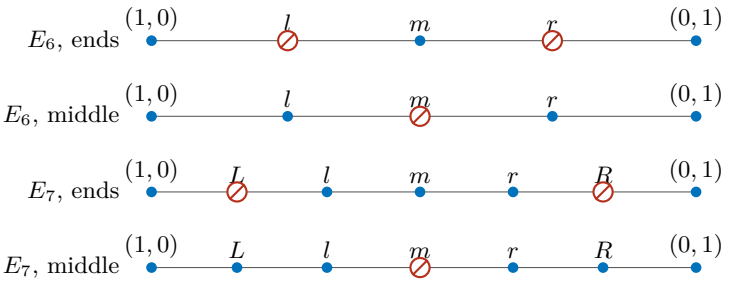


Figure XV.6.7: The four coarsenings. Each row lists the ordered rays of a full fan, with an open crossed marker for a ray to be deleted. Adjacent surviving rays bound the restored cones. The end cuts restore smooth cones of determinant one; the middle cuts insert one cone of determinant three.

Consequently the invariant square separates as

$$I_{\mathrm{GS}} = \tfrac{1}{2} Z^t B^{-1} Z + \tfrac{1}{2} W_*^t D_*^{-1} W_*. \tag{XV.6.92}$$

The source must be shifted along with the matrix. Keeping W and merely changing the pairing would fail (XV.6.91). This change of source coordinates is an identity for the full quadratic term, including gauge, flavor, R and gravity entries.

For the two end curves $B = \mathbf{1}_2$, with an adjacent entry -1 in C for each end. In the E_6 branch both ends touch the center. Thus

$$\begin{gathered} Z_i = c - p/4 - (e_i + 2s_C)/4, \qquad D_* = [3 - 2] = [1], \\ W_* = s_C/2 + 5c - p/4 - (e_L + e_R)/4. \end{gathered} \tag{XV.6.93}$$

For the last equality the old central source is $3s_C/2 + 3c + p/4$, and we add both Z_i's. For E_7 each end touches a different side node. We have $Z_i = c - p/4 - (e_i + 2s_i)/4$, $i = L, R$, and the shift reduces each side's diagonal by one:

$$D_* = \begin{pmatrix} 1 & -1 & 0 \\ -1 & 3 & -1 \\ 0 & -1 & 1 \end{pmatrix}, \qquad W_* = \begin{pmatrix} s_L/2 - s_C/4 + 3c - p/4 - e_L/4 \\ 3s_C/4 - (s_L + s_R)/2 + 5c + p/4 \\ s_R/2 - s_C/4 + 3c - p/4 - e_R/4 \end{pmatrix}. \tag{XV.6.94}$$

For example the old side source is $s_L - s_C/4 + 2c$; adding Z_L increases the R coefficient to three and introduces the external curvature on that same row. The integer retained matrices also follow directly by intersecting the surviving curves in the smooth blown-down bases of (XV.6.89).

Each end's cut term together with its tensor loop now equals the E-string expression (XV.6.72) with the substitution $h = e_i + 2s_j$, where j is its gauge neighbor. Indeed $I_T + Z_i^2/2$ has precisely that source by (XV.6.66). For example in E_6 the $h^2/32$ term produces $e_i s_C/8$, while the retained square in (XV.6.93) produces $-e_i s_C/8$. This term would have been missed if the neighboring gauge curvature had been dropped from Z_i. Replacing each end tensor and cut square by its interacting E-string polynomial leaves

the total local anomaly unchanged by (XV.6.92). The interpretation uses the ordinary E-string link rule. The finite-area gauge fields still couple to both interacting ends.

Consider instead shrinking only the middle ray m. In both fans its neighbors are $l = (2, 1)$ and $r = (1, 2)$, with $l+r = 3m$. Deleting m merges just the cones $(l, m), (m, r)$. In the integral basis (l, m), the surviving cone generators have coordinates $(1, 0)$ and $(-1, 3)$. Thus

$$\det(l, r) = 3, \qquad \mathbb{Z}^2 = \langle l, r\rangle + \mathbb{Z}\frac{l+r}{3}. \tag{XV.6.95}$$

Using l, r as a basis of the sublattice gives a smooth affine plane cover of the coarse chart. In this frame the additional lattice point is $(1/3, 1/3)$, so the coarse chart is $\mathbb{C}^2/\mu_3$ with weights $(1, 1)$. This is a quotient of the base chart, with no inference about the global form of any gauge or flavor group.

We can exhibit a geometric path to this face. Write $a_i = J \cdot C_i$ and take $a_m = \epsilon > 0$, $a_i = L > 0$ for every other compact curve. For rational a_i, the divisor $\sum_i d_i C_i$ with

$$d = -\Omega^{-1}a, \qquad \left(\sum_i d_i C_i\right) \cdot C_j = (-\Omega d)_j = a_j \tag{XV.6.96}$$

is relatively rational Cartier. The smooth fan was obtained by projective blowups over $\mathbb{A}^2$. Any complete curve in a fiber of this projection is supported on the compact chain. Therefore positivity on the indicated curves gives relative ampleness; in toric terms the support function is strictly convex across their rays. The ample cone extends to real degrees. When $\epsilon = 0$, the convex function is linear across m and strict at the other compact rays, giving the displayed coarsening. This is a geometric construction of the area face, not a calculation of the physical scalar metric.

For example, the equation $-\Omega_7 d = a$ with the reflection-symmetric degrees $a = (L, L, \epsilon, L, L)^t$ reduces to three equations. Denote the repeated end and side coefficients by d_e, d_s, and the middle one by d_m. Then

$$-d_e + d_s = L, \quad d_e - 2d_s + d_m = L, \quad 2d_s - 3d_m = \epsilon. \tag{XV.6.97}$$

Eliminating in this order gives

$$(d_e, d_s, d_m) = (-7L - \epsilon, -6L - \epsilon, -4L - \epsilon). \tag{XV.6.98}$$

The two side and two end degrees are still L after setting $\epsilon = 0$; only the central intersection of this relative class becomes zero. For E_6, setting $A_L = A_R = L$ in (XV.6.26) gives $(-3L - \epsilon, -2L - \epsilon, -3L - \epsilon)$. The zero degree occurs on the same ray whose deletion gave the index-three cone.

For a fixed charge column q in the effective compact curve cone, the period and tension behave as

$$q_i \in \mathbb{Z}_{\geq 0}, \qquad q^t a = q_m \epsilon + L \sum_{i \neq m} q_i, \qquad T_q = \frac{q^t a}{(2\pi)^3 \alpha'^2}. \tag{XV.6.99}$$

At fixed L the limiting period is zero exactly when the charge is supported on m. A formal charge such as $(0, 1, 0, -1, 0)$ in the E_7 ordering has zero period for every ϵ.

It is a difference of two finite spectator classes, so it is not an effective holomorphic curve charge. It does not give a physical tensionless wrapped BPS string on this path. Positivity is essential to the implication from the period to the support.

The Schur calculation for the middle cut now uses $B = [3]$. In E_6, both end sources shift by $+Z/3$, giving

$$Z = 3s_C/2 + 3c + p/4, \qquad D_* = \begin{pmatrix} 2/3 & -1/3 \\ -1/3 & 2/3 \end{pmatrix}, \qquad W_* = \begin{pmatrix} 2c - p/6 - e_L/4 \\ 2c - p/6 - e_R/4 \end{pmatrix}. \tag{XV.6.100}$$

The s_C dependence cancels out of W_*. In the cut square $Z^2/6$, the terms with s_C are $3s_C^2/8 + (3c/2 + p/8)s_C$, so they cancel the central vector's gauge terms. Its background polynomial is

$$I_{\text{cut}}^{(6)} = I_T + V(0,0,8) + (3c+p/4)^2/6 = 29c^2/24 + 5cp/48 + 3p^2/640 - 7P/480. \tag{XV.6.101}$$

Here $V(0,0,8)$ is the vector index at zero gauge curvature; its R and gravitational terms are still present.

For the E_7 cut write $S = s_L + s_R$. The central source and the retained data in order (L, l, r, R) are

$$Z = 3s_C/4 + 5c + p/4 - S/2. \tag{XV.6.102}$$

Since the middle touches the two side nodes and neither end, the two nonzero components of the elimination row are both $1/3$. The same operation on the pairing and the source gives

$$D_* = \begin{pmatrix} 1 & -1 & 0 & 0 \\ -1 & 5/3 & -1/3 & 0 \\ 0 & -1/3 & 5/3 & -1 \\ 0 & 0 & -1 & 1 \end{pmatrix}, \qquad W_* = \begin{pmatrix} c - p/4 - e_L/4 - s_L/2 \\ 11c/3 + p/12 + 5s_L/6 - s_R/6 \\ 11c/3 + p/12 + 5s_R/6 - s_L/6 \\ c - p/4 - e_R/4 - s_R/2 \end{pmatrix}. \tag{XV.6.103}$$

In particular the left side starts at $s_L - s_C/4 + 2c$, and gets $+Z/3$. The right-side curvature enters with coefficient $-1/6$ on this row. There is no middle gauge curvature left in W_*. The ends are unchanged. These fractions describe an orthogonal projection of the original positive pairing, not a new integral string charge lattice on the singular base.

The cut loop contains its tensor, the central vector and both half products. The side gauge curvatures are treated as backgrounds for this cut calculation. The two half products cancel the independent quartic as in (XV.6.54). The remaining central terms in the cut loop are

$$-3s_C^2/32 + Ss_C/8 - (5c/4 + p/16)s_C. \tag{XV.6.104}$$

Expansion of $Z^2/6$ gives their negatives. To compute what is left, write $A = 5c + p/4$. The background from the cut loop and from the cut square is, respectively,

$$I_{\text{cut,loop},b} = I_T + V(0,0,21) + 16G + (s_L^2 + s_R^2)/12 + pS/12, \tag{XV.6.105}$$

$$I_{\text{cut,GS},b} = (A - S/2)^2/6 = A^2/6 - AS/6 + S^2/24. \tag{XV.6.106}$$

No loop hyper touches both side nodes. The entire $s_L s_R$ term comes from the last square. Combining the two lines,

$$\begin{aligned} I^{(7)}_{\rm cut} &= \tfrac{10}{3}c^2 + \tfrac{p^2}{120} - \tfrac{P}{60} + \left(-\tfrac{5c}{6} + \tfrac{p}{24}\right)(s_L + s_R) \\ &\quad + \tfrac{1}{8}(s_L^2 + s_R^2) + \tfrac{1}{12} s_L s_R. \end{aligned} \tag{XV.6.107}$$

The cp terms cancel between the cut loop and $A^2/6$.

There is a direct way to check the opposite mixed coefficient without inverting the four by four matrix. The spectator curvatures in W_* are exactly $D_* x_*$ with $x_* = (0, s_L/2, s_R/2, 0)^t$, as can be checked row by row in (XV.6.103). The remaining part of W_* has no dynamical gauge curvature. Thus the only term quadratic in s_L, s_R is $x_*^t D_* x_*/2$, and

$$[s_L s_R] I_{\rm cut,GS} = \frac{2(1/2)(1/2)}{6} = \frac{1}{12}, \qquad [s_L s_R] I_{\rm kept,GS} = \frac{1}{2}\left(-\frac{1}{3}\right)\frac{1}{2} = -\frac{1}{12}. \tag{XV.6.108}$$

The first term comes from squaring $-S/2$ and the second from the off-diagonal entry of D_*. Simply deleting the central row and column would leave the retained matrix block diagonal and miss the compensating mixed term. Switching off both curvatures also erases this test, even though neither step repairs the coupled calculation.

The local anomaly before and after the middle cut can also be checked on the side self terms. Retain the original E_7 sides, put the central curvature to zero in the cut polynomial, and keep s_L, s_R arbitrary. A side vector gives $-s_i^2/3 - c s_i - p s_i/12$. The spectator square in the full retained term gives $5 s_i^2/24$ from the diagonal $5/3$. Its linear part follows from the same $W_* = D_* x_* + B_*$ decomposition used in (XV.6.108). On a side row, $B_{*,i} = 11c/3 + p/12$, so the linear part is $s_i(11c/3 + p/12)/2$. Combining these with the cut contribution yields

$$[s_i^2] I_{\rm coupled} = \tfrac{1}{8} - \tfrac{1}{3} + \tfrac{5}{24} = 0, \tag{XV.6.109}$$

$$[c s_i] I_{\rm coupled} = -\tfrac{5}{6} - 1 + \tfrac{11}{6} = 0, \tag{XV.6.110}$$

$$[p s_i] I_{\rm coupled} = \tfrac{1}{24} - \tfrac{1}{12} + \tfrac{1}{24} = 0. \tag{XV.6.111}$$

There is no pure $e_i s_j$ contribution: the flavor entries in B_* remain on the unpaired end rows, where x_* is zero. This is the same coupled gauge test in different source coordinates. It illustrates why the background polynomial of the cut subsystem is useful precisely when one knows which couplings the spectators still carry.

The finite areas have not been taken to a weak gauging infinity. In the leading six-dimensional Yang–Mills description the dimensionless strength at energy E scales as $g_6 E$; it can become small in a further low energy scaling regime. That observation does not delete the finite-area gauge fields from the branch or establish that the contracted sector factorizes. The ordinary local construction and anomaly matching specify a partially contracted sector coupled to spectators. We have neither a normalizability or Kaluza–Klein isolation argument nor a full ultraviolet construction from these pairings. Changing boundary flavor or changing the matter via a Higgs flow requires a different calculation.

Exercises

1. Take $f = -Au^4$, $g = Bu^5v^k$ with A, B nonzero integers and $0 \le k \le 4$. Compute the two first-blowup coefficient pairs when a blowup is possible. Determine the remaining candidate point's orders in the second chart and count the required blowups. Show why the blowup stops. For $k = 0$ explain the pole that would result from an illegal blowup.

2. Keep $g_3 = 0$ and replace the middle leading section by a nonzero $f_2 = a_0 + a_1 s + a_2 s^2$. Compute both framed coefficient lists, their orders at the two ends and the number of generic cover factors. Try $1 + 2s + s^2$ and $s + 2s^2$. Explain where the two branch points go in the nonsquare example.

3. On the fixed E_7 branch, change the left half product to a half vector product and the right half product to a full spinor product. Give both selected orthogonal index rows and every gauge-dependent residual after adding the unchanged geometric square. Explain how the quartic residual distinguishes the errors.

4. In rank-one inflow replace h by kh for a signed nonzero integer k. Compare subtracting or keeping the free hyper. Give the seven interacting coefficient slots, including the changed mixed terms, and the coefficients of $\ell^2, \ell p, \ell c, \ell h$. Why does the flavor square alone not see the sign of k?

5. Keep the middle cut in E_7, and choose a new compact charge and rescale the side probe curvatures independently. Give the period coefficients of ϵ, L and say whether the charge lies in the effective cone. Give the cut and retained mixed coefficients and the two slopes of the left retained source with respect to the rescaled side probe variables.

6. Explain why the zero of a signed lattice period can persist throughout the ample cone path, and why neither the vanishing effective period nor the rational Schur pairing proves an isolated theory or a new integral lattice.

Use `benchmark/tasks.json` for the bounded JSON fields and `benchmark/PROTOCOL.md` for submission. Written explanations are assessed by a reader.

Status and sources

§1. The geometric E-string. The point orders, charts and incidence, compact elliptic surface, crepant modified total line bundle and changes of the leading zero are [MATH]. For the sectioned surface, fiber classification, RDP resolution and canonical formula see Miranda (1989), II.4, III.1.3, III.3.2, III.5.4–5.7, IV.1.1 and IV.3.2. The wrapped tension and ordinary E-string identification are [GEO-E], with the calibrated local premise of B.2 and the unpaired link in Heckman, Morrison, et al. (2015), §6.3; see also Heckman and Rudelius (2019), eq. (5.44).

§2. The pure E_6 collision. The fan, base orders and pairing, both cover frames, and restricted end surfaces are [MATH]. The pure polynomial is from Del Zotto et al. (2015),

eq. (2.2). The ordinary algebra assignments are [GEO-E], in the transverse minimal frame of Katz et al. (2011), §5 and Weigand (2018), Table 4.1 and eqs. (4.13)–(4.17).

§3. The pure E_7 collision. The fan and pairing, both cover frames and square obstruction, and restricted end surfaces are [MATH]. The pure polynomial is from Del Zotto et al. (2015), eq. (2.3); the ordinary algebra assignments are [GEO-E], using Katz et al. (2011), §6 and Weigand (2018), Table 4.1. No total resolution of these collision threefolds is used.

§4. Matter and the chiral index. The ordinary branch content is [GEO-E]; see Del Zotto et al. (2015), eqs. (2.5),(2.6) and Heckman, Morrison, et al. (2015), §§6.1–6.2 and Appendix E.3. The raw moments and normalized embeddings are [MATH]; for trace conventions see Heckman, Morrison, et al. (2015), eq. (2.1), footnote 7, and Ohmori, Shimizu, Tachikawa, and Yonekura (2014), Appendix A. The gauge calculation is [ANOM], using the index in the latter source, eqs. (A.1)–(A.4).

§5. Full local backgrounds. The source and gauge check and the full comparisons are [ANOM]. For sources use Ohmori, Shimizu, Tachikawa, and Yonekura (2014), eqs. (3.26)–(3.33), (3.39)–(3.42); for the E-string inflow and free hyper use Ohmori, Shimizu, and Tachikawa (2014), arXiv:1404.3887v2, eqs. (1.1)–(1.5). The one-unit ALE expression and center subtraction are Ohmori, Shimizu, Tachikawa, and Yonekura (2014), arXiv:1408.5572v2, eqs. (3.23),(3.24),(B.20). The comparisons match seven, eleven and eleven local background monomials, respectively, with reflection relating three pairs in each exceptional result.

§6. The two partial contractions. The actual coarsenings, quotient cone and geometric area face are [MATH]. The tensor source identity and local anomaly matching are [ANOM]; the end link uses Ohmori, Shimizu, Tachikawa, and Yonekura (2014), eqs. (3.10),(3.11),(3.15),(3.41),(3.42). The finite-spectator and wrapped-charge interpretation is [GEO-E], with the ordinary retained-sector and leading calibrated-brane premises. The projected form is rational; the local polynomial does not establish dynamical factorization.

References

Del Zotto, M. et al. (2015). "6d Conformal Matter". In: *JHEP* 02, p. 054. arXiv: 1407.6359.

Heckman, J. J., D. R. Morrison, et al. (2015). "Atomic Classification of 6D SCFTs". In: *Fortsch. Phys.* 63, pp. 468–530. arXiv: 1502.05405.

Heckman, J. J. and T. Rudelius (2019). "Top Down Approach to 6D SCFTs". In: *J. Phys. A* 52, p. 093001. arXiv: 1805.06467.

Katz, S. et al. (2011). "Tate's Algorithm and F-theory". In: *JHEP* 08, p. 094. arXiv: 1106.3854.

Miranda, R. (1989). *The Basic Theory of Elliptic Surfaces*. Pisa: ETS Editrice.

Ohmori, K., H. Shimizu, and Y. Tachikawa (2014). "Anomaly Polynomial of E-string Theories". In: *JHEP* 08, p. 002. arXiv: 1404.3887.

Ohmori, K., H. Shimizu, Y. Tachikawa, and K. Yonekura (2014). "Anomaly Polynomial of General 6d SCFTs". In: *PTEP* 2014, 103B07. arXiv: 1408.5572.

Weigand, T. (2018). “F-theory”. In: *PoS* TASI2017, p. 016. arXiv: 1806.01854.

Chapter XV.7

Organization of SCFTs and RG flows

XV.7.1 Organizing the constructions already obtained

What has to change in a six-dimensional construction before we can recognize a new low energy theory? A diagram of intersecting curves does not record all the operations we can perform. We can change the areas while holding the elliptic coefficients fixed, or change the coefficients so that a collision separates or recombines. We will follow both operations on a rank-two E-string and compare the resulting theories. First we need to identify what the diagrams of Chapters B.3–6 actually record.

Let C_i be the compact base curves and let $a_i = \int_{C_i} J$ be their areas for a Kähler class J. The integral tensor pairing on their span is $\Omega_{ij} = -C_i \cdot C_j$. A diagonal entry gives minus the self-intersection; an off-diagonal entry counts intersections with a minus sign. This is a pairing of base curves. The Dynkin diagrams that identify gauge algebras come from a different calculation, on the resolved elliptic fibers. The pairing and the fiber labels of the two ordinary examples in Figure XV.7.1 are

$$\Omega_{45} = \begin{pmatrix} 2 & -1 \\ -1 & 2 \end{pmatrix}, \qquad \text{fibers: } I_4^{\text{s}}, I_5^{\text{s}}. \tag{XV.7.1}$$

$$\Omega_{414} = \begin{pmatrix} 4 & -1 & 0 \\ -1 & 1 & -1 \\ 0 & -1 & 4 \end{pmatrix}, \qquad \text{fibers: } I_0^{*\text{s}}, I_0, I_0^{*\text{s}}. \tag{XV.7.2}$$

The first example, CHAIN45, uses split multiplicative fibers and ordinary matter at a transverse intersection and at the selected simple zeros of the residual discriminants. In the second example the compact middle curve is the exceptional curve of the blowup of the transverse meeting of two -3 curves. It has a smooth generic fiber. It still contributes a compact string charge. The middle tensor and the $\mathfrak{so}(8)$ sectors at the ends have to be distinguished even before specifying a limit.

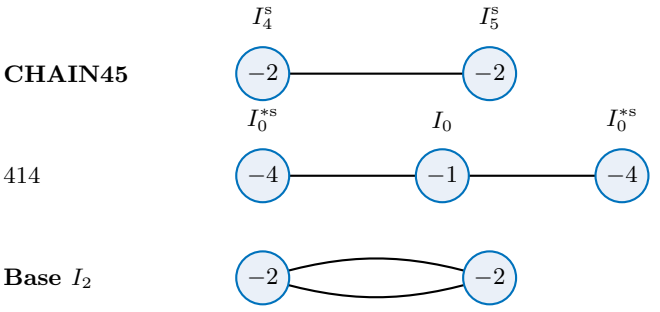


Figure XV.7.1: Three base pairings. The labels inside the vertices are self-intersections. Above the first two panels are the elliptic fibers over the compact curves; the superscript s denotes split. The lower panel depicts components of the actual degenerating base cubic of B.5, with two intersections between the same components. Its I_2 label describes that base fiber as a whole.

The leading principal minors test the sign of the tensor pairing as a bilinear form, independently of the actual positive areas used in a geometry. For 414 the first two minors are $4, 4-1=3$; expansion in the third row gives the third as $4\cdot 3-4=8$. The two lists are

$$m(\Omega_{45})=(2,3), \qquad m(\Omega_{414})=(4,3,8). \tag{XV.7.3}$$

For the second matrix an equivalent direct positivity test is

$$q^{\mathsf{T}}\Omega_{414}q = 4(q_1-q_2/4)^2+\tfrac{1}{2}q_2^2+4(q_3-q_2/4)^2. \tag{XV.7.4}$$

Here q_i are coefficients of a base curve class. Both pairings are positive definite, though the second has three independent charges and a different set of elliptic fibers. For the actual contractions of B.5 one also constructs the relative Kähler path and specifies which other scales are held fixed. Positivity alone supplies neither those data nor the identification of the limiting sector.

The compact I_2 fiber of B.5 is a useful control because a change of just one incidence would reverse the definite-versus-null diagnosis. In a neighborhood of the old node, the cubic is $y^2=s^2(3+s)+t^2$, where t is the base parameter of this cubic family and $s=x-1$. At $t=0$ the two limiting directions are $y/s=\pm\sqrt{3}$. The exceptional conic meets the strict curve at both directions. Their sum $D=C_1+C_2$ is the divisor of t and has zero intersection with either curve. Since $C_1\cdot C_2=2$, this gives

$$C_i^2=-2, \qquad \Omega_{I_2}=\begin{pmatrix}2&-2\\-2&2\end{pmatrix}, \qquad \Omega_{I_2}\begin{pmatrix}1\\1\end{pmatrix}=0. \tag{XV.7.5}$$

If we keep the self-intersections but replace the two edges by a single edge, the result is Ω_{45}, which sends $(1,1)^{\mathsf{T}}$ to itself and has determinant 3. The mistake changes a geometric obstruction: a whole compact configuration with this nonzero null fiber class fails the negative definiteness test for contraction to a surface point. Chapter B.8 will use null classes in a different limit. A null direction in this example does not assign an elliptic decoration or identify a physical little string theory.

The null class does not have zero area in the positive chamber. In the I_2 example the area of the principal fiber is $a_1 + a_2$; it can stay finite even as the relative component areas change. For instance, compare the choices $(a_1, a_2) = (2, 3)$ and $(1, 4)$ in common units. For $q_+ = (1, 1)^{\mathsf{T}}$ and $q_- = (1, -1)^{\mathsf{T}}$,

$$q_+^{\mathsf{T}} \Omega_{I_2} q_+ = 0, \qquad q_-^{\mathsf{T}} \Omega_{I_2} q_- = 8, \tag{XV.7.6}$$

$$q_+^{\mathsf{T}} a = 5 \quad \text{in both cases}, \qquad q_-^{\mathsf{T}} a = -1 \text{ or } -3. \tag{XV.7.7}$$

The last two numbers are signed periods; q_- is a difference of components, not an effective sum. These data explain why neither the norm of a charge nor the number of visible vertices can be substituted for a wrapped-string area. In the positive definite 414 lattice the primitive sum of the three curves instead has squared norm 5, by (XV.7.4) with each $q_i = 1$. The presence of the middle -1 tensor changes both the charge span and how to read the periods, even without a gauge field there.

Even a correct pairing with correct generic fibers leaves the behavior at marked points to be determined. In the short Weierstrass convention we use $\Delta = 4f^3 + 27g^2$; the orders are those of f, g, Δ. Chapter B.4 computes the following inherited point data in the two lifts with the same designated generic multiplicative fibers:

$$\text{ordinary corner} : (0, 0, 9), \qquad \text{changed residual tangency at another point} : (0, 0, 5). \tag{XV.7.8}$$

These refer to distinct loci. The latter is a double residual zero on the designated I_4 curve, not a new value for the old corner. The point data distinguish the two tunings even when the tensor pairing is unchanged. In particular, the old ordinary simple-root spectrum does not follow for the altered tangency. In the next section we first compute the gauge test with the old specified matter and then replace the ordinary link by an interacting one.

XV.7.2 Gauging and compatibility

Which pieces of two neighboring sectors can be gauged by the same six-dimensional vector? On CHAIN45 we can answer the anomaly part of the question by summing weights. We take one full bifundamental hyper, F_i full external fundamentals at each node, and one vector in each adjoint. These are the ordinary matter hypotheses of the selected split model. At node i, the gauge size N_i is the dimension of the defining representation of $SU(N_i)$; the Lie rank is $N_i - 1$. For the gauge-only calculation, let $\mathcal{F}_i$ be the curvature in the fundamental trace, and put $s_i = \operatorname{tr}_{\mathrm{f}} \mathcal{F}_i^2$ and $q_i^{(4)} = \operatorname{tr}_{\mathrm{f}} \mathcal{F}_i^4$. Take Cartan weights x_a, y_b with zero sum in their respective fundamentals. Then

$$\sum_{a,b} (x_a - y_b)^4 = N_2 q_1^{(4)} + N_1 q_2^{(4)} + 6 s_1 s_2, \tag{XV.7.9}$$

$$\sum_{a,b=1}^{N_i} (x_a - x_b)^4 = 2 N_i q_i^{(4)} + 6 s_i^2. \tag{XV.7.10}$$

The terms cubic in one set of weights and linear in the other vanish by tracelessness. The adjoint sum can include the diagonal terms, because their weights are zero. The

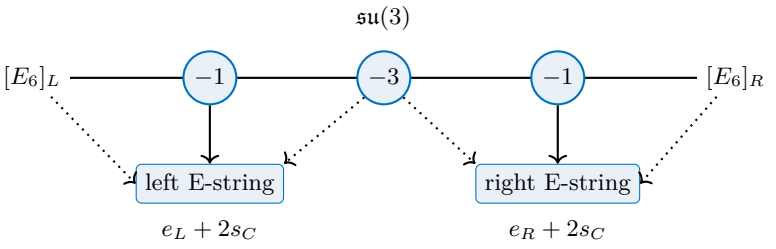


Figure XV.7.2: The pure E_6 collision on the 131 base. The noncompact ends carry background currents. The arrows below the two -1 curves mark their contraction into distinct E-string sectors. Both sectors couple to the retained central gauge field; the dotted arrows indicate source restriction, not additional matter or additional compact curves.

chiral index gives a full hyper with sign $+1/24$ in the fourth trace and a vector with the opposite sign. For $N_i \geq 4$ the quartic invariant is independent of the square of the quadratic, so the irreducible terms must vanish before the Green–Schwarz comparison:

$$I_{\text{loop}}^{\text{gauge}} = \frac{(F_1 + N_2 - 2N_1)q_1^{(4)} + (F_2 + N_1 - 2N_2)q_2^{(4)}}{24} - \frac{1}{8}s^{\mathsf{T}}\Omega_{45}s, \tag{XV.7.11}$$

$$\begin{pmatrix} F_1 \\ F_2 \end{pmatrix} = \Omega_{45}\begin{pmatrix} N_1 \\ N_2 \end{pmatrix}. \tag{XV.7.12}$$

Here $s = (s_1, s_2)^{\mathsf{T}}$. With source $Y = \Omega_{45}s/2$, the pure gauge part of $I_{\text{GS}} = Y^{\mathsf{T}}\Omega_{45}^{-1}Y/2$ is $+s^{\mathsf{T}}\Omega_{45}s/8$. This cancels the reducible gauge terms. For $(N_1, N_2) = (4, 5)$ the fundamentals are $(3, 6)$. Set $N_2 = 6$, as in the explicit split I_4–I_6 construction in Chapter B.3. The required pair is now $(2, 8)$. Keeping the old counts instead would leave

$$I_{\text{loop}}^{\text{gauge}} + I_{\text{GS}}^{\text{gauge}} = \frac{q_1^{(4)}}{24} - \frac{q_2^{(4)}}{12}. \tag{XV.7.13}$$

The counts here are necessary gauge arithmetic. Chapter B.3 separately realizes this particular changed model by Tate coefficient sections and verifies its ordinary matter loci; the arithmetic alone does not supply that geometry.

For the pure E_6 collision of B.6, each unpaired -1 curve can instead be contracted to an interacting E-string link. The two ends attach to different links, as shown in Figure XV.7.2. The ordinary $\mathfrak{e}_8$ restriction of a single link supplies commuting $\mathfrak{e}_6 \oplus \mathfrak{su}(3)$ currents, one of which couples to the central vector. Another example of this restriction is $\mathfrak{e}_7 \oplus \mathfrak{su}(2)$. Both have total rank 8; trying to attach both $\mathfrak{e}_6$ ends to a single link would already fail because $6+6 > 8$. Passing this screen would still leave the actual embedding and its trace index to be established. We use the specified index-one embeddings at the Lie-algebra level.

We now change the tensor variables used in the anomaly calculation. The positive pairing of the strict central curve is 3, and it meets each end once. Write C_L, C_C, C_R for the strict curves, and C_C' for the central curve after blowing down both ends. Its

total pullback is $C_C + C_L + C_R$: its intersection with each end is zero, as required of a pullback. In this basis

$$\Omega = \begin{pmatrix} 1 & -1 & 0 \\ -1 & 3 & -1 \\ 0 & -1 & 1 \end{pmatrix}, \qquad -\big(C_C + C_L + C_R\big)^2 = 3 - 1 - 1 = 1. \tag{XV.7.14}$$

A source component on the retained tensor also changes; evaluating it on the total pullback adds the two end components to the strict central one. Use the B.6 curvature $F_O = -iF_{\rm phys}/(2\pi)$ in the index $\widehat{A}(T)\,\mathrm{tr}\exp(iF_O)$. Let $c = c_2(R)$, $p = p_1(T)$, $p_2 = p_2(T)$, $s_C = \mathrm{tr}_{\rm f}\, F_{O,C}^2$, and e_L, e_R be the normalized $\mathfrak{e}_6$ quadratic traces. For each simple algebra the normalized trace is $\mathrm{Tr} = \mathrm{tr}_{\rm adj}\,/h^\vee$. Thus in this trace convention the quadratic argument $h = \mathrm{Tr}_{E_8} F_O^2$ of the left or right E-string restricts to $e_i + 2s_C$. The original and retained tensor sources are

$$Y = \Omega \begin{pmatrix} 0 \\ s_C/2 \\ 0 \end{pmatrix} + \begin{pmatrix} c - (p + e_L)/4 \\ 3c + p/4 \\ c - (p + e_R)/4 \end{pmatrix}, \tag{XV.7.15}$$

$$Y'_C = Y_L + Y_C + Y_R = 5c - \tfrac{1}{4}(p + e_L + e_R) + \tfrac{1}{2}s_C. \tag{XV.7.16}$$

The source vector with no s_C is the branch input of B.6. Treating a contraction as deletion of the end rows would give both the wrong central pairing and the wrong central source.

To check the resulting gauging, the rank-one interacting anomaly of B.6 can be written $J_1(h) = K + (p/16 - c/4)h + h^2/32$, with

$$G = \frac{7p^2 - 4p_2}{5760}, \qquad K = \frac{13c^2}{24} - \frac{11cp}{48} + 29G. \tag{XV.7.17}$$

The two copies of J_1 already include the local anomaly contributions of the contracted tensors. We do not add their squares a second time. For the central vector, (XV.7.10) with $N = 3$ gives $\mathrm{tr}_{\rm adj}\, F_{O,C}^4 = 9s_C^2$ since $\mathrm{tr}_{\rm f}\, F_{O,C}^4 = s_C^2/2$ for three eigenvalues of zero sum. The second trace is $6s_C$. The vector and free tensor polynomials are

$$V_3 = -\frac{9s_C^2}{24} - 6s_C\left(\frac{c}{4} + \frac{p}{48}\right) - 8\left(\frac{c^2}{24} + \frac{cp}{48} + G\right), \tag{XV.7.18}$$

$$T = \frac{c^2}{24} + \frac{cp}{48} + \frac{23p^2 - 116p_2}{5760}. \tag{XV.7.19}$$

Set $B = 5c - (p + e_L + e_R)/4$. The coefficient of s_C^2 in $J_1(e_L + 2s_C) + J_1(e_R + 2s_C) + T + V_3 + (Y'_C)^2/2$ is $1/4 - 3/8 + 1/8 = 0$. Its linear coefficient is

$$\left(\frac{e_L + e_R}{8} + \frac{p}{4} - c\right) - \left(\frac{3c}{2} + \frac{p}{8}\right) + \frac{B}{2} = 0. \tag{XV.7.20}$$

For example, replace just the left trace restriction by $e_L + s_C$, holding the actual central source and right embedding fixed. The s_C^2 coefficient drops by $3/32$ and gauge

dependence returns. The two actual restrictions cancel all terms containing the gauge curvature, including the terms mixed with backgrounds. The remaining background polynomial is

$$I_{E_6}(e_L,e_R)=\frac{319c^2}{24}-\frac{89cp}{48}-\frac{3c}{2}(e_L+e_R)+\frac{p(e_L+e_R)}{8}\\ +\frac{e_L^2+e_Le_R+e_R^2}{16}+79G. \tag{XV.7.21}$$

To see how the mixed flavor term arose, put $S_e=e_L+e_R$ and $U_e=e_L^2+e_R^2$. The two end indices contain $U_e/32$; only the retained square can generate an e_Le_R term. Its pure flavor part is $S_e^2/32$, which adds another $U_e/32$ and gives the mixed term $e_Le_R/16$. Likewise the tangent contributions from T and the neutral parts of the indices must all be included. In the convention above

$$T\big|_{c=0}=29G-\frac{p^2}{32}. \tag{XV.7.22}$$

At $c=e_L=e_R=s_C=0$ the retained square restores $p^2/32$, leaving $(2\cdot29+29-8)G=79G$. This is the full tangent contribution, not only the p_2 slot. The e_Le_R term and the gravitational term will separately test the proposed spectrum after recombination.

This agrees with the exceptional branch result of B.6 and will be used again when the two external backgrounds are identified by recombination. The calculation tests local gauge compatibility of the prescribed sectors; it neither determines a global group nor regards the central Yang–Mills field at finite tensor area as a free conformal multiplet.

XV.7.3 A tensor branch deformation

Can one keep a finite tensor scale and still reach an interacting theory? The geometry must have a partial contraction: some wrapped strings must become tensionless while another curve remains at positive area. We construct the parent model and its last blowdown before identifying the massless sectors.

Take the short Weierstrass family on $\mathbb{C}^2_{u,v}$

$$f=-3u^4,\qquad g=u^5(v^2-b^2),\qquad \Delta=27u^{10}\big((v^2-b^2)^2-4u^2\big). \tag{XV.7.23}$$

The divisor $u=0$ is noncompact. At its generic point it has orders $(4,5,10)$, so it supplies a II^* background. Set $b=0$ first. The orders at the origin are $(4,7,12)$, because the least-degree term in Δ is $-108u^{12}$, not the term with v^4. Every point with $u\neq0$ has $f\neq0$. On $u=0$ away from the origin the factor v^2 is a unit. Thus the origin is the only point meeting the nonminimal bounds $(4,6,12)$.

At a base point blowup with local exceptional equation $e=0$, the new short coefficients are $f_{\mathrm{new}}=\pi^*f/e^4$ and $g_{\mathrm{new}}=\pi^*g/e^6$. This follows from $K_{\widetilde{B}}=\pi^*K_B+E$, so the line bundle $-K_{\widetilde{B}}$ has one exceptional subtraction. The discriminant correspondingly divides by e^{12}. The two pivot charts of the first blowup give

$$u=st,\quad v=t:\quad (f_1,g_1,\Delta_1)=(-3s^4,\ s^5t,\ 27s^{10}(t^2-4s^2)), \tag{XV.7.24}$$

$$u=a,\quad v=az:\quad (f_1,g_1,\Delta_1)=(-3,\ az^2,\ 27(a^2z^4-4)). \tag{XV.7.25}$$

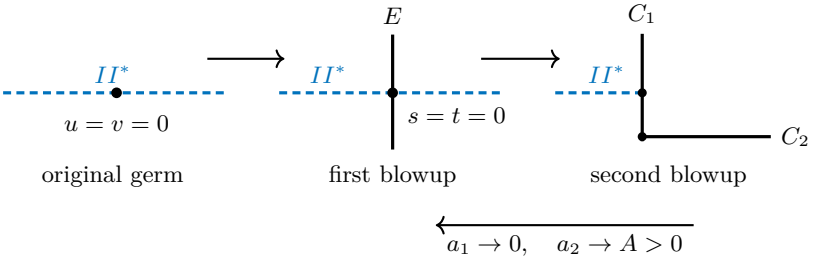


Figure XV.7.3: The first exceptional E meets strict II^* at the second blowup center. After that blowup the two strict curves meet the new C_1 in different directions. Contracting C_1 alone restores the middle panel with its rank-one nonminimal germ, while the area of the old exceptional remains positive.

In the second chart f_1 is a unit. In the first chart $t = 0$ is the first exceptional and $s = 0$ is strict II^*. Their meeting still has $(4, 6, 12)$. Equation (XV.7.24) is exactly the rank-one germ used in B.6. This identifies what the reverse of the next blowup will recover.

Blow up $s = t = 0$, writing $(s, t) = (\sigma\tau, \tau)$ or $(a', a'z')$. Apply the same powers as before, now with exceptionals $\tau = 0$ and $a' = 0$:

$$(f_2, g_2, \Delta_2)_\tau = (-3\sigma^4,\ \sigma^5,\ 27\sigma^{10}(1 - 4\sigma^2)), \tag{XV.7.26}$$

$$(f_2, g_2, \Delta_2)_{a'} = (-3,\ z',\ 27((z')^2 - 4)). \tag{XV.7.27}$$

In the τ chart, the new exceptional C_1 meets strict II^* at $\sigma = 0$, of orders $(4, 5, 10)$. The other direction, strict $t = 0$ of the first step, meets C_1 at $z' = 0$ in the a' chart, where f_2 is a unit. The two intersection points are distinct directions on C_1. The zeros of the residual discriminant at $\sigma = \pm 1/2$ and $z' = \pm 2$ describe the same two points in the overlap and do not give nonminimal centers. Neither exceptional carries a generically singular elliptic fiber. There is no further nonminimal point in the new charts or in the part unchanged from the first step. Figure XV.7.3 follows the two distinguished directions through the construction.

Call the strict old curve C_2; its self-intersection decreases by one since the second blowup lies on it with multiplicity one. In the column notation $C = (C_1, C_2)$, the total pullback of the old exceptional is $C_1 + C_2$. Its intersection with C_1 is zero. The change $C \mapsto CP$ is integral:

$$\Omega = \begin{pmatrix} 1 & -1 \\ -1 & 2 \end{pmatrix}, \qquad P = \begin{pmatrix} 1 & 1 \\ 0 & 1 \end{pmatrix}, \qquad P^{\mathsf{T}}\Omega P = \mathbf{1}_2. \tag{XV.7.28}$$

This is not a change in the effective generators: a total pullback is a sum of effective curves. The old exceptional has self-intersection -1 on the blown-down base, rather than the strict -2 read from the old principal submatrix. In coordinates the blowdown is precisely the inverse of the two chart maps above, including restoration of the line bundle powers used to obtain (XV.7.24).

Choose the areas $a_1 = \varepsilon > 0,\ a_2 = A > 0$. The relative curve cone over $\mathbb{C}^2$ is generated by the two exceptional curves, so positivity on them specifies the relative ample chamber. Explicitly a relative class in the compact divisor span with coefficient column j has $a = -\Omega j$; solving gives

$$j = -\begin{pmatrix} 2 & 1 \\ 1 & 1 \end{pmatrix} \begin{pmatrix} \varepsilon \\ A \end{pmatrix}, \qquad P^{\mathsf{T}} a = \begin{pmatrix} \varepsilon \\ A + \varepsilon \end{pmatrix}. \tag{XV.7.29}$$

Here relative ample rational classes and their real positive cone suffice; no physical metric is constructed. As $\varepsilon \to 0$, the period of the total pullback stays finite. For example at $A = 5$, the calibrated tension of a string of class $2C_1 + 3C_2$, if present in this dictionary, is

$$\mathcal{T}_{(2,3)} = \tau_3(2\varepsilon + 15), \qquad \tau_3 = \frac{1}{(2\pi)^3 \alpha'^2}. \tag{XV.7.30}$$

The general expression is $\tau_3 q^{\mathsf{T}} a$. With area of dimension length squared, the tension has dimension length to the minus two. This is a fixed microscopic calibration, not an existence claim for a BPS state of every effective charge. In the total basis the charge column becomes $P^{-1}q = (-1, 3)^{\mathsf{T}}$, and the period sum is unchanged: $-\varepsilon + 3(A + \varepsilon) = 2\varepsilon + 3A$. The negative new component is not a negative curve area. It reflects the distinction between the effective generators and the basis that makes the blowdown pairing diagonal.

The opposite wall $a_2 \to 0,\ a_1 = A > 0$ is different already at the level of periods and pairing. In the total basis both periods tend to A; $P^{\mathsf{T}} a$ does not contain a zero component. For a comparison orthogonal to C_2 one can project the strict C_1 to $C_1 + C_2/2$, which pairs to zero with C_2:

$$\left(1, \tfrac{1}{2}\right) \Omega \begin{pmatrix} 0 \\ 1 \end{pmatrix} = 0, \qquad \left(1, \tfrac{1}{2}\right) \Omega \begin{pmatrix} 1 \\ 1/2 \end{pmatrix} = \tfrac{1}{2}. \tag{XV.7.31}$$

The rational value is not a new integral pairing. In particular it is not the -1 blowdown pairing of the wall in Figure XV.7.3. A smooth point blowup has exceptional self-intersection -1; reversing that operation here specifically removes C_1, not the strict -2 curve. This is why the area path specifies which anomaly basis is relevant.

Under the isolated small-instanton interpretation, the vanishing area is the rank-one E-string sector and the positive area separates one brane from the wall. At energies far below the scale set by this finite tensor expectation value, the endpoint contains a rank-one E-string including its center hyper, and one free $(2, 0)$ tensor multiplet. With the common $(1, 0)$ supercharges, the detached multiplet is a free tensor plus an E_8-neutral half-hyper in the doublet of $SU(2)_L$. A single detached brane has no relative interacting $(2, 0)$ sector. The free multiplet must be kept even though the finite-tension strings on the positive-area direction are not part of the deep infrared theory. At finite energy the area calculation alone does not imply factorization of coupled sectors.

XV.7.4 A Higgs branch deformation

What changes if we keep the tensor scales at zero and instead separate the zeros in the coefficient family? We do not need a different noncompact flavor divisor. In (XV.7.23)

let $b \neq 0$. On $u = 0$ the coefficient g/u^5 now vanishes at two points $v = V = \pm b$. Near either point use $\eta = v - V$:

$$v^2 - b^2 = \eta(2V + \eta), \qquad \Delta = 27u^{10}\big(\eta^2(2V + \eta)^2 - 4u^2\big). \tag{XV.7.32}$$

The second factor $2V + \eta$ in the expression for $v^2 - b^2$ is a unit in a neighborhood excluding the other zero. At the center the least degree in g is six and that in Δ is twelve. The leading discriminant polynomial contains both $u^{10}\eta^2$ and u^{12}, so the two terms cannot cancel as polynomials. The orders are therefore $(4, 6, 12)$ at each of the two centers.

There are two ways to see which branch each center gives. First, $w = v^2 - b^2$ is an analytic coordinate near either center since

$$\left.\frac{\partial w}{\partial v}\right|_V = 2V \neq 0, \qquad (f, g) = (-3u^4, u^5 w). \tag{XV.7.33}$$

These coefficients retain the original Weierstrass trivialization and only rewrite the arguments. Here $du \wedge dw = 2v\, du \wedge dv$, with $2v$ a unit near $v = V$. The new anticanonical generator dual to $du \wedge dw$ is $(2v)^{-1}$ times the original. The coefficients in that frame acquire factors $(2v)^4, (2v)^6, (2v)^{12}$, respectively for f, g, Δ. These units preserve the rank-one orders at each center. We can also keep the marked v coordinate and compute both blowup charts to track the signs of the coefficients and the incidence with II^*. With $(u, \eta) = (st, t)$ and (a, az), respectively, the results are

$$(f'_V, g'_V, \Delta'_V)_t = \big(-3s^4,\ s^5(2V + t),\ 27s^{10}((2V + t)^2 - 4s^2)\big), \tag{XV.7.34}$$

$$(f'_V, g'_V, \Delta'_V)_a = \big(-3,\ z(2V + az),\ 27(z^2(2V + az)^2 - 4)\big). \tag{XV.7.35}$$

On the strict noncompact divisor $s = 0$, $2V + t$ is a unit within the chosen neighborhood, so the transformed orders there are $(4, 5, 10)$. In the a chart f'_V is a unit. Both exceptionals have generic I_0, and there is no further nonminimal center. Since the blowup centers are disjoint, the exceptionals are disjoint and each has self-intersection -1:

$$C_- \cdot C_+ = 0, \qquad \Omega_{\text{split}} = \operatorname{diag}(1, 1). \tag{XV.7.36}$$

This is an intersection matrix in the actual effective basis of a different base. To compare chambers, use a'_1, a'_2 for the periods in a basis with matrix $\mathbf{1}_2$ in both cases. In the coincident model the second effective generator is the second total-basis curve minus the first. For the split model the total and effective bases are the same. Thus the respective ample conditions are

$$\text{coincident}: \quad a'_1 > 0, \qquad a'_2 - a'_1 > 0, \tag{XV.7.37}$$

$$\text{split}: \quad a'_1 > 0, \qquad a'_2 > 0. \tag{XV.7.38}$$

For example the period pair $(3, 2)$ is admissible only in the split geometry. The equal matrices are not a comparison of identical contraction diagrams.

For example take $b = 2$. The t-chart leading factor of g'_V is $s^5(t - 4)$ at the negative root and $s^5(t + 4)$ at the positive root. In the other chart the coefficient on the

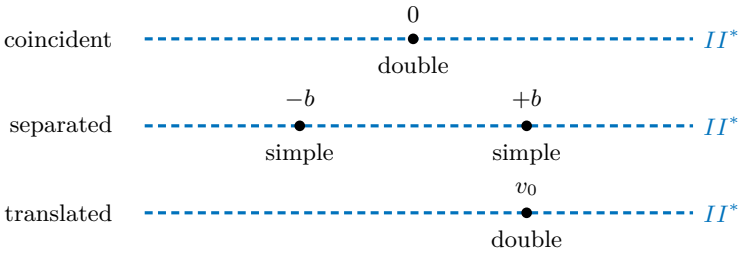


Figure XV.7.4: The coefficient g/u^5 on the same noncompact II^* divisor. A double zero uses a second center above the first. The separated simple zeros have one exceptional each, at distinct points of strict II^*. Translating a double zero preserves the two-step blowup at a single location.

exceptional is $-4z$ or $+4z$, respectively. The charts overlap where $a = st,\ z = 1/s$, so the new g in the a frame differs from that in the t frame by $(t/a)^6$. In particular,

$$\frac{s^5(2V + t)}{s^6} = z(2V + az). \tag{XV.7.39}$$

The residual discriminant meets the exceptional at $s = \pm V$ in the first chart and $z = \pm 1/V$ in the second. These are two points, not four; the reciprocal map identifies the lists. At either point the s derivative of the residual factor in (XV.7.34) is $-8s \neq 0$, and $f'_V \neq 0$. The residual is transverse to the exceptional and locally has ordinary nodal fibers along it. The meeting at $s = 0$ is the distinct II^* point. Thus a generic I_0 label on the compact curve does not suppress the marked fibers that the chart actually exhibits.

By contrast the change $v^2 \mapsto (v - 2)^2$ gives a single double zero. In the translated coordinate $\eta = v - 2$ the first blowup in the t chart again produces $s^5 t$, so the same second blowup is necessary. This control shows why multiplicity of a zero is better information than the movement of its position.

To interpret the change as a Higgs flow, we use the small-instanton identification of the relative displacement along the E_8 wall with a hypermultiplet VEV in the isolated local theory. The displayed equations exhibit the actual coincident and separated germs. They do not by themselves show that the parameter is a normalizable mode of a physical metric. In the deep infrared there are two rank-one E-string sectors, each including its own center hyper. The two centers account for the original center and the relative degrees of freedom; adding a separate relative hyper would count it twice.

The noncompact II^* divisor is common to the two germs and remains external. The two rank-one theories can have separate E_8 symmetries in the isolated infrared description, but the original E_8 connection restricts to both. Likewise a relative displacement is a fixed nonzero vector in the real four-dimensional transverse representation of $SU(2)_L \times SU(2)_R$. Represent that vector by a nonzero quaternion Q with action $Q \mapsto g_L Q g_R^{-1}$. In a frame in which the VEV is real, its stabilizer satisfies $g_L = g_R$. Thus the conserved background for the flow is the common diagonal in the two normal rotations, as well as the common external E_8. This identifies the anomaly compari-

son that we can do, without assuming the ultraviolet and infrared superconformal R symmetries themselves are the same.

XV.7.5 Tracking sectors and anomalies

Which anomalies can compare the endpoints, and which fields enter each comparison? On the tensor branch the scalar VEV is neutral under the normal rotations; we can keep the same R, L, E_8 backgrounds. On the Higgs branch the relative displacement leaves only the diagonal subgroup just described. Neither of these comparisons uses the conformal anomaly until the massless sectors and their superconformal R symmetries have been identified.

In the inflow formula $E(n)$ is the anomaly polynomial of n E-strings *including* one free center hyper. We retain $c = c_2(R)$, write $\ell = c_2(L)$, and set $h = \mathrm{Tr}_{E_8} F_O^2$. The Euler class of the normal four-plane is $\chi = \ell - c$; its first and second Pontryagin classes are $n_1 = -2(\ell + c)$ and χ^2. The inflow formula uses the tangent Pontryagin classes p, p_2:

$$I_4 = \frac{n_1 + p + h}{4}, \qquad I_8^0 = \frac{1}{48}\left(\chi^2 + p_2 - \frac{(n_1 - p)^2}{4}\right), \tag{XV.7.40}$$

$$E(n) = \frac{n^3}{6}\chi^2 + \frac{n^2}{2}\chi I_4 + n\left(\frac{I_4^2}{2} - I_8^0\right). \tag{XV.7.41}$$

The normal Euler orientation matters in the term linear in χ. To compute the center polynomial, let the two weights of the $SU(2)_L$ doublet be $x, -x$ with $x^2 = -\ell$. The half-hyper multiplies the tangent genus by half of $e^x + e^{-x}$, with x the index root. Its degree-four part is $-\ell/2$ and its degree-eight part is $\ell^2/24$. Multiplication by the degree-four tangent term $-p/24$ gives the mixed term:

$$H_L = G + \frac{\ell p}{48} + \frac{\ell^2}{24}, \qquad H_{20} = T + H_L. \tag{XV.7.42}$$

The half-doublet is one hyper unit in the gravity index. It is neutral under E_8, but dropping its $SU(2)_L$ source would be incorrect when comparing normal-rotation backgrounds.

For a check on the inflow normalization, set $n = 1$. Inserting (XV.7.40) and collecting the terms depending on ℓ gives $\ell^2/24 + \ell p/48$; these are exactly the center terms. The remaining h, c, and gravity terms give

$$E(1) - H_L = \frac{13c^2}{24} - \frac{11cp}{48} + \left(\frac{p}{16} - \frac{c}{4}\right)h + \frac{h^2}{32} + 29G. \tag{XV.7.43}$$

This gives J_1 used in the gauging calculation. In particular there is no $SU(2)_L$ anomaly in the rank-one interacting factor. We still keep H_L whenever the whole rank-one small-instanton sector enters an endpoint.

One way to reconstruct every term at rank two is to use $E(2) - 2E(1) = \chi^2 + \chi I_4$, so that the part linear in n, including the irreducible p_2 term, comes directly from $E(1)$.

Since $I_4 = (p+h)/4 - (\ell+c)/2$, this gives

$$E(2) = \frac{31c^2}{12} - 2c\ell - \frac{3ch}{4} - \frac{17cp}{24} + \frac{7\ell^2}{12} + \frac{\ell h}{4} + \frac{7\ell p}{24} + \frac{h^2}{16} + \frac{hp}{8} + \frac{7p^2}{96} - \frac{p_2}{24}. \tag{XV.7.44}$$

The linear gravity term in p_2 also follows from two H_{20} multiplets on the full tensor branch. Subtract them and use $Z = (p+h)/4$. Directly from the displayed coefficients,

$$E(2) - 2H_{20} = \tfrac{5}{2}c^2 - 2c\ell + \tfrac{1}{2}\ell^2 - 3cZ + \ell Z + Z^2. \tag{XV.7.45}$$

Here Z^2 reproduces the h^2, hp, p^2 terms in the remainder; the cZ and ℓZ terms fix both the mixed tangent and mixed flavor coefficients. In the strict curve basis of (XV.7.28), define the source Y by the following factorization:

$$Y = \begin{pmatrix} c - Z \\ c - \ell \end{pmatrix}, \qquad \Omega^{-1} = \begin{pmatrix} 2 & 1 \\ 1 & 1 \end{pmatrix}, \tag{XV.7.46}$$

$$\tfrac{1}{2}Y^{\mathsf{T}}\Omega^{-1}Y = Y_1^2 + Y_1Y_2 + \tfrac{1}{2}Y_2^2 = \tfrac{1}{2}Y_1^2 + \tfrac{1}{2}(Y_1+Y_2)^2. \tag{XV.7.47}$$

Expansion gives (XV.7.45). This supplies the full anomaly comparison for these particular sources. It is not a prescription for the R source of an arbitrary unpaired -2 curve.

The rank-one sector already contains $Y_1^2/2$: by (XV.7.43) and (XV.7.42), $E(1) - H_{20} = (c-Z)^2/2$. On the tensor wall the source column in the total basis is $P^{\mathsf{T}}Y = (Y_1, Y_1+Y_2)^{\mathsf{T}}$. Thus the mismatch with the rank-one daughter and the complete free multiplet is

$$E(2) - E(1) - H_{20} = \tfrac{1}{2}(Y_1+Y_2)^2 = \frac{(p+h+4\ell-8c)^2}{32}. \tag{XV.7.48}$$

In particular hp has coefficient $1/16$, whereas using the unshifted Y_2 for the finite-area direction would give zero. The p_2 coefficient vanishes because a square of four-forms cannot supply an irreducible gravity term. Omitting the free half-doublet instead leaves $-1/1440$ in the mismatch; omitting the free tensor leaves $-29/1440$. These tests isolate two separate omissions. The positive finite-area direction is therefore visible in the anomaly comparison even though the contracted rank drops by one.

For Higgs splitting the two daughters have $I_{\mathrm{IR}} = E(1,h_1) + E(1,h_2)$ before background restriction. The common E_8 connection sends both h_i to h. The difference on this partially restricted background is

$$E(2) - 2E(1,h) = \chi^2 + \chi I_4 = \frac{(\ell-c)(2\ell-6c+p+h)}{4}, \tag{XV.7.49}$$

$$c = \ell = d, \qquad h_1 = h_2 = h \quad \Longrightarrow \quad (E(2) - I_{\mathrm{IR}})\big|_{\mathrm{common}} = 0. \tag{XV.7.50}$$

Here $d = c_2(SU(2)_{\mathrm{diag}})$, and the normal classes on each rank-one sector are pulled back along the same common subgroup. Setting $\ell = 0$ while leaving an independent c gives $3c^2/2 - c(p+h)/4$; that is a different background. Leaving one daughter E_8

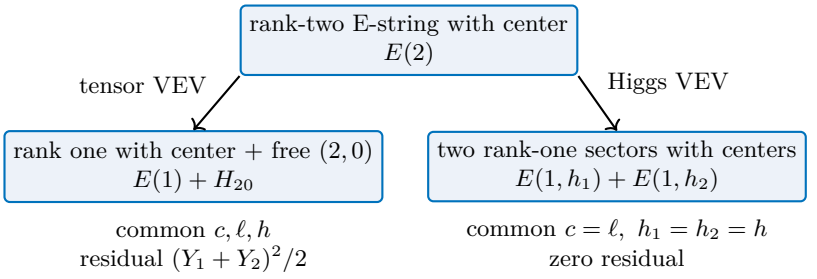


Figure XV.7.5: The same parent with two different comparisons. The tensor direction keeps the original background classes and leaves the shifted source square. The Higgs direction compares the two rank-one sectors on the common diagonal; their separate center hypers are part of the sum. $H_{20} = T + H_L$ is the detached free multiplet.

source off instead gives a mismatch $h^2/32 + hp/16 - dh/4$ on the common normal subgroup. Dropping one center hyper while keeping both flavor sources gives a residual p_2 coefficient $-1/1440$. These comparisons identify precisely which sources or free fields were lost.

Finally, to evaluate the Euler Weyl anomaly a for a six-dimensional $(1,0)$ superconformal sector, turn off flavors and use that sector's own superconformal $c = c_2(R)$. In the normalization in which one free $(2,0)$ tensor has $a = 1$, the polynomial coefficients give

$$I_8\big|_{\text{flavor}=0} = \tfrac{1}{24}(\alpha c^2 + \beta cp + \gamma p^2 + \delta p_2), \qquad a = \frac{16}{7}(\alpha - \beta + \gamma) + \frac{6}{7}\delta. \tag{XV.7.51}$$

For $E(2), E(1), H_{20}$ the coefficient tuples are respectively

$$(62, -17, 7/4, -1), \qquad (13, -11/2, 7/8, -1/2), \qquad (1, 1/2, 1/8, -1/2). \tag{XV.7.52}$$

The tuples follow by setting $\ell = h = 0$ in the polynomials for these sectors and keeping their respective R source. The formula yields $1286/7, 307/7, 1$. The tensor and Higgs endpoints of Figure XV.7.5 then give

$$\Delta a_{\text{tensor}} = \frac{1286}{7} - \frac{307}{7} - 1 = \frac{972}{7}, \qquad \Delta a_{\text{Higgs}} = \frac{1286}{7} - 2\,\frac{307}{7} = 96. \tag{XV.7.53}$$

The tensor calculation also gives the difference directly in terms of the retained source. With the flavor backgrounds off, (XV.7.48) gives $(8c - p)^2/32$. In the convention of (XV.7.51), its coefficient differences are

$$(\Delta\alpha, \Delta\beta, \Delta\gamma, \Delta\delta)_{\text{tensor}} = (48, -12, 3/4, 0). \tag{XV.7.54}$$

This agrees with subtracting the three tuples and explains the sign: the negative mixed coefficient enters a with a minus sign. The shortcut uses the R class preserved on that tensor branch. For Higgs splitting, applying the same shortcut to the common diagonal would give zero because the anomalies match there. The separate superconformal

polynomials instead give $(36,-6,0,0)$ upon subtraction with flavors off. Using the unbroken Higgs diagonal in (XV.7.51) would conflate a common-background identity with a superconformal Ward identity. The values in (XV.7.53) compare the stated endpoints and do not establish a general Higgs-branch monotonicity result.

XV.7.6 The scope of the classification

How much of the exceptional recombination can we determine without first assuming an infrared spectrum? Begin with the pure E_6, E_7 collisions of B.6, whose local equations contain the product uv for the two transverse noncompact flavor divisors. For E_6 the short coefficients are $(0,(uv)^4)$, so at the crossing the orders are $(\infty,8,16)$. For E_7 they are $((uv)^3,0)$, giving $(6,\infty,18)$. Here ∞ denotes the order of an identically zero polynomial. The respective resolutions of the base require the compact chains 131 and 12321. Replace uv in both equations by $w = uv - b$. If $b \neq 0$, the entire discriminant is supported on $w = 0$, where $u \neq 0$ and $v = b/u$. We can use u, w as coordinates near every point of this divisor, since

$$v = (w+b)/u, \qquad du \wedge dw = u\, du \wedge dv. \tag{XV.7.55}$$

Keeping the original Weierstrass trivialization and rewriting only the arguments gives the transverse powers:

$$E_6: \quad (f,g,\Delta) = (0, w^4, 27w^8), \qquad \mathrm{ord}_w = (\infty,4,8), \tag{XV.7.56}$$

$$E_7: \quad (f,g,\Delta) = (w^3, 0, 4w^9), \qquad \mathrm{ord}_w = (3,\infty,9). \tag{XV.7.57}$$

The new anticanonical generator dual to $du \wedge dw$ is u^{-1} times the original one. In that frame f, g, Δ acquire factors u^4, u^6, u^{12}, respectively, since they multiply the corresponding powers of the generator. These are units wherever $u \neq 0$, unlike the exceptional division at a blowup in Section XV.7.3. In the original frame the IV^* cover is $\psi^2 - g/w^4 = \psi^2 - 1$, so the fiber is split and the ordinary algebra is $\mathfrak{e}_6$. In the new frame g/w^4 is multiplied by $u^6 = (u^3)^2$ on the divisor, which preserves the split test. The second is III^* with algebra $\mathfrak{e}_7$. The orders remain minimal along the whole support, including in point ideals, and w is a unit away from it. There is no center requiring a base blowup. The compact base lattice in these local models thus changes rank from three or five to zero. This conclusion concerns base tensor curves, not the resolved fiber curves or the full brane charge lattice.

For $b = 2$ the origin is no longer on the support, and for example the point $(u,v) = (1,2)$ on the support has the minimal transverse orders in (XV.7.56) or (XV.7.57). Compare replacing uv by $(u-2)v$. In coordinates $\widetilde{u} = u - 2, v$ this is the original product. It has two components and retains the original nonminimal orders at $(2,0)$. The control in Figure XV.7.6 distinguishes a moving crossing from the change to one irreducible divisor.

The physical recombination interpretation identifies the two external flavor algebras along their diagonal. As a separate hypothesis, try a free infrared spectrum consisting of one full adjoint hyper and one singlet, without additional normalizable sectors. This is the candidate obtained by applying the adjoint-plus-singlet prescription of the pure

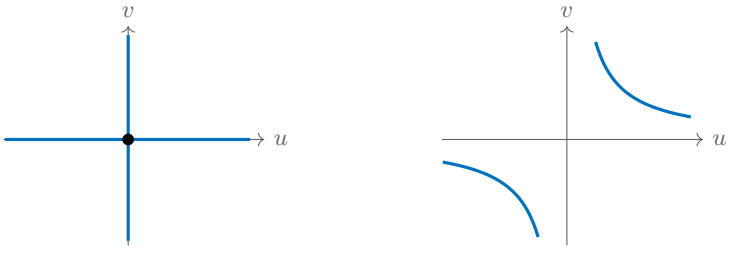


Figure XV.7.6: Real slices of the discriminant supports at $b = 0$ and $b = 2$. The right panel shows two real branches of one smooth complex curve $\mathbb{C}^*$. Its fiber is $IV^{*\mathrm{s}}$ in the E_6 model or III^* in the E_7 model. The two axes on the left meet at a nonminimal point; this is a picture of the base, not a total-space resolution.

E_8 recombination to these two examples. The geometric change does not establish this transfer of spectra. We can test it with the complete diagonal flavor and tangent anomaly, setting $c = 0$ so no identification of an ultraviolet R connection with an infrared one is needed.

Let F be a Cartan element and $h = \mathrm{tr}_{\mathrm{adj}}\, F^2/h^\vee$ the diagonal quadratic trace. To compute the raw adjoint traces, start from the E_8 roots $\pm e_i \pm e_j$ and the half-sums $(\pm e_1 \pm \cdots \pm e_8)/2$ with an even number of minus signs. Use roots orthogonal to $e_7 + e_8$ for E_7, and also to $e_6 + e_7$ for E_6. Corresponding Cartan elements have coordinates $(x_1, \ldots, x_6, z, -z)$ and $(x_1, \ldots, x_5, -z, z, -z)$. The roots wholly supported on the x_i form the D_m integer roots with $m = 6$ or 5; E_7 has an extra pair with weights $\pm 2z$. The half-root sets have 64 or 32 elements, respectively, with tail weights $\pm z$ or $\pm 3z/2$. The parity rule fixes one sign but averages all lower moments of up to four distinct x_i signs to zero.

The count can be done before summing any weights. Orthogonality to $e_7 + e_8$ forces the last two half-root signs to be opposite. For either choice of their order, parity allows 2^5 choices of the first six signs. Orthogonality also to $e_6 + e_7$ fixes one more tail sign for the E_6 roots, leaving 2^4 choices for the first five for each allowed tail. For fixed tail, any assignment to fewer than all of the first signs admits the same number of completions. In particular every monomial of degree at most four in distinct first signs averages just as with independent fair signs. This supplies the moment calculation without assuming from the start that the fourth trace is a multiple of the square of the second.

To perform the sums, put $X_2 = \sum x_i^2$, $X_4 = \sum x_i^4$, $B_4 = \sum_{i<j} x_i^2 x_j^2$. A pair of D_m indices contributes $4(x_i^2 + x_j^2)$ at order two and $4(x_i^4 + x_j^4) + 24 x_i^2 x_j^2$ at order four. With M half-roots whose tail has weight $\pm\lambda z$, their totals are

$$\sum_{\text{half}} (r \cdot F)^2 = M\big(X_2/4 + \lambda^2 z^2\big), \tag{XV.7.58}$$

$$\sum_{\text{half}} (r \cdot F)^4 = M\big((X_4 + 6B_4)/16 + \tfrac{3}{2}\lambda^2 z^2 X_2 + \lambda^4 z^4\big). \tag{XV.7.59}$$

Combining the integer and half-root contributions and adding the zero Cartan weights for the dimension, we obtain

$$\dim E_6 = 40 + 32 + 6 = 78, \qquad \dim E_7 = 60 + 2 + 64 + 7 = 133, \tag{XV.7.60}$$

$$E_6: \quad \mathrm{tr}_{\mathrm{adj}}\, F^2 = 24(X_2 + 3z^2), \qquad \mathrm{tr}_{\mathrm{adj}}\, F^4 = 18(X_2 + 3z^2)^2, \tag{XV.7.61}$$

$$E_7: \quad \mathrm{tr}_{\mathrm{adj}}\, F^2 = 36(X_2 + 2z^2), \qquad \mathrm{tr}_{\mathrm{adj}}\, F^4 = 24(X_2 + 2z^2)^2. \tag{XV.7.62}$$

Since $h^\vee = 12, 18$, the fourth traces are $\frac{9}{2}h^2, 6h^2$. For instance in E_7 take $x_1 = 1, x_2 = 2, z = 1$, others zero. The three quantities $(h, \mathrm{tr}_{\mathrm{adj}}\, F^2, \mathrm{tr}_{\mathrm{adj}}\, F^4) = (14, 252, 1176)$ probe both the integer and half-root weights. Neutral hypers have zero fourth trace in the same direction.

For the proposed adjoint and singlet the tangent and flavor polynomial from the hyper index is

$$I_{\mathrm{cand}} = (\dim + 1)G + \frac{p}{48}\,\mathrm{tr}_{\mathrm{adj}}\, F^2 + \frac{1}{24}\,\mathrm{tr}_{\mathrm{adj}}\, F^4. \tag{XV.7.63}$$

To compare the UV indices, pull both e_L, e_R back to h. In E_6, (XV.7.21) gives $3h^2/16 + hp/4 + 79G$ at $c = 0$. In the pure E_7 index from B.6 the flavor terms at $c = 0$ are $3(e_L^2 + e_R^2)/32 + e_L e_R/16 + 3p(e_L + e_R)/16$; the gravity term is $134G$. The diagonal comparison therefore gives

$$I_{E_6}(h, h)\big|_{c=0} = 79G + \frac{hp}{4} + \frac{3h^2}{16}, \tag{XV.7.64}$$

$$I_{E_7}(h, h)\big|_{c=0} = 134G + \frac{3hp}{8} + \frac{h^2}{4}. \tag{XV.7.65}$$

These are the four coefficients of p^2, p_2, hp, h^2 in each candidate index. The inherited full branch counts give a separate way to obtain the gravity coefficients: the irreducible term counts $H - V + 29n_T$, where H is the hyper dimension counted with half-hyper weights, V is the dimension of the gauge algebra, and n_T is the number of compact tensors. In these examples,

$$E_6: \quad 0 - 8 + 29 \cdot 3 = 79, \qquad E_7: \quad 16 - 27 + 29 \cdot 5 = 134. \tag{XV.7.66}$$

For E_7 the three gauge algebras on the resolved branch are $\mathfrak{su}(2)$, $\mathfrak{so}(7)$, $\mathfrak{su}(2)$, of dimensions $3, 21, 3$. Each neighboring gauge pair supports the specified half-hyper in the doublet times the spinor. Each contributes $(2 \cdot 8)/2 = 8$ to H. Thus the number 134 in (XV.7.66) uses the actual branch matter assignment of B.6 rather than deducing matter from a gravity count.

A candidate consisting of 134 neutral hypers passes the E_7 gravity count but misses both flavor coefficients. An adjoint alone passes the flavor test but misses G. Keeping $e_R = 0$ with $e_L = h$ instead would give

$$I_{E_7}(h, 0)\big|_{c=0} = 134G + \frac{3hp}{16} + \frac{3h^2}{32}. \tag{XV.7.67}$$

The smaller mixed coefficient in particular distinguishes a restriction to one factor from a restriction to the diagonal.

For completeness the residuals outside this comparison are

$$I_{E_6}(h,h) - I_{\text{cand}} = c\left(\tfrac{319}{24}c - 3h - \tfrac{89}{48}p\right), \tag{XV.7.68}$$

$$I_{E_7}(h,h) - I_{\text{cand}} = c\left(\tfrac{835}{12}c - \tfrac{15}{2}h - \tfrac{125}{24}p\right). \tag{XV.7.69}$$

The residual is allowed to contain R terms because the test was only on the tangent and diagonal flavor backgrounds. Under the free spectrum hypothesis, the four coefficients entering the difference of a's come from setting $h = 0$ in (XV.7.69), with the IR hyperfermions neutral under their superconformal R. The p^2, p_2 coefficients cancel, so (XV.7.51) gives

$$\Delta a_{E_6} = \frac{16}{7}\left(319 + \frac{89}{2}\right) = \frac{5816}{7}, \qquad \Delta a_{E_7} = \frac{16}{7}(1670 + 125) = \frac{28720}{7}. \tag{XV.7.70}$$

These numbers are conditional on the candidate being the full infrared spectrum. Neither the anomaly match nor the absence of compact base curves derives that spectrum.

These constructions illustrate the order of a classification argument. One first constrains the contractible bases, then the allowed elliptic decorations and charged sectors for each base. The organization by fission and fusion relates known ordinary constructions: fission first makes a tensor move and then takes a restricted Higgs deformation of the resulting theory. This second step, called a homplex deformation, is specified by a continuous $\mathfrak{su}(2) \to \mathfrak{g}_{\text{flav}}$ or discrete $\Gamma_{\text{ADE}} \to E_8$ homomorphism. Recombination in general need not be a step of this kind. Fusion runs the gauging construction in the other direction: gauge a common flavor algebra on an added tensor, then go to the tensor origin when the geometry allows this limit. The rank screen or cancellation in Section XV.7.2 alone cannot provide the added tensor or its contraction. Within some fixed Higgs families, closure relations between nilpotent orbits organize a partial order of deformations. This is an organization of source-specified families, not a classification of all possible six-dimensional flows. In the examples here a pairing tests a contraction, explicit coefficients locate the change in the geometry, the physical interpretation identifies the VEV, and anomaly matching tests the proposed massless content on the surviving backgrounds. Each step supplies information the preceding one did not determine.

XV.7.7 Exercises

1. **Change the gauge sizes N_1, N_2.** Keep one ordinary full bifundamental and the two -2 curves. Change the gauge sizes (N_1, N_2) from $(4,5)$ to $(4,6)$. Give the required external fundamentals, the ordered quartic coefficients at those counts, and the coefficients if the external counts stay at $(3,6)$. Show that the reducible Green–Schwarz slice is unaffected by this change of gauge sizes. Explain which part of the calculation would be invalid if the ordinary matter locus were replaced by an uncomputed tangency.

2. **Separate or translate.** In the family (XV.7.23) take $b = 3$. At each labeled center calculate the order triple, the derivative of $v^2 - b^2$, and the two transformed

(f, g) pairs in the marked charts $(u, \eta) = (st, t)$ and (a, az). Give the orders at the meeting of each exceptional with strict II^*. Compare with the translated family $g = u^5(v-3)^2$: give the order triple at the unique root and the first t-chart pair there. Explain why the translated example needs a second blowup.

3. **Keep a different tensor area.** Use strict areas $(\varepsilon, 7)$ and effective charge $(1, 3)$ in the exact coincident geometry. Give the total-pullback periods, charge in the total basis, period pairing, and retained self-pairing at the wall. Give the two transformed sources and the coefficient of hp in the retained square. Explain why a negative total-basis charge component need not violate effectiveness.

4. **Account for the free fields.** Use (XV.7.41) to give the coefficients of p_2 and hp, in that order, in the correct tensor mismatch and in the mismatch without the detached half-doublet. On the Higgs side compare the common background, the common normal subgroup with only one daughter E_8 turned on, and the common background with one center omitted. Give the same two coefficients in each difference. Explain why the conformal a comparison does not use $c = \ell$.

5. **Test a proposed exceptional spectrum.** In the E_7 Cartan frame of (XV.7.62), set $x_1 = 2, x_2 = -1, z = 2$, all other $x_i = 0$. Compute the root count, h, the second and fourth adjoint moments, the p_2 coefficient of the adjoint-plus-singlet candidate, and the value of its quartic term on this Cartan element. Give the same two index slots for 134 neutral hypers. Explain which observations this test cannot make about a physical spectrum.

6. **Compare the evidence for flows.** Suppose a change of coefficients smooths the support of a noncompact discriminant and a proposed daughter matches all four diagonal coefficients in (XV.7.65). Explain what each test establishes. Identify the additional physical information needed to turn these tests into evidence for a Higgs flow. Compare with the role of a specified area path and complete detached multiplet on the tensor branch.

For Exercises 1–5, use `benchmark/tasks.json` for the JSON fields and `benchmark/PROTOCOL.md` for submission. Written explanations, including Exercise 6, are assessed by a reader.

Status and sources

§1. What the base records. The base-pairing comparisons are [MATH], using the actual 414 and two-component I_2 objects of B.5. The separate $(0, 0, 9)$ and $(0, 0, 5)$ orders ([MATH]) are inherited from B.4, including its selected split Tate lift and residual mutation. The ordinary matter interpretation uses B.1 and B.4 under the split, transverse and simple-root premises there. No changed tangency spectrum is assigned.

§2. Ordinary and exceptional gauging. The CHAIN45 quartic and Green–Schwarz comparisons and the changed gauge size calculation ([ANOM]) use the integral anomaly normalization of Chapter 3. The two distinct interacting E-string links and the ordinary

index-one restrictions ([GEO-E]) use Ohmori, Shimizu, Tachikawa, and Yonekura (2014), arXiv:1408.5572v2, §3.2.1, eqs. (3.9), (3.10) and (3.15): the first is the coalesced E_6 diagram, the latter two are the embeddings. For the unpaired -1 constraint see Heckman, Morrison, et al. (2015a), arXiv:1502.05405v3, PDF pp. 13–14. The retained pairing and transformed source are derived on the B.6 branch. The two-link polynomial calculation ([ANOM]) uses Ohmori, Shimizu, Tachikawa, and Yonekura (2014), arXiv:1408.5572v2, eq. (3.11) for the retained square and eq. (3.12) for the full E_6 result, along with the inherited ordinary source choice. It compares the full local gauge slice and the eleven displayed independent background monomials.

§3. The partial tensor contraction. The coincident orders, both blowups, reverse chart operation, curve lattice and relative areas are [MATH]; the calculation uses the Weierstrass convention $\Delta_{\text{book}} = 4f^3 + 27g^2$ and the rank-one comparison uses B.6. The wrapped D3 calibration and small-instanton tensor endpoint ([GEO-E]) assume the fixed microscopic frame and an isolated local deep infrared sector. See Heckman, Morrison, et al. (2015b), published §4.1, eqs. (4.1)–(4.3), and Córdova et al. (2016), arXiv:1506.03807v2, §5, eqs. (5.1)–(5.6) and Fig. 2. There is no metric convergence or spectrum of every effective charge claimed by the relative calculation.

§4. Displacing the two centers. The disjoint germs, both charts and the translated control are [MATH]. The physical VEV, the two daughters with their centers, and the common background interpretation ([GEO-E]) use Heckman, Morrison, et al. (2015b), published §4.2.1, eqs. (4.17)–(4.24). The gauged model of eq. (4.24) is a distinct example; its E_8 gauge node is not imported. Normalizability and physical isolation are premises in the local interpretation.

§5. Inflow and endpoint anomalies. The inflow, free subtraction, transformed square, common subgroup comparison and two Weyl-anomaly differences ([ANOM]) use Ohmori, Shimizu, and Tachikawa (2014), eqs. (1.1)–(1.5) and curvature footnote, and Córdova et al. (2016), §2.2, §4 and §5. For the tensor comparison the ten monomials in c, ℓ, p, h of degree eight and the p_2 coefficient are checked; for Higgs splitting the six degree-eight monomials in d, p, h and p_2 are compared on the common subgroup. For a, use CDI eqs. (1.6)–(1.7) in each sector's own superconformal frame; §5 checks the small-instanton values.

§6. Recombination and the scope of the examples. The changed exceptional support, orders, cover and compact base ranks ([MATH]) use the original equations of B.6. The sourced recombination operation ([GEO-E]) uses Del Zotto et al. (2015), arXiv:1407.6359v3, §2.1, and we separately transfer the adjoint-plus-singlet candidate of Heckman, Morrison, et al. (2015b), published §4.2, eq. (4.16). The root moments and four-coefficient diagonal comparison and conditional Weyl differences ([ANOM]) establish neither the infrared representations nor an isolated vacuum. For the scoped organization see Heckman, Rudelius, et al. (2019), §2, §4 and §5. In particular the available operations and classifications concern the theories and deformations specified there.

References

Córdova, C., T. T. Dumitrescu, and K. Intriligator (2016). "Anomalies, Renormalization Group Flows, and the a-Theorem in Six-Dimensional $(1,0)$ Theories". In: *JHEP* 10, p. 080. arXiv: 1506.03807 [hep-th].

Del Zotto, M. et al. (2015). "6d Conformal Matter". In: *JHEP* 02, p. 054. arXiv: 1407.6359 [hep-th].

Heckman, J. J., D. R. Morrison, et al. (2015a). "Atomic Classification of 6D SCFTs". In: *Fortsch. Phys.* 63, pp. 468–530. arXiv: 1502.05405 [hep-th].

Heckman, J. J., D. R. Morrison, et al. (2015b). "Geometry of 6D RG Flows". In: *JHEP* 09, p. 052. arXiv: 1505.00009 [hep-th].

Heckman, J. J., T. Rudelius, and A. Tomasiello (2019). "Fission, Fusion, and 6D RG Flows". In: *JHEP* 02, p. 167. arXiv: 1807.10274 [hep-th].

Ohmori, K., H. Shimizu, and Y. Tachikawa (2014). "Anomaly Polynomial of E-string Theories". In: *JHEP* 08, p. 002. arXiv: 1404.3887 [hep-th].

Ohmori, K., H. Shimizu, Y. Tachikawa, and K. Yonekura (2014). "Anomaly Polynomial of General 6D SCFTs". In: *PTEP* 2014.10, 103B07. arXiv: 1408.5572 [hep-th].

Chapter XV.8

Geometric little string limits and the string scale

XV.8.1 A finite string scale after gravity decouples

Can gravitational coupling go to zero while a wrapped string keeps finite tension? The wrapped D3-branes of Chapter 2 give a way to arrange this. The tension of such a string measures the area of a particular compact curve in the F-theory base. The gravitational coupling measures the volume of the entire internal base. If the compact curves form a fiber over a noncompact complex line of motion, one can stretch the transverse direction while keeping their areas fixed. We will construct two examples: a genus-one fiber that degenerates to a triangle, and a rational fiber that degenerates to an interval of curves. We use the point-contraction criterion of Chapter 5 to see which parts of these configurations can become tensionless independently of the rest.

Let B be a smooth complex base surface and $\pi : B \to D$ a proper map to an open disc, with smooth connected general fiber F_t. In the second example the external coordinate is called ψ instead of t. Over the origin the compact fiber D_0 is reduced; each of its irreducible components C_i occurs once. The disc variable is a coordinate of the F-theory base. The curve F_t is a fiber of π, distinct from the auxiliary elliptic fiber of the Calabi–Yau threefold. Write J_0 for a reference Einstein-frame Kähler form on B and define

$$D_0 = \sum_i C_i, \qquad a_i = \int_{C_i} J_0, \qquad A_D = \int_{F_t} J_0 = \sum_i a_i. \tag{XV.8.1}$$

The last equality integrates the same closed form over a smooth fiber and its specialization as a cycle. In a small family one may sweep the smooth fibers along a path to the central fiber; the limiting cycle counts the components with their multiplicities. In particular, an individual C_i need not be homologous to F_t. It is their sum that can be moved to a nearby value of t.

Choose a smooth positive two-form ω on D, for example the area form of the

complete hyperbolic metric. The two-form is closed by degree. Stretch the disc using

$$J_\lambda = J_0 + \lambda \pi^* \omega, \qquad \lambda \geq 0. \tag{XV.8.2}$$

The pullback is nonnegative on a complex tangent line: it evaluates as the positive area of the image line under $d\pi$, or zero if the image vanishes. This remains true at a critical point. The sum is closed and remains strictly positive because J_0 is positive. On the smooth part of C_i, $d\pi$ kills every tangent vector. It also kills the tangent directions of a regular fiber. Consequently

$$\int_{C_i} J_\lambda = a_i, \qquad \int_{F_t} J_\lambda = A_D. \tag{XV.8.3}$$

This operation changes the metric even on a disc where ω is de Rham exact. There is no need to interpret λ as a compact Kähler modulus.

Take a fixed closed subdisc D' inside D, with the origin in its interior. Its inverse image is compact by properness. In the Kähler volume form there is no term quadratic in the stretch:

$$(\pi^*\omega)^2 = \pi^*(\omega \wedge \omega) = 0, \qquad \tfrac{1}{2} J_\lambda^2 = \tfrac{1}{2} J_0^2 + \lambda J_0 \wedge \pi^* \omega. \tag{XV.8.4}$$

A local product coordinate system on the regular part shows what is integrated in the second term. Wedging with the external area form removes the pieces of J_0 with an external leg. Integrating the remaining vertical two-form first gives $\int_{F_t} J_0$. The exceptional value $t = 0$ is a set of measure zero in the base integral. Hence

$$\int_{\pi^{-1}(D')} J_0 \wedge \pi^* \omega = \int_{D'} \left(\int_{F_t} J_0 \right) \omega = A_D \int_{D'} \omega, \tag{XV.8.5}$$

$$V_\lambda(D') = V_0(D') + \lambda A_D \int_{D'} \omega. \tag{XV.8.6}$$

In particular, it suffices to stretch over a fixed patch to make its volume diverge. Enlarging the cutoff on the already noncompact disc is a different operation. Figure XV.8.1 shows the cutoff within the disc and the fibers it contains.

For a numerical comparison put $V_0(D') = 7$, $A_D = 10$, and $\int_{D'} \omega = 3$ in common units, with λ dimensionless. If an area unit is ℓ^2, the two factors in the product carry ℓ^2 each and V_0 carries ℓ^4. The three choices $\lambda = 1, 4, 20$ give

$$(V_1, V_4, V_{20}) = (37, 127, 607)\ell^4, \qquad \int_{F_t} J_\lambda = 10\ell^2 \quad \text{in all three cases.} \tag{XV.8.7}$$

Scaling the whole Kähler form would also scale the fiber area and the D3 tension. The distinction is visible before any gravitational interpretation: only the second term in (XV.8.2) has vanishing restriction to every compact component.

It is useful to make the competing rescaling explicit. If $\widehat{J}_\rho = \rho J_0$ with $\rho > 0$, the volumes and areas obey

$$\widehat{V}_\rho(D') = \rho^2 V_0(D'), \qquad \int_{F_t} \widehat{J}_\rho = \rho A_D, \qquad \frac{\left(\int_{F_t} \widehat{J}_\rho\right)^2}{\widehat{V}_\rho(D')} = \frac{A_D^2}{V_0(D')}. \tag{XV.8.8}$$

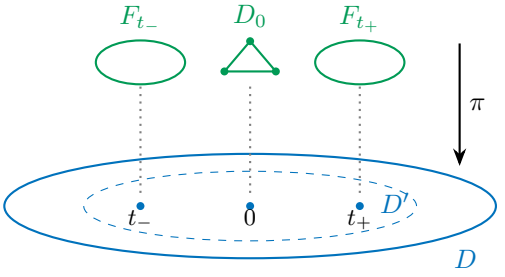


Figure XV.8.1: A proper map to a disc. The central triangle sketches the reducible fiber in the first example; the two ovals represent smooth fibers. The outer contour marks the open disc and the dashed contour is the regulator. At a fixed regulator the stretch raises the transverse area and leaves the area of every displayed fiber unchanged.

By contrast this last ratio for J_λ is $A_D^2/(V_0 + \lambda A_D \int_{D'} \omega)$, which tends to zero. The ratio is dimensionless and tests whether the two geometric measurements can separate. In the numerical example, matching the stretched volume at $\lambda = 20$ by an overall rescaling would require $\rho = \sqrt{607/7}$ and multiply the fiber area by the same factor. Matching the bulk volumes does not match the local theory at a fixed wrapped tension.

To relate this volume to gravity, start from the ten-dimensional Einstein term and retain an internal constant graviton profile. On the regulated unwarped product, the part proportional to the six-dimensional curvature is

$$S_{10,E} = \frac{1}{2\kappa_{10,E}^2} \int d^{10}x \sqrt{|g_{10,E}|}\, R_{10,E}, \tag{XV.8.9}$$

$$S_{6,\mathrm{red}} = \frac{V_\lambda(D')}{2\kappa_{10,E}^2} \int d^{6}x \sqrt{|g_{6,E}|}\, R_{6,E}, \tag{XV.8.10}$$

$$M_{6,\mathrm{red}}^4 = \frac{V_\lambda(D')}{\kappa_{10,E}^2}. \tag{XV.8.11}$$

The length dimension of $\kappa_{10,E}^2$ is eight, so the coefficient has the correct inverse fourth power of length. At fixed microscopic units this Einstein coefficient diverges as λ grows. The kinetic norm of a constant profile grows with the same volume. A canonically normalized constant mode therefore carries a factor proportional to $V_\lambda^{-1/2}$ in its coupling to a fixed local source in this reduction. Meanwhile a calibrated D3 wrapping the full base fiber has leading tension

$$T_{F_t} = \tau_3 \int_{F_t} J_\lambda = \tau_3 A_D, \tag{XV.8.12}$$

where τ_3 is the Einstein-frame D3 tension.

The regulated unwarped estimate tests the uniform gravitational mode. A localized state can still couple to nonconstant modes of the bulk, whose norm and overlap depend on their profiles and the actual background. The calculation neither gives that

background nor controls the continuum at the noncompact end. The little string theory (LST) interpretation below uses the rigid brane construction, in which the interacting local sector is taken with the appropriate bulk-decoupling conditions. In that setting the finite tension in (XV.8.12) is an intrinsic scale. The ultraviolet theory retains extended strings, although sufficiently low energy can admit a description in local field theory. The next step is to realize the compact fiber by equations and determine its charge pairing.

XV.8.2 From a negative-definite to a semidefinite pairing

Where does a corank-one string pairing come from in a smooth base? We construct it by resolving a degeneration, so that the proper transform and each exceptional curve can be counted separately. Take the projective Weierstrass surface over $|t|<1$ whose affine equation is

$$y^2 = x^3 - 3x + 2 + t^3, \qquad \Delta = 4f^3 + 27g^2 = 27t^3(4+t^3), \qquad c_4 = -48f = 144. \tag{XV.8.13}$$

The other discriminant roots have $|t|^3 = 4$ and lie outside the disc. In homogeneous cubic coordinates $[X:Y:Z]$, the infinity section is $[0:1:0]$. On $Y=1$, put $\xi = X/Y$ and $\zeta = Z/Y$. The equation and the derivative there are

$$\zeta - \xi^3 - f\xi\zeta^2 - g\zeta^3 = 0, \qquad \partial_\zeta(\zeta - \xi^3 - f\xi\zeta^2 - g\zeta^3)\big|_{(0,0)} = 1. \tag{XV.8.14}$$

Thus the section survives the resolution away from its center. At $t=0$ the right-hand side of (XV.8.13) is $(x-1)^2(x+2)$. Near $(x,y)=(1,0)$ the two tangent directions are $y = \pm\sqrt{3}(x-1)$. Globally the cubic is irreducible: $x+2$ prevents the polynomial from being a square. Its normalization is rational, as is also seen by parametrizing the cubic by $y/(x-1)$ away from the node.

Choose the local analytic branch $h = (x-1)\sqrt{x+2}$. Since $h'(1) = \sqrt{3}$, the following change has nonzero Jacobian in the transverse variables:

$$U = y - h, \qquad V = y + h, \qquad UV = t^3. \tag{XV.8.15}$$

The gradient of $UV - t^3$ vanishes only at the origin. This is the single total-space singularity. In its point blowup, start with the chart in which t supplies the exceptional factor. Then use the chart in which U supplies it:

$$U = tu, \quad V = tv: \qquad uv = t, \tag{XV.8.16}$$

$$t = Ur, \quad V = Up: \qquad p = Ur^3, \qquad t = Ur. \tag{XV.8.17}$$

In the first line u, v are coordinates on the resolved surface. The exceptional locus $t=0$ consists of $u=0$ and $v=0$ and they meet once at $(u,v)=(0,0)$. In the second line the surface has coordinates U, r. The two loci $U=0$ and $r=0$ are, respectively, one exceptional component and a proper branch of the old nodal cubic. They meet transversely at $(U,r)=(0,0)$. The third chart is

$$t = Vs, \quad U = V\widetilde{p}: \qquad \widetilde{p} = Vs^3, \qquad t = Vs. \tag{XV.8.18}$$

The proper branch there is $s = 0$ and its intersection with $V = 0$ is also transverse.

One can see how the affine pieces make complete curves without relying on the diagram. On the overlap of the U and t charts, $r = t/U$ is nonzero and the same point has

$$u = \frac{1}{r}, \qquad v = \frac{V}{t} = Ur^2. \tag{XV.8.19}$$

Thus the line $U = 0$ on the U chart and the line $v = 0$ on the central chart patch by reciprocal coordinates. The point $r = 0$ is present only in the U chart and the point $u = 0$ on this line is the mutual exceptional intersection. On the other line the analogous transition is $v = 1/s$, $u = Vs^2$. The U-chart and V-chart proper branches do not glue through the exceptional. Instead they glue in the original cubic away from the node. For $x \neq 1$, writing $\xi = y/(x-1)$ there gives

$$x = \xi^2 - 2, \qquad y = \xi(\xi^2 - 3), \qquad \xi_{\text{node}} = \pm\sqrt{3}. \tag{XV.8.20}$$

The two values of ξ give the two different preimages of the node; $\xi = \infty$ adds the smooth point at infinity. This accounts for why the global incidence closes into a triangle even though the two proper branches are separate in the local resolution.

The projective exceptional directions $[U : V : t]$ distinguish all three intersections. The exceptional components C_1, C_2 are the lines $[U : 0 : t]$ and $[0 : V : t]$ of the projectivized tangent cone. Their mutual intersection is $[0 : 0 : 1]$. The proper cubic C_0 meets them at $[1 : 0 : 0]$ and $[0 : 1 : 0]$, respectively. Each C_i is rational; on C_0 the two proper branches of the node now lie at different points of its normalization. All multiplicities are one because t is locally a product of two coordinates at each meeting and vanishes to order one along either coordinate axis. The incidence in Figure XV.8.2 comes from these three distinct points.

Exceptional directions

U chart : $[1 : 0 : 0]$

t chart : $[0 : 0 : 1]$

V chart : $[0 : 1 : 0]$

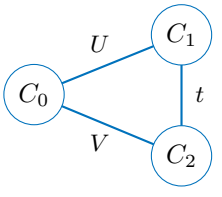


Figure XV.8.2: The three I_3 nodes in their exceptional direction charts (left). Each triangle edge at right records one of the three transverse intersections. The vertex C_0 denotes the entire proper cubic, joining the two proper branches visible in the local charts.

For a self-intersection calculation, intersect each component with a smooth fiber F_t that misses it. Specializing F_t to D_0, the same intersection number becomes a sum of the self-intersection and the two neighboring intersections. Thus in the ordered basis (C_0, C_1, C_2),

$$0 = F_t \cdot C_i = C_i^2 + 1 + 1, \qquad Q = (C_i \cdot C_j) = \begin{pmatrix} -2 & 1 & 1 \\ 1 & -2 & 1 \\ 1 & 1 & -2 \end{pmatrix}, \qquad A = -Q. \tag{XV.8.21}$$

We use A for the positive-sign string pairing. On an ordered column q of coefficients,

$$q^t A q = (q_0 - q_1)^2 + (q_1 - q_2)^2 + (q_2 - q_0)^2. \tag{XV.8.22}$$

Any nonconstant column has positive pairing with itself. The full fiber column $(1,1,1)^t$ spans the null space. A negative-definite set could not have a nonzero such direction. Here it occurs because every member of the reducible fiber is disjoint from a nearby representative of the full fiber class.

We also need a holomorphic two-form on the resolved surface. The residue of the Weierstrass equation gives $dx \wedge dt/(2y)$ away from the zero of the displayed denominator. Near the singular point the analytic change of variables takes it to a unit times $dU \wedge dt/U$, up to orientation. Use $t = uv$ and $U = tu$ in the first chart to compute

$$\frac{dU \wedge dt}{U} = \frac{du}{u} \wedge dt = du \wedge dv. \tag{XV.8.23}$$

In the U chart $dt = r\,dU + U\,dr$, so the same residue is $dU \wedge dr$. In the V chart $dU/U = 3\,dt/t - dV/V$ away from the coordinate divisors. Hence it is $-dV \wedge ds$ there. All three expressions extend as nonvanishing holomorphic forms. Away from the resolution center, the surface residue can be written with any nonzero equation derivative. It extends at the regular section by adjunction for the projective cubic in the trivial projective bundle over the disc. The resolution S therefore has trivial canonical bundle. Its reduced nodal triangle is a split I_3 fiber.

Now take the fixed smooth elliptic curve $E : y_E^2 = x_E^3 - x_E$ with section at infinity. The product is a smooth local Calabi–Yau threefold with nowhere-vanishing form given by the product of the two residue forms. The two maps of interest are

$$E \times S \longrightarrow S, \quad (e, s_0) \longmapsto s_0, \qquad E \times S \longrightarrow E \times D, \quad (e, s_0) \longmapsto (e, t(s_0)). \tag{XV.8.24}$$

In the first map, E is smooth over every point. Thus there is no seven-brane gauge decoration on C_0, C_1, C_2. The second map has a split I_3 fiber over $E \times \{0\}$. We keep the first map for the physical construction in this chapter; the second supplies a geometric input for the later comparison of circle reductions.

The charts give a sensitive comparison if t^3 is replaced by t^2 in the Weierstrass equation. The nodal cubic at zero is unchanged, but now $UV = t^2$. The central chart is $uv = 1$, so there is no central meeting of two exceptional lines. The exceptional conic $UV = t^2$ in the direction plane is smooth. On the U chart $p = r^2$ with $t = Ur$, and on the V chart $\widetilde{p} = s^2$ with $t = Vs$. The same single exceptional curve meets the two proper branches at $[1:0:0]$ and $[0:1:0]$, which are distinct points. The reduced I_2 fiber gives

$$Q_{I_2} = \begin{pmatrix} -2 & 2 \\ 2 & -2 \end{pmatrix}, \qquad q^t(-Q_{I_2})q = 2(q_0 - q_1)^2. \tag{XV.8.25}$$

The transition also explains why the changed model has only one exceptional curve. In the overlap $r = 1/u$ and $p = r^2$. The exceptional part with $U = 0, r \neq 0$ maps to the $uv = 1$ locus, where u is invertible and $v = 1/u$. In the V chart the coordinate $s = 1/v$ gives the other end of this same locus. The two points where an exceptional

coordinate vanishes on the outer charts compactify it to a conic. They each meet one proper branch, in contrast to the separate exceptional lines of the I_3 chart.

The entry 2 counts two local intersections of multiplicity one. A single edge of multiplicity one with diagonal entries -2 would instead give the negative-definite matrix of a point-contractible pair. Here the geometry has changed by changing the polynomial; deleting a vertex from the triangle would retain the latter single-edge intersection. The actual changed object retains a whole fiber and a null direction. We now identify the string carried by that direction.

XV.8.3 The null charge and its wrapped string

Why can a charge in the radical have strictly positive tension? The pairing and the tension are different measurements of the same wrapped curve. For an ordered integer column q, write $[C_q] = \sum_i q_i [C_i]$. Signed coefficients are useful for the lattice. For tension examples we take $q_i \geq 0$ and use the calibrated effective cycle. In the product geometry the primitive column δ represents the full fiber:

$$\delta = (1,1,1)^t, \qquad [C_\delta] = [F_t], \qquad Q\delta = 0. \tag{XV.8.26}$$

The entries have greatest common divisor one. There is no relation setting this column to zero in homology: its period against the closed Kähler form is $A_D > 0$. The vanishing of $Q\delta$ says that the cycle has zero intersection with all the compact components in our lattice.

The D3 worldvolume occupies two spacetime directions and wraps a holomorphic curve in B. The restriction of the Einstein-frame Kähler form to the curve is its area form. To leading calibrated order with no worldvolume flux, the tension per unit spacetime string length is the D3 tension times the internal area:

$$\tau_3 = \frac{1}{(2\pi)^3 \alpha'^2}, \qquad T(q) = \tau_3 \int_{C_q} J_E = \tau_3 q^t a, \tag{XV.8.27}$$

$$M_{\mathrm{LST}}^2 := T(\delta) = \tau_3 A_D. \tag{XV.8.28}$$

Here a is the column of Einstein areas and J_E can be any J_λ in (XV.8.2). Since $[\alpha'] = \text{length}^2$, τ_3 is an inverse fourth power of length, and multiplying by area gives a mass squared. With the scalar convention $g_{8,E}^2 = 2(2\pi)^5 \alpha'^2$ and $\phi_i = a_i / g_{8,E}^2$, the same formula reads

$$T(q) = \tau_3 g_{8,E}^2 q^t \phi = 8\pi^2 q^t \phi. \tag{XV.8.29}$$

We use M_{LST}^2 to name this tension, without assigning a numerical oscillator gap. The full fiber here is a curve in S. In the product frame it is this base curve that the D3 wraps. The auxiliary elliptic curve E does not enter its wrapped area.

The periods a_i must come from a Kähler form. To see which positive rational partitions can be prescribed, use the infinity section S_∞ as a reference divisor of degree one on F_t. This section meets C_0 once and is disjoint from C_1, C_2. Consider the rational divisor class

$$L = A_D S_\infty + b_1 C_1 + b_2 C_2. \tag{XV.8.30}$$

We measure areas in a common unit, so the coefficients denote dimensionless degrees in this equation. The intersections in (XV.8.21) give

$$\begin{pmatrix} L\cdot C_0 \\ L\cdot C_1 \\ L\cdot C_2 \end{pmatrix} = \begin{pmatrix} A_D + b_1 + b_2 \\ -2b_1 + b_2 \\ b_1 - 2b_2 \end{pmatrix}, \qquad L\cdot F_t = A_D. \tag{XV.8.31}$$

The component contributions from b_1, b_2 add to zero. Thus these two coefficients redistribute area at fixed total. To give prescribed a_1, a_2, solve the last two rows:

$$b_1 = -\frac{2a_1 + a_2}{3}, \qquad b_2 = -\frac{a_1 + 2a_2}{3}, \qquad a_0 = A_D - a_1 - a_2. \tag{XV.8.32}$$

The minus signs follow from the negative intersection of each exceptional curve with itself. A negative coefficient in L therefore need not give a negative period.

If all three areas are positive and rational, multiply L by a common denominator to get an integral relative polarization. A line bundle of positive degree on each component of every proper curve fiber is relatively ample. In our disc all other fibers are irreducible and have positive degree A_D. After restriction to a smaller disc, a sufficiently high power gives a relative projective embedding. Pull back the projective Kähler form, rescale it to the desired degrees, and add a positive form from the disc to obtain a reference Kähler form. This establishes the chosen periods in the local family; it does not require a description of a compact completion's Kähler cone.

For example, compare two ordered partitions at total area ten. The required coefficients, read by (XV.8.32), are

(a_0, a_1, a_2)	b_1	b_2
$(2, 3, 5)$	$-11/3$	$-13/3$
$(1, 4, 5)$	$-13/3$	$-14/3$

(XV.8.33)

Moving one unit from C_0 to C_1 increases the C_1 tension by τ_3 in these units and leaves the full-fiber tension unchanged. Figure XV.8.3 represents the first partition. The lengths in its bar encode areas; they do not represent intersection numbers.

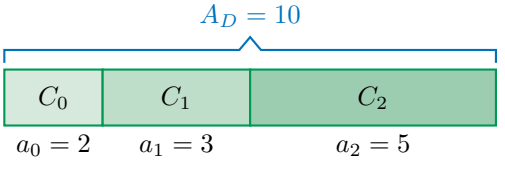


Figure XV.8.3: The ordered area partition $(2, 3, 5)$ of the base fiber $D_0 = C_0 + C_1 + C_2$. The upper brace marks the cycle used for the whole-fiber D3 tension, while the lower marks show the component periods.

The reference-class calculation can also be run in the forward direction. At fixed total, the shift from the first to the second row is $(\Delta b_1, \Delta b_2) = (-2/3, -1/3)$. Its period variation follows directly by intersecting the divisor difference:

$$\left(-\tfrac{2}{3}C_1 - \tfrac{1}{3}C_2\right)\cdot(C_0, C_1, C_2) = (-1, 1, 0). \tag{XV.8.34}$$

Changing b_1 alone would also change the period on C_2. The two coefficients must be solved together if a_2 is to stay fixed. Because the section has degree one on a smooth fiber and the two exceptional curves are disjoint from a regular fiber, the same difference has zero pairing with that class.

In the first partition, the two effective cycles with columns $q = (1, 2, 0)^t$ and $q + \delta = (2, 3, 1)^t$ have

$$T(q)/\tau_3 = 2 + 2(3) = 8, \tag{XV.8.35}$$

$$T(q + \delta)/\tau_3 = 2(2) + 3(3) + 5 = 18, \tag{XV.8.36}$$

$$(q + \delta)^t A(q + \delta) = q^t A q = 6. \tag{XV.8.37}$$

The tension difference is exactly the tension of the added fiber. The formula assigns the calibrated area to an effective configuration and does not count single-string bound states. In the rigid product construction the full-fiber D3 is the little string, and the S-base model realizes the gauge-free $(2, 0)$ affine A_2 LST. This identification uses the ordinary rigid background described above. The same algebra would assign a radical to any matrix of the same shape; it would not supply the physical construction. We next determine precisely which data that algebra retains.

XV.8.4 Dynamical and nondynamical tensor directions

Which variables can vary at fixed string scale, and which charge data determine tensor pairings? In Chapter 2 the tensor fields came from reducing the four-form on internal two-forms. In a noncompact construction the corresponding fluctuations are dynamical only when the internal modes obey the required boundary conditions and have finite kinetic norms. The pairing calculation below characterizes the candidate local charge sector in the ordinary rigid construction. It does not determine the norms of the modes or the full kinetic metric.

First let $n_i > 0$ be the multiplicities in a connected compact fiber, so $Qn = 0$. Use the off-diagonal intersections Q_{ij} to eliminate the diagonal by $Q_{ii} n_i = -\sum_{j \neq i} Q_{ij} n_j$. Combining the contributions of each unordered pair to $q^t(-Q)q$ gives

$$\begin{aligned} q^t A q &= \sum_{i<j} Q_{ij} \left(\frac{n_j}{n_i} q_i^2 - 2 q_i q_j + \frac{n_i}{n_j} q_j^2 \right) \\ &= \sum_{i<j} Q_{ij} n_i n_j \left(\frac{q_i}{n_i} - \frac{q_j}{n_j} \right)^2 . \end{aligned} \tag{XV.8.38}$$

Every intersection between distinct components of a smooth surface is nonnegative. The form vanishes only when the ratios agree across every edge. Connectedness then makes them all equal. In the two examples all $n_i = 1$, and for N components the integral radical is $\mathbb{Z}\delta$ with $\delta = (1, \ldots, 1)^t$.

To coordinatize the quotient $\mathbb{Z}^N/\mathbb{Z}\delta$, choose the last component as reference and put

$$Pq = (q_1 - q_N, \ldots, q_{N-1} - q_N)^t \tag{XV.8.39}$$

using labels $1, \dots, N$ here for the ordered positions. Every quotient class has a unique representative with last entry zero, obtained by subtracting $q_N \delta$. Every integer column of length $N-1$ occurs. Write $\iota p = (p, 0)^t$ and let M be the leading principal block of A. Then $q = \iota P q + q_N \delta$, so for all q, q'

$$q^t A q' = (Pq)^t M (Pq'), \qquad A = P^t M P. \tag{XV.8.40}$$

Since a nonzero ιp cannot lie in the radical, M is positive definite. This calculation removes the radical from the bilinear form without inverting a singular matrix.

For the triangle return to labels $0, 1, 2$ and take C_2 as reference. For the three-component chain constructed in Section XV.8.6, order the components from its left flavor end and again take the last one as reference. The two quotient matrices are

$$M_{I_3} = \begin{pmatrix} 2 & -1 \\ -1 & 2 \end{pmatrix}, \qquad M_{121} = \begin{pmatrix} 1 & -1 \\ -1 & 2 \end{pmatrix}, \qquad (\det M_{I_3}, \det M_{121}) = (3, 1). \tag{XV.8.41}$$

The notation 121 records the magnitudes of the three compact self-intersections. It gives two independent differences, as the triangle does, but the determinants show that the integral pairings differ. Choosing a different reference on the same triangle gives the same determinant. For instance reference C_0 gives coordinates $(q_1 - q_0, q_2 - q_0) = (p_2 - p_1, -p_1)$ for $p = (q_0 - q_2, q_1 - q_2)$. This coordinate change has determinant one and preserves the finite A_2 form. For the two-component chain the block is simply (1).

It matters which object is deleted when using a principal block. Algebraically, the omitted coefficient has been removed by choosing a representative of a class, not by discarding a component of the geometric fiber. For example the triangle charge $(0, 0, 1)^t$ has representative $(-1, -1, 0)^t$; in the quotient it is the negative sum of the other two basis charges. Its pairings with the C_0 and C_1 basis charges are both -1:

$$M_{I_3} \begin{pmatrix} -1 \\ -1 \end{pmatrix} = \begin{pmatrix} -1 \\ -1 \end{pmatrix}. \tag{XV.8.42}$$

The representative need not be effective even if the original cycle is effective. Its signed coefficients are legitimate for evaluating the bilinear form but cannot be substituted for a wrapped effective configuration when computing the absolute tension.

Now treat the areas as variables. Since $A_D = \delta^t a$, their variation at fixed scale satisfies

$$\delta^t da = 0, \qquad da = P^t \eta = (\eta_1, \dots, \eta_{N-1}, -\textstyle\sum_i \eta_i)^t. \tag{XV.8.43}$$

The real image of Q is this same hyperplane because Q is symmetric with one-dimensional kernel. Equation (XV.8.43) describes a tangent in period coordinates. The two descriptions are dual in the sense that

$$q^t da = (Pq)^t \eta. \tag{XV.8.44}$$

The variation of tension pairs with a quotient charge, whereas the absolute tension in (XV.8.27) pairs with the full charge. In the example of (XV.8.37), shifting by δ leaves Pq fixed at $(1, 2)$ but adds $10\tau_3$ to T. There is no contradiction: the added tension is constant along the fixed-scale slice.

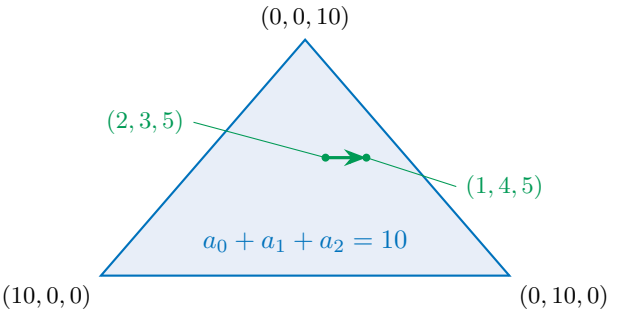


Figure XV.8.4: The fixed-total-area simplex for the triangle. The vertices have all the area on one component and are boundary configurations. The arrow at $(2, 3, 5)$ redistributes area from C_0 to C_1, giving $(1, 4, 5)$ at the same A_D. Its tangent is $(-1, 1, 0)$ in the period coordinates.

There is a geometric reason why a localized deformation cannot change the full-fiber area. Suppose da comes from a closed variation d_J of the Kähler form with compact support in B. The image of the support under π is compact in the open disc. Choose a regular t_* outside that image. Then

$$\delta^t da = \int_{D_0} d_J = \int_{F_{t_*}} d_J = 0. \tag{XV.8.45}$$

Here d_J denotes a variation of the form, not its exterior derivative. Compact support is a sufficient condition for the displayed period identity. Determining which fluctuations are normalizable requires the actual noncompact geometry and its boundary conditions. In the local tensor interpretation the positive quotient is the pairing of the dynamical sector and the null combination is fixed background data. The full-fiber string still exists at that background value. The geometry of Figure XV.8.4 now makes a further question possible: which subset can shrink while that value stays nonzero?

XV.8.5 Comparing an SCFT limit with an LST limit

When can tensionless strings appear while the theory keeps its little string scale? The distinction is between shrinking a set of components to a point and fixing the area of the complete fiber. For a connected fiber as above, take a proper subset of its components and extend a nonzero vector x on that subset by zero to the full column $\widetilde{x}$. Write A_{sub} for the principal block. Then

$$x^t A_{\mathrm{sub}} x = \widetilde{x}^t A \widetilde{x} > 0. \tag{XV.8.46}$$

Indeed, equality in (XV.8.38) would make $\widetilde{x}$ a multiple of the positive multiplicity column, but one of its entries is zero. Thus the selected compact intersection matrix is negative definite. The same argument fails for the full set because there is no removed entry.

For the triangle choose the two exceptional components, keeping C_0 outside the selected set. Their intersection block and the area path at fixed total are

$$Q_{\mathrm{sub}} = \begin{pmatrix} -2 & 1 \\ 1 & -2 \end{pmatrix}, \qquad a(\epsilon) = (10 - 3\epsilon, \epsilon, 2\epsilon)^t, \qquad 0 < \epsilon < 10/3. \tag{XV.8.47}$$

The path lies inside the positive chamber. For positive rational ϵ the periods are realized by (XV.8.32); one can also interpolate the positive reference forms for interior real points. Along this path the two exceptional coefficients are $b_1 = -4\epsilon/3$ and $b_2 = -5\epsilon/3$. Their collapse leaves the positive area from the section term in L. At leading calibrated order,

$$(T(C_1), T(C_2), T(\delta)) = \tau_3(\epsilon, 2\epsilon, 10). \tag{XV.8.48}$$

The first two tensions vanish as $\epsilon \to 0$, but the little string still has finite tension.

For a concrete comparison on the fixed-scale path, take $\epsilon = 1/2$ and $1/10$ in the chosen area unit. The corresponding ordered triples and the tension ratio for the exceptional pair are

$$\begin{gathered} a(1/2) = (17/2, 1/2, 1)^t, \qquad a(1/10) = (97/10, 1/10, 1/5)^t, \\ \frac{T(C_1 + C_2)}{T(\delta)} = \frac{3\epsilon}{10}. \end{gathered} \tag{XV.8.49}$$

The ratio falls from $3/20$ to $3/100$. This measures the hierarchy of calibrated scales but does not establish that the light sector is isolated. Even after the two exceptional areas vanish, the surviving component still meets the locus where they contract.

In this example there is an actual analytic contraction of precisely the two exceptional components. The blowup map gives, in the central chart (XV.8.16) and the U chart (XV.8.17),

$$(u, v) \longmapsto (U, V, t) = (u^2 v, uv^2, uv), \tag{XV.8.50}$$

$$(U, r) \longmapsto (U, V, t) = (U, U^2 r^3, Ur). \tag{XV.8.51}$$

Both images satisfy $UV = t^3$. The corresponding V chart exchanges the first two coordinates. In the central chart $uv = 0$ maps to the origin. In the U chart the exceptional component $U = 0$ maps to the origin, but the proper branch $r = 0$ maps to $(U, 0, 0)$ and survives away from its meeting point. Similarly the proper branch in the V chart maps to $(0, V, 0)$. Outside the origin the blowup is an isomorphism. This proves that the exceptional pair contracts inside the local germ while the proper cubic, viewed globally in the fiber, is not contracted by that map.

Analytic contractibility provides the local geometry required for the corresponding point-limit construction. Under the ordinary physical decoupling assumptions, an isolated tensionless point-contracted sector can give an SCFT. The contraction map alone supplies neither its isolation from other modes nor an identification of the entire fixed-scale theory with that SCFT. In the point-contraction construction the special limit uses zero areas for the contracted curves, as distinct from the positive-area tensor branch obtained by supplying a reference Kähler form. The limit in (XV.8.47) approaches a possible point-contracted subsector while holding the whole-fiber scale fixed.

The intersection criterion and the map answer different parts of the contraction question. Negative definiteness of the pair is the local analytic contractibility criterion for this compact curve configuration. The explicit blowup map gives a specific target, with the A_2 hypersurface equation $UV = t^3$. Neither argument makes the full special fiber a point-contractible set: the normal intersection of that set is degenerate, and the displayed map sends the proper branches to the two coordinate axes instead of to the origin. This is why deleting a row to compute a positive pairing, as in Section XV.8.4, is not itself a choice of a physical limit.

A different path keeps the same two small areas but shrinks the remaining component as well:

$$a_{\mathrm{all}}(\epsilon) = (3\epsilon, \epsilon, 2\epsilon)^t, \qquad T_{\mathrm{all}}(\delta) = 6\tau_3\epsilon. \tag{XV.8.52}$$

Now the little string scale is going to zero, so this is not a path within the given fixed-scale LST family. Nor does it give a negative-definite full intersection matrix or an analytic point contraction of the entire fiber. Tensionlessness alone is insufficient to infer a whole-theory SCFT. Figure XV.8.5 distinguishes the two paths in area space.

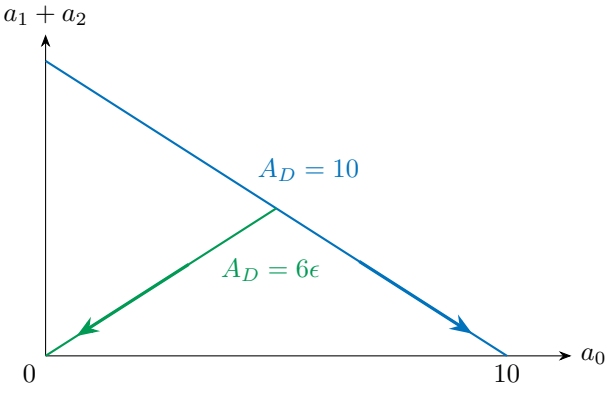


Figure XV.8.5: The two limits projected to the $(a_0, a_1 + a_2)$ plane, with $a_2 = 2a_1$ on both paths. The fixed-scale path approaches $(10, 0)$ on the line $A_D = 10$. The all-shrink path approaches the origin and changes the total area.

One can instead make C_0 heavy in the area calculation, for instance by taking $a_0 = R$ at fixed $\epsilon > 0$:

$$T(C_0) = \tau_3 R, \qquad T(\delta) = \tau_3(R + 3\epsilon) \xrightarrow{R\to\infty} \infty. \tag{XV.8.53}$$

This comparison separates the cost of wrapping the outside component from the costs of wrapping the exceptional pair. It takes the whole-fiber scale to infinity, unlike the fixed-total path. To extract a physically isolated sector one still needs the appropriate boundary and decoupling conditions. Having distinguished these limits on the affine model, we can ask how the same fixed-scale mechanism is realized on a base with rational general fiber and noncompact flavor divisors.

XV.8.6 Geometric existence beyond the lattice

What must a rational-fiber chain satisfy beyond reproducing a null matrix? Its compact curves must occur together in an actual base. A Weierstrass equation over that base must realize the desired boundary divisors without leaving unwanted nonminimal points. Both checks matter: moving a blowup center can preserve the compact intersection matrix and spoil the Weierstrass construction. We will see this directly in a two-step resolution and repeat the calculation with a changed exponent that requires only one step.

Start from $B_0 = \mathbb{P}^1_{[\sigma:\tau]} \times D_\psi$. The canonical bundle of the disc is trivial and $K_{\mathbb{P}^1} = \mathcal{O}(-2)$. Therefore $-4K_{B_0}$ and $-6K_{B_0}$ have degrees eight and twelve along $\mathbb{P}^1$. In the exact interval family we take

$$f = -3\sigma^4\tau^4, \tag{XV.8.54}$$

$$g = \psi^m\sigma^5\tau^7 + \sigma^6\tau^6 + \sigma^7\tau^5, \qquad m = 2 \text{ or } 1. \tag{XV.8.55}$$

The coefficient ψ^m is a holomorphic function on the disc and does not alter the homogeneous degrees. In the two affine trivializations the coefficients read

$$z = \sigma/\tau: \qquad (f, g) = \big(-3z^4, z^5(\psi^m + z + z^2)\big), \tag{XV.8.56}$$

$$w = \tau/\sigma: \qquad (f, g) = \big(-3w^4, w^5(1 + w + \psi^m w^2)\big). \tag{XV.8.57}$$

Away from $z = 0$ and $w = 0$ the coefficient f is nonzero. Along $w = 0$ the factor multiplying w^5 is a unit, including at $\psi = 0$. At $z = 0$ it is a unit when $\psi \neq 0$, but not at the origin. At the left origin, the lowest degree of f in (z, ψ) is four, and the z^6 term in g guarantees degree six for both $m = 1$ and $m = 2$. This is the only nonminimal point on the initial small neighborhood.

The blowup of a smooth surface point has exceptional curve E_{exc} and projection p. Its canonical divisor is

$$K_{B'} = p^*K_B + E_{\text{exc}}. \tag{XV.8.58}$$

To express the new coefficients as sections of $-4K_{B'}$ and $-6K_{B'}$, divide their pullbacks by e^4 and e^6, with $e = 0$ the local exceptional equation. These divisions are regular at a center of point orders at least $(4, 6)$. In Weierstrass coordinates this is the change $x = e^2x'$, $y = e^3y'$. In the residue $dx \wedge dz \wedge d\psi/(2y)$ the dx terms proportional to de wedge to zero against the pulled-back base two-form. The remaining relative factor is e^{-1}. For example, in $z = ez_1, \psi = e$ the base wedge has one factor of e, so the factors cancel. The other chart gives the same cancellation up to orientation. This explains crepancy at the level of the base blowup and normalized Weierstrass form. The ordinary fiber resolution over the flavor divisors is a separate operation.

For the first blowup use $z = \psi z_1$ on the chart containing the strict left section. The chart at the other end of the exceptional uses $z = e, \psi = ev$. Divide by the exceptional powers in each chart to get

$$z = \psi z_1: \qquad (f_1, g_1) = \big(-3z_1^4, z_1^5(\psi^{m-1} + z_1 + \psi z_1^2)\big), \tag{XV.8.59}$$

$$z = e, \quad \psi = ev: \qquad (f_1', g_1') = \big(-3, 1 + e + e^{m-1}v^m\big). \tag{XV.8.60}$$

The primed chart has unit f_1', so it has no nonminimal point. At $(\psi, z_1) = (0,0)$ on the first chart, the orders are $(4,6)$ when $m = 2$, since the bracket starts with $\psi + z_1$. For $m = 1$ they are $(4,5)$, since the bracket starts with one. Thus the number of required blowups is already distinguished by a point-order calculation, although both initial centers had the same orders.

For $m = 2$, blow up the continuing point. Use $z_1 = \psi z_2$ on the continuing chart and $z_1 = e, \psi = ev$ on the other chart, reusing the local symbols e, v for this step. The normalized coefficients are

$$z_1 = \psi z_2 : \qquad (f_2, g_2) = \big(-3z_2^4, z_2^5(1 + z_2 + \psi^2 z_2^2)\big), \tag{XV.8.61}$$

$$z_1 = e, \quad \psi = ev : \qquad (f_2', g_2') = \big(-3, 1 + v + e^2 v\big). \tag{XV.8.62}$$

Now the continuing point has orders $(4,5)$ and the other chart again has unit f_2'.

The same transformations can be organized by a step index $j \le m$ for these two families. In the continuing chart $z = \psi^j z_j$, and the pullback coefficient g contains a factor of ψ^{6j}:

$$z^5(\psi^m + z + z^2) = \psi^{6j} z_j^5(\psi^{m-j} + z_j + \psi^j z_j^2). \tag{XV.8.63}$$

The exponent $6j$ comes from accumulating the crepant divisions; the remaining coefficient is the one tested at the next point. A quick check on the noncontinuing chart of the jth step starts from its previous bracket $\psi^{m-j+1} + z_{j-1} + \psi^{j-1} z_{j-1}^2$. Substituting $z_{j-1} = e, \psi = ev$ and dividing the remaining bracket by e gives

$$g_j' = 1 + e^{m-j} v^{m-j+1} + e^j v^{j-1}. \tag{XV.8.64}$$

In particular on the new exceptional in the final noncontinuing chart, $g_m' = 1 + v$ at $e = 0$. This equality holds for either final step, though the preceding steps and the adjacent components differ.

The map to D_ψ remains proper. Its central fiber in either noncontinuing blowup chart has local equation $ev = 0$, which accounts for the transverse compact nodes and the multiplicities one. In the continuing charts the new exceptional is $\psi = 0$ and the strict flavor section is $z_j = 0$. They are transverse. Figure XV.8.6 records the resulting incidence; the final exceptional enters next to the strict left section.

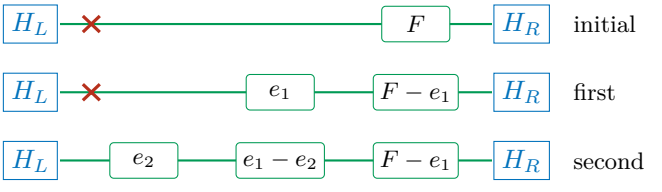


Figure XV.8.6: The central rational fiber and the left and right flavor sections before and after the two base blowups for $m = 2$. A cross marks the next center. The second blowup separates the left section from the first exceptional, whose proper transform becomes the middle curve. All solid compact links indicate a single transverse intersection.

To calculate self-intersections, use total-transform classes. Write F for the original vertical fiber class and H for a horizontal section class on B_0. The exceptional classes

e_i in this calculation are total transforms on the final surface; in particular e_1 is not the strict middle curve after two steps. The basic intersections are

$$F^2 = H^2 = 0, \qquad H \cdot F = 1, \qquad e_i \cdot e_j = -\delta_{ij}, \qquad e_i \cdot F = e_i \cdot H = 0. \quad \text{(XV.8.65)}$$

The first center lies on F and the left section. The second lies on the first exceptional and the strict left section, away from the strict transform of F. Hence for $m = 2$ the compact components from left to right and the flavor section classes are

$$(C_L, C_M, C_R) = (e_2, e_1 - e_2, F - e_1), \qquad C_L + C_M + C_R = F, \quad \text{(XV.8.66)}$$

$$(H_L, H_R) = (H - e_1 - e_2, H). \quad \text{(XV.8.67)}$$

Their pairings follow by multiplication. For example $(e_1 - e_2)^2 = -2$ and $(e_1 - e_2) \cdot (F - e_1) = 1$. The left section has intersection $(H - e_1 - e_2) \cdot (e_1 - e_2) = 0$ and meets e_2 once. The matrices and boundary incidence are

$$Q_{121} = \begin{pmatrix} -1 & 1 & 0 \\ 1 & -2 & 1 \\ 0 & 1 & -1 \end{pmatrix}, \qquad \begin{pmatrix} H_L \cdot C_i \\ H_R \cdot C_i \end{pmatrix} = \begin{pmatrix} 1 & 0 & 0 \\ 0 & 0 & 1 \end{pmatrix}. \quad \text{(XV.8.68)}$$

For $m = 1$ the second center is absent. The compact order is $(e_1, F - e_1)$ and the end sections are $H - e_1$ and H. Their intersection data become

$$Q_{11} = \begin{pmatrix} -1 & 1 \\ 1 & -1 \end{pmatrix}, \qquad \begin{pmatrix} H_L \cdot C_i \\ H_R \cdot C_i \end{pmatrix} = \begin{pmatrix} 1 & 0 \\ 0 & 1 \end{pmatrix}. \quad \text{(XV.8.69)}$$

In each case the rows of Q sum to zero. Adjunction also distinguishes these configurations from the triangle. For $m = 2$, $K_B = -2H + e_1 + e_2$ in these local classes, so its intersections with the compact chain are $(-1, 0, -1)$ and $K_B \cdot F = -2$. For $m = 1$ omit e_2 to obtain the same canonical degree of the total fiber. The smooth general fiber has genus zero by $2g - 2 = (K_B + F) \cdot F$. On the affine surface K_S is trivial and the smooth fiber has genus one. A corank-one condition on the pairing is not a genus calculation.

We next check where the elliptic Weierstrass fiber of the threefold degenerates over this resolved base. On C_R, away from the first exceptional, the restriction to $\psi = 0$ uses $f = -3z^4$, $g = z^6(1 + z)$. On C_L use the final continuing chart of either family and restrict to $\psi = 0$. Its coefficients are $f = -3z_m^4$, $g = z_m^5(1 + z_m)$. The discriminants along the two end curves in these charts are

$$\Delta|_{C_R} = 27z^{12}(z - 1)(z + 3), \quad \text{(XV.8.70)}$$

$$\Delta|_{C_L} = 27z_m^{10}(1 - z_m)(1 + 3z_m). \quad \text{(XV.8.71)}$$

The factor z^{12} in the first line occurs at the old left point, where this chart does not describe the blown-up C_R. Near the relevant compact node the first primed chart in (XV.8.60) gives $f = -3, g = 1$ at $e = v = 0$. In the second primed chart for $m = 2$ the node likewise has $f = -3, g = 1$. In both cases $\Delta = -81$ there. On the middle curve for $m = 2$ the first continuing chart has $g_1 = z_1^6$ and $f_1 = -3z_1^4$ at generic $\psi = 0$, with discriminant $-81z_1^{12}$. The primed charts cover its ends. Hence there are no additional residual zeros on that curve.

The continuing and noncontinuing descriptions also cross-check the location of the last two residual roots. On the final exceptional their overlap has $v = 1/z_m$. In the primed trivialization the discriminant at $e = 0$ is $27[(1+v)^2 - 4] = 27(v-1)(v+3)$. Its two roots become $z_m = 1, -1/3$ in the continuing chart. At $v = 0$ the primed expression is nonzero, so the node at the other end of the exceptional has no residual zero hidden by the change of trivialization. For C_R the first primed chart at $v = 0$ gives $27[(1+e)^2 - 4]$ with $z = e$, as expected after removing the exceptional powers from the right-end discriminant (XV.8.70).

The residual intersections are at $z = 1, -3$ and $z_m = 1, -1/3$. They are simple and disjoint from the two compact nodes when both nodes are present. At each residual root $f \neq 0$, so the Weierstrass fiber is nodal of type I_1. For a double root $x = x_*$ of the cubic, $f = -3x_*^2$ and $g = 2x_*^3$. In a base direction along the compact curve the derivative of the discriminant there is $108x_*^3(x_*\, df + dg)$. Since $x_* \neq 0$ and the root is simple, the Weierstrass hypersurface derivative $-(x_*\, df + dg)$ in that direction is nonzero. Thus these nodal fibers have smooth total space near their singular points. Simplicity also makes the residual discriminant transverse to the compact end curve there. Properness lets us restrict to a smaller external disc so that these local neighborhoods and the regular parts cover all residual loci near the central fiber. In particular the residual discriminant does not collide with a flavor divisor in that smaller neighborhood.

The two end curves each meet a compact neighbor, a noncompact flavor section, and two residual discriminant branches. Figure XV.8.7 records the positions in their own affine coordinates. The I_1 roots do not enter the compact intersection matrix: they are points of degeneration of the elliptic fiber *over* the base curves. They must nevertheless be checked to decide whether the Weierstrass model introduces a further singularity that changes the construction. In particular the two labels 1 on the diagram are values of different coordinates and refer to points on different curves.

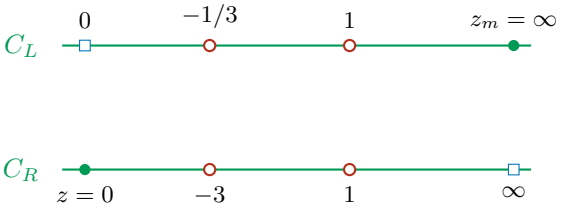


Figure XV.8.7: Marked loci on the two end curves of the rational central fiber. Each row is a projective line with its own affine coordinate. Markers are schematic, with the coordinate values written beside them. Squares mark flavor-section incidence, open circles mark simple residual I_1 intersections, and solid points mark the compact nodes. For $m = 1$ the two solid markers describe the same compact node.

At the final left section $z_m = 0$ the bracket multiplying z_m^5 has constant term one. At the right section $w = 0$ the corresponding bracket in (XV.8.57) also has constant term one. The g^2 term therefore contributes order ten and cannot be canceled by f^3, which starts at order twelve. Both noncompact sections have

$$\operatorname{ord}(f, g, \Delta) = (4, 5, 10). \tag{XV.8.72}$$

The ordinary type is II^*. We use the ordinary local crepant fiber resolution along the two flavor sections as a construction ingredient. In a transverse germ, normalizing the unit multiplying the fifth power gives the weighted leading form $y^2 - x^3 - u^5$, where u is a normal coordinate to the section. This is the transverse E_8 type; it is not by itself an analytic simultaneous resolution of the threefold family. Our blowups and residual checks do not construct such a global resolution. The compact components are generically I_0, meaning smooth Weierstrass fiber. The two E_8 algebras come from the noncompact ends and act as flavor algebras in the ordinary local rigid interpretation.

Here is why the coefficient checks are essential. In the $m = 2$ family move the second center to $(\psi, z_1) = (0, 1)$ on the first exceptional. The strict transform of the first exceptional still has self-intersection -2, and the same three compact classes and matrix (XV.8.68) result. But the center misses the left section, whose class stays $H - e_1$ and whose incidence changes to $(0, 1, 0)$. Worse, the first continuing coefficients are units at the proposed center, with values $-3, 1$. For example, the chart $z_1 = 1 + e, \psi = ev$ would give after the proposed division

$$f' = -3e^{-4}(1 + e)^4, \qquad g' = e^{-6}(1 + e)^5\big(ev + 1 + e + ev(1 + e)^2\big). \tag{XV.8.73}$$

The complementary chart $\psi = e, z_1 = 1 + ev$ gives

$$f' = -3e^{-4}(1 + ev)^4, \tag{XV.8.74}$$

$$g' = e^{-6}(1 + ev)^5\big(e + 1 + ev + e(1 + ev)^2\big). \tag{XV.8.75}$$

Both normalized coefficients would have poles on either chart, since the numerators there restrict to $-3, 1$. The true nonminimal point remains: in the first wrong-center chart it is at $e = -1, v = 0$. There e is a unit, the factors z_1^4, z_1^5 persist as $(1 + e)^4, (1 + e)^5$, and the bracket vanishes to first order. Thus the point still has orders $(4, 6)$. The unchanged compact matrix cannot diagnose this failure.

There is a second possible error at the correct center: retaining the bare pullback. For the $m = 2$ second step, for example, on the other chart those coefficients would be

$$p^* f_1 = -3e^4, \qquad p^* g_1 = e^6(1 + v + e^2 v). \tag{XV.8.76}$$

These have the divisorial orders $(4, 6)$ along $e = 0$. Their orders reflect the old line bundles on the new base. Dividing by the exceptional powers as in (XV.8.58) gives unit f_2' and removes this divisorial failure. In the wrong-center calculation there are no exceptional factors to remove. Thus the base blowup must be made at a point with the required orders, and the Weierstrass coefficients must be transformed in the new bundles.

Finally the positive reference forms for the chain can be constructed as in the affine case. For $m = 2$ use the class $L = A_D H - \epsilon_1 e_1 - \epsilon_2 e_2$. Its degrees in the order of (XV.8.67) and their positivity condition are

$$(a_L, a_M, a_R) = (\epsilon_2, \epsilon_1 - \epsilon_2, A_D - \epsilon_1), \tag{XV.8.77}$$

$$a_i > 0 \text{ for all } i \quad \Longleftrightarrow \quad 0 < \epsilon_2 < \epsilon_1 < A_D. \tag{XV.8.78}$$

Given a rational partition one recovers $\epsilon_2 = a_L$ and $\epsilon_1 = a_L + a_M$. The generic fiber has degree A_D, so the relative ampleness and reference-metric argument applies. For $m = 1$

use $L = A_D H - \epsilon_1 e_1$. The period pair is $(\epsilon_1, A_D - \epsilon_1)$, for example $(2, 8)$ at $A_D = 10$. Both realizations can be stretched by (XV.8.2) and retain the full-fiber tension $\tau_3 A_D$. The flavor sections play no role in the sum of the compact areas.

To realize the same ordered partition $(2, 3, 5)$ used for the affine example in this chain, take $\epsilon_2 = 2$, $\epsilon_1 = 5$ and $A_D = 10$. Thus $L = 10H - 5e_1 - 2e_2$, very different from the affine section and exceptional class in (XV.8.33). If ϵ_1 fell to ϵ_2 the middle curve would have zero degree and the class would reach a wall, despite leaving both end degrees positive. Equal numerical periods in the two examples give equal tensions for the corresponding effective coefficient columns at leading order. Their intersection pairings and flavor incidences still differ. In particular, the middle component has no intersection with either flavor section here.

Under the bulk-decoupling hypotheses of the rigid heterotic interval construction this gives a $(1, 0)$ LST with $E_8 \times E_8$ flavor. In the interval frame the special gravity-decoupling scaling collapses the transverse interval while keeping the effective string scale finite. The ratios of the subinterval lengths can stay positive and supply tensor-branch parameters. This distinguishes that microscopic scaling from setting the normalized compact periods to zero: our positive reference areas describe the finite-tension branch in the F-theory frame. The later chapters will vary the gauge data and compare circle reductions. Both tasks require more than the compact matrix. Here the separate base and Weierstrass calculations identify what survives the gravity limit, where the flavor loci meet it, and which scale remains fixed.

XV.8.7 Exercises

1. **Resolve the changed affine exponent.** Replace t^3 by t^2 in (XV.8.13). Give the discriminant order at zero and the compact intersection matrix in the order (proper cubic, exceptional conic). Give the primitive effective null column. Assign the two curves areas $(7/2, 5/2)$ in common units and compute $T(\delta)/T(C_0)$. Explain how the two actual intersections are distinguished in the direction plane.

2. **Redistribute area and add one fiber.** In the triangle, prescribe $(a_0, a_1, a_2) = (3, 5/2, 9/2)$ at $A_D = 10$. Solve for (b_1, b_2) in (XV.8.30). For $q = (2, 0, 1)^t$ and $q + \delta$, submit their quotient columns with reference C_2 and both tensions in units of τ_3. Check the periods from your class. Explain how equal quotient classes can give different answers for the two tensions.

3. **Stop or continue the chain resolution.** Compare the $m = 1$ family to the $m = 2$ family stopped after its first blowup. In each case give the (f, g) point orders at the strict left section on the continuing chart. Give the powers of the three bracket terms in g_j/z_j^5, and the generic exceptional orders of (f_j', g_j') on the other chart. Give the compact intersection matrix Q, left and right section incidences and central fiber multiplicities at the stage you have computed, in order from left to right. For $m = 2$ also complete the second blowup and give the corresponding final data. Explain why two identical compact matrices at the first stage give different answers to the question of whether the model has a nonminimal point.

4. **Diagnose gravitational isolation.** Explain how the regulated Einstein coefficient tests gravity decoupling. Which profile is assumed, and which information about other modes would be needed to infer that a chosen local interacting sector is isolated from a continuum? Distinguish the fixed-area stretch from a uniform rescaling of J_0.

Use `benchmark/tasks.json` for the JSON fields and `benchmark/PROTOCOL.md` for submission. Written explanations, including all of Exercise 4, are human-assessed.

Status and sources

§1. Regulated gravity and a fixed fiber period. The Kähler and volume identities are [MATH]. The regulated unwarped constant-mode estimate is [SUGRA]. The rigid-sector interpretation with bulk decoupling is [DEC]; see Bhardwaj et al. (2016), arXiv:1511.05565v3, pp. 11–14, §3.1 and eq. (3.17). For the independent NS5 finite-scale mechanism in its own microscopic units see Seiberg (1997), hep-th/9705221v2, pp. 1–4, §2.1, eqs. (2.1)–(2.4). The regulated volume identity makes no assertion about the continuum or a backreacted metric.

§2. The affine base. The nodal polynomial, resolved charts and residue, and the changed I_2 object are [MATH]. The pairing computation uses the sign opposite to geometric intersection, as in Bhardwaj et al. (2016), §3, eqs. (3.5)–(3.7). The product input is from §4.1, pp. 14–17, eq. (4.1); the exact I_3 polynomial and its local charts are the derivation here. The calculation uses the Weierstrass convention $\Delta_{\text{book}} = 4f^3 + 27g^2$. The two projections do not by themselves identify two six-dimensional theories.

§3. Periods and the full-fiber string. The relative period construction and calibrated area comparison are [MATH] with the stated reference-class and leading-order hypotheses. The wrapped-fiber identification and rigid product interpretation are [GEO-E]; see Bhardwaj et al. (2016), §3.1.2 and §4.1, pp. 13–17, in the leading Einstein-frame D3 tension normalization. No multiplicity of bound states or oscillator gap follows from the area calculation.

§4. Local pairing and period variations. The positive quotient and the fixed-scale duality of variations and quotient charges are [MATH]. The local physical interpretation is [GEO-E] in the ordinary rigid background; see Bhardwaj et al. (2016), §2, pp. 6–8, eqs. (2.1)–(2.7), and §3, eqs. (3.5)–(3.7). Compact support proves a period condition; it is not a complete kinetic or normalizability analysis.

§5. Point contraction and the area paths. The positive proper blocks, paths and analytic subset contraction are [MATH]. The local SCFT interpretation under the tensionless and isolation conditions is [DEC]; see Bhardwaj et al. (2016), §3.1.2, p. 13, and the opening of §5, pp. 19–20. Shrinking a subset at fixed total area is compatible with a finite little string tension.

§6. Rational chain and its flavor ends. The base blowups, component classes, residual discriminant and reference periods are [MATH]. See Bhardwaj et al. (2016), Appendix F, pp. 63–64, eq. (F.1), specialized here to $m = 1, 2$ and coefficients $-3, 1$.

The imported ordinary local crepant E_8 resolution is [MATH] at its stated local scope; for formal transverse recognition see Cossec et al. (n.d.), p. 73, Remark 0.4.14. The flavor and heterotic interval interpretation is [GEO-E]; see Bhardwaj et al. (2016), §4.2, eq. (4.3), and Figure 3. We use the exponent m rather than the source's two component-count conventions. The exact chain uses the $E_8 \times E_8$ frame only.

References

Bhardwaj, L. et al. (2016). "F-theory and the Classification of Little Strings". In: *Phys. Rev. Lett.* 116, p. 161601. DOI: 10.1103/PhysRevLett.116.161601. arXiv: 1511.05565 [hep-th].

Cossec, F., I. Dolgachev, and C. Liedtke (n.d.). *Enriques Surfaces I*. Online manuscript, §0.4, Remark 0.4.14.

Seiberg, N. (1997). "New Theories in Six-Dimensions and Matrix Description of M-theory on T^5 and $T^5/\mathbb{Z}_2$". In: *Phys. Lett. B* 408, pp. 98–104. DOI: 10.1016/S0370-2693(97)00805-8. arXiv: hep-th/9705221.

Chapter XV.9

Worked little string constructions and SCFT subsectors

XV.9.1 A loop of actual curves

What extra geometry turns a loop of tensor charges into a gauge theory on its tensor branch? We will use the same base surface twice, first with a smooth elliptic fiber and then with a singular one. In the second construction a hypermultiplet will come from an actual crossing of two gauge divisors. We will also build a different little string geometry in which the compact curves form an interval and the two gauge algebras live on noncompact flavor divisors. To find the local conformal sectors inside these examples, we will keep track of the curves that shrink and of the fibers that still meet them.

Recall the two maps involved in the first example. An elliptic threefold projects to the F-theory base surface S. The base in turn maps to the external disc $D = \{|t| < 1\}$. It is a compact curve of S, rather than the elliptic fiber of the first map, that a D3-brane wraps to give a six-dimensional string. We construct S from the sectioned family of projective cubics whose affine equation is

$$y_b^2 = x_b^3 - 3x_b + 2 + t^3. \tag{XV.9.1}$$

The subscript b marks the coordinates of the cubic inside the base surface. In the convention $\Delta = 4f^3 + 27g^2$, the discriminant of this family is $27t^3(4 + t^3)$. Only the central cubic is singular on D. To see what the central fiber becomes after resolution, set $\xi_b = x_b - 1$. In the analytic branch with $\sqrt{\xi_b + 3} = \sqrt{3}$ at $\xi_b = 0$, the coordinates

$$u_b = y_b - \xi_b\sqrt{\xi_b + 3}, \qquad v_b = y_b + \xi_b\sqrt{\xi_b + 3} \quad \Longrightarrow \quad u_b v_b = t^3 \tag{XV.9.2}$$

separate the tangents of the node. Their Jacobian with respect to (ξ_b, y_b) is $-2\sqrt{3}$ there. At $t = 0$ the cubic is irreducible and nodal: the slope $y_b/(x_b - 1)$ parametrizes its normalization, and takes the two values $\pm\sqrt{3}$ above the node.

One can resolve this A_2 surface singularity by blowing up the point. In the u_b chart put $t = u_b r$ and $v_b = u_b s$, so the strict transform has $s = u_b r^3$. In the v_b chart the expression is exchanged. In the t chart set $u_b = tU_b$ and $v_b = tV_b$, so the strict transform has $t = U_b V_b$. Thus the base map has the following local products at the three joint points:

$$t = u_b r, \qquad t = U_b V_b, \qquad t = v_b r', \tag{XV.9.3}$$

where $r' = t/v_b$ on the last chart. The two lines in the t chart extend to the two exceptional rational curves C_1, C_2. Choose C_1 to meet the branch on which u_b is a coordinate, and C_2 to meet the branch on which v_b is a coordinate. The other component, C_0, is the proper transform of the original cubic. It meets one end of each exceptional. The three products in (XV.9.3) show that the meetings are transverse and all multiplicities are one.

This resolution also gives a trivialization of K_S, needed to write global Weierstrass coefficients later. On the smooth affine part of the cubic family, a residue representative is $dx_b \wedge dt/(2y_b)$, with the equivalent residue charts where $y_b = 0$. Adjunction for the degree-three equation makes the relative residue regular and nonzero also at the infinity section. In the analytic coordinates of (XV.9.2) the two-form is a holomorphic unit times $du_b \wedge dt/u_b$. For example,

$$\frac{du_b \wedge dt}{u_b} = du_b \wedge dr \quad (t = u_b r), \qquad \frac{du_b \wedge dt}{u_b} = dU_b \wedge dV_b \quad (u_b = tU_b,\ t = U_b V_b). \tag{XV.9.4}$$

On the v_b chart one uses $du_b \wedge dt/u_b = -dv_b \wedge dt/v_b$. These forms have neither poles nor zeros. The product coordinate t itself extends through the resolution, so the central fiber is the principal divisor

$$D_0 = \operatorname{div}(t) = C_0 + C_1 + C_2, \qquad D_0 \cdot C_i = 0. \tag{XV.9.5}$$

The second identity is the degree of a trivial line bundle on each proper curve. Each C_i meets the other two once. Expanding the degree in (XV.9.5) therefore gives $C_i^2 = -2$. This is also the adjunction value for a rational curve with $K_S \cdot C_i = 0$.

Write $Q_{ij} = C_i \cdot C_j$ for the geometric form and $\Omega_A = -Q$ for the positive-sign charge pairing. For a column of wrapped-curve coefficients $\ell = (\ell_0, \ell_1, \ell_2)^t$,

$$\Omega_A = \begin{pmatrix} 2 & -1 & -1 \\ -1 & 2 & -1 \\ -1 & -1 & 2 \end{pmatrix}. \tag{XV.9.6}$$

The quadratic and the integral radical are

$$\ell^t \Omega_A \ell = (\ell_0 - \ell_1)^2 + (\ell_1 - \ell_2)^2 + (\ell_2 - \ell_0)^2, \tag{XV.9.7}$$

$$\ker_{\mathbb{Z}} \Omega_A = \mathbb{Z}\delta, \qquad \delta = (1,1,1)^t. \tag{XV.9.8}$$

The pairing measures differences along the three joints. A charge with equal coefficients has zero pairing with all compact charges. It still wraps the full effective fiber. A nearby smooth fiber can replace that cycle without changing its area, so a nonzero area and a zero pairing are compatible.

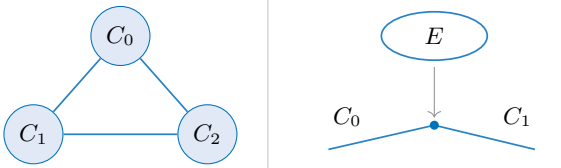


Figure XV.9.1: Left: the two exceptional curves connect the two preimages of the node of the original cubic. Each link denotes a different transverse base point. Right: the constant elliptic fiber E sits above the base, including above a joint of base curves. The two kinds of curve belong to different maps.

For a first elliptic threefold take $E \times S \to S$, with the constant curve E given by $y_E^2 = x_E^3 - x_E$. Its Weierstrass coefficients and discriminant are

$$(f_E, g_E) = (-1, 0), \qquad \Delta_E = -4. \tag{XV.9.9}$$

In particular, none of the three C_i carries a seven-brane gauge algebra. A joint in the lower surface of Figure XV.9.1 does not cause any degeneration upstairs. With the ordinary rigid limit of Chapter 8, including decoupling of the local sector from bulk modes, this product gives the $(2, 0)$ little string example. We next keep (XV.9.7) exactly fixed and change the elliptic map. That comparison separates the information carried by the charge lattice from the information carried by the seven-branes.

The two compact directions in the quotient already appear in the intersection geometry. For example, let $\mathbf{e}_i$ denote the charge wrapping C_i once. The full charge and two finite differences give the following exact decompositions:

$$\ell = \ell_0\delta + (\ell_1 - \ell_0)\mathbf{e}_1 + (\ell_2 - \ell_0)\mathbf{e}_2, \tag{XV.9.10}$$

$$\ell^t \Omega_A \ell = 2\big[(\ell_1 - \ell_0)^2 + (\ell_2 - \ell_0)^2 - (\ell_1 - \ell_0)(\ell_2 - \ell_0)\big]. \tag{XV.9.11}$$

Thus the classes of $\mathbf{e}_1, \mathbf{e}_2$ give an integral basis of the quotient. For instance $\mathbf{e}_1$ and $\mathbf{e}_1 + \delta$ have equal pairing against every compact charge. In a positive Kähler class the area of the latter is larger by the whole fiber area. The base calculation tells us which information is lost by the quotient. In Section XV.9.4 the Green–Schwarz square will depend only on the differences; in Section XV.9.5 the string tensions will use the full effective charge.

XV.9.2 A split elliptic fiber over the loop

Can a single sectioned threefold put split I_4 fibers over all three components? We start with a second cubic family $W_n \to D$ and pull it back to S, using $n = 4$ for the first example and $n = 5$ for a changed rank. In projective coordinates $[X : Y : Z]$ the family is

$$W_n : \quad Y^2Z = X^3 - 3XZ^2 + (2 + t^n)Z^3, \qquad W_n \times_D S \longrightarrow S. \tag{XV.9.12}$$

The nonzero two-form on S trivializes the Weierstrass line bundle. Thus $f=-3$ and $g=2+t^n$ are actual sections on the whole S. The section $[0:1:0]$ is smooth: in the $Y=1$ chart the equation has derivative one with respect to Z at the section. On the affine chart the only relative singular point above $t=0$ is $(X,Y)=(1,0)$.

The leading quadratic at that point decides whether its two branches are exchanged by monodromy. Put $X=1+\xi$, $Y=\eta+\sqrt{3}\xi$. The exact Tate equation, with coefficients in the order $1,2,3,4,6$, is

$$\eta^2+2\sqrt{3}\xi\eta=\xi^3+t^n,\qquad (a_1,a_2,a_3,a_4,a_6)=(2\sqrt{3},0,0,0,t^n). \tag{XV.9.13}$$

These sections have no transition along the C_i in the chosen frame. In this equation the degree-two term on the central divisor is $\eta(\eta+2\sqrt{3}\xi)$. Equivalently, with tangent slope $\lambda=\eta/\xi$, the two descriptions of the tangent cover are

$$\lambda(\lambda+2\sqrt{3})=0,\qquad w=2\lambda+a_1,\qquad w^2=b_2=a_1^2+4a_2=12. \tag{XV.9.14}$$

The two distinct constant roots $w=\pm 2\sqrt{3}$ are defined over every component, giving the split multiplicative case. The calculation uses the actual shift and the actual leading coefficient. In a different Tate equation the square test is over the generic residue field of the gauge divisor: a varying function may itself be a square in that field. Failure to have these two fixed constant roots rules out this particular fixed-frame calculation, not splitness for a general varying cover.

The discriminant identifies all the degenerations that have to be resolved:

$$\Delta=27t^n(4+t^n), \tag{XV.9.15}$$

$$\Delta\big|_{t=uv}=27u^nv^n(4+u^nv^n), \tag{XV.9.16}$$

$$\operatorname{ord}_{C_i}(f,g,\Delta)=(0,0,n),\qquad \operatorname{ord}_{(u,v)}(f,g,\Delta)=(0,0,2n). \tag{XV.9.17}$$

Here u,v are the two base coordinates at a joint, and the second order in (XV.9.17) is the order in the maximal ideal of that point. The residual factor never vanishes for $|t|<1$. The nonzero constant f excludes a nonminimal point. This order calculation locates the singular fibers. To read the crossing, we still need the resolution.

First resolve the surface W_n. The analytic change

$$a=Y-\xi\sqrt{\xi+3},\qquad b=Y+\xi\sqrt{\xi+3},\qquad ab=t^n \tag{XV.9.18}$$

uses the same square-root branch as in the base calculation and again has Jacobian $-2\sqrt{3}$ at the node. Blow up (a,t) in this local model. The t chart $a=ta'$ has $a'b=t^{n-1}$. The a chart $t=ar$ has $b=a^{n-1}r^n$ and is smooth. Iterating in the unresolved chart gives the following n smooth charts indexed by j:

$$a=A_jt^{j-1},\qquad b=B_jt^{n-j},\qquad t=A_jB_j,\qquad j=1,\dots,n, \tag{XV.9.19}$$

$$A_{j+1}=1/B_j,\qquad B_{j+1}=tB_j\qquad (B_j\neq 0). \tag{XV.9.20}$$

To check the overlap, divide a by one more power of t and use $A_j/t=1/B_j$. The coordinate lines over $t=0$ then glue to the chain of $n-1$ exceptional projective lines and the two branches of the same normalized cubic. This closes the chain into a reduced

I_n polygon. Denote the resolved surface by T_n, and its ordered central components by $D_0^T, D_1^T, \dots, D_{n-1}^T$, with D_0^T the proper transform. The superscript distinguishes them from the full fiber D_0 of the base.

For $n = 4$ the exponents of t multiplying A_j, B_j can be listed in the order of the charts:

$$(j-1, n-j) = (0,3),\ (1,2),\ (2,1),\ (3,0). \tag{XV.9.21}$$

In the first chart the axis $B_1 = 0$ with $A_1 \neq 0$ maps to a smooth point of one old branch. The other axis, $A_1 = 0$, maps to the node and is one chart of the first exceptional. On its open set $B_1 \neq 0$ it becomes $B_2 = 0$, $A_2 = 1/B_1$ in the next chart. Thus it closes into a projective line with the two joint points $B_1 = 0$ and $A_2 = 0$. Continuing the same calculation gives the middle and last exceptionals. This explains why there are four joint points on T_4, rather than one joint for each of its three exceptional curves. The old cubic accounts for the fourth component. For $n = 5$ there is one extra overlap and one extra exceptional; the two endpoints are again supplied by the same old cubic.

A global construction of T_n does not require the analytic branches a, b to be global divisors on W_n. Blow up its singular point instead. For a germ $ab = t^k$ the t chart has $a'b' = t^{k-2}$, while the a chart has $b' = a^{k-2}(t')^k$ with $t' = t/a$; the b chart is exchanged. Continue only at the unresolved singular points. Each blowup has ambient discrepancy two, canceled by the multiplicity two of the hypersurface. The resulting smooth surface is crepant; an exceptional (-1) curve would contradict adjunction since the canonical bundle pairs trivially with an exceptional curve. This is the minimal resolution, described locally by (XV.9.19). In those charts one can check the residue directly:

$$\frac{da \wedge dt}{a} = \frac{dA_j \wedge dt}{A_j} = dA_j \wedge dB_j. \tag{XV.9.22}$$

The first equality loses only a term proportional to $dt \wedge dt$. It is the residue of the original cubic two-form, up to a holomorphic unit, that extends.

Now form $Z_n = S \times_D T_n$. Away from pairs of central nodes, one surface map is a submersion, so the product is smooth there. At a pair of nodes use u, v in S and now use a, b for the two *resolved* coordinates in T_n. Since $t = uv = ab$, the product has one ordinary double point for every such pair. There are three nodes on S and n on T_n, hence $3n$ ordinary double points. The product of a chosen base branch with a chosen fiber branch has ideal (a, u) after labeling the two branches accordingly. Blowing it up gives two smooth charts:

$$a = uh, \quad v = hb, \qquad (u, h, b), \tag{XV.9.23}$$

$$u = ak, \quad b = kv, \qquad (a, k, v), \tag{XV.9.24}$$

$$hk = 1, \qquad u = ak, \qquad b = kv \quad \text{on the overlap.} \tag{XV.9.25}$$

For instance $a = uh$ gives $u(hb - v) = 0$ before taking the strict transform, and the strict transform has $hb = v$. Over the ordinary double point the two charts give an exceptional $\mathbb{P}^1$ with coordinates h, k. Over the base point $u = v = 0$, the scheme fibers in the two charts have ideals

$$(u, hb) \ \subset\ \mathbb{C}\{u, h, b\}, \qquad (v, ak) \ \subset\ \mathbb{C}\{a, k, v\}. \tag{XV.9.26}$$

The product of two distinct coordinates shows reducedness. In the first chart the two axes meet at $h = b = 0$; in the second they meet at $a = k = 0$. They are the two different endpoints of the exceptional line. Thus the new line separates the old branches and meets each once. For clarity, the axis $b = 0$ of the first chart maps entirely to the old node because then $u = a = v = 0$. The other axis, $h = 0$, has b free and maps to the original b branch. In the second chart the axis $a = 0$ continues the exceptional line, and the axis $k = 0$ maps to the original a branch. On the exceptional axes the transition $hk = 1$ identifies the two affine charts of the line. Each old branch meets that line at the endpoint of exactly one chart. In particular the scheme calculation distinguishes a doubled component from two simple ones: $\mathbb{C}\{h, b\}/(hb)$ has two minimal primes (h) and (b), and neither has multiplicity two.

The same expressions give regular sequences: for example u is regular, and hb is a nonzero element in the domain after quotienting by u. The source is smooth and the base is a regular surface; the fibers have the expected pure dimension one. The flatness criterion for a Cohen–Macaulay source over a smooth base therefore applies. The unchanged product charts are flat by base change from the curve fibration $T_n \to D$.

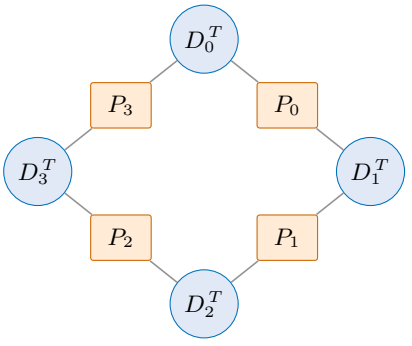


Figure XV.9.2: The reduced fiber of the resolved threefold over one base joint for $n = 4$. Each old D_j^T remains a curve; a new line P_j is inserted at its former meeting with D_{j+1}^T. Subscripts on the old curves are cyclic. The two endpoints of each P_j are the two separate axis intersections in (XV.9.26).

The same resolution can be made at all nodes by an ordered global sequence. Take the closed product surfaces $C_i \times D_j^T$ in Z_n, in lexicographic (i, j) order, and blow up their strict transforms. At any unresolved node exactly four such surfaces are incident, one for each pair of branches. The first incident center is the local product just analyzed, up to swapping branch labels. Near any smooth point of the product or of a partial resolution the strict transform of a product surface is a divisor and hence Cartier, so its blowup there is an isomorphism. A center not incident to a node misses it. This gives the same two charts at every node without demanding that one branch label work at every joint. No subsequent center alters an already resolved node. Projectivity over Z_n follows from the sequence of blowups; the exceptional locus over Z_n consists of curves, so the resolution is small.

For the original pullback cubic, adjunction gives a three-form from the two-form on

S and the relative residue of W_n. The passage to T_n extends that residue by (XV.9.22): after wedging with the base two-form, any dt ambiguity in the relative one-form drops out. Near a pair of nodes the three-form is a unit times $da \wedge du \wedge dv/a$. In the two small-resolution charts it becomes

$$\frac{da \wedge du \wedge dv}{a} = dh \wedge du \wedge db \qquad (a = uh,\ v = hb), \tag{XV.9.27}$$

$$\frac{da \wedge du \wedge dv}{a} = da \wedge dk \wedge dv \qquad (u = ak). \tag{XV.9.28}$$

This checks crepancy with respect to the original equation, as well as the absence of a pole on the small exceptional curves. The resulting threefold, denoted X_n, is projective over S and has the original section. The base has not been blown up. This distinguishes the procedure from the point blowups we will need at a nonminimal collision in the interval example. Here the equation $ab = uv$ is a singularity of the threefold at fixed base coordinates. Its blowup ideal selects a surface in the threefold; the map to the (u, v) chart stays defined and neither coordinate is divided by a base exceptional equation.

At a general point of C_i, the fiber has its n old components. At each base joint it also contains the n inserted lines, as in Figure XV.9.2. The two cases give

n	nodes of Z_n	base joints	components per crossing
4	12	3	8
5	15	3	10

(XV.9.29)

Here an I_{2n}-shaped crossing fiber is a curve configuration over a point, not an I_{2n} Kodaira divisor. To identify the local charged matter, return to the unresolved cubic germ $ab = (uv)^n$. The slices $u = z$, $v = z + \mu$ separate the two roots for $\mu \neq 0$:

$$ab = z^n(z + \mu)^n. \tag{XV.9.30}$$

This is the ordinary A-type matter slice with two stacks of size n. At $\mu = 0$ the enhanced algebra is $\mathfrak{su}(2n)$; at distinct roots the two blocks give $\mathfrak{su}(n) \oplus \mathfrak{su}(n)$. The upper right block transforms as $\mathbf{n} \otimes \overline{\mathbf{n}}$ and the lower left as its conjugate. The ordinary local F-theory matter rule for this transverse two-stack slice assigns one full hypermultiplet to this complex representation, with its conjugate already included. This rule supplies the multiplicity; an enhanced root count by itself does not supply a six-dimensional spectrum.

We can now read the compact tensor-branch quiver. There is one $\mathfrak{su}(n)$ on each C_i and one full bifundamental on each of the three edges. The curves are rational and carry no genus adjoints; there is no additional compact charged locus because the residual factor is a unit. With the ordinary rigid decoupling conditions this is a $(1, 0)$ little string example. Its distinction from the $(2, 0)$ product follows from the elliptic geometry, before any anomaly calculation. We will return to the two projections of X_n after examining what happens if one tries to vary the ranks.

XV.9.3 The two ends of an interval

Can the full-fiber charge survive if the base fiber is rational and the gauge divisors are moved to the ends? Start from the ruling $\mathbb{P}^1_{[\sigma:\tau]} \times D_\psi$. Write F for a fiber of the ruling

over the disc and H for the class of a section at fixed $[\sigma:\tau]$. Since $K=-2H$ before blowup, the coefficients of a Calabi–Yau Weierstrass model must be homogeneous of degrees eight and twelve in $[\sigma:\tau]$. Choose the two families

$$f=-3\sigma^4\tau^4, \qquad g=\psi^m\sigma^5\tau^7+\sigma^6\tau^6+\sigma^7\tau^5, \qquad m=1,2. \tag{XV.9.31}$$

The noncompact sections $\sigma=0$ and $\tau=0$ mark the two ends of the fiber. At the right end, in $v=\tau/\sigma$, the coefficients are $f=-3v^4$ and $g=v^5(1+v+\psi^m v^2)$, with a unit in parentheses at $v=0$. At the left end set $z=\sigma/\tau$:

$$f=-3z^4, \qquad g=z^5(\psi^m+z+z^2). \tag{XV.9.32}$$

Here the bracket vanishes to first order at $(\psi,z)=(0,0)$. Both choices of m begin at a nonminimal $(4,6)$ point. To see how m controls the interval, we must track where that point goes under the blowup.

Let p denote a point blowup and $E_{\rm exc}$ its exceptional curve with local defining equation $e=0$. The new canonical bundle is $K'=p^*K+E_{\rm exc}$. Therefore the coefficients in the new bundles are

$$f'=\frac{p^*f}{e^4}, \qquad g'=\frac{p^*g}{e^6}. \tag{XV.9.33}$$

This prescription is also the one obtained by setting the old fiber coordinates to $x=e^2x'$ and $y=e^3y'$. It produces holomorphic sections when the pullbacks contain the required factors. Bare pullback instead leaves an entire exceptional divisor with the high orders and has the wrong line bundles.

At the jth center use the continuing chart $z_{j-1}=\psi z_j$, starting with $z_0=z$. The exceptional equation there is $\psi=0$. The companion chart uses $z_{j-1}=e,\ \psi=ew$, with exceptional equation $e=0$. The transformed sections are

$$z=\psi^j z_j, \qquad f_j=-3z_j^4, \qquad g_j=z_j^5(\psi^{m-j}+z_j+\psi^j z_j^2), \tag{XV.9.34}$$

$$f_j'=-3, \qquad g_j'=1+e^{m-j}w^{m-j+1}+e^j w^{j-1}, \qquad 1\le j\le m. \tag{XV.9.35}$$

For the continuing chart, the power ψ^5 from z_{j-1}^5 combines with a power ψ from each bracket term. In the companion chart the term z_{j-1} in the bracket provides e and becomes the constant one after division. The two charts overlap by $z_j=1/w$, $\psi=ew$. One can check the line-bundle transition explicitly: substituting these two identities in the first row and multiplying by the corresponding exceptional ratios gives

$$f_j'=w^4 f_j\big|_{(z_j,\psi)=(1/w,ew)}, \qquad g_j'=w^6 g_j\big|_{(z_j,\psi)=(1/w,ew)}. \tag{XV.9.36}$$

Thus a location such as $z_j=\infty$ in one chart is precisely the end $w=0$ in the other, with a different trivialization of the coefficient bundles.

For $m=1$ the first continuing chart has $g_1=z_1^5(1+z_1+\psi z_1^2)$, and the first companion chart has $g_1'=1+w+e$. At the intersection of the exceptional and the left flavor section, the continuing chart now has orders $(4,5)$ and Δ has order ten. In the companion chart the compact joint is $e=w=0$ and $g_1'=1$ there. For $m=2$ the first step instead gives

$$g_1=z_1^5(\psi+z_1+\psi z_1^2), \qquad g_1'=1+ew^2+e. \tag{XV.9.37}$$

The joint with the old fiber is again regular, but the intersection with the strict left flavor is still $(4,6)$. The second blowup is at that intersection. It yields

$$g_2 = z_2^5(1 + z_2 + \psi^2 z_2^2), \qquad g_2' = 1 + w + e^2 w. \tag{XV.9.38}$$

In the second companion chart $w = 0$ is the strict transform of the first exceptional. There $g_2' = 1$ and $f_2' = -3$. At the new joint $e = w = 0$ the discriminant is -81. In the old first companion chart the strict middle component lies on $e = 0$ and again has $\Delta = -81$. On the rest of that middle component $g_1 = z_1^6$ and $\Delta = -81 z_1^{12}$ at $\psi = 0$ away from the center. These checks cover the middle component and show that no degeneration is missed at either joint.

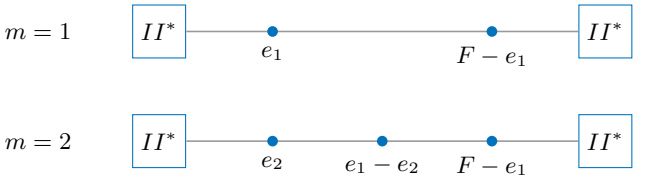


Figure XV.9.3: The left section is followed through the two allowed blowups. The upper row for $m = 1$ has one new compact end; the lower row for $m = 2$ has a strict middle curve between the new end and the original fiber. Open squares are the noncompact II^* sections. Each filled node denotes a compact curve and its label is the curve class in the total pullback basis.

The lattice follows from these actual centers. Use e_j for the total pullback class of the jth exceptional, in contrast to the local equation e. Then $F^2 = H^2 = 0$, $F \cdot H = 1$, $e_j^2 = -1$, and the other pairings vanish. In particular, e_1 for $m = 2$ is not the class of the middle component. In left-to-right order,

$$m = 1: \quad (C_L, C_R) = (e_1, F - e_1), \tag{XV.9.39}$$

$$m = 2: \quad (C_L, C_M, C_R) = (e_2, e_1 - e_2, F - e_1). \tag{XV.9.40}$$

Each second center used here is on just one compact component, so each new exceptional has multiplicity one in the pullback of the central fiber. The sum in each line is F. The left section is $H - \sum_{j=1}^{m} e_j$, and the right is H. Pairing them with (XV.9.40) gives

m	left incidence	right incidence	$(K' \cdot C_i)_i$
1	$(1,0)$	$(0,1)$	$(-1,-1)$
2	$(1,0,0)$	$(0,0,1)$	$(-1,0,-1)$

(XV.9.41)

where $K' = -2H + \sum_j e_j$. The intersections between adjacent compact curves are one, and the others vanish. Consequently the two charge pairings are

$$\Omega_1 = \begin{pmatrix} 1 & -1 \\ -1 & 1 \end{pmatrix}, \qquad \Omega_2 = \begin{pmatrix} 1 & -1 & 0 \\ -1 & 2 & -1 \\ 0 & -1 & 1 \end{pmatrix}. \tag{XV.9.42}$$

These are the path Laplacians. Their quadratic forms sum the squared difference across each compact joint. On either interval the only zero is a column with all coefficients equal, so the full-fiber charge is again primitive, with all coefficients one. This time its curve can move to a smooth rational fiber.

To distinguish a flavor divisor from other discriminant branches, restrict the discriminant to the compact ends. On the left put $z_m = \zeta$ in the final continuing chart and set $\psi = 0$. On the right use $v = \tau/\sigma$. In these two distinct coordinates the restrictions have the same expression:

$$\Delta|_{C_L} = 27\zeta^{10}(1-\zeta)(1+3\zeta), \qquad \Delta|_{C_R} = 27v^{10}(1-v)(1+3v). \tag{XV.9.43}$$

The common factorization comes from $(1+\zeta)^2 - 4\zeta^2$, or its counterpart in v. The tenth power is the ordinary II^* section; at either end the bracket multiplying g has value one at the flavor. The remaining roots $1, -1/3$ are simple in each end's own coordinate. On the old right fiber the same points in $z = \sigma/\tau$ have coordinates $1, -3$. Neither root is at the flavor point or at the compact joint. On the left the joint $z_m = \infty$ is checked in (XV.9.35); the right joint is checked in the first companion chart.

The left exceptional provides a check with no reference to the right end. Its final companion chart gives $g'_m = 1 + w$ at $e = 0$. Therefore on that chart

$$\Delta'_m\big|_{e=0} = 27[(1+w)^2 - 4] = 27(w-1)(w+3). \tag{XV.9.44}$$

The two roots become $\zeta = 1, -1/3$ under $\zeta = 1/w$. The value at the compact joint $w = 0$ is nonzero. Figure XV.9.4 shows why matching roots with the same printed coordinate in the two end charts does not identify the underlying points.

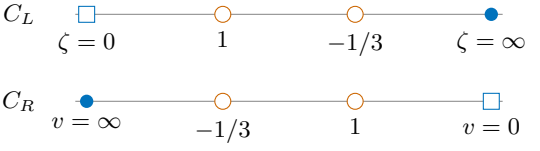


Figure XV.9.4: Schematic marked points on the two different compact ends, each in its own coordinate. The squares denote the flavor points, open circles denote simple residual intersections, and the filled dots denote the compact joints. The coordinate $v = 0$ on the right is the point $z = \infty$ in the original chart.

These restrictions exhaust the intersections near the central fiber. For example the line bundle of Δ has degree 12 on C_L by (XV.9.41); the flavor section uses ten of these degrees. If R_Δ denotes the divisor left after removing the two noncompact flavor contributions, then

$$(R_\Delta \cdot C_i)_i = (2,2) \quad (m=1), \qquad (R_\Delta \cdot C_i)_i = (2,0,2) \quad (m=2). \tag{XV.9.45}$$

At each residual root $f \neq 0$ and Δ has nonzero derivative along the compact curve. To check that this really is an ordinary nodal degeneration of the total model, let x_* be the double root of $x^3 + fx + g$. Then $x_* \neq 0$, $f = -3x_*^2$, $g = 2x_*^3$. Differentiating at this point gives

$$d\Delta = 12f^2\,df + 54g\,dg = 108x_*^3(x_*\,df + dg). \tag{XV.9.46}$$

The hypersurface derivative in a base direction at $(x, y) = (x_*, 0)$ is $-(x_*\, df + dg)$ in that direction. Nonzero derivative of the restriction therefore rules out a singular total space at the node of this fiber. The residual branch is transverse there and its ordinary fiber is I_1. The compact curves themselves are generically I_0 and have no nonabelian gauge decoration. In the ordinary local resolution of the transverse II^* fibers, the two noncompact sections furnish the two E_8 flavor algebras. This uses the ordinary local E_8 fiber resolution and the rigid construction with its decoupling conditions. The chart calculation above resolves the base and tests the residual loci; it is not a construction of a global simultaneous projective fiber resolution for this interval.

There is a useful way to fail while keeping (XV.9.42) unchanged. In the $m = 2$ model, move the second center from $z_1 = 0$ to $z_1 = 1$ on the first exceptional. It is still on just that compact curve, so the compact classes stay the same. In the companion chart $z_1 = 1 + e,\ \psi = ew$, the tentative division gives

$$f'_{\text{wrong}} = -3e^{-4}(1 + e)^4, \tag{XV.9.47}$$

$$g'_{\text{wrong}} = e^{-6}(1 + e)^5\big(ew + 1 + e + ew(1 + e)^2\big). \tag{XV.9.48}$$

In the other chart $\psi = e,\ z_1 = 1 + ew$ the transformed coefficients would likewise be

$$f'_{\text{wrong}} = -3e^{-4}(1+ew)^4, \qquad g'_{\text{wrong}} = e^{-6}(1+ew)^5\big(e+1+ew+e(1+ew)^2\big). \tag{XV.9.49}$$

Both numerators are units on the new exceptional. The poles of orders four and six disallow these Weierstrass sections in the required bundles. Also the true $(4, 6)$ point still occurs at $(e, w) = (-1, 0)$, where the exceptional factor is a unit. This is a geometric obstruction that the compact pairing does not see. The interval and the decorated loop now give opposite examples of where gauge data can live: the interval has flavor algebras at its ends and no compact gauge algebra; the loop gauges every compact node.

XV.9.4 Gauge anomaly without an inverse

Which gauge anomalies can two dynamical tensors cancel on a loop with three gauge factors? We can answer this question without a formal inverse of the charge pairing. Start with the ordinary $(1, 0)$ one-loop contributions of the actual vector and hypermultiplets. Let F_i be the normalized gauge curvature $-iF_{i,\text{phys}}/(2\pi)$, and let the defining trace be $\text{tr}_{\mathbf{n}}$. Define

$$s_i = \text{tr}_{\mathbf{n}}\, F_i^2, \qquad q_i = \text{tr}_{\mathbf{n}}\, F_i^4, \qquad p = p_1(T), \qquad c = c_2(R). \tag{XV.9.50}$$

Here q_i is a quartic invariant, not a charge component. The characteristic forms have even degree, so they commute in the expressions below.

For an oriented edge (i, j), the weights of $\mathbf{n} \otimes \overline{\mathbf{n}}$ evaluate as $x_a - y_b$, where x, y are the defining Cartan eigenvalues at the two ends. Both sums of eigenvalues vanish. In the fourth power expansion the terms involving an odd power at one end times a linear power at the other therefore sum to zero. In the quadratic trace the cross term vanishes

for the same reason. We get

$$\sum_{a,b}(x_a - y_b)^2 = n(s_i + s_j), \tag{XV.9.51}$$

$$\sum_{a,b}(x_a - y_b)^4 = n(q_i + q_j) + 6s_i s_j. \tag{XV.9.52}$$

Setting $y = x$ gives the adjoint trace, since the extra zero weights in the defining tensor product make no contribution. Thus $\mathrm{tr}_{\mathrm{adj}}\, F_i^2 = 2ns_i$ and $\mathrm{tr}_{\mathrm{adj}}\, F_i^4 = 2nq_i + 6s_i^2$. The quartic and the square of the quadratic are independent here. For example, the traceless eigenvalue lists $(1, -1, 0, 0)$ and $(1, 1, -1, -1)$, padded with zeros if needed, give the two rows

$$(q, s^2) = (2, 4), (4, 16), \qquad \det \begin{pmatrix} 2 & 4 \\ 4 & 16 \end{pmatrix} = 16. \tag{XV.9.53}$$

These two probes prevent an independent quartic residue from being hidden in a reducible square.

In this curvature convention the gauge-containing part of a full hypermultiplet index is $+\,\mathrm{tr}\, F^4/24 + p\,\mathrm{tr}\, F^2/48$. The vector contributes the negative of the corresponding adjoint terms and $-c\ \mathrm{tr}_{\mathrm{adj}}\, F^2/4$. This is the ordinary tensor-branch index rule. It counts the trace of one oriented complex bifundamental for the full hyper. At each node the two edges together give $2n$ in the defining quadratic and quartic parts, equal to the $2n$ in the vector. For $c = 0$ this leaves

$$[q_i]I_{8,\mathrm{loop}} = (2n - 2n)/24 = 0, \qquad [ps_i]I_{8,\mathrm{loop}} = (2n - 2n)/48 = 0, \tag{XV.9.54}$$

$$I_{8,\mathrm{loop}}\big|_{\mathrm{gauge},\, c=0} = -\frac{1}{4}\sum_i s_i^2 + \frac{1}{4}\sum_{\{i,j\}\ \mathrm{edge}} s_i s_j = -\frac{1}{8} s^t \Omega_A s, \tag{XV.9.55}$$

where s is the column of s_i. The diagonal square comes from the vector; the edge square comes from the one hyper at that crossing. These coefficients reflect $C_i^2 = -2$, $C_i \cdot C_j = 1$, and $K_S \cdot C_i = 0$ in the geometric pairing. For $n = 4$ the three q_i coefficients and three tangent-mixed coefficients vanish separately, leaving three coefficients $-1/4$ and three $+1/4$ in (XV.9.55). Counting both orientations as two full hypers on every edge would instead give $(4n - 2n)/24 = n/12 = 1/3$ at each quartic. That error cannot be repaired by changing a tensor source quadratic in s.

To cancel the surviving form at $c = 0$, quotient by the radical. Let $P\ell = (\ell_1 - \ell_0, \ell_2 - \ell_0)^t$ and let K_A be its Gram matrix. Direct multiplication gives

$$P = \begin{pmatrix} -1 & 1 & 0 \\ -1 & 0 & 1 \end{pmatrix}, \qquad K_A = \begin{pmatrix} 2 & -1 \\ -1 & 2 \end{pmatrix}, \qquad \Omega_A = P^t K_A P. \tag{XV.9.56}$$

The integral kernel is generated by δ and P is surjective over the integers. This gives two dynamical directions in the ordinary rigid construction. The gauge source in the node-aligned basis is $X = s/2$; its paired column is $Y = \Omega_A X$. The Green–Schwarz contribution from the quotient is

$$I_{8,\mathrm{GS}}\big|_{\mathrm{gauge},\, c=0} = \tfrac{1}{2}(PX)^t K_A (PX) = \tfrac{1}{2} X^t \Omega_A X = \tfrac{1}{8} s^t \Omega_A s. \tag{XV.9.57}$$

As an explicit check, the two entries of PX are $(s_1 - s_0)/2$ and $(s_2 - s_0)/2$. The coefficient of s_0^2 in the quotient quadratic is $(2 + 2 - 2)/8 = 1/4$. The coefficient of $s_1 s_2$ comes only from the off-diagonal term, and is $-2/8 = -1/4$. The coefficient of $s_0 s_1$ combines a square and the off-diagonal term, giving $(-4 + 2)/8 = -1/4$. The other three coefficients follow by the exchange of nodes or by the same expansion. It cancels all six reducible terms in (XV.9.55); the tangent-mixed terms already vanish at one loop. Shifting X by a multiple of δ does not change the paired source or the quadratic. Conversely a paired column Y can come from such a source only if it annihilates δ. Over the real numbers this condition is sufficient, since Ω_A is symmetric of rank two and its image is $\delta^\perp$.

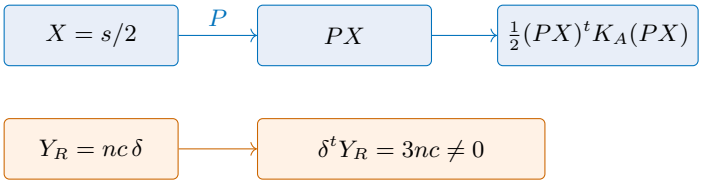


Figure XV.9.5: At vanishing R background, P retains the two source differences and the quotient form cancels the gauge square. The putative paired R source has nonzero evaluation on δ, so it lies outside the image. The null-charge Bianchi identity instead concerns a separate background field.

Now turn on c. The mixed one-loop term is $-nc \sum_i s_i/2$. To cancel it by the same dynamical quotient ansatz, the cross term between $s/2$ and an additional source X_R would have to be its negative. Thus the required paired column is

$$Y_R = \Omega_A X_R = nc(1, 1, 1)^t, \qquad \delta^t Y_R = 3nc. \tag{XV.9.58}$$

It is outside the image for nonzero c. Projecting Y_R onto that image would discard the very source we wanted to match. The obstruction is visible directly on the physical Cartan probes: set $s_0 = s_1 = s_2 = s_*$ for the purpose of evaluating the gauge-mixed polynomial. Then $Ps = 0$, so every cross term from the proposed quotient gauge source vanishes, while the vector contribution is $-3ncs_*/2$. This evaluation compares the two polynomial expressions; it does not identify the gauge factors or their backgrounds. It shows why a projection of the paired source cannot reproduce the mixed term. The failed image condition obstructs the naive full-rank SCFT source ansatz on the LST quotient. It does not diagnose an inconsistent rigid theory.

The ordinary $(1, 0)$ LST background prescription gives a separate Bianchi identity for a background two-form associated to the primitive null string. In its own convention, let H_{LST} be the corresponding three-form field strength. With all other background curvatures turned off, the R-symmetry and tangent part is

$$\frac{dH_{\mathrm{LST}}}{2\pi} = \widehat{\kappa}_R\, c - \widehat{\kappa}_P\, p/4, \tag{XV.9.59}$$

$$\widehat{\kappa}_R = \sum_i \delta_i h_i^\vee, \qquad \widehat{\kappa}_P = -\sum_i \delta_i(\Omega_{ii} - 2). \tag{XV.9.60}$$

For a gauged $\mathfrak{su}(n)$ node $h_i^\vee = n$; this prescription gives $h_i^\vee = 1$ to the ordinary unpaired (-1) and (-2) nodes of the interval. Thus the loop gives $(3n, 0)$, and the two intervals give $(m+1, 2)$. In the latter calculation only the two ends contribute to $\widehat{\kappa}_P$, each with one unit. The loop value changes from $(12, 0)$ to $(15, 0)$ when the common rank changes from four to five. This background projection is not an extra dynamical GS tensor and is not the complete LST anomaly polynomial. It applies here only to the ordinary $(1, 0)$ examples. In particular the $(2, 0)$ product is outside this formula's use here. The interval has no compact gauge anomaly to cancel. Its tangent coefficient is nevertheless nonzero: a compact (-1) end has canonical degree -1, whereas a (-2) interior curve has canonical degree zero. In this convention $\Omega_{ii} - 2 = K' \cdot C_i$ for each rational component, so the sum is also $-K' \cdot F = 2$. This explains why changing m adds one unit to the R projection while leaving the tangent projection unchanged. The source problem changes again when we pass from either full LST to an actual proper retained configuration.

XV.9.5 Taking a limit on a proper subchain

What survives if we make some of the compact curves infinitely large and then contract the rest? There are three things to check: the intersection pairing of the retained curves, a path of positive periods to the proposed limit, and the actual fiber geometry and boundary data at the retained curves. The last check matters because a gauge field that becomes a background may still act on matter at an old crossing.

First consider any of the three graphs in (XV.9.7) and (XV.9.42). For a nonempty proper retained set I, extend a vector x on I by zero to a column $\widetilde{x}$ on all vertices. Then

$$x^t \Omega_{II} x = \widetilde{x}^t \Omega \widetilde{x} = \sum_{\{i,j\} \text{ edge}} (\widetilde{x}_i - \widetilde{x}_j)^2. \tag{XV.9.61}$$

If this vanishes, connectedness makes $\widetilde{x}$ constant, and the zero entry outside I makes it zero. The principal restriction is positive definite, even if the retained set is disconnected. This is a criterion for the compact contraction. A principal restriction retains specific geometric generators; the quotient of the full lattice in (XV.9.56) identifies columns that differ by a multiple of the full fiber. The two operations may give the same matrix in particular coordinates, but they have different meanings and background data.

Let $a_i = \int_{C_i} J_E$ be the Einstein-frame periods, with J_E a reference Kähler form. On the affine surface let H_{sec} be the section meeting only C_0. A relative divisor class with prescribed positive periods is

$$\mathcal{L}_A = A_D H_{\mathrm{sec}} + b_1 C_1 + b_2 C_2, \qquad A_D = a_0 + a_1 + a_2, \tag{XV.9.62}$$

$$b_1 = -(2a_1 + a_2)/3, \qquad b_2 = -(a_1 + 2a_2)/3. \tag{XV.9.63}$$

The degrees on C_1, C_2 follow from $-K_A (b_1, b_2)^t = (a_1, a_2)^t$. Subtracting these degrees

from the fiber sum gives a_0. For the interval put

$$\mathcal{L}_E = A_D H - \sum_{j=1}^{m} \epsilon_j e_j, \tag{XV.9.64}$$

$$(a_L, a_R) = (\epsilon_1, A_D - \epsilon_1) \qquad (m = 1), \tag{XV.9.65}$$

$$(a_L, a_M, a_R) = (\epsilon_2, \epsilon_1 - \epsilon_2, A_D - \epsilon_1) \qquad (m = 2). \tag{XV.9.66}$$

Every positive ordered partition is realized by these degree formulas; for $m = 2$ the inequalities are $0 < \epsilon_2 < \epsilon_1 < A_D$. In both families the degree on a general fiber is A_D. For rational samples, clearing denominators gives a line bundle positive on every component of every fiber, hence relatively ample over the disc. As in Chapter 8, a curvature representative can be made positive in the horizontal directions by adding a form from the disc. This establishes positive reference classes at finite samples, independently of any statement about convergence of a physical metric.

The area identities give a useful scale comparison. For an effective charge ℓ in the leading flux-free calibrated D3 description, keep α' fixed and set $\tau_3 = 1/((2\pi)^3 \alpha'^2)$. Then

$$T(\ell) = \tau_3 \, \ell^t a, \qquad T(\delta) = \tau_3 A_D. \tag{XV.9.67}$$

An area has dimension length squared, so T has dimension inverse length squared. The first equality is the leading calibrated tension for an effective wrapped charge. It does not count stable bound states. The area relation $A_D = \sum_i a_i$ used in it is an independent cycle identity.

For the affine cut take areas $L, \epsilon, 2\epsilon$ in order from C_0 to C_2. For the left interval cut put the same areas in order $\epsilon, 2\epsilon, L$ from left to right. Send $L \to \infty$ first at fixed $\epsilon > 0$, and then take $\epsilon \to 0$ in the retained region. A different operation at fixed total period A_* uses $L = A_* - 3\epsilon$. In the two cases,

$$T(\delta)/\tau_3 = L + 3\epsilon \qquad \text{for the growing complement,} \tag{XV.9.68}$$

$$T(\delta)/\tau_3 = A_* \qquad \text{on the fixed-total-period path.} \tag{XV.9.69}$$

For example $(L, \epsilon) = (10, 1/2)$ and $(100, 1/10)$ give $23/2$ and $1003/10$ in units of τ_3 on the first type of path. Both values would be 10 on the second type at $A_* = 10$, using $L = 10 - 3\epsilon$ at each sample. The fixed-scale face has light retained strings while the full-fiber string stays at finite tension. On the first path it leaves the finite-tension region. Neither conclusion about tension establishes bulk continuum isolation.

In the affine case with C_0 large, contract C_1, C_2 using the actual map back to $u_b v_b = t^3$ in (XV.9.2). Near the contracted point the image of C_0 has the two branches

$$\{v_b = t = 0\}, \qquad \{u_b = t = 0\}. \tag{XV.9.70}$$

Their proper transforms hit the two opposite ends of the retained A_2 chain. In the product with smooth E this is the ordinary local $(2,0)$ A_2 construction. In the decorated model each branch still carries split I_n near its meeting with the retained chain. The leading gauge kinetic coefficient on C_0 grows with L; at fixed normalization its gauging

is turned off in the local limit. Under the ordinary local decoupling and normalizability conditions the $(1,0)$ retained tensor branch is

$$[\mathfrak{su}(n)_L] \;-\; \mathfrak{su}(n) \;-\; \mathfrak{su}(n) \;-\; [\mathfrak{su}(n)_R]. \tag{XV.9.71}$$

The square brackets denote local background flavor algebras. Each old edge still supplies its hypermultiplet; the kinetic scaling removes the old gauge interaction and does not remove the endpoint matter. One can vary the two flavor probes independently in the local SCFT. Turning on just the inherited C_0 background sets them equal. This is a statement about local Lie algebra probes and does not determine a global flavor group.

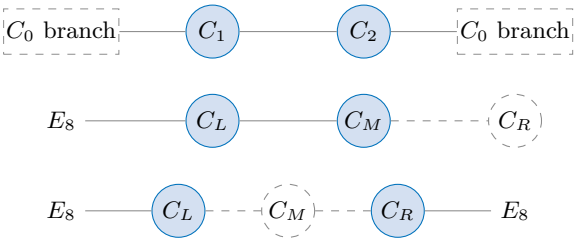


Figure XV.9.6: Retained geometry in three limits. Filled nodes shrink after the large-area limit; dashed nodes have area $L \to \infty$. Top: the same C_0 has a branch meeting each end of the affine cut. Middle: the left interval cut retains the $(-1,-2)$ chain. Bottom: a large middle curve separates the two endpoint neighborhoods. The last picture describes the local geometry; independence of the two physical sectors requires compatible boundary conditions.

The retained gauge calculation illustrates why the endpoint matter matters. Now set $s = (s_1, s_2)^t$ and denote by s_L, s_R the defining traces of the two flavor probes. The gauge-containing one-loop terms are

$$-\frac{1}{8} s^t K_A s + \frac{1}{4}(s_1 s_L + s_2 s_R) - \frac{n}{2} c(s_1 + s_2). \tag{XV.9.72}$$

The two endpoint hypers provide n defining fundamentals each for the quadratic and quartic gauge indices. Without either one, its adjacent gauge node would have an independent quartic residue $-n/24$. To cancel (XV.9.72), the paired source Y for the retained two tensors has the following background part B:

$$Y = K_A s/2 + B, \qquad B = nc \begin{pmatrix} 1 \\ 1 \end{pmatrix} - \tfrac{1}{2} \begin{pmatrix} s_L \\ s_R \end{pmatrix}. \tag{XV.9.73}$$

For a concrete probe, set $s_L = 0$ and keep s_R arbitrary. With $n = 4$ the paired background column is $(4c, 4c - s_R/2)^t$. The GS cross term then gives $-s_2 s_R/4$ and no $s_1 s_R$ term, although the inverse of the retained form is not diagonal. This locality of the gauge cancellation follows because multiplying $K_A s/2$ by K_A^{-1} undoes the gauge pairing. The background square itself still knows about the two ends of the chain. Here K_A is positive definite on the actual retained lattice. In $\frac{1}{2} Y^t K_A^{-1} Y$ the gauge square is

$+s^tK_As/8$ and the cross term is $s^tB/2$, with exactly the signs needed. The inverse is the inverse of this two-curve form, not of Ω_A. Its background-only contribution is

$$\tfrac{1}{2}B^tK_A^{-1}B = n^2c^2 - \tfrac{n}{2}c(s_L+s_R) + \tfrac{1}{12}(s_L^2+s_Ls_R+s_R^2). \tag{XV.9.74}$$

The s_Ls_R term is a background anomaly even after the gauge terms cancel. The flavor-dependent one-loop pieces are separately $n(q_L+q_R)/24 + np(s_L+s_R)/48$, with q_L, q_R the fourth-order defining traces. No purely background term is being required to vanish.

The interval gives a different extraction. Take $a_R = L$ and keep the left curve for $m = 1$, or the left and middle curves for $m = 2$. Equation (XV.9.66) realizes this limit without changing their intersections with the flavor section. After sending L to infinity, the retained contraction is the inverse of the one or two actual point blowups in (XV.9.34)–(XV.9.38). The local base returns to a smooth patch with the noncompact E_8 section and the order-m small-instanton point. The right II^* section meets only the discarded curve. With the ordinary local decoupling premise, the one-ended (-1) and $(-1,-2)$ neighborhoods are the rank-one and rank-two E-string sectors. Alternatively, taking $a_M = L$ at $m = 2$ keeps two disjoint (-1) neighborhoods and the two independent incidences. Their retained form is $\mathrm{diag}(1,1)$; each neighborhood has the rank-one local geometry. The periods give an explicit comparison of the two cuts. For the middle cut choose $a_L = a_R = \epsilon$ and $a_M = L$; for the right cut choose $a_L = \epsilon$, $a_M = 2\epsilon$, $a_R = L$. In (XV.9.66) they correspond to

$$(A_D, \epsilon_1, \epsilon_2) = (L+2\epsilon, L+\epsilon, \epsilon) \qquad \text{for a large middle curve,} \tag{XV.9.75}$$

$$(A_D, \epsilon_1, \epsilon_2) = (L+3\epsilon, 3\epsilon, \epsilon) \qquad \text{for a large right curve.} \tag{XV.9.76}$$

Both satisfy the same relative positivity inequalities for every $L, \epsilon > 0$. They retain different cycles and different flavor incidences. For the first restriction, the two endpoint curves are disjoint even before taking any limit; each II^* section still meets its own end once. For the second restriction only the left II^* section meets a retained curve, while the retained compact joint has intersection one. A product of isolated physical sectors would additionally require factorization of the spectator boundary conditions and decoupling of any mediating modes. That does not follow from $a_M \to \infty$.

We can test the left E-string identification through its E_8-bearing anomaly terms. Set $U = \mathrm{tr}_{\mathrm{adj}}\, F_{E_8}^2/30$, and let c_L, c_R be the second Chern classes of the two $SU(2)$ factors of the transverse rotation bundle, with c_R the R symmetry class in the inflow convention. Inflow at rank m has U-dependent terms only through

$$\frac{m^2}{2}(c_L - c_R)I_4 + \frac{m}{2}I_4^2, \qquad I_4 = \frac{U+p-2c_L-2c_R}{4}. \tag{XV.9.77}$$

The free center-of-mass hypermultiplet is E_8-neutral. The first term supplies $m^2U(c_L - c_R)/8$; the square supplies $mU^2/32 + mU(p-2c_L-2c_R)/16$. The resulting flavor-containing polynomial is

$$\frac{m}{32}U^2 + \frac{m}{16}Up + \frac{m(m-1)}{8}Uc_L - \frac{m(m+1)}{8}Uc_R. \tag{XV.9.78}$$

Independently the geometric principal forms and their inverses are

$$K_{E,1} = (1), \quad K_{E,1}^{-1} = (1), \qquad K_{E,2} = \begin{pmatrix} 1 & -1 \\ -1 & 2 \end{pmatrix}, \quad K_{E,2}^{-1} = \begin{pmatrix} 2 & 1 \\ 1 & 1 \end{pmatrix}. \quad \text{(XV.9.79)}$$

In the ordinary E-string tensor-branch anomaly convention, the paired sources are $Y_1 = c_R - p/4 - U/4$ at the end that meets II^* and $Y_2 = c_R - c_L$ at the second curve when it is present. The negative flavor sign is part of this four-form convention. The geometric incidence itself is positive and selects the first entry only. To isolate the flavor dependence of $\frac{1}{2}Y^t K_E^{-1} Y$, write $Y = B_E - (U/4)\mathbf{e}_L$ with B_E the column at $U = 0$ and $\mathbf{e}_L$ its first unit vector:

$$I_{8,\mathrm{GS}}\big|_U = \frac{U^2}{32}(K_E^{-1})_{11} - \frac{U}{4}\,\mathbf{e}_L^t K_E^{-1} B_E. \quad \text{(XV.9.80)}$$

For rank one the linear term uses $c_R - p/4$. For rank two it uses $2(c_R - p/4) + (c_R - c_L)$. The tensor-branch free fields in this comparison are E_8-neutral. We can therefore compare each coefficient from (XV.9.80) directly with (XV.9.78):

	U^2	Up	Uc_L	Uc_R
$m = 1$	$1/32$	$1/16$	0	$-1/4$
$m = 2$	$1/16$	$1/8$	$1/4$	$-3/4$

(XV.9.81)

In particular the second curve changes the Uc_L term even though it does not meet the flavor section. It contributes through the off-diagonal entry of $K_{E,2}^{-1}$. If one incorrectly attached the same E_8 source to both curves, the quadratic coefficient would be $(2 + 1 + 1 + 1)/32 = 5/32$ instead of $1/16$. For the middle cut there is a separate incidence calculation. With independent curvatures U_L, U_R on the two II^* sections, the paired flavor column is $-(U_L, U_R)^t/4$ in the two retained geometric blocks. With the positive form $\mathrm{diag}(1, 1)$ its square contribution is

$$\frac{U_L^2 + U_R^2}{32}. \quad \text{(XV.9.82)}$$

There is no cross term from this restricted tensor lattice. This calculation is compatible with the two local rank-one neighborhoods; it cannot establish physical factorization. In the one-ended rank-two cut the corresponding coefficients are $U_L^2/16$ and zero for the absent right source. Thus an equality of total retained rank would miss the different flavor couplings. The one-ended inflow comparison checks four flavor-bearing coefficients for each of two extracted SCFTs. It is not a calculation of the complete anomaly of either parent interval.

XV.9.6 Changing a tuning and testing it

Can we raise the order on just one compact curve and make up the matter with fundamentals? A quick anomaly count can suggest what matter would be needed, but a proposed set of orders must first be the divisor of an actual section. We compare a

uniform change that comes from the cubic with a nonuniform change that cannot occur on this base.

Replace t^4 by t^5 in (XV.9.12). The quadratic term in the Tate coordinates is unchanged, because only a_6 changes. The same roots of (XV.9.14) distinguish the two branches. The discriminant and the node model at each base joint become

$$\Delta_5 = 27u^5v^5(4+u^5v^5), \qquad ab = z^5(z+\mu)^5. \tag{XV.9.83}$$

The auxiliary surface has four exceptional curves and its proper cubic transform. Hence the product has $3\cdot 5$ ordinary double points, each crossing has five old and five inserted components, and each hyper is a full $(\mathbf{5},\overline{\mathbf{5}})$. The edge's quartic trace changes from $4(q_i+q_j)+6s_is_j$ to $5(q_i+q_j)+6s_is_j$. Each vector now contributes $10q_i+6s_i^2$ before its index coefficient. The defining quartic cancellation therefore persists, as does the normalized reducible form, because the coefficients of s_i^2 and s_is_j did not change.

For a further test replace a_6 by t^6 in the same cubic. The generic order of Δ on each base curve becomes six; the total order at each joint becomes twelve. The residual factor is $27(4+t^6)$, still nowhere zero on the disc. The charts (XV.9.19) have six indices and the point blowups reduce $ab=t^6$ through the exponents four and two. Thus the ordered product construction has $3\cdot 6$ ordinary double points to resolve. There are six old and six inserted curves at each crossing. This verifies the change using the equation as well as the equal orders. One can summarize the variation as

n	$\operatorname{ord}_{C_i}\Delta$	$\operatorname{ord}_{C_i\cap C_j}\Delta$	ordinary double points of Z_n
4	4	8	12
5	5	10	15
6	6	12	18

(XV.9.84)

The extra $n=6$ example stays in the same fixed frame and uses the same resolution argument. In particular, a positive cover test requires the leading Tate coefficient and its two actual roots; an I_n order alone cannot establish it. The distinction can be seen even without changing the threefold. On a patch of a compact curve take a nonconstant holomorphic unit $\chi = 1+z$ near $z=0$. Change the frame of the Tate equation by $\xi=\chi^2\xi'$, $\eta=\chi^3\eta'$. Dividing the equation by χ^6 gives

$$(\eta')^2 + \frac{2\sqrt{3}}{\chi}\xi'\eta' = (\xi')^3 + \frac{t^n}{\chi^6}, \qquad b_2' = \frac{12}{\chi^2}. \tag{XV.9.85}$$

It has roots $\pm 2\sqrt{3}/\chi$. These vary in the chosen patch and can be read as functions in the residue field when z is the rational coordinate on the curve. They still distinguish the branches over the generic point. In particular, rejecting this frame as an input to a test that asks for $b_2=12$ and the two fixed constant roots would be correct. Calling the cover nonsplit on that basis would be wrong. The local frame change does not give new global coefficients or new singular fibers.

Now suppose a putative multiplicative model on S has generic orders r_i on the three compact divisors. Remove those orders from its actual discriminant. The rest must be an effective divisor R_Δ without any C_i as a component:

$$\operatorname{div}(\Delta) = \sum_i r_iC_i + R_\Delta, \qquad \big(R_\Delta\cdot C_i\big)_i = \Omega_A r. \tag{XV.9.86}$$

The second equality follows because the discriminant is a section of $-12K_S$, whose degree on each C_i is zero. The degree of an effective divisor on a proper curve it does not contain is the sum of its local intersection multiplicities, all nonnegative. But their total is

$$\sum_i R_\Delta \cdot C_i = \delta^t \Omega_A r = 0. \tag{XV.9.87}$$

Thus each degree must vanish. By (XV.9.7) the column r must be constant. A uniform tuple satisfies this necessary condition; existence still requires a section, a cover and the crossing geometry. The cubic supplies them for the rows above.

For $r = (4, 4, 5)^t$, the proposed residual degrees are

$$\Omega_A r = (-1, -1, 2)^t. \tag{XV.9.88}$$

The first two entries already contradict effectivity. The obstruction precedes the choice of a Tate frame. It also explains why the simple field-theory repair cannot work: with one ordinary bifundamental per edge and only extra fundamentals, the independent quartic equation would demand

$$N_i^{\text{fund}} = 2r_i - r_j - r_k = (\Omega_A r)_i, \qquad \{i, j, k\} = \{0, 1, 2\}. \tag{XV.9.89}$$

At each low-rank node that is a negative number of fundamentals. This count assumes precisely the stated matter types. The effectivity calculation gives the obstruction to the specified multiplicative discriminant orders without that assumption about how one would repair the quiver.

For comparison, the uniform $r = (5, 5, 5)^t$ has zero degree at each node, not just zero total. Its residual factor $27(4 + t^5)$ is a unit, and the cubic realizes exactly that absence of residual intersections. The failure of the nonuniform tuple is more specific than a negative total degree: the positive value 2 on C_2 cannot compensate for a negative intersection on C_0. Intersection multiplicities are tested curve by curve. Moving a residual branch away from a joint might remove one positive contribution, but cannot make any contribution negative.

The two ways to change these examples test different geometry. On the loop, (XV.9.88) obstructs an effective discriminant. On the interval, the wrong center in (XV.9.48) fails at the level of the two coefficient sections, even though its compact classes and their negative intersections agree with those of the correct resolution. The comparison shows why one starts with sections and their transforms when proposing a new construction.

Finally the resolved product has two actual projection morphisms. If $\rho : X_n \to Z_n$ is the ordered resolution and π_S, π_T are the maps of the surfaces to the disc, then

$$p_S = \mathrm{pr}_S \circ \rho : X_n \longrightarrow S, \qquad p_T = \mathrm{pr}_{T_n} \circ \rho : X_n \longrightarrow T_n, \qquad \pi_S \circ p_S = \pi_T \circ p_T. \tag{XV.9.90}$$

Over $t \neq 0$ the blowups are absent and the fiber over t is the product of the two smooth genus-one curves. Figure XV.9.7 records the two choices of base. The first projection takes the I_3 surface as its base; the second takes the resolved I_n surface. The ordered centers can be used for both maps because they are centers in the product. One can check the common smooth region without following any exceptional curves. For fixed

$t = t_* \neq 0$ write S_{t_*} and $(T_n)_{t_*}$ for the two surface fibers. Then

$$X_n\big|_{t_*} = S_{t_*} \times (T_n)_{t_*}, \quad (p_S)^{-1}(s) \cong (T_n)_{t_*}, \quad (p_T)^{-1}(d) \cong S_{t_*} \tag{XV.9.91}$$

for $s \in S_{t_*}$ and $d \in (T_n)_{t_*}$. The two curves appear in opposite roles. Their areas and the wrapped-brane interpretations have not been identified by this algebraic statement. Having these maps specifies the geometric input for the circle-reduction comparison in Chapter 10. No identification of the two six-dimensional theories or exchange of their charges follows from the maps alone.

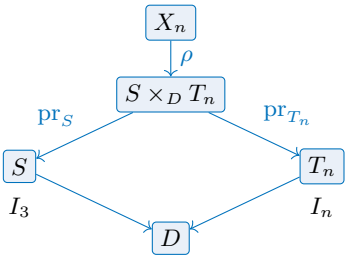


Figure XV.9.7: The resolution ρ is followed by either product projection. Both compositions down to the disc give the same t. The labels below the surfaces are their central fibers over $t = 0$, rather than the elliptic fibers of the threefold projections.

XV.9.7 Exercises

1. **Transport the split calculation.** Use the explicit cubic with $n = 7$. Derive b_2 and both cover roots, the residual factor, the generic and crossing orders of (f, g, Δ), the number of conifolds and the number of components in each reduced crossing fiber. Explain how the tangent test differs from the order test.

2. **Blow up the wrong point.** In the $m = 2$ interval move the second center to $(z_1, \psi) = (2, 0)$. Use the companion chart $z_1 = 2 + e$, $\psi = ew$. Give the generic orders of the putative f', g' along the new exceptional and locate the remaining nonminimal point in (e, w) coordinates. Explain why the compact pairing is unchanged.

3. **Remove one edge.** For the hypothetical rank-six loop spectrum omit the hyper on $(0, 2)$. Compute the one-loop coefficient rows of q_i and ps_i, then of s_i^2 and of $s_0 s_1, s_1 s_2, s_0 s_2$. Use $c = 0$. Explain which residual terms cannot be changed by the gauge GS square.

4. **Keep the two flavor probes distinct.** Take the rank-five cut C_0. Find the background part of the paired source with s_R alone and with both probes. Give the $s_L s_R$ coefficient of the background GS term and check the one-loop and GS gauge cross terms at the right end.

5. **Compare interval cuts.** For $m = 2$, first remove the middle curve and retain the two endpoints. Then remove the right curve and retain the left two. Use $(a_L, a_M, a_R) = (2, 17, 3)$ and $(2, 3, 17)$, respectively, as finite samples. Compute the restricted forms, the two flavor incidence columns, each retained U_L^2, U_R^2 coefficient and the full-fiber area at the sample. Explain the growing-complement limits.

6. **Test residual effectivity.** Compute the degree rows for $r = (5, 4, 4)^t$ and $r = (6, 6, 6)^t$. Explain which survives the test and why an explicit Weierstrass witness is still needed.

7. **Distinguish three charge operations.** Compare the full effective null charge, the quotient by the radical, and the principal restriction to retained curves. Explain why equal quotient charges need not give equal tensions and why a positive principal block does not supply a new tensor for the parent LST.

Use `benchmark/tasks.json` for the JSON fields and `benchmark/PROTOCOL.md` for submission. Written explanations and the final problem are human-assessed.

Status and sources

§1. The affine base and the constant fiber. The reduced base, canonical trivialization and intersection form are [MATH]. The gauge-free product with the stated ordinary rigid limit is [GEO-E]; see Bhardwaj et al. (2016), arXiv:1511.05565v3, §3.1.2 and §4.1, eq. (4.1). The explicit base is the family from Chapter 8.

§2. Split fibers and ordinary matter. The Tate coefficients, surface and threefold resolutions, fiber counts and projection maps are [MATH]. For the monodromy test see Katz, Morrison, et al. (2011), arXiv:1106.3854v1, §4.2, eq. (4.5), and Appendix A. The charged matter of the exact two-stack slice is [GEO-E]; see Katz and Vafa (1997), hep-th/9606086v1, §4.1, eq. (4.1). The ordinary rigid LST interpretation is [DEC]; see Bhardwaj et al. (2016), §4.2.

§3. The rational interval. The two crepant base blowup sequences, endpoint and residual intersections, and path forms are [MATH]; see Bhardwaj et al. (2016), Appendix F, eq. (F.1) for the starting coefficients, and Chapter 8 for the specialized family and ordinary local II^* resolution. The ordinary flavor interpretation is [GEO-E]; see §4.2, eq. (4.3) and Figure 3 of the same source. The exponent m counts the actual left blowups in these charts.

§4. The quotient and the background projection. Gauge and tangent-mixed cancellation in the stated projection is [ANOM]; see Ohmori, Shimizu, Tachikawa, and Yonekura (2014), arXiv:1408.5572v2, Appendix A, eqs. (A.2)–(A.4), for the index, and Bhardwaj et al. (2016), §2, for the distinction between null and dynamical tensors. The image test is [MATH]. The hatted background projection is [ANOM] in Del Zotto and Ohmori (2021), arXiv:2009.03489v3, §3, eqs. (3.1)–(3.6). We use the stated Weierstrass, integral curvature and curve-pairing conventions; the hatted coefficients use their source convention.

§5. Proper restrictions and extracted sectors. Positive proper blocks and the period paths are [MATH]; the calibrated leading wrapped tension is [GEO-E] with the Chapter 2 normalization. The affine and interval local SCFT interpretations are [DEC]; see Bhardwaj et al. (2016), §3.1.2, §4.2 and the opening of §5. The retained flavor-dependent comparisons are [ANOM]. For the full-rank GS rule see Ohmori, Shimizu, Tachikawa, and Yonekura (2014), §3.1. For the E_8 terms compare Ohmori, Shimizu, and Tachikawa (2014), arXiv:1404.3887v2, eqs. (1.1)–(1.5), with Apruzzi et al. (2018), JHEP 02 (2018) 157, Appendix A.2.1, eqs. (A.26)–(A.31).

§6. Changing the order. The equal-rank residual obstruction and the changed families are [MATH]. See also Bhardwaj et al. (2016), §7.2.1 and §9.1, for the general multiplicative comparison. The matter and gauge calculation in this section uses the same localized matter and gauge-sector hypotheses stated above. The projections leave the duality question to the next chapter.

References

Apruzzi, F., J. J. Heckman, and T. Rudelius (2018). "Green-Schwarz Automorphisms and 6D SCFTs". In: *JHEP* 02, p. 157. arXiv: 1707.06242 [hep-th].

Bhardwaj, L. et al. (2016). "F-theory and the Classification of Little Strings". In: *Phys. Rev. Lett.* 116, p. 161601. DOI: 10.1103/PhysRevLett.116.161601. arXiv: 1511.05565 [hep-th].

Del Zotto, M. and K. Ohmori (2021). "2-Group Symmetries of 6d Little String Theories and T-duality". In: arXiv: 2009.03489 [hep-th].

Katz, S., D. R. Morrison, et al. (2011). "Tate's algorithm and F-theory". In: *JHEP* 08, p. 094. arXiv: 1106.3854 [hep-th].

Katz, S. and C. Vafa (1997). "Matter from geometry". In: *Nucl. Phys. B* 497, pp. 146–154. arXiv: hep-th/9606086.

Ohmori, K., H. Shimizu, and Y. Tachikawa (2014). "Anomaly polynomial of E-string theories". In: *JHEP* 08, p. 002. arXiv: 1404.3887 [hep-th].

Ohmori, K., H. Shimizu, Y. Tachikawa, and K. Yonekura (2014). "Anomaly polynomial of general 6D SCFTs". In: *PTEP* 2014, 103B07. arXiv: 1408.5572 [hep-th].

Chapter XV.10

Circle compactification, five-dimensional theories and LST T-duality

XV.10.1 Two elliptic projections of one geometry

Which cycle of a Calabi–Yau threefold supplies the momentum of the emergent F-theory circle? The answer requires a projection and a section. For the product from Chapter 8 there are two concrete choices. We will calculate their marks on the same compact curves and then see what the two choices do to the six-dimensional strings and the five-dimensional particles. The example requires the ordinary circle dictionary of XIV.1, the split multiplicative fibers of Volume IV, and the tension of a wrapped D3-brane from Chapter 2.

Let $D = \{|t| < 1\}$ be a disc. Write S for the crepant resolution of the projective Weierstrass family with projection $t : S \to D$ and section o_S at infinity. Write E for a fixed smooth cubic with point at infinity o_E. The defining equations in affine coordinates are

$$E : \; y_E^2 = x_E^3 - x_E, \qquad S_{\mathrm{W}} : \; y^2 = x^3 - 3x + 2 + t^3. \tag{XV.10.1}$$

The holomorphic two-form on the regular chart of S_{W} is proportional to $dt \wedge dx/y$ and extends through the crepant resolution. Together with the nowhere vanishing one-form on E it supplies a nowhere vanishing three-form on $X = E \times S$.

To distinguish the fibers, use $\Delta = 4f^3 + 27g^2$ for $y^2 = x^3 + fx + g$, and $j = 1728(4f^3)/\Delta$. In the two factors these are

$$\Delta_E = -4, \qquad j_E = 1728, \tag{XV.10.2}$$

$$\Delta_S = 27t^3(4 + t^3), \qquad j_S = -\frac{6912}{t^3(4 + t^3)}. \tag{XV.10.3}$$

The second discriminant has only one zero in D, since $|t^3| < 1$. Its varying j distinguishes the generic S_t from E. Exchanging the roles of these curves means changing the map out of X; it does not require an automorphism of X that exchanges the two elliptic curves.

For the first map retain the point of S. For the second map retain the point of E and only the projection of S to the disc:

$$p_A : X \longrightarrow S, \quad (e,s) \longmapsto s, \qquad s_A(s) = (o_E, s), \tag{XV.10.4}$$

$$p_B : X \longrightarrow E \times D, \quad (e,s) \longmapsto (e, t(s)), \qquad s_B(e,t) = (e, o_S(t)). \tag{XV.10.5}$$

The fibers of the two maps are respectively E and S_t; the section in each row picks the point at infinity of that fiber. Both maps are proper with connected fibers, by the product with a compact elliptic curve in the first row and the base change of the proper elliptic surface in the second. The threefold itself is noncompact. The two base surfaces are different even at the level of where one finds compact curves.

At $t = 0$ the surface fiber has its node at $(x, y) = (1, 0)$. Near that point choose a holomorphic square root of $x + 2$ and set $u = y - (x-1)\sqrt{x+2}$, $v = y + (x-1)\sqrt{x+2}$. The coordinates are independent at the node, since the derivatives of the second terms with respect to x are $\mp\sqrt{3}$. The equation becomes

$$x^3 - 3x + 2 = (x-1)^2(x+2), \qquad uv = t^3. \tag{XV.10.6}$$

This local surface has an A_2 singularity. Its minimal resolution inserts a chain of two rational curves, C_1, C_2, between the two branches of the normalized nodal cubic. The proper transform C_0 is also rational, and meets opposite ends of the chain. The central fiber is a reduced I_3; the section meets C_0 transversely at a point away from the nodes. The square of each component follows without a normal-coordinate calculation: the entire fiber is equivalent to a nearby disjoint fiber. Hence

$$0 = (C_0 + C_1 + C_2) \cdot C_i = C_i^2 + 2, \qquad C_i^2 = -2. \tag{XV.10.7}$$

One can also see the multiplicities in local charts of the resolution of $uv = t^3$. For $j = 0, 1, 2$ take a chart (U_j, V_j) with monomials

$$u = U_j^{j+1} V_j^{\,j}, \qquad v = U_j^{2-j} V_j^{\,3-j}, \qquad t = U_j V_j. \tag{XV.10.8}$$

These obey $uv = t^3$. The consecutive overlaps are $U_{j+1} = 1/V_j$, $V_{j+1} = U_j V_j^2$ for $V_j \neq 0$. Thus the curve $U_j = 0$ is glued to $V_{j+1} = 0$ through the coordinate inversion along the curve. For $j = 0, 1$ this gives a projective line. In the middle chart they meet at $U_1 = V_1 = 0$. The other two coordinate axes, $V_0 = 0$ and $U_2 = 0$, map to the two branches of the original node. The global proper transform joins these two ends. This local calculation accounts for the three distinct intersections of the central fiber; $t = U_j V_j$ also shows that each branch occurs with multiplicity one.

Choose $e_* \in E$ and $s_* \in S$ on a smooth fiber, and put $F_E = E \times \{s_*\}$, $c_i = \{e_*\} \times C_i$. The class of $\{e_*\} \times S_t$ is $F_S = c_0 + c_1 + c_2$, because fibers over different disc points are homologous and the central multiplicities are one. Use the section divisors $Z_A = \{o_E\} \times S$, $Z_B = E \times o_S(D)$, and the exceptional divisors $D_i = E \times C_i$ for $i = 1, 2$. The

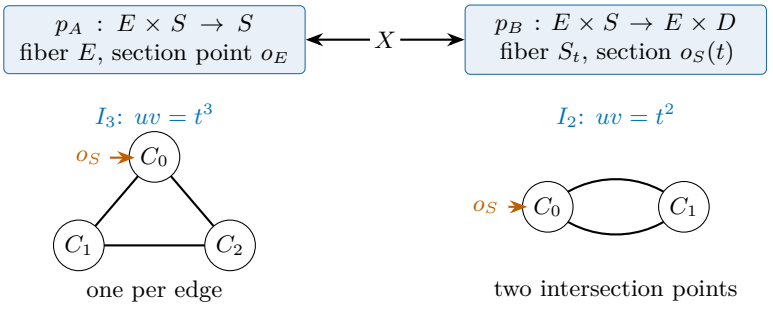


Figure XV.10.1: The two projections of $E \times S$. The upper row shows what each map forgets and which point its section selects. The lower left shows the three intersections of the reduced I_3 fiber. In the I_2 control on the right the two curves meet at two distinct points. In both cases the section meets the proper transform C_0.

entries of the following matrix are degrees of the divisor line bundles restricted to the corresponding compact curves:

	F_E	c_0	c_1	c_2
Z_A	1	0	0	0
Z_B	0	1	0	0
D_1	0	1	-2	1
D_2	0	1	1	-2

(XV.10.9)

For example $\mathcal{O}_X(D_1)$ is pulled back from $\mathcal{O}_S(C_1)$. Its restriction along F_E is a constant line, while along c_2 its degree is $C_1 \cdot C_2 = 1$. The first row instead comes from pulling back the point divisor on E; only F_E projects with degree one to E. The section in the second row measures the degree along the full S-fiber, but does not meet either of the two exceptional curves. These rules reproduce the entire matrix.

The determinant of (XV.10.9) is 3. An integral relation among the four curves would give a vector in its kernel, so these curves generate a rank-four free subgroup of the curve homology. The determinant computes the index of its evaluation image in the four-dimensional target $\mathbb{Z}^4$. It does not establish saturation in the full homology of the threefold, or determine a gauge group or line-operator lattice. In particular a nontrivial cokernel of the displayed map does not establish that a curve with a missing evaluation vector exists.

The choice of basis (F_E, F_S, c_1, c_2) separates the two section degrees from the roots. In fact $c_0 = F_S - c_1 - c_2$, an integral basis change with inverse over the integers. If q is a class in the displayed lattice, then

$$q = dF_E + b_0 c_0 + b_1 c_1 + b_2 c_2 \tag{XV.10.10}$$

$$= dF_E + b_0 F_S + \beta_1 c_1 + \beta_2 c_2, \quad \beta_i = b_i - b_0, \tag{XV.10.11}$$

$$(Z_A \cdot q, Z_B \cdot q) = (d, b_0). \tag{XV.10.12}$$

The remaining two evaluations then take the form

$$\begin{pmatrix} D_1 \cdot q \\ D_2 \cdot q \end{pmatrix} = \begin{pmatrix} -2 & 1 \\ 1 & -2 \end{pmatrix} \begin{pmatrix} \beta_1 \\ \beta_2 \end{pmatrix}. \tag{XV.10.13}$$

In the marked momentum and null-string sublattice we will use $(n_A, w_A) = (d, b_0)$ and $(n_B, w_B) = (b_0, d)$, retaining β as separate relative coordinates. This assignment follows physically in Section XV.10.5. For $(d, b_0, b_1, b_2) = (2, 3, 1, 4)$, the relative coordinates are $(-2, 1)$, so the four evaluations are $(2, 3, 5, -4)$. A negative relative coordinate can arise even for a sum of effective components, because we subtracted a multiple of the full fiber. The charge vector alone is not a one-particle existence claim.

The index has a useful operational meaning. Suppose we are given the four evaluations and want to reconstruct the charge in this basis. Write $u_1 = D_1 \cdot q$, $u_2 = D_2 \cdot q$. The two section degrees already give d, b_0; the finite block gives

$$\beta_1 = -\frac{2u_1 + u_2}{3}, \qquad \beta_2 = -\frac{u_1 + 2u_2}{3}. \tag{XV.10.14}$$

So a pair of Cartan evaluations with $u_1 \not\equiv u_2 \pmod 3$ cannot come from this displayed span. For instance the marks $(u_1, u_2) = (1, 0)$ would require the fractional coefficients $(-2/3, -1/3)$ here. By contrast $(5, -4)$ passes the congruence and reproduces $(-2, 1)$. This is a condition on an evaluation image, not on an independently specified probe charge. We inverted only the finite two-by-two matrix. Inverting the full fiber intersection form would fail, since it annihilates the full-fiber vector.

Now replace t^3 by t^2 in (XV.10.1). The local equation is $uv = t^2$; one exceptional curve replaces the two-curve chain, meeting the two original branches at separate points. Here the analogous calculation is

$$Q_{I_2} = \begin{pmatrix} -2 & 2 \\ 2 & -2 \end{pmatrix}, \qquad \begin{array}{c|ccc} & F_E & c_0 & c_1 \\ \hline Z_A & 1 & 0 & 0 \\ Z_B & 0 & 1 & 0 \\ D_1 & 0 & 2 & -2 \end{array} \tag{XV.10.15}$$

The index of this evaluation image is two. Counting only one intersection, with the -2 self-intersections held fixed, would give $D_1 \cdot F_S = -1$. That contradicts the disjoint nearby fiber and would give the full fiber a spurious Cartan charge. A section fixes a marking, whereas the vanishing evaluation on the entire fiber follows from the geometry. We next determine which masses a physical circle assigns to such marked curves.

XV.10.2 Momentum and winding on a circle

A finite string tension gives a light winding sector on a small circle. To compare it with momentum on a large circle, we need the distinction between a particle propagating along a compact direction and a string lying along it. Start with an external spacelike circle of proper circumference $2\pi R$. Let $\theta \sim \theta + 2\pi$, so its metric is $R^2 d\theta^2$. For periodic fields in the absence of Wilson or other twists, $-i\partial_\theta$ has integer eigenvalues. A

six-dimensional particle of mass M gives a five-dimensional mode with

$$\varphi(x,\theta)=\sum_{n\in\mathbb{Z}}\varphi_n(x)e^{in\theta}, \qquad p_{\hat{\theta}}=\frac{n}{R}, \tag{XV.10.16}$$

$$E^2=\boldsymbol{p}^2+M^2+\frac{n^2}{R^2}, \qquad m_n=\sqrt{M^2+\frac{n^2}{R^2}}. \tag{XV.10.17}$$

The five-dimensional rest mass m_n is the energy at zero noncompact spatial momentum $\boldsymbol{p}$. A pure KK gap $1/R$ refers to a mode of a massless parent. At $(M,n,R)=(1,2,3/2)$, the massive-parent result is $5/3$, while setting $M=0$ gives $4/3$. The integer is signed even though either energy is even in n.

For winding let a string of tension T lie straight along the external circle, with map $\theta(\sigma)=w\sigma$ for $0\le\sigma<2\pi$ and no other excitation. In the static gauge the energy is tension times the induced length:

$$L_w=\int_0^{2\pi}R|\partial_\sigma\theta|\,d\sigma=2\pi R|w|, \qquad m_w=2\pi RT|w|. \tag{XV.10.18}$$

The sign records the orientation of the wrapped string. In contrast to $p_{\hat{\theta}}$, the string length depends on the metric even before any momentum is excited. We compare separate pure sectors using (XV.10.17) and (XV.10.18); they give no rule for a mixed state, its worldsheet level matching, or its degeneracy.

The two expressions also show how to find the circle scale from the spectrum when only pure energies are supplied. For nonzero n,w of a massless parent and a straight string, respectively,

$$\frac{m_n}{|n|}=R^{-1}, \qquad \frac{m_w}{|w|}=2\pi RT, \qquad \frac{m_nm_w}{|nw|}=2\pi T. \tag{XV.10.19}$$

If T is fixed, changing R to $(2\pi TR)^{-1}$ exchanges the two unit gaps. One cannot infer this exchange by measuring the lightest mode of a massive parent and calling it $1/R$. Nor does this calculation identify which string in the theory supplies T. We will determine that string geometrically for both projections.

The external circle extends along both five-branes in the ordinary separated NS5 construction. It is distinct from the transverse circle used when an M5 system is related to IIA, and from either one-cycle of the auxiliary F-theory elliptic fiber. The external circle is the one along which momentum becomes winding in the type-II comparison. Figure XV.10.2 shows why a relative D2 strip and a stretched D1 can test this circle map: the D2 wraps the longitudinal direction and spans the transverse separation L. Dualizing along its wrapped direction removes that direction from its worldvolume.

Use an ordinary untwisted isometry, periodic spin structure, and no metric or two-form mixing along the dualized direction in the ambient comparison. In common asymptotic string units $\ell_s^2=\alpha'$, Buscher duality sends the IIA radius R_{IIA} and coupling g_{IIA} to

$$R_{\mathrm{IIB}}=\frac{\ell_s^2}{R_{\mathrm{IIA}}}, \qquad g_{\mathrm{IIB}}=g_{\mathrm{IIA}}\frac{\ell_s}{R_{\mathrm{IIA}}}. \tag{XV.10.20}$$

The spectator block is unchanged in these string units. With the underlying fundamental tension $1/(2\pi\ell_s^2)$, the dual unit winding mass is $R_{\mathrm{IIB}}/\ell_s^2=1/R_{\mathrm{IIA}}$. This check uses

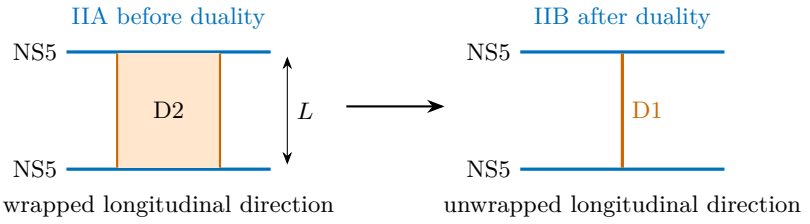


Figure XV.10.2: A relative D2 strip wraps the longitudinal circle and stretches between the two NS5-branes; longitudinal T-duality leaves a relative D1 on the transverse segment. The transverse M circle and auxiliary torus cycles are separate from this worldvolume operation. The diagram represents brane directions, not a metric in a five-brane core.

the intrinsic string tension in this weak NS5 realization; it is not a conversion between arbitrary native metrics of the two F-theory lifts.

The signed comparison at finite radius uses the orientation of the dualized circle. Choose it so that a positive pure momentum in IIA gives positive winding in IIB. The opposite assignment is then obtained by orientation reversal, and the exchange preserves the pair of integer labels. For instance, at $\ell_s = 2$, $R_{\mathrm{IIA}} = 3$ and signed momentum $n = -2$, the corresponding pure IIB winding gives

$$n = -2, \qquad w' = -2, \qquad \frac{|n|}{R_{\mathrm{IIA}}} = \frac{2}{3} = \frac{|w'|R_{\mathrm{IIB}}}{\ell_s^2}. \tag{XV.10.21}$$

The equality of positive masses would survive a change of the sign in only one label. It is therefore essential to state the orientation rule separately from the energy test. The geometric section markings later supply exactly such signed labels.

The relative D2 and D1 use the ordinary leading brane tensions. With separation L measured in the common spectator string metric, the wrapped strip and segment have masses

$$m_{\mathrm{D2}} = (2\pi R_{\mathrm{IIA}})L\,\frac{1}{(2\pi)^2 g_{\mathrm{IIA}}\ell_s^3} = \frac{R_{\mathrm{IIA}}L}{2\pi g_{\mathrm{IIA}}\ell_s^3}, \tag{XV.10.22}$$

$$m_{\mathrm{D1}} = L\,\frac{1}{2\pi g_{\mathrm{IIB}}\ell_s^2} = \frac{R_{\mathrm{IIA}}L}{2\pi g_{\mathrm{IIA}}\ell_s^3}. \tag{XV.10.23}$$

The equalities test the relative-sector identification away from coincident branes. For $(g_{\mathrm{IIA}}, \ell_s, R_{\mathrm{IIA}}, L) = (1/5, 2, 3, 7)$ one obtains $g_{\mathrm{IIB}} = 2/15$, $R_{\mathrm{IIB}} = 4/3$, and both masses are $105/(16\pi)$. The two factors of length in the first line and the one in the second give the same dimension of energy, since the branes have different tensions.

The finite weak limit keeps the intrinsic tension while separating it from the ambient gravitational scale. With ℓ_s fixed, scaling the separation along with the coupling is necessary if the stretched sector is to stay at a finite mass: its six-dimensional tension is proportional to L/g_{IIA}. For instance, with the other parameters of the preceding

example held fixed, replacing g_{IIA} by $z/5$ and L by $7z$ gives

$$g_{\mathrm{IIB}} = \frac{2z}{15}, \qquad \frac{m_{\mathrm{D2}}}{2\pi R_{\mathrm{IIA}}} = \frac{35}{32\pi^2}, \qquad m_{\mathrm{D1}} = \frac{105}{16\pi}. \tag{XV.10.24}$$

The first equality tests the ambient coupling; the second and third test the relative probe. At fixed separation instead, both relative masses would grow as $1/z$. Keeping the fundamental tension alone would then retain the null-string scale while losing the finite stretched sector of this example.

For a limiting test write $(g_{\mathrm{IIA}}, \ell_s, L, R_{\mathrm{IIA}}) \sim (z^a, z^b, z^c, z^d)$ as $z \to 0^+$. The exponents of the dual coupling, dual radius, intrinsic tension and relative mass are respectively

$$a + b - d, \qquad 2b - d, \qquad -2b, \qquad d + c - a - 3b. \tag{XV.10.25}$$

At $(a, b, c, d) = (1, 0, 1, 0)$, both ambient couplings tend to zero, the radii and fundamental tension stay finite, and the wrapped relative mass stays finite because L/g_{IIA} is fixed. If we change only d to 2, the dual coupling grows as z^{-1} and the dual radius grows as z^{-2}. The wrapped relative mass now tends to zero. Thus the weak finite-radius argument must precede a decompactification limit; one cannot use weak coupling in both ambient frames on this changed path. The survival and identification of the decoupled ordinary NS5 relative sectors is physical input to the comparison. The powers alone do not establish it.

XV.10.3 The M-theory description

The product has no preferred longitudinal radius until we choose the auxiliary fiber and a mass metric. The normalization can be derived first on a smooth rectangular torus. Let r_{11}, r_{10} be the proper radii in the eleven-dimensional metric, with no warping or off-diagonal terms. Let ℓ_p be the eleven-dimensional Planck length. A membrane wrapping both cycles once has area and static rest mass

$$A_f = (2\pi)^2 r_{11} r_{10}, \qquad T_{\mathrm{M2}} = \frac{1}{(2\pi)^2 \ell_p^3}, \qquad m_{11} = T_{\mathrm{M2}} A_f. \tag{XV.10.26}$$

The rest action is $-m_{11} \int ds_{11}$. The radius in the last frame will be read by comparing this action to a pure KK action, and not by identifying one torus circumference with the final circumference.

Reduce first along the r_{11} cycle. The once-wrapped M2 becomes the IIA fundamental string. Write $ds_\sigma = \lambda\, ds_{11}$ in the spectator block for a constant positive factor λ, including the remaining r_{10} circle before dualizing it. Matching the worldsheet areas gives the tension transformation, while matching the spectator length gives the IIA radius:

$$T_{\mathrm{F1},\sigma}\, \lambda^2 = 2\pi r_{11} T_{\mathrm{M2}}, \qquad R_{\mathrm{IIA},\sigma} = \lambda r_{10}. \tag{XV.10.27}$$

There is one power of the metric conversion for each worldsheet direction. Using

$\alpha'_\sigma = (2\pi T_{\mathrm{F1},\sigma})^{-1}$ in the rectangular Buscher step then gives

$$R_{\mathrm{IIB},\sigma} = \frac{\alpha'_\sigma}{R_{\mathrm{IIA},\sigma}} = \frac{\lambda}{T_{\mathrm{M2}} A_f}, \tag{XV.10.28}$$

$$m_\sigma = \frac{m_{11}}{\lambda} = \frac{1}{R_{\mathrm{IIB},\sigma}}, \qquad R_{\mathrm{IIB},11} := \frac{R_{\mathrm{IIB},\sigma}}{\lambda} = \frac{1}{T_{\mathrm{M2}} A_f}. \tag{XV.10.29}$$

The last quantity is a radius expressed in eleven-dimensional external mass units. The action of the particle and the string-frame Buscher relation give the same inverse radius only after this conversion.

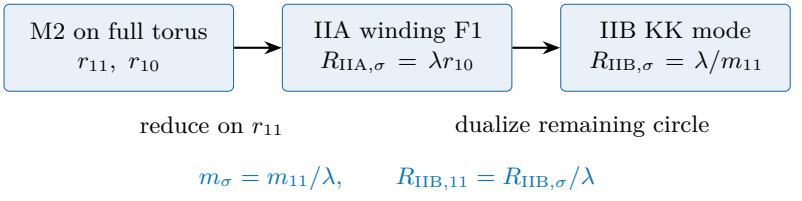


Figure XV.10.3: Two steps from the rectangular M-theory torus to the IIB circle. Reduction of the cycle of radius r_{11} produces a winding fundamental string; duality on the remaining cycle turns its winding into KK momentum. The σ labels refer to the string metric; $R_{\mathrm{IIB},11}$ is inferred in the original external mass units.

As an exact normalization test set $r_{11} = 3/2$, $r_{10} = 5/2$, $4\pi^2 T_{\mathrm{M2}} = 7$, $\lambda = 3$ in compatible units. Then

$$m_{11} = \frac{105}{4}, \quad \alpha'_\sigma = \frac{6}{7}, \quad R_{\mathrm{IIA},\sigma} = \frac{15}{2}, \quad R_{\mathrm{IIB},\sigma} = \frac{4}{35}, \quad R_{\mathrm{IIB},11} = \frac{4}{105}. \tag{XV.10.30}$$

For example, the first rest energy in string units is $35/4$, the inverse of $4/35$. If we change the external convention by doubling λ at the same eleven-dimensional input, α'_σ grows by four and both string radii by two. The inferred eleven-dimensional radius remains $4/105$. This is a conversion test for the chosen rectangular calculation, not an instruction for varying a physical dilaton while fixing all microscopic parameters.

The dimensionful quantities can be recovered from two measurements that transform differently. In the original metric the once-wrapped membrane with one circle left unwrapped has string tension $2\pi r_{11} T_{\mathrm{M2}}$. The wound string particle acquires a further factor $2\pi r_{10}$. After reduction the tension carries two inverse powers of λ, while the winding length carries one positive power:

$$(2\pi R_{\mathrm{IIA},\sigma}) T_{\mathrm{F1},\sigma} = (2\pi\lambda r_{10}) \frac{2\pi r_{11} T_{\mathrm{M2}}}{\lambda^2} = \frac{m_{11}}{\lambda}. \tag{XV.10.31}$$

In the final frame the same mass is pure momentum. A mistaken use of r_{10} as the string-frame proper radius would introduce an extra $1/\lambda$ in the winding mass and hence a wrong inferred KK radius. Thus the metric issue is present already for the completely nonsingular torus. It is not specific to F-theory seven-branes.

A related comparison holds when the conversion itself depends on the area. For clarity, let T_0 be a fixed tension parameter in the IIB metric convention in which the conversion is $ds_{\mathrm{IIB}} = \beta\, ds_{11}$, with the ordinary M/IIB relation $\beta^2 = \sqrt{A_f}\, T_{\mathrm{M2}}/T_0$. In this convention the inferred radius R_{IIB} and the one expressed in the original mass units obey

$$R_{\mathrm{IIB}}^{-2} = \frac{(T_{\mathrm{M2}} A_f)^2}{\beta^2} = T_0 T_{\mathrm{M2}} A_f^{3/2}, \qquad (R_{\mathrm{IIB}}/\beta)^{-1} = T_{\mathrm{M2}} A_f. \tag{XV.10.32}$$

The relation for β is specific to this ordinary fixed-tension convention; the algebra illustrates which area power changes with the metric. Doubling A_f at fixed tensions multiplies the first inverse radius by $2^{3/4}$ and the second by 2. It would be inconsistent to use the first power with an area measured in a different metric or to take it as a result about the native B frame over a varying axiodilaton.

For the product comparison, fix a common noncompact five-dimensional mass metric and let $ds_I = \lambda_I ds_{\mathrm{c}}$ be any constant alternative normalization of the external block in description I. The worldline and worldsheet actions separately imply

$$m_I = \frac{m_{\mathrm{c}}}{\lambda_I}, \qquad T_I = \frac{T_{\mathrm{c}}}{\lambda_I^2}, \qquad R_{I,\mathrm{native}} = \lambda_I R_I. \tag{XV.10.33}$$

The radius law follows from a KK mass in these units. It is useful even when an explicit native metric is unavailable. An inverse area in common units need not be an inverse area with the same power in a string frame whose conversion depends on the moduli. In the varying-fiber geometry the ordinary adiabatic M/F interpretation is an additional premise, with its usual local Kodaira dictionary at degenerate fibers. We do not apply the rectangular free isometry at the I_3 core. With these qualifications, either primitive elliptic fiber of (XV.10.5) can supply a KK gap in the same common external mass metric.

XV.10.4 Two six-dimensional readings of the product

The fiber in a sectioned model fixes where its seven-branes are located. With E as the fiber, the discriminant is nowhere zero. With S_t as the fiber, the factor t^3 in (XV.10.3) is present over the entire copy of E at $t = 0$. Thus, denoting the discriminant divisors with multiplicity by $\mathcal{D}_I$, we have

$$\mathcal{D}_A = 0, \qquad \mathcal{D}_B = 3\Gamma, \qquad \Gamma = E \times \{0\} \subset E \times D. \tag{XV.10.34}$$

The branch coordinates in (XV.10.6) have no dependence on e. The two branches are defined everywhere along Γ; there is no permutation of components along it. In the ordinary unfrozen dictionary a split I_3 gives local Lie algebra $\mathfrak{su}(3)$. The residual factor $4 + t^3$ is a unit and there are no isolated enhancements in this neighborhood.

In reading A the ordinary IIB construction on the local A-type surface, or equivalently the corresponding ordinary type IIA NS5 description, gives the relative $(2, 0)$ little string theory of type A_2. Here we use the unquotiented, unfrozen local product with sixteen supercharges and the boundary and isolation prescription of the ordinary little

string sector. We set aside the center of mass. These are physical conditions, not a consequence of $\Delta_E \neq 0$. In particular the absence of a nonabelian seven-brane factor does not remove the tensor strings. Their charges come from D3-branes wrapped on curves in the base S. With $Q_{ij} = C_i \cdot C_j$, the sign convention for their geometric pairing is $\Omega = -Q$. It has one null direction:

$$Q = \begin{pmatrix} -2 & 1 & 1 \\ 1 & -2 & 1 \\ 1 & 1 & -2 \end{pmatrix}, \qquad Q \begin{pmatrix} 1 \\ 1 \\ 1 \end{pmatrix} = 0. \tag{XV.10.35}$$

The primitive sum $C_0 + C_1 + C_2$ is a base fiber that can move away from the singular configuration. Its D3 tension is positive if its area is positive. In the ordinary unwarped leading D3 normalization, with calibrated curve areas measured in the same frame as the D3 tension, this reads

$$T_A = T_3 \operatorname{Area}(S_t) = T_3 \sum_i \operatorname{Area}(C_i) > 0. \tag{XV.10.36}$$

The quotient by the null direction retains the finite root pairing. The tension does not descend to that quotient when the full fiber has finite positive area. A null vector of the pairing is not a zero of the area functional.

For a concrete tension comparison, take two curve charges $v = C_1$ and $v' = C_1 + (C_0 + C_1 + C_2)$ on the A base. Their finite pairings agree, because for every component C_j,

$$Q(v', C_j) = Q(v, C_j), \qquad T(v') - T(v) = T_A. \tag{XV.10.37}$$

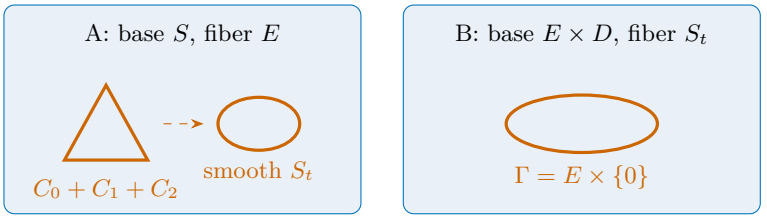
The second identity evaluates the positive calibrated tension functional on the effective sums. It is not an assertion of a bound state in class v'. It explains why keeping only the finite pairing would lose the intrinsic scale. The corresponding five-dimensional charge coordinates retain both the root label and the coefficient of the full fiber.

In reading B the relevant compact base curve is Γ, not any c_i. Its normal line is trivial: t is a transverse coordinate globally along the product curve, and the displacement from Γ to $E \times \{t\}$ gives a nonzero section of the normal. Equivalently,

$$g(\Gamma) = 1, \qquad N_{\Gamma/(E\times D)} \simeq \mathcal{O}_\Gamma, \qquad \Gamma^2 = \deg N_{\Gamma/(E\times D)} = 0. \tag{XV.10.38}$$

Here Γ is a single square-zero curve that supports a gauge algebra, whereas in A the displayed null charge is a sum of three negative-square components. The D3 on Γ gives the little string in the ordinary $(1,1)$ reading, identified with the corresponding relative type IIB NS5 sector at finite intrinsic scale. The same string has a leading gauge description as an instanton on the seven-branes, to be normalized in Section XV.10.6.

For the light B gauge multiplet, take the ordinary eight-dimensional gauge fields on a flat Γ with trivial background bundle, no background flux, no twist or quotient, and periodic spin structure. Count fields at energies below the nonconstant internal modes and other brane thresholds. A scalar has a constant zero mode, since on the compact torus a harmonic function has vanishing gradient. An internal gauge component instead comes from a harmonic real one-form. The two independent periods around the torus



Orange: compact base support of the wrapped D3

Figure XV.10.4: The base supports of the null D3 charges. In A a D3 wraps a full fiber in S, which can be represented by the sum of the three central components. In B it wraps $\Gamma \subset E \times D$, the support of the split I_3. The auxiliary fibers for the two F-theory readings are indicated separately.

give two such forms. Writing z for the internal coordinate and x for six-dimensional spacetime, the zero-mode part of the connection is

$$\begin{aligned} A(x,z) &= A^{(6)}(x) + \phi_1(x)\omega_1(z) + \phi_2(x)\omega_2(z), \\ \dim H^0(\Gamma,\mathbb{R}) &= 1, \qquad \dim H^1(\Gamma,\mathbb{R}) = 2. \end{aligned} \tag{XV.10.39}$$

Both ϕ_i are real adjoint scalars. The two transverse real scalars of the eight-dimensional multiplet also give one constant mode each. Thus a six-dimensional vector comes with $2+2=4$ real adjoint scalars, and the periodic fermions give their superpartners. This is one $(1,1)$ vector, or one $(1,0)$ vector and one adjoint hypermultiplet in that notation. This counting is a calculation for the light gauge fields under the stated assumptions. A twist or a nontrivial bundle changes the zero-mode operator; a compact completion may add other fields and couple gravity. Neither construction is identified with the spectrum of a compact Schoen threefold by this calculation.

The difference between the six-dimensional supersymmetry assignments can also be seen without comparing charged multiplicities. A ten-dimensional ordinary D7 has sixteen worldvolume supercharges. Reducing its eight-dimensional gauge multiplet along the flat internal two-torus preserves the constant spinors of both six-dimensional chiralities. The eight on-shell bosonic polarizations decompose as $6+2$ in eight dimensions (vector and transverse scalars), or as $4+2+2$ in six dimensions (vector, Wilson scalars, transverse scalars):

$$8 = 6 + 2 = 4 + 4. \tag{XV.10.40}$$

The A tensor branch is chiral. Its relative tensors are not the polarizations just counted in B. Reduction to five dimensions removes the distinction between the two six-dimensional spinor chiralities; for example a free chiral two-form on the circle gives a five-dimensional vector from its components with one circle index, with the other components tied to it by self-duality. This makes a common five-dimensional gauge interpretation possible. It does not identify the full interacting compactifications by polarization counting.

To see the tensor reduction explicitly, take a product circle with orthonormal length one-form e^5. For the six-dimensional self-dual field strength write $H = H_3 + F_2 \wedge e^5$, where the forms on the right are five-dimensional and independent of the circle coordinate. Choose the orientation $\mathrm{vol}_6 = \mathrm{vol}_5 \wedge e^5$. With the mostly-plus Lorentzian metric the self-duality and Bianchi conditions give

$$H_3 = - *_5 F_2, \qquad dF_2 = 0, \qquad d *_5 F_2 = 0. \tag{XV.10.41}$$

The Hodge identities behind the reduction are

$$*_6 H_3 = (*_5 H_3) \wedge e^5, \qquad *_6 (F_2 \wedge e^5) = - *_5 F_2. \tag{XV.10.42}$$

The equality of the components without a circle leg gives the first equation in (XV.10.41). The other component gives $F_2 = *_5 H_3$, consistent with $*_5^2 F_2 = -F_2$. The resulting massless five-dimensional vector has three on-shell polarizations. In A the five tensor-multiplet scalars then give $3 + 5 = 8$ bosonic polarizations. In B a six-dimensional vector has four polarizations, splitting into a five-dimensional vector and one Wilson scalar; adding the other four scalars gives the same count. This is a free zero-mode calculation. It explains how the two six-dimensional tensor and vector descriptions can lead to the same kind of five-dimensional multiplet without implying that their six-dimensional field content agrees.

We can follow the null D3 charges into the common M-theory description. At finite radius let a calibrated D3 wrap a compact base curve and the longitudinal spacetime circle. In a local ordinary dictionary, T-duality along the circle turns it into a D2 on the same curve, and the M lift is an M2. In the product there are simple lifted representatives because the other factor can be fixed:

$$A: \quad S_t \subset S \;\longmapsto\; \{e_*\} \times S_t, \; B: \qquad \Gamma \subset E \times D \;\longmapsto\; E \times \{o_S(0)\}. \tag{XV.10.43}$$

The section in B is a choice of representative; the lifted curve has class F_E. It can also be moved to a point of the smooth surface fiber. In A the lifted class is F_S. This use of the wrapped-brane dictionary in a fibration is a physical continuation from the ordinary circle construction, including the ordinary description at the discriminant. It is not a flat Buscher calculation of the seven-brane background. The result provides the two crossed identifications: each lifted base curve is the other projection's full elliptic fiber.

XV.10.5 Matching charges and finite scales

The same membrane mass can now be read twice. Let J be the product Kähler form at the chosen finite background. Define $a_E = \int_{F_E} J$, $a_i = \int_{c_i} J > 0$, and $a_S = \int_{F_S} J = \sum_i a_i$. On a holomorphic curve the Kähler form restricts to its area form with the complex orientation. The ordinary calibrated M2 central masses in the common external metric are therefore

$$m_E = \mu a_E, \qquad m_i = \mu a_i, \qquad m_S = \mu a_S = \sum_i m_i, \tag{XV.10.44}$$

where μ is the shared mass per area, equal to T_{M2} with eleven-dimensional proper areas and external metric in the unwarped convention. Reversing a curve's orientation reverses the charge. The pure energy scale for k units is $|k|$ times the unit scale; these calibrations do not count stable bound states or guarantee a single-particle tower for every wrapping.

For F_E the A interpretation is one unit of KK momentum by (XV.10.29), and the B interpretation is one winding by (XV.10.43). The opposite holds for F_S. With compatible spin, flux, flat-field and boundary data, the dictionary for the two primitive legs in the common external mass metric is

curve	A	B
F_E	$1/R_A = m_E$	$2\pi R_B T_B = m_E$
F_S	$2\pi R_A T_A = m_S$	$1/R_B = m_S$

(XV.10.45)

Here the radii are inferred from the external KK masses; the D3 tensions are in the same external metric. In particular a_E and a_S are M-theory periods. They are not inserted as proper IIB base areas into the D3 action. Applying the markings in (XV.10.12) to (XV.10.45) gives the signed dictionary

$$n_A = w_B = d, \qquad w_A = n_B = b_0. \tag{XV.10.46}$$

The two equalities are oriented identifications on separate legs, with relative coordinates carried by c_1, c_2. They are not a rest-energy rule for a general charge vector.

The matching can also be organized as a test of the tension on an individual base curve. Let C be one of the holomorphic base curves with a calibrated representative on the M side of the ordinary lift, and write $a(C)$ for the area of that lift. If $T_I(C)$ is the external tension in the common frame, the once-wrapped worldsheet action has coefficient

$$\mu a(C) = 2\pi R_I T_I(C). \tag{XV.10.47}$$

Thus on side A the relative tensions inferred for C_1, C_2 are $m_E m_1/(2\pi)$ and $m_E m_2/(2\pi)$. In the reference periods below their ratio is $3:5$, and changing only a_E changes both by the same factor, without changing the two wrapped-particle masses. This distinction between a tension and a wrapped mass matters when the circle is varied. The equality presupposes a calibrated ordinary brane and the absence of additional charges in the wrapped configuration.

Eliminating the radii in (XV.10.45) yields

$$T_A = T_B =: T = \frac{m_E m_S}{2\pi}, \qquad R_A R_B = \frac{1}{m_E m_S} = \frac{1}{2\pi T} =: \alpha_{\mathrm{eff}}. \tag{XV.10.48}$$

The two pure sectors have exchanged roles, at a common finite intrinsic tension. The dimensions are consistent: μ has dimension length to the power -3, each m inverse length, and α_{eff} length squared. Its equality to the underlying ℓ_s^2 is used only in the fundamental-string realization in the appropriate string metric. The physical equivalence of the two ordinary circle compactifications uses the longitudinal type-II duality of the corresponding decoupled NS5 sectors, with the same relative-sector and compatible background prescriptions on the two sides. The geometric calculation verifies this charge

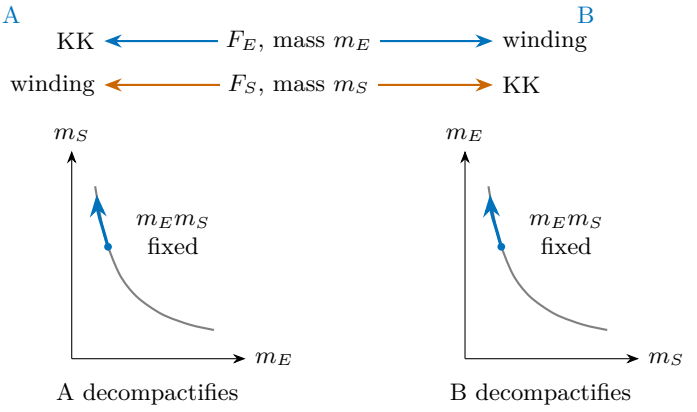


Figure XV.10.5: The two primitive mass legs. The KK leg of A is the winding leg of B, and conversely. The arrows in the lower panels indicate the fixed-tension limits in mass coordinates: one gap tends to zero while the other tends to infinity. Neither plot uses radii from different native frames.

and scale map under those physical identifications. Two maps out of an unmarked threefold would not establish the equivalence of arbitrary compactified quantum theories.

There is a dimensionless parameter that says which circle reading has the lighter momentum modes at fixed T. Let $\ell_{\text{eff}} = \sqrt{\alpha_{\text{eff}}}$ in the common frame and set $\rho = R_A/\ell_{\text{eff}}$. Then

$$\frac{R_B}{\ell_{\text{eff}}} = \rho^{-1}, \qquad m_E \ell_{\text{eff}} = \rho^{-1}, \qquad m_S \ell_{\text{eff}} = \rho. \tag{XV.10.49}$$

At $\rho = 1$ the two gaps coincide, so the masses alone cannot distinguish the two charge labels. The section marking still does. For $\rho > 1$ the A momentum sector is lighter than its winding sector; for B the order is reversed. This is why a low-energy truncation to the lightest pure scales made separately in each description can omit a leg that is needed for the full circle comparison.

For an example take $\mu = 1$, $a_E = 3/2$ and $(a_0, a_1, a_2) = (2, 3, 5)$ in compatible units. The inverse radii are $3/2$ and 10, so

$$R_A = \frac{2}{3}, \qquad R_B = \frac{1}{10}, \qquad 2\pi T = 15, \qquad \alpha_{\text{eff}} = \frac{1}{15}. \tag{XV.10.50}$$

A pure $n_A = 2$ mode has common mass 3, and a pure $w_A = -1$ configuration has mass 10. In B these are $w_B = 2$ and $n_B = -1$ respectively. For the native conventions $(\lambda_A, \lambda_B) = (2, 3)$, the pair of masses reads $(3/2, 5)$ in A and $(1, 10/3)$ in B. This does not violate (XV.10.45): each mass must be multiplied by its own λ_I before comparison. Likewise

$$R_{A,\text{native}} R_{B,\text{native}} = \frac{4}{3}\frac{3}{10} = \frac{2}{5} = \lambda_A \lambda_B \alpha_{\text{eff}}. \tag{XV.10.51}$$

The native slope inferred from A's tension would be $4/15$, and from B's tension $9/15$. Neither is $2/5$. The discrepancy in a direct native-radius comparison comes from mixing the two normalizations.

The full-fiber area a_S fixes one KK spacing, but does not fix the allocation among components. Change (a_0, a_1, a_2) from $(2, 3, 5)$ to $(1, 4, 5)$. The two radii and $2\pi T$ remain as in (XV.10.50), while the two finite simple periods move from $(3, 5)$ to $(4, 5)$ in mass units. Conversely, holding the components fixed and changing only a_E to $5/2$ gives

$$(R_A, R_B, 2\pi T) = (2/5, 1/10, 25). \tag{XV.10.52}$$

Thus a change of one auxiliary area alone is not a radius change at fixed intrinsic tension. The first control instead varies a relative parameter without altering either longitudinal spacing. We will identify these relative parameters with Wilson gaps in the gauge description.

There is also a way to vary the radius without changing the little-string tension. For example double R_A starting from (XV.10.50). The A momentum mass must halve. Fixing $m_E m_S = 15$ then doubles the B momentum mass, so B's radius halves. If we keep the three component fractions fixed, the input and output are

$$(a_E; a_0, a_1, a_2) = (3/4; 4, 6, 10), \tag{XV.10.53}$$

$$(R_A, R_B, 2\pi T) = (4/3, 1/20, 15). \tag{XV.10.54}$$

The A winding gap doubles and its KK gap halves; the opposite statements hold in B. This trajectory changes both area parameters. It is different from both the fixed-sum redistribution and the single-area change, even though all three operations are easy to describe in terms of Kähler periods.

The two six-dimensional limits occur at opposite ends of the finite-circle comparison. If the intrinsic tension is to remain fixed, (XV.10.48) gives the two mass-coordinate paths

$$\begin{aligned} &(m_E, m_S) = (z m_E^{(0)}, m_S^{(0)}/z), \quad R_A \to \infty, \\ &(m_E, m_S) = (m_E^{(0)}/z, z m_S^{(0)}), \quad R_B \to \infty \end{aligned} \qquad (z \to 0^+). \tag{XV.10.55}$$

One may hold the fractions a_i/a_S fixed while comparing the rays. The tower becoming light in each case is its own KK tower. For example in the first line the A KK gap is $z m_E^{(0)}$, while the A winding gap grows as $m_S^{(0)}/z$. If instead one gap tends to zero while the other stays finite, T tends to zero. These are conditional scale trajectories in the chosen external normalization, not constructed limiting metrics. Their behavior does not make the distinct chiralities of the six-dimensional endpoints equivalent as six-dimensional theories.

XV.10.6 The five-dimensional gauge theory

In B the unit little string can be measured using a gauge configuration on the seven-brane. We first derive its tension in the leading ordinary action. This calculation is independent of the mass comparison between the two projections. Take the background pullback of the two-form plus the background gauge curvature to vanish, $P[B] + 2\pi\alpha' F_{\mathrm{bg}} = 0$. Use the unwarped leading action, with the same proper length and area conventions

in the brane tensions and volume integrals. The kinetic and charge conventions for a fundamental trace are

$$\operatorname{tr}_f(T_a T_b) = \frac{\delta_{ab}}{2}, \qquad \mathcal{L}_{\mathrm{YM}} = -\frac{1}{2g^2}\operatorname{tr}_f F_{\mu\nu}F^{\mu\nu}, \qquad k = \frac{1}{8\pi^2}\int \operatorname{tr}_f F\wedge F. \tag{XV.10.56}$$

The integral is over the four spatial directions transverse to the string within six dimensions. Choose the orientation so that a self-dual unit instanton has $k = 1$.

Let $T_p = [(2\pi)^p g_s(\alpha')^{(p+1)/2}]^{-1}$ and $\mu_p = g_s T_p$ be the ordinary string-frame tension and RR charge, respectively. To quadratic order in the fluctuating field, the D7 determinant contributes $(2\pi\alpha')^2 \operatorname{tr}_f F^2/4$ times the volume and tension. Integrating over Γ, of area A_Γ, and comparing with (XV.10.56) gives

$$\mathcal{L}_6^{(2)} = -\frac{A_\Gamma T_7 (2\pi\alpha')^2}{4}\operatorname{tr}_f F^2, \qquad \frac{1}{g_{6,B}^2} = \frac{A_\Gamma T_7 (2\pi\alpha')^2}{2}. \tag{XV.10.57}$$

One way to check the determinant coefficient is to use $\log\det(1+M) = \operatorname{Tr}(M - M^2/2 + \cdots)$ for $M^\mu{}_\nu = 2\pi\alpha' F^\mu{}_\nu$ and then take the square root. The spacetime matrix has vanishing linear trace and $\operatorname{Tr} M^2 = -(2\pi\alpha')^2 F_{\mu\nu}F^{\mu\nu}$ at quadratic order. This spacetime trace is separate from the gauge trace. In particular substituting a stack identity for the fundamental trace of the fluctuating field would not compute the same coefficient.

The incremental Wess–Zumino coupling to the RR four-form is obtained instead from the quadratic term of the gauge-field exponential. The wedge product of two two-forms has even degree, so it comes with $1/2!$ and the chosen orientation:

$$S_{C_4}^{(2)} = \frac{\mu_7(2\pi\alpha')^2}{2}\int C_4 \wedge \operatorname{tr}_f(F\wedge F), \qquad \frac{\mu_7(2\pi\alpha')^2}{2}\,8\pi^2 k = k\mu_3. \tag{XV.10.58}$$

The integrated charge is that of k D3-branes wrapping Γ and the string worldsheet. This is an incremental charge, so no background contribution is being interpreted as an instanton. The equality uses $\mu_3/\mu_7 = (2\pi)^4(\alpha')^2$. The corresponding tension ratio uses $T_3/T_7 = (2\pi)^4(\alpha')^2$ and (XV.10.57):

$$\frac{8\pi^2}{g_{6,B}^2} = 4\pi^2(2\pi\alpha')^2 A_\Gamma T_7 = A_\Gamma T_3 = T_B. \tag{XV.10.59}$$

The two ratios agree, but the RR calculation and the kinetic calculation are distinct. In six dimensions $g_{6,B}^2$ has dimension length squared, so the coefficient of $8\pi^2$ in (XV.10.59) has the dimension of a string tension.

The factor of two in the kinetic coefficient is visible by restricting to a single normalized generator. If $F_{\mu\nu} = F^a_{\mu\nu}T_a$, the Lagrangian and the quadratic brane term for this polarization give

$$-\frac{(F^a)^2}{4g_{6,B}^2} = -\frac{A_\Gamma T_7(2\pi\alpha')^2}{8}(F^a)^2. \tag{XV.10.60}$$

Equating instead the coefficient on the right to $1/(2g_{6,B}^2)$ would mix the component normalization with the trace normalization. On the RR side one could check the same

issue using an $\mathfrak{su}(2)$ block acting on the first two colors. The fundamental trace on the 3×3 matrices restricts to the two-dimensional trace on that block; an embedded unit instanton has $\int \operatorname{tr}_f F \wedge F = 8\pi^2$, not three times this integral. Both tests use a genuine nonabelian fluctuating field.

Reduce the six-dimensional action on the longitudinal B circle. For the ordinary leading zero modes, integrating the kinetic coefficient over the circle of proper length $2\pi R_B$ yields, in matched units,

$$\frac{1}{g_5^2} = \frac{2\pi R_B}{g_{6,B}^2}, \qquad \frac{8\pi^2}{g_5^2} = 2\pi R_B T_B = m_E = \frac{1}{R_A}. \tag{XV.10.61}$$

The equality to $1/R_A$ uses the wrapped-brane identification of (XV.10.45); it is not contained in the gauge action. This is the leading unit topological mass scale. To decide if it is the mass of a smooth pure classical configuration, one must ask whether the leading energy bound can be saturated in the chosen Wilson background.

In the reduced theory put the electric field and other scalars to zero. Let $\Phi = A_\ell$ be the Wilson scalar in a proper length coordinate ℓ on the B circle. Circle independence gives $F_{i\ell} = D_i \Phi$; here $i, j = 1, \dots, 4$ refer to transverse spatial directions of a static particle. With a positive spatial trace norm the energy is

$$E = \frac{1}{2g_5^2} \int_{\mathbb{R}^4} d^4x \, \operatorname{tr}_f(F_{ij}F_{ij} + 2D_i\Phi D_i\Phi). \tag{XV.10.62}$$

Writing $\operatorname{tr}_f(F \wedge F) = \frac{1}{2} \operatorname{tr}_f(F_{ij}(*F)_{ij}) d^4x$ and choosing the sign by k gives

$$\begin{aligned} E = {} & \frac{8\pi^2|k|}{g_5^2} + \frac{1}{4g_5^2} \int d^4x \, \operatorname{tr}_f\big[(F_{ij} \mp (*F)_{ij})^2\big] \\ & + \frac{1}{g_5^2} \int d^4x \, \operatorname{tr}_f(D_i\Phi D_i\Phi). \end{aligned} \tag{XV.10.63}$$

The last term is nonnegative and vanishes only for a parallel scalar. At the unbroken wall with trivial Wilson scalar an embedded smooth self-dual instanton of unit charge saturates the bound. In a regular Wilson chamber, the scalar has distinct asymptotic eigenvalues. If it is parallel, these eigenvalues and their multiplicities are constant everywhere, and the connection preserves the three eigenline bundles. Its structure reduces to the Cartan. On compactified transverse $\mathbb{R}^4 = S^4$, for smooth finite-action data with the ordinary instanton boundary condition, these lines have zero first Chern class because $H^2(S^4) = 0$. Their direct sum has

$$c_2(L_1 \oplus L_2 \oplus L_3) = \sum_{i<j} c_1(L_i) c_1(L_j) = 0. \tag{XV.10.64}$$

So $k = 0$. A regular Wilson chamber cannot have a smooth pure unit solution saturating (XV.10.63). Dropping the gradient term would erase this distinction and would confuse a leading coefficient of the action with a statement about its solutions. The argument does not exclude a quantum, dyonic or ultraviolet state, or determine a quantum coupling.

The classical distinction also follows by asking whether a simple trial configuration saturates the bound. Take a smooth unit instanton embedded in colors 1 and 2. If Φ is constant with $\Phi_1 = \Phi_2$ on this block, its commutator with the embedded connection vanishes. A scalar with $\Phi_1 \neq \Phi_2$ does not commute with the off-diagonal generators of that connection. In a gauge with diagonal constant Φ, for the entry $A_i{}^1{}_2$ the magnitude of the commutator is

$$\left|[A_i, \Phi]^1{}_2\right| = |\Phi_1 - \Phi_2|\,|A_i{}^1{}_2|. \tag{XV.10.65}$$

Letting Φ vary can change the local gradient energy, but cannot evade the global parallel-scalar argument if saturation is required. This is why a result at the unbroken wall cannot be transported to a regular chamber simply by keeping the numeric coupling fixed.

The same chamber gives a direct check on the relative curve masses. Let $x_i = a_i/a_S$, so $x_0 + x_1 + x_2 = 1$ and each $x_i > 0$. Choose trace-free holonomy phases in turns, so the eigenphases are $e^{2\pi i h_j}$, with a lift

$$(h_1, h_2, h_3) = \tfrac{1}{3}(2x_1 + x_2, -x_1 + x_2, -x_1 - 2x_2). \tag{XV.10.66}$$

In the adjoint the off-diagonal entry with root $e_i - e_j$ sees the difference $h_i - h_j$. In a convention where the background enters with plus sign, its circle derivative on Fourier mode k gives the signed covariant momentum $(k + h_i - h_j)/R_B$. This integer labels a Fourier mode and is independent of the instanton number in (XV.10.56). The differences obtained from (XV.10.66) are

$$h_1 - h_2 = x_1, \quad h_2 - h_3 = x_2, \quad h_1 - h_3 = x_1 + x_2, \quad 1 + h_3 - h_1 = x_0. \tag{XV.10.67}$$

The first three gaps, divided by R_B, are $m_1, m_2, m_1 + m_2$. The highest positive finite root has Fourier number zero in this lift. The affine gap is m_0; it is the mode of the opposite highest root with Fourier number one. This is precisely the decomposition $c_0 = F_S - c_1 - c_2$. Neither the affine mode nor the full KK fiber is a new finite simple root. This calculation uses the local algebra; the trace-free holonomy lift does not select a global gauge group.

The eigenphases themselves make a useful numerical check. With $(a_0, a_1, a_2) = (2, 3, 5)$ the trace-free lift and two ways to go between the extreme eigenphases are

$$h = \frac{1}{30}(11, 2, -13), \qquad \frac{h_1 - h_3}{R_B} = 8, \qquad \frac{1 + h_3 - h_1}{R_B} = 2. \tag{XV.10.68}$$

Both energies refer to the same two color labels but differ by which oriented arc is taken and which KK shift is used. The gaps sum to $1/R_B$. With the changed allocation the lift becomes $(13, 1, -14)/30$, so these gaps become 9 and 1 without any change in the KK spacing. A numerical test that accidentally sets $h_1 - h_3 = 1/2$ would give equal gaps and would not distinguish the two readings.

For the reference periods the simple gaps are $(3, 5)$, the highest is 8, and the affine gap is 2. For the fixed-sum change they are $(4, 5)$, 9 and 1. These highest-root masses follow from the ordinary gauge dictionary; they do not follow from assuming that every sum of effective curves yields a new isolated M2 state. On the A side the relative particles come from the corresponding wrapped tensor strings. In the interior of the

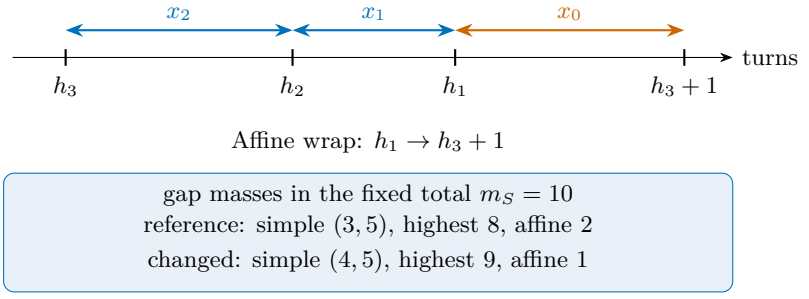


Figure XV.10.6: Phase differences in the B circle holonomy. In the upper row the simple gaps lie between successive phases, and the affine gap reaches the first phase translated by one turn. The lower row compares the allocation $(2, 3, 5)$ with $(1, 4, 5)$ at the same $a_S = 10$. The first two gaps sum to the highest finite root; all three gaps sum to the KK spacing.

chamber the gauge theory is in its Coulomb regime, and the largest root gap need not be below all other thresholds. There is a different regime near the partial wall $m_1, m_2 \to 0$ with $m_E, m_S > 0$ fixed:

$$m_1 + m_2 \longrightarrow 0, \qquad m_0 = m_S - m_1 - m_2 \longrightarrow m_S. \tag{XV.10.69}$$

At any fixed positive pair of gaps an external energy $\mathcal{E}$ must satisfy

$$\mathcal{E} \ll \min(m_E, m_S) \tag{XV.10.70}$$

to omit the two pure towers in this leading description. The inequality is necessary for that truncation; other thresholds must be checked separately. The reference parameters give $\min(m_E, m_S) = 3/2$, so the finite gaps $3, 5, 8$ are not all light in that example. By contrast choose $a_E = 3/2$ and $(a_0, a_1, a_2) = (10 - 2\delta, \delta, \delta)$ at $\mu = 1$. The highest finite gap is 2δ, while the gaps $3/2$ and 10 stay fixed. At $\delta \ll 1$ there is room to include the light relative fields and still stay below both tower thresholds. This hierarchy, rather than the existence of the root labels by itself, makes the approach to the unbroken five-dimensional gauge regime useful.

The finite-root modes become light while the affine mode and both full-fiber gaps remain heavy. With the other compactification and brane thresholds also above the energies in question, this is the ordinary unbroken maximally supersymmetric local five-dimensional $\mathfrak{su}(3)$ gauge sector. The partial wall limit does not shrink the little-string scale to zero. The finite-circle compactification supplies thresholds beyond the leading gauge theory; the leading theory alone is not a local ultraviolet completion. This is the same distinction between KK and Coulomb periods used in the five-dimensional geometric engineering of XIII.9, now with two actual sectioned F-theory projections of one threefold.

XV.10.7 A birational comparison from Appendix F

The product calculation started with two regular maps. What can we conclude if the change of fibration is given by rational coordinates instead? Consider a different local Weierstrass family from Appendix F of the little-string construction. Its coefficients have two useful choices, $m = 2$ and $m = 1$, with $a = -3$, $c = 1$. Let (σ, τ) be the old homogeneous base coordinates, (X, Y) the old fiber coordinates, and ψ an external coordinate. The old equation is

$$Y^2 = X^3 + a\sigma^4\tau^4 X + \psi^m\sigma^5\tau^7 + c\sigma^6\tau^6 + \sigma^7\tau^5. \tag{XV.10.71}$$

To try a new base coordinate s, take the forward substitution from (s, τ, x, y) to the old variables,

$$\sigma = \frac{x}{\tau^3}, \qquad X = \frac{sx^2}{\tau^5}, \qquad Y = \frac{x^2 y}{\tau^8}. \tag{XV.10.72}$$

Multiply the transformed equation by τ^{16}/x^4, which is allowed on the open $x\tau \neq 0$. For instance the X^3 term becomes $s^3x^2\tau$ and the ψ^m term becomes $\psi^m x\tau^8$. The new cubic is

$$y^2 = x^3 + Ax^2 + Bx, \qquad A = \tau(s^3 + as\tau^2 + c\tau^3), \qquad B = \psi^m\tau^8. \tag{XV.10.73}$$

Solving (XV.10.72) in order for x, s, y gives

$$x = \sigma\tau^3, \qquad s = \frac{X}{\sigma^2\tau}, \qquad y = \frac{\tau^2 Y}{\sigma^2}. \tag{XV.10.74}$$

The last power is two; the printed power one returns Y/τ on the old-coordinate roundtrip. It also has the wrong homogeneous weight. Under old weights $(1, 1, 4, 6)$ for (σ, τ, X, Y), the new (s, τ, x, y) have weights $(1, 1, 4, 6)$ using (XV.10.74), but y would have weight five with power one.

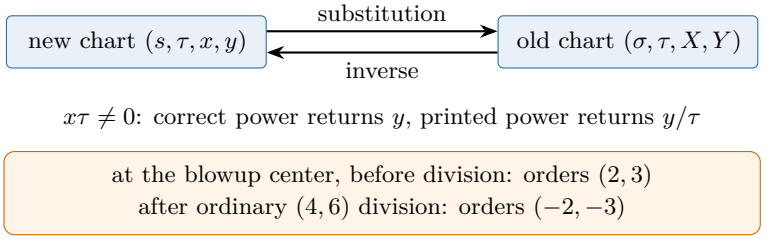


Figure XV.10.7: The rational coordinate change on $x\tau \neq 0$. The corrected inverse gives the original point on the roundtrip; the printed inverse rescales the fiber coordinate by $1/\tau$. The lower row tests the separate extension problem at the base blowup of $\tau = \psi = 0$.

Setting $\tau = 1$ before checking the inverse would miss the problem. At $s = x = \psi = 1$, $\tau = 2$, $a = -3$, $c = 1$ and either $m = 1$ or 2, the new cubic has $A = -6$, $B = 256$ and $y^2 = 251$. The roundtrip with the printed inverse gives $y/2$, which fails the new

equation at that point. The two powers of ψ agree at the chosen point, but distinguish the transverse discriminant orders.

To check the boundary, translate $x = z - A/3$ to short form. The resulting coefficients and discriminant are

$$f = B - \frac{A^2}{3}, \qquad g = \frac{2A^3}{27} - \frac{AB}{3}, \qquad \Delta = -B^2(A^2 - 4B). \tag{XV.10.75}$$

For a further chart test choose $s = x = 1$, $\tau = \psi = 2$. The ψ-dependent term now distinguishes the two members:

$$A = -6, \qquad B = 256 \cdot 2^m, \qquad y^2 = \begin{cases} 507, & m = 1, \\ 1019, & m = 2. \end{cases} \tag{XV.10.76}$$

The corresponding old coordinates are $\sigma = 1/8$, $X = 1/32$, $Y = y/256$. Substituting them into (XV.10.74) gives y for both choices; replacing τ^2 by τ gives $y/2$ in both. The inverse defect therefore has nothing to do with a specific value of the power of ψ. It is an algebraic defect in the coordinate formula on an otherwise regular dense open.

The shift also shows why the order at the intersection of the divisors has to be computed separately. Write $P = s^3 + as\tau^2 + c\tau^3$ and expand

$$\Delta = -\psi^{2m}\tau^{18}\big(P^2 - 4\psi^m\tau^6\big). \tag{XV.10.77}$$

A generic divisor order reads off one power while holding the other coordinate away from zero. The exceptional order in a blowup chart instead follows a path on which both coordinates vanish. For example, on $\tau = \epsilon$, $\psi = \epsilon\eta$ at $s = 1$, $\eta \neq 0$, this expression has discriminant order $18 + 2m$. That large number alone does not ensure divisibility of each short coefficient by the powers required by a crepant blowup.

At generic $\tau = 0$ the first term of A is τs^3 and B has order eight, so the discriminant has order $16 + 2 = 18$. At generic $\psi = 0$ it has order $2m$. In the patch $\tau = 1$ on $\psi = 0$, the square of the tangent slope at the node $x = y = 0$ is $s^3 - 3s + 1$. Its discriminant is 81 and its three simple roots preclude a rational square in $\mathbb{C}(s)$. If c is changed to 2 the polynomial becomes $(s-1)^2(s+2)$, and the discriminant becomes zero. The remaining simple root still precludes a square. The change affects the branch locus, but does not change that generic nonsquare test.

The required division follows from the Weierstrass line bundle. Locally a base blowup of a smooth surface changes the canonical class by one exceptional divisor, as one can check from

$$d\tau \wedge d\psi = \epsilon\, d\epsilon \wedge d\eta. \tag{XV.10.78}$$

For the Calabi–Yau Weierstrass choice, x and y transform as the second and third powers of the anticanonical bundle. Requiring the same Calabi–Yau choice on the blown-up base changes the pulled-back fiber coordinates by $x = \epsilon^2 x'$, $y = \epsilon^3 y'$ in a short chart. The cubic equation divided by ϵ^6 is then short with coefficients f/ϵ^4 and g/ϵ^6. An ordinary blowup of the base as a surface is possible regardless of these orders; regularity of this transformed Weierstrass model is the extra condition.

The ordinary blowup of the base center has chart $\tau = \epsilon$, $\psi = \epsilon\eta$. On the slice $s = 1$ we have $A = \epsilon(1 - 3\epsilon^2 + \epsilon^3)$, $B = \epsilon^{m+8}\eta^m$, so f starts at order two and g at order three.

For an ordinary crepant base blowup of a short Weierstrass model the new coefficients would be $f/\epsilon^4, g/\epsilon^6$, from the usual $(2,3)$ rescaling of the fiber coordinates. Here the orders are

$$(\mathrm{ord}_\epsilon f, \mathrm{ord}_\epsilon g) = (2,3), \qquad (\mathrm{ord}_\epsilon(f/\epsilon^4), \mathrm{ord}_\epsilon(g/\epsilon^6)) = (-2,-3), \qquad \text{(XV.10.79)}$$

where each order on the right is that of the displayed quotient. The poles obstruct this literal ordinary crepant procedure. They do not obstruct every birational model or disprove a heterotic duality. One would need further boundary and resolution data to use this second chart in a resolved fibration comparison. In the product example the two sectioned maps and the marked curves were available directly, which is why its charge and finite-scale calculation does not rely on this extension.

Exercises

Submit the quantities in the order specified below. Use `benchmark/tasks.json` for the JSON fields and `benchmark/PROTOCOL.md` for submission. The written parts, including all of Exercise 5, are assessed by a reader.

1. **A different parent mass.** For a free particle with $M = 2$, take $n = 3$, $R = 2$. Separately, wind a straight string with $2\pi T = 3$ and $w = -2$ on a circle of radius $3/2$. Submit the two masses in order. Explain why neither the momentum sign nor the winding sign can make the rest mass negative.

2. **Resolve the two intersections.** In the I_2 product take $q = 2F_E + c_0 + 4c_1$. Submit the evaluations in the order (Z_A, Z_B, D_1), and both marked pairs (n_A, w_A), (n_B, w_B). Give the relative coefficient of c_1 after changing basis to the full fiber. Explain which incidence would make the full fiber appear charged.

3. **Change the periods and frames.** Take $\mu = 1$, $a_E = 4$, $(a_0, a_1, a_2) = (2, 3, 1)$, $\lambda_A = 3/2$, and $\lambda_B = 2$. Start with signed $(n_A, w_A) = (-2, 2)$. Submit the two pure legs in the order A momentum, A winding. For each give the A and B signed labels and their charge types, the common mass, and the mass in each native convention. Give both simple gaps, the highest finite gap and the affine gap in common units. Submit also α_{eff} and the product of the two native radii. Why does agreement of the two leading topological scales not give a pure smooth unit instanton in the regular chamber?

4. **Test an inverse away from the unit chart.** In (XV.10.73) use $m = 1$, $a = -3$, $c = 1$ at $\tau = 3$, $s = x = \psi = 1$, $y = \sqrt{6565}$. Submit the exponent of τ in the inverse for y, the returned y, and the returned value that the printed inverse would give. Check the given point in the new cubic and submit the orders of both short coefficients after ordinary crepant division in the chart $\tau = \epsilon$, $\psi = \epsilon\eta$ at $s = 1$. Explain what those orders say about the extension.

5. **Compare backgrounds.** Suppose two elliptic morphisms are equipped with different spin structures or different flat three-form backgrounds. Explain why

the same unmarked geometry and a correct mass table do not identify their compactified relative quantum theories. Distinguish the two six-dimensional limits, the finite-radius duality of the ordinary little-string sectors, and the leading five-dimensional gauge regime.

To check your reasoning across these exercises, keep track of what the proposed counterexample is allowed to change. In Exercise 2 you can change the relative curve coefficient while keeping both marked charges. In Exercise 3 you can change the two native units while keeping the common masses, or move periods at fixed total area while changing the relative gaps. Identify one measured quantity that distinguishes each such change. In Exercise 4, explain why a successful roundtrip at a generic point and a failed coefficient division at the blowup center are compatible. A numerical match is useful only if you can say which competing interpretation it rules out.

Status and sources

§1. Product and marking. The product equations, incidence and integral evaluations are [MATH]. The exact models are those of Chapter 8; the underlying product construction is in Bhardwaj et al. (2016), arXiv:1511.05565v3, §4.1, printed pp. 14–16, eq. (4.1) and Fig. 2. The calculation uses the Weierstrass convention $\Delta_{\text{book}} = 4f^3+27g^2$. The I2 determinant is -2 in the displayed order; only the evaluation indices are asserted.

§2. The longitudinal circle. Periodic free Fourier modes are [MATH]. The winding, finite-circle weak comparison and relative segment are [GEO-E], under the isometric product-circle and weak-reference hypotheses. See Seiberg (1997), arXiv:hep-th/9705221v2, §2.1, printed pp. 2–4, eqs. (2.1)–(2.4) and the following paragraphs.

§3. Membrane area and radius. The ordinary rectangular M/IIA/IIB interpretation is [GEO-E]; constant conversions at a common mass point are [MATH]. See Schwarz (1995), arXiv:hep-th/9508143v5, eqs. (25)–(32), including the fixed-tension metric conversion, and Vafa (1996), arXiv:hep-th/9602022v1, §2–4, printed pp. 5, 7, 10, for the separate adiabatic input. The comparison uses the calibrated M2 units, the ordinary rectangular torus reduction and the separate qualified adiabatic fiberwise interpretation.

§4. Six-dimensional readings. The discriminant support and normal line are [MATH]. The ordinary relative $(2,0)$ and $(1,1)$ interpretations, the B adjoint and the D3 lift are [GEO-E]. See Bhardwaj et al., v3, §4.1 and §9.1, printed pp. 14–16, 38–40, and Seiberg, v2, §2.1. The wrapped-brane map uses the qualified adiabatic fiberwise interpretation.

§5. Finite scale. The matched masses and inferred tension are [GEO-E], and the fixed-tension scale trajectories are [MATH] within those inputs. For this A-type product see Seiberg, v2, eq. (2.4) and following text, and Bhardwaj et al., v3, §4.1, eq. (4.1), the opening of §9, and the first paragraph of §9.1. We count components using eq. (4.1) and the explicitly resolved cubic rather than adopting the index wording of the first §9.1 example. The ordinary physical equivalence is sourced in this specific setting; the lattice calculation gives no new general QFT-transfer claim.

§6. Gauge scale and Wilson chamber. The leading gauge interpretation, topological normalization, chamber and finite wall are [GEO-E] under the ordinary background,

with the Einstein-frame D3 tension and fundamental-trace conventions of Chapter 2. See Seiberg, v2, after eq. (2.4), and Bhardwaj et al., v3, §4.1. The energy square and Cartan obstruction use the pure leading classical sector; no quantum nonexistence assertion follows. The comparison with XIII.9 uses only the period arithmetic of that chapter.

§7. Dense chart and boundary. The inverse, discriminant and ordinary blowup tests are [MATH] for the literal family in Bhardwaj et al., v3, Appendix F, printed pp. 63–64, eqs. (F.1)–(F.12). The inverse in (XV.10.74) corrects the printed (F.10). The tested obstruction concerns the ordinary blowup of the displayed short Weierstrass model.

References

Bhardwaj, L. et al. (2016). "F-theory and the Classification of Little Strings". In: *Phys. Rev. Lett.* 116, p. 161601. DOI: 10.1103/PhysRevLett.116.161601. arXiv: 1511.05565 [hep-th].

Schwarz, J. H. (1995). "An SL(2,Z) multiplet of type IIB superstrings". In: *Phys. Lett. B* 360, pp. 13–18. DOI: 10.1016/0370-2693(95)01138-G. arXiv: hep-th/9508143.

Seiberg, N. (1997). "New Theories in Six-Dimensions and Matrix Description of M-theory on T^5 and $T^5/\mathbb{Z}_2$". In: *Phys. Lett. B* 408, pp. 98–104. DOI: 10.1016/S0370-2693(97)00805-8. arXiv: hep-th/9705221.

Vafa, C. (1996). "Evidence for F-Theory". In: *Nucl. Phys. B* 469, pp. 403–418. DOI: 10.1016/0550-3213(96)00172-1. arXiv: hep-th/9602022.

Chapter XV.11

An atlas of six-dimensional constructions

A list of curve self-intersections is often the shortest way to describe a six-dimensional construction. How much can one reconstruct from it? Consider two intersecting rational curves of square -2. They can carry split gauge fibers with several choices of defining dimensions, or they can lie in the base of a product with a smooth elliptic curve. Their intersection pairing is the same. To recover the physical interpretation we must specify what is fibered over them, which periods are realized and what limit is taken. The examples below keep one ingredient fixed at a time, so that we can locate the origin of each change in the physics.

We use the ordinary elliptic and wrapped D3-brane dictionaries developed in Chapters 1–4, then the contractions and source calculations of Chapters 5–7, and the full-fiber and circle constructions of Chapters 8–10. In each example Q is the geometric curve intersection matrix and $\Omega = -Q$ is the tensor pairing. A period is an unnormalized Kähler area. We distinguish an integral charge, an effective calibrated representative and the existence of an isolated six-dimensional theory.

XV.11.1 Gauge theories on finite tensor branches

Which pieces of a gauge theory change when we tune its fiber but keep its gauge curves? Start with the two compact constructions with split I_4 on C_1 and split I_N on C_2, where $N = 5, 6$. The surface is the blowup of $\mathbb{F}_2$ at two points on the same ruling fiber away from the negative section. Let (S, F, E_1, E_2) be the total-pullback basis, with F a ruling fiber and E_i the exceptional classes. The strict gauge curves and ambient intersection matrix are

$$C = (C_1, C_2) = (S, F - E_1 - E_2), \qquad M = \begin{pmatrix} -2 & 1 & 0 & 0 \\ 1 & 0 & 0 & 0 \\ 0 & 0 & -1 & 0 \\ 0 & 0 & 0 & -1 \end{pmatrix}. \tag{XV.11.1}$$

The first block has determinant -1, so it has one eigenvalue of each sign. The two exceptional directions add two negative eigenvalues. But the coefficient columns of the strict curves in (XV.11.1) give

$$\Omega = -C^{\mathsf{T}}MC = \begin{pmatrix} 2 & -1 \\ -1 & 2 \end{pmatrix}, \qquad C^{\mathsf{T}}MK = 0, \qquad K = -2S - 4F + E_1 + E_2. \tag{XV.11.2}$$

The eigenvalues of Ω are $1, 3$, so the marked two-curve sector is positive definite even though the ambient surface has inertia $(1, 3, 0)$. Adjunction gives $K \cdot C_i = 0$, also visible in the displayed product. The exceptional curves in Figure XV.11.1 change the self-intersection of the strict fiber; their intersections with it need their own coefficient test.

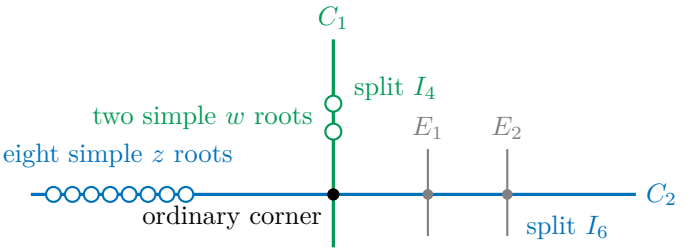


Figure XV.11.1: Strict gauge curves of the compact split I_4/I_6 model. The two blowup centers lie away from the ordinary gauge corner. The open circles label simple residual loci schematically and are grouped by their counts; they are not the exceptional intersections.

To count those residual loci, use $\Delta = 4f^3 + 27g^2$. Removing the prescribed gauge vanishing gives a section of $-12K - 4C_1 - NC_2$. Intersecting it with the two curves gives

$$((-12K - 4C_1 - NC_2) \cdot C_i)_{i=1,2} = (8 - N, 2N - 4). \tag{XV.11.3}$$

Degrees only count zeros with multiplicity. In the actual $N = 5$ model the residuals are $w^3 - w + 1$ and $z^6 + z + 1$, and in the $N = 6$ model they are $2 + w^2$ and $2 + z^8$. The first pair is relatively prime to its derivatives, and the derivatives of the second pair vanish only at the respective origins, where the residuals are nonzero. The polynomials exhaust the displayed degrees in these coordinates. Thus we have distinct simple roots away from the gauge corner.

The degree calculation did not construct the even tuning. To see the change of geometry, put $C_1 : z = 0$, $C_2 : w = 0$ downstairs, and put $D(z) = (z - 1)(z - 2)/2$. In Tate coefficient order $i = 1, 2, 3, 4, 6$, the new powers and numerators are

$$k = (0, 1, 2, 2, 4), \qquad j = (0, 1, 3, 3, 6), \qquad (m_i) = (1, 1, 0, 1, 0), \tag{XV.11.4}$$

$$a_i = z^{k_i} w^{j_i} H_i, \qquad (H_i) = (D, D, 1, D, 4 + w^2 + z^8). \tag{XV.11.5}$$

For the downstairs class $A_i S + B_i F$, where $A_i = 2i - k_i$ and $B_i = 4i - j_i$, a monomial $z^a w^b$ is allowed if $0 \le a \le A_i$ and $0 \le b \le B_i - 2(A_i - a)$. For example the last class is

$8S + 18F$: w^2 exhausts the base degree at $a = 0$, and z^8 exhausts the fiber degree. The three numerators D have the required simple zeros at both centers. This establishes why the prescribed restrictions come from sections.

Use the Tate discriminant sign of Chapter 3. Here $B_2 = a_1^2 + 4a_2 = D^2 + 4zwD$, and the five terms in B_8 give

$$\frac{B_8}{z^4w^6} = D^2(H_6 - 2) + zwD(1 + 4H_6).$$

In $16\Delta = B_2^2B_8 + 8B_4^3 + 27B_6^2 - 9B_2B_4B_6$, the last three terms vanish on either axis after division by z^4w^6: B_4 is divisible by z^2w^3 and B_6 by z^4w^6. Since $B_2 = D^2$ on either axis, the divided 16Δ restricts to $D^6(H_6 - 2)$. On $z = 0$ this is $2 + w^2$; on $w = 0$ it is $D^6(2 + z^8)$. The next step removes the extra downstairs zeros at the blowup centers.

At $z = a$, $a = 1, 2$, the two blowup charts are $(z, w) = (a + u, uv)$ and $(a + \tilde{u}\tilde{v}, \tilde{v})$. The crepant coefficient in the first chart is divided by u^i, in the second by $\tilde{v}^i$, as follows from the canonical divisor change. Here $m_i = i - j_i$. After removing the prescribed w-powers, the remaining divisions are

$$\frac{D(a + u)}{u} = \frac{2a - 3 + u}{2}, \qquad \frac{D(a + \tilde{u}\tilde{v})}{\tilde{v}} = \frac{\tilde{u}(2a - 3 + \tilde{u}\tilde{v})}{2}. \tag{XV.11.6}$$

On their overlap $\tilde{u} = 1/v$, $\tilde{v} = uv$, the full coefficients differ by v^i, as required. In the first chart the discriminant is divided by u^{12}, while $w^6 = u^6v^6$. On the strict fiber $v = 0$, the residual after removing v^6 is proportional to

$$(a + u)^4 \left(\frac{D(a + u)}{u}\right)^6 \left(2 + (a + u)^8\right), \tag{XV.11.7}$$

nonzero at $u = 0$, where a_1 is a unit. The two and eight simple roots of $2 + w^2$ and $2 + z^8$ therefore count the residual loci on the strict curves. At the gauge corner the divided discriminant has value $1/8$, and the node is analytically $UV = z^4w^6$ after absorbing a unit. Along $z = w = \tau$ the orders of (f, g, Δ) are $(0, 0, 10)$. This disk order is the sum of the two divisor orders $4, 6$ because the residual is a unit at the point. The old tuning has the corresponding $(0, 0, 9)$ disk orders. The split ordinary dictionary then gives one full bifundamental at each corner and one external fundamental at each simple residual locus. This is a statement near the named ordinary curves. Changing $2 + w^2$ to $(w + \sqrt{2})^2$ by adding an allowed monomial preserves the degree and the corner unit but loses the argument for two separated enhancements.

The trace test explains why the changed matter is necessary for the changed gauge ranks. Let $s_i = \mathrm{tr}_{\mathrm{fund}}\, F_i^2$, $q_i = \mathrm{tr}_{\mathrm{fund}}\, F_i^4$, $c = c_2(R)$, and $p = p_1(T)$. For defining dimensions $n_i \geq 4$, the independent quartic and mixed gauge-gravitational pieces for m_i external fundamentals and a full bifundamental are

$$\sum_{i=1}^{2} (m_i + n_{3-i} - 2n_i) \left(\frac{q_i}{24} + \frac{ps_i}{48}\right). \tag{XV.11.8}$$

The adjoint trace is $2n_iq_i + 6s_i^2$; the other defining dimension multiplies the single-node trace of the bifundamental. The independent quartic thus asks for $m_i = 2n_i - n_{3-i}$.

This reproduces $(3,6)$ and $(2,8)$. Using the old multiplicities for the new fibers, with background flavor off, leaves

$$\frac{q_1}{24}-\frac{q_2}{12}+\frac{ps_1}{48}-\frac{ps_2}{24}. \tag{XV.11.9}$$

A Green–Schwarz square of four-forms cannot remove an independent quartic. Even with the right multiplicities the projected source changes. Write $Y=\Omega X$, so the retained Green–Schwarz square is $Y^{\mathsf{T}}\Omega^{-1}Y/2$. The coefficients of c in Y are the two defining dimensions. Therefore

$$\Delta Y_R=(0,c)^{\mathsf{T}},\qquad \Delta X_R=\Omega^{-1}\Delta Y_R=(c/3,2c/3)^{\mathsf{T}}. \tag{XV.11.10}$$

The lattice fixes the relation between source frames, while the fiber data fix the source. For an arbitrary changed pair the quartic test gives conditional matter arithmetic; it does not give a Cox lift or a compact neutral spectrum.

Two other calculations separate the same ingredients more sharply. On $\mathbb{F}_1$ the gauge section has $S^2=K\cdot S=-1$, so the split I_5 residual degree is $12+5=17$. The defining-hyper polynomial is $(w+1)(w^{12}-w^{11}+\cdots-w+1)=w^{13}+1$, with thirteen simple roots. The remaining degree is localized at the ordinary antisymmetric locus, whose residual vanishing is weighted by four. Thus $17=13+4$ in the divisor computation but the charged spectrum has thirteen defining hypers and one antisymmetric. On the negative section of $\mathbb{F}_2$, a smooth I_0 and two ordinary IV choices share the same [2] pairing. For the two IV choices the orders $(2,2,4)$ agree. The residual cover equations are

$$\xi^2=UV(U-2V)(U-V),\qquad (\xi-U^2-V^2)(\xi+U^2+V^2)=0. \tag{XV.11.11}$$

The first cover has four simple branch points and $2g-2=2(-2)+4=0$. The second splits over the generic field. The ordinary dictionary gives $\mathfrak{su}(2)$ and $\mathfrak{su}(3)$, respectively, while the smooth fiber gives no gauge algebra; the connected cover genus is not the gauge-curve genus. Table XV.11.1 collects the finite choices. At positive realized periods the weak tensor-branch interpretation uses $g_{6,i}^{-2}\propto a_i$, with the fixed microscopic normalization of Chapter 2. The rank change considered here changes the charged and source data without requiring a change of those periods. We next keep the compact geometry and instead change the path through its period cone.

Fiber data	Ordinary output	Diagonal	Chs.
Split I_4/I_5	$(3,6)$ external; one bifundamental	$(2,2)$	1, 2, 3, 4, 5, 7
Split I_4/I_6	$(2,8)$ external; one bifundamental	$(2,2)$	2, 3, 7
Split I_5 on $\mathbb{F}_1$	13 defining, 1 antisym.; weighted 17	(1)	1, 2, 3
I_0 on $\mathbb{F}_2$	Generic orders $(0,0,0)$	(2)	4
IV connected on $\mathbb{F}_2$	Generic orders $(2,2,4)$	(2)	4
IV split on $\mathbb{F}_2$	Generic orders $(2,2,4)$	(2)	4

Table XV.11.1: Finite curve constructions. The displayed diagonal is that of the retained pairing; the two-node entries have off-diagonal -1.

XV.11.2 Surface contractions and tensor limits

Can a large base volume be used to tell whether a charged string becomes tensionless? The answer depends on which periods control the volume and which control the string. There is also a preliminary geometric question: does the proposed chain really arise in a surface? Both questions can be tested before making an isolated fixed-point interpretation.

Begin with the two (-3)-curves in the actual regular fan, bounded by two external rays. Its consecutive generators, in order, are

$$v_0 = (1,0), \quad v_1 = (0,1), \quad v_2 = (-1,3), \quad v_3 = (-3,8). \tag{XV.11.12}$$

For adjacent determinant one, the relation $v_{i-1} + v_{i+1} = b_i v_i$ gives square $-b_i$ for an interior ray. Here the two coefficients are $(3,3)$. Inserting $v_* = v_1 + v_2 = (-1,4)$ preserves the consecutive determinants. The old inner intersection is replaced by two intersections with the exceptional curve, and the new relations are

$$v_0 + v_* = 4v_1, \qquad v_1 + v_2 = v_*, \qquad v_* + v_3 = 4v_2. \tag{XV.11.13}$$

So the new pairing and its leading principal minors are

$$\Omega_{414} = \begin{pmatrix} 4 & -1 & 0 \\ -1 & 1 & -1 \\ 0 & -1 & 4 \end{pmatrix}, \qquad (D_1, D_2, D_3) = (4,3,8). \tag{XV.11.14}$$

The elliptic coefficients must also be transformed. The actual old corner has $f = u^2 v^2$, $g = u^3 v^3$. In either chart $(u,v) = (e, et)$ or (et, e), canonical division gives

$$(f/e^4, g/e^6, \Delta/e^{12}) = (t^2, t^3, 31t^6). \tag{XV.11.15}$$

The two values $t = 0$ in these charts mark different meetings with the strict ends. At a generic point of the exceptional curve $t \neq 0$ and the elliptic fiber is smooth. The two end fibers have split I_0^* over the ordinary branches: their leading cubic $x^3 + x + 1$ has three distinct constant roots. Thus the additional compact tensor does not come with a new generic gauge algebra. Chapter 5 constructs the ordinary resolved model; its isolated simultaneous contraction has the sourced $(1,0)$ interpretation when the rigid physical premises hold.

The exceptional period adds a new variable. Its blowdown is a geometric return to the original corner, not a claim that the whole negative chain is already collapsed. The existing compact chain satisfies the negative definiteness criterion for analytic surface contraction in the stated setting. That criterion does not provide an elliptic lift or a proof of a decoupled fixed point for an arbitrary proposed chain.

For a concrete period test return to the compact split I_4/I_5 construction. In the basis of (XV.11.1), fix $0 < h < 1$ and choose

$$J = (\rho, A + 2\rho, -h(\rho - B), -(1-h)(\rho - B))^{\mathsf{T}}. \tag{XV.11.16}$$

Here A, B will be the two strict periods and ρ controls the total ruling fiber period. Intersecting with the strict and exceptional curves gives

$$C^{\mathsf{T}} M J = (A, B)^{\mathsf{T}}, \quad (J \cdot E_1, J \cdot E_2) = (h, 1-h)(\rho - B), \quad J \cdot F = \rho. \tag{XV.11.17}$$

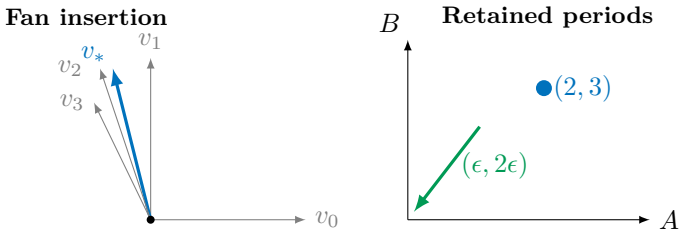


Figure XV.11.2: At left the inserted ray subdivides the regular cone of the two (-3)-curves, giving the $(-4,-1,-4)$ chain. At right two paths on the same compact I_4/I_5 base are projected to the plane of its retained curve periods. The parameter ρ controls a bulk direction not plotted in that plane.

Geometry	Comparison	Diagonal	Chs.
Regular fan insertion	Old diagonal $(3,3)$	$(4,1,4)$	5
Smooth elliptic product	Exceptional A_2 configuration	$(2,2)$	5

Table XV.11.2: Two definite curve configurations. Adjacent compact curves have pairing -1.

In the realized cone chart of this surface these periods are positive for $A, B > 0$ and $\rho > B$. The volume is obtained by squaring the same class, rather than independently sending every area to infinity:

$$\mathcal{V}_B = \frac{1}{2} J^{\mathsf{T}} M J = \rho A + \rho^2 - \frac{h^2 + (1-h)^2}{2}(\rho - B)^2. \tag{XV.11.18}$$

The ambient positive direction contributes to this leading volume. At $h = 1/3$, two ways to use it are

$$(A,B) = (2,3): \quad \mathcal{V}_B = 13\rho^2/18 + 11\rho/3 - 5/2, \tag{XV.11.19}$$

$$(A,B) = (\epsilon, 2\epsilon): \quad \mathcal{V}_B = 13\rho^2/18 + 19\epsilon\rho/9 - 10\epsilon^2/9. \tag{XV.11.20}$$

At fixed microscopic units the leading gravitational coupling can vanish as $\rho \to \infty$ on either path. The wrapped curve tensions remain positive on the first. On the second take $\epsilon \to 0^+$, for example $\epsilon = 1/\rho$; both retained strings become tensionless and the two exceptional periods grow. The geometric volume limit alone does not ensure that the would-be local modes are normalizable or that all coupling to the bulk has disappeared.

As a control, resolve the surface $xy = t^3$ at its isolated A_2 singularity. The two exceptional spheres have square -2 and meet once. The product with a fixed smooth elliptic curve has the same positive pairing (XV.11.2). Its elliptic projection is smooth over both exceptional spheres. Under the ordinary ADE contraction dictionary with its decoupling assumptions, contraction gives the local $(2,0)$ interpretation, rather than the split-gauge $(1,0)$ construction. Comparing the two fibrations explains why the retained pairing cannot decide the supersymmetry or gauge algebra. A further test arises when a contraction changes the tensor source frame itself.

XV.11.3 Conformal matter and source transfer

What is retained when we coarsen a resolved conformal matter base? Shrinking a curve affects its couplings to neighboring tensors. We first identify the curves geometrically; then we compare the Green–Schwarz square in the resolved and coarsened descriptions.

For pure E_6 and E_7 collisions take the leading models $f = 0,\ g = (uv)^4$ and $f = (uv)^3,\ g = 0$, respectively. The bounding rays $(1,0), (0,1)$ carry the external flavor divisors. The ordered interior rays of the regular fans are

$$E_6: \quad (2,1),\ (1,1),\ (1,2), \tag{XV.11.21}$$

$$E_7: \quad (3,1),\ (2,1),\ (1,1),\ (1,2),\ (1,3). \tag{XV.11.22}$$

For a ray (a,b), the relative canonical discrepancy is $a+b-1$. Subtract four or six times this number from the valuation of f or g to obtain the transformed coefficient order. For the E_6 fan the input g-valuation is $4(a+b)$, giving transformed order $6-2(a+b)$. Thus the orders on the three rays are $(0,2,0)$, giving I_0, IV, I_0. For E_7, the analogous f-order is $4-(a+b)$, giving $(0,1,2,1,0)$ and $I_0, III, I_0^*, III, I_0$. From the regular-fan neighbor relation used in (XV.11.13) the diagonal entries are

$$\operatorname{diag}\Omega_{E_6} = (1,3,1), \qquad \operatorname{diag}\Omega_{E_7} = (1,2,3,2,1), \qquad \Omega_{i,i+1} = -1. \tag{XV.11.23}$$

For instance $(2,1)+(1,2) = 3(1,1)$ determines the middle (-3)-curve in both. The compact block is a chain, so all nonadjacent off-diagonal entries vanish.

In the ordinary local branch dictionary for these named pure collisions, the E_6 middle curve carries split IV with algebra $\mathfrak{su}(3)$. For E_7 the three inner curves carry $\mathfrak{su}(2)$, $\mathfrak{so}(7)$, and $\mathfrak{su}(2)$ from left to right. Each adjacency supplies one half-hypermultiplet: $(\mathbf{2},\mathbf{8})$ for the left and middle factors, and $(\mathbf{8},\mathbf{2})$ for the middle and right factors, with $\mathbf{8}$ the $\mathfrak{so}(7)$ spinor Del Zotto, Heckman, et al. 2014, (2.5)–(2.6). These are the gauge and matter assignments on the resolved local branches; interpreting their contractions as isolated endpoints still requires the corresponding decoupling conditions.

In the E_7 fan remove the middle ray $(1,1)$ but keep the neighbors $v_L = (2,1)$ and $v_R = (1,2)$. Their determinant is three. Their cone contains $(v_L + v_R)/3$, which is exactly the removed ray. The numerical pullback of each neighboring divisor to the regular surface must have zero intersection with the removed curve D. Since $D^2 = -3$ and each neighbor meets D once,

$$\widehat{C}_L = C_L + D/3, \qquad \widehat{C}_R = C_R + D/3, \qquad \widehat{C}_L \cdot \widehat{C}_R = 1/3. \tag{XV.11.24}$$

The same substitution gives square $-5/3$ for each neighbor. This computes the rational pairing of the coarser fan. It does not turn the fractional pullbacks into integral dynamical string charges.

For the source transfer write the resolved pairing in blocks $\Omega = \left(\begin{smallmatrix} A & b \\ b^{\mathsf{T}} & d_0 \end{smallmatrix}\right)$, putting the removed curve last for this formula. Write the source in the same order as (Y_A, Y_D). Eliminating the last variable in $\Omega X = Y$ gives

$$S = A - bb^{\mathsf{T}}/d_0, \qquad Y_A' = Y_A - bY_D/d_0, \qquad SX_A = Y_A'. \tag{XV.11.25}$$

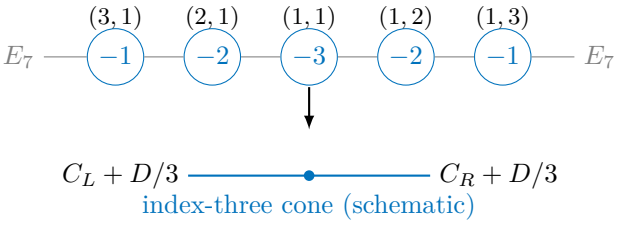


Figure XV.11.3: The upper line shows the resolved E_7 chain and its external flavor divisors. The lower line schematically marks the two neighbors and their singular cone of determinant three. Each neighbor acquires a $D/3$ term in its numerical pullback.

Multiplying the eliminated equations by the appropriate components of Y, or expanding the completed square, yields the full identity

$$\tfrac{1}{2}Y^{\mathsf{T}}\Omega^{-1}Y = \frac{Y_D^2}{2d_0} + \tfrac{1}{2}(Y'_A)^{\mathsf{T}}S^{-1}Y'_A. \tag{XV.11.26}$$

Here $d_0 = 3$ and $b = (0,-1,-1,0)^{\mathsf{T}}$. The Schur correction precisely agrees with the geometric pullback in (XV.11.24). In particular the coupling between the inner neighbors is $-1/3$; the raw principal block would have zero there.

To see what happens to the source, let s_L, s_R be the two side $SU(2)$ four-forms in the normalization of Chapter 6, and let $s_C = \mathrm{tr}_{\mathbf{7}}\, F_{\mathrm{O},C}^2$ be the central $\mathfrak{so}(7)$ gauge four-form in the same frame. Here $\mathbf{7}$ is the vector and $F_{\mathrm{O},C} = -iF_{\mathrm{phys},C}/(2\pi)$ as in Chapter 6. With c, p as in Section XV.11.1, the removed source and neighboring sources are

$$Y_D = 5c + p/4 + 3s_C/4 - (s_L + s_R)/2, \tag{XV.11.27}$$
$$Y_{L,R} = 2c - s_C/4 + s_{L,R}, \tag{XV.11.28}$$
$$Y'_{L,R} = 11c/3 + p/12 + (5s_{L,R} - s_{R,L})/6. \tag{XV.11.29}$$

The outer sources retain the side dependence $-s_{L,R}/2$. Their other terms, including the outer flavor four-forms, cannot contribute to the $s_L s_R$ coefficient. The eliminated outer block is the identity and couples to the inner block by minus the identity. Its two source entries are therefore added to the corresponding inner entries, left to left and right to right. This leaves the inner pairing and inner side-source contribution

$$K = \frac{1}{3}\begin{pmatrix} 2 & -1 \\ -1 & 2 \end{pmatrix}, \qquad (Y'_{\mathrm{inner}} + Y'_{\mathrm{outer}})\big|_{s_L,s_R} = \frac{1}{6}\begin{pmatrix} 2s_L - s_R \\ 2s_R - s_L \end{pmatrix}. \tag{XV.11.30}$$

The outer squares are separate by side. The mixed term is $-s_L s_R/12$ from the inner square with K^{-1}, while $Y_D^2/6$ contributes $+s_L s_R/12$. Under the formal pullback $(s_L, s_R) = (2d, 3d)$, the two mixed pieces become $+d^2/2$ and $-d^2/2$. This changes polynomial variables; it supplies no physical background bundle. With the unshifted sources the inner side column would be $(s_L, s_R)^{\mathsf{T}}/2$, giving mixed coefficient $+1/4$ in the coarsened pairing. Using the raw principal block instead would disconnect the two

sides and give zero. Thus two different shortcuts give different wrong answers. Only the coarsened pairing and the shifted source together reproduce the resolved square.

There is also an integral geometric transfer, with a different physical interpretation. For the rank-two E-string model of Chapter 7 take $f = -3u^4$, $g = u^5(v^2 - b_0^2)$, with the flavor divisor $u = 0$. The coefficient that must vanish for the additional point order is $v^2 - b_0^2$. At $b_0 = 0$ it has a double root, giving two successive centers. At $b_0 = 2$ it gives one center at each of $v = \pm 2$, both on the same flavor divisor. At coincidence order the strict classes as $(D_1, D_2) = (e_2, e_1 - e_2)$, with e_i the total exceptional classes. The total-basis transformation and strict pairing are

$$P = \begin{pmatrix} 1 & 1 \\ 0 & 1 \end{pmatrix}, \qquad \Omega_{\text{strict}} = \begin{pmatrix} 1 & -1 \\ -1 & 2 \end{pmatrix}, \qquad P^{\mathsf{T}} \Omega_{\text{strict}} P = \mathbf{1}_2. \tag{XV.11.31}$$

Here the columns of P are $D_1, D_1 + D_2$. Removing the first charge by principal restriction leaves [2]; blowing down D_1 leaves $[2 - 1] = [1]$, since the pulled-back outer class is $D_2 + D_1$. The source in the total basis is $P^{\mathsf{T}} Y = (Y_1, Y_1 + Y_2)^{\mathsf{T}}$, so the outer square uses the sum rather than the original outer entry. The separated geometry has pairing $\mathbf{1}_2$ on its two effective exceptional generators, not just in a total basis of the old geometry. Indeed the old total-basis periods (a_1', a_2') must satisfy $a_2' > a_1' > 0$, since $D_2 = e_1 - e_2$. The new two effective periods need only be positive in the selected chamber.

For the rank-two paired source in the normalization of Chapter 7, let h be the E_8 four-form, $\ell = c_2(SU(2)_L)$ and $Z = (p + h)/4$. The strict entries and the finite outer square are

$$Y = (c - Z, c - \ell)^{\mathsf{T}}, \qquad \frac{1}{2}(Y_1 + Y_2)^2 = \frac{(p + h + 4\ell - 8c)^2}{32}. \tag{XV.11.32}$$

In particular the hp coefficient in the outer square is $1/16$; it would vanish if we used Y_2 alone. This is a trace of the finite tensor direction in the anomaly comparison, even though that direction is not one of the contracting curves.

The rank-one E-string has one compact (-1)-curve meeting an E_8 flavor divisor. In the isolated small-instanton interpretation, the rank-two tensor flow shrinking D_1 at fixed positive D_2 period has a rank-one sector, including its center hyper, and a detached free $(2, 0)$ tensor multiplet. In the common $(1, 0)$ notation that multiplet includes an E_8-neutral half-hyper in an $SU(2)_L$ doublet. For the separated-center Higgs interpretation the endpoint instead has two rank-one sectors with their own center hypers; a separate relative hyper would count a displacement twice. These endpoint statements concern the isolated deep infrared under the corresponding physical premises. This distinction will matter when a rank-two neighborhood sits at the end of a chain with a nonzero full-fiber period.

XV.11.4 Affine fibers and the heterotic interval

When does a null tensor pairing measure a physical string? It has to come with an effective full-fiber class and an actual positive period. Even then, the same primitive

Configuration	Fibers or effective basis	Diagonal	Chs.
Pure E_6	IV^*, I_0, IV, I_0, IV^*	$(1,3,1)$	5, 6
Pure E_7	III^*, I_0, III, I_0^*, III, I_0, III^*	$(1,2,3,2,1)$	6
Rank-one E-string	II^*, I_0, I_0	(1)	6
Rank two, coincident	Effective exceptional basis; adjacent	$(1,2)$	6, 7
Rank two, separated	Effective exceptional basis; disjoint	$(1,1)$	6, 7

Table XV.11.3: Conformal matter and E-string configurations. Fiber lists include their exterior ends. The diagonal is read in the effective compact basis.

null coefficients can describe different curves and different background sources. We will compare fibers whose geometry lets us evaluate those differences.

For the affine example use the surface family $y^2 = x^3 - 3x + 2 + t^k$ on a small disc, with its minimal resolution. Near the node at $(1,0)$, the factorization $x^3 - 3x + 2 = (x-1)^2(x+2)$ gives analytic coordinates with equation $UV = t^k$. For $k = 3$, two inserted rational curves join the proper transform of the nodal fiber into a triangle. For $k = 2$, one inserted curve joins both branches at two distinct points. The full reduced fiber is disjoint from a nearby smooth fiber in the same class, so its intersection with each component is zero. Each component has two local intersections with other components, counted with multiplicity, hence has square -2. Thus

$$\Omega_{I_3} = \begin{pmatrix} 2 & -1 & -1 \\ -1 & 2 & -1 \\ -1 & -1 & 2 \end{pmatrix}, \qquad \Omega_{I_2} = \begin{pmatrix} 2 & -2 \\ -2 & 2 \end{pmatrix}, \qquad D = \sum_i C_i. \tag{XV.11.33}$$

The primitive radical is the all-ones vector in each case. Replacing the two I_2 intersections by one while keeping the diagonals would instead give determinant three. The actual D has genus one because it is the class of the smooth elliptic fiber. With a smooth constant auxiliary elliptic curve as the F-theory fiber, the affine surface serves as the six-dimensional base of the gauge-free product example.

For the interval, start from the ruling $\mathbb{P}^1_{[\sigma:\tau]} \times D_\psi$, with compact fiber F and a horizontal section H. Take

$$f = -3\sigma^4\tau^4, \qquad g = \psi^m\sigma^5\tau^7 + \sigma^6\tau^6 + \sigma^7\tau^5, \qquad m = 1, 2. \tag{XV.11.34}$$

Near the left section put $z = \sigma/\tau$. After the first blowup set $z = \psi z_1$ and divide by the crepant powers of ψ. The coefficients become

$$f_1 = -3z_1^4, \qquad g_1 = z_1^5(\psi^{m-1} + z_1 + \psi z_1^2). \tag{XV.11.35}$$

Thus the remaining left center has point orders $(4,5)$ for $m = 1$, and $(4,6)$ for $m = 2$. The latter calls for a second blowup on the first exceptional where it meets the strict left section. The other charts give the ordinary regular compact branches described in Chapter 8. In the $m = 2$ case the compact classes, ordered left to right, are

$$(C_L, C_M, C_R) = (e_2, e_1 - e_2, F - e_1), \qquad M_{\mathrm{rul}} = \begin{pmatrix} 0 & 1 \\ 1 & 0 \end{pmatrix} \oplus (-\mathbf{1}_2), \tag{XV.11.36}$$

with M_{rul} written in total-pullback coordinates (F, H, e_1, e_2). For $m = 1$ the classes are $(e_1, F - e_1)$. Taking their pairwise products gives

$$\Omega_{m=2} = \begin{pmatrix} 1 & -1 & 0 \\ -1 & 2 & -1 \\ 0 & -1 & 1 \end{pmatrix}, \qquad \Omega_{m=1} = \begin{pmatrix} 1 & -1 \\ -1 & 1 \end{pmatrix}. \tag{XV.11.37}$$

Again the all-ones vector is primitive null. This time the sum of the strict classes is the ruling class F; its canonical degree is -2 and its square is zero. By adjunction the nearby smooth full fiber is rational. Figure XV.11.4 distinguishes the two geometries and marks the interval flavor incidences. The ordinary rigid-limit interpretations in Table XV.11.4 require appropriate backgrounds, normalizable modes and isolation from bulk dynamics, in addition to a fixed positive full-fiber tension. Under the ordinary local dictionary these are the gauge-free $(2, 0)$ product and the $(1, 0)$ heterotic interval with $E_8 \times E_8$ flavor, respectively.

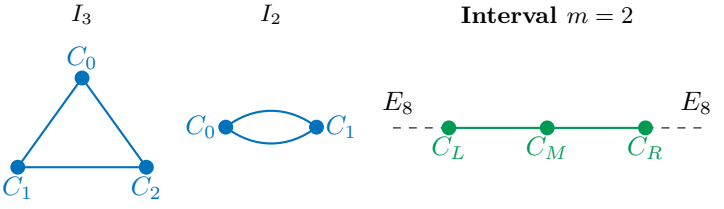


Figure XV.11.4: The reduced I_3 cycle and I_2 double edge have elliptic full-fiber class. The two-ended $m = 2$ interval has rational full-fiber class. Its left E_8 section meets only C_L, even though the left two compact components intersect.

The flavor marks supply information that is invisible even to the full compact matrix. In (XV.11.36) the strict left section is $H - e_1 - e_2$, which meets the compact classes with incidence $(1, 0, 0)$. If we move the second center to $(\psi, z_1) = (0, 1)$, the compact classes and matrix stay the same, but the left section is now $H - e_1$ with incidence $(0, 1, 0)$. Worse, (XV.11.35) has $f_1 = -3, g_1 = 1$ there; dividing the pulled-back coefficients by the fourth and sixth exceptional powers introduces poles. This changed blowup is a surface operation, not a valid crepant repair of the chosen elliptic model.

For the actual left two components the principal pairing is the rank-two strict E-string block (XV.11.31). The source must also use the actual incidence. Let U be the E_8 four-form in the paired inflow frame, and c_L, c_R the two rotation four-forms in that frame. The selected source and its inverse pairing are

$$Y = \begin{pmatrix} c_R - p/4 \\ c_R - c_L \end{pmatrix} - \frac{U}{4}\begin{pmatrix} 1 \\ 0 \end{pmatrix}, \qquad \Omega_L^{-1} = \begin{pmatrix} 2 & 1 \\ 1 & 1 \end{pmatrix}. \tag{XV.11.38}$$

To extract the terms involving U, the square of the second summand gives $U^2(\Omega_L^{-1})_{11}/32$, and its cross term evaluates the first row of the inverse on the background column. The result is

$$I_8\big|_U = \frac{U^2}{16} + \frac{U c_L}{4} - \frac{3U c_R}{4} + \frac{Up}{8}. \tag{XV.11.39}$$

This reproduces four rank-two inflow slots at the endpoint, using the inherited paired source. Uniform incidence on both nodes would give $5U^2/32$ instead. These are the selected E_8 terms, not the full LST anomaly; a geometric limit isolating the endpoint still has to be specified.

Now hold the I_3 base fixed and change the auxiliary elliptic family. Locally its Tate form can be written $Y^2 + 2\sqrt{3}\,zY = z^3 + t^n$, for $n = 4, 5$. Completing the square and translating z gives the short form with $f = -3, g = 2 + t^n$. The distinct tangents at the generic node give the split multiplicative fiber. At a transverse crossing of base components take $t = uv$; then $\Delta = 27(uv)^n(4 + (uv)^n)$ has total order $2n$. Each decorated branch carries $\mathfrak{su}(n)$ in the ordinary local chamber. For these $(1, 0)$ configurations the selected background projection is

$$\widehat{\kappa}_R = \sum_i \delta_i h_i^\vee, \qquad \widehat{\kappa}_P = \sum_i \delta_i (2 - \Omega_{ii}). \tag{XV.11.40}$$

Here $h_i^\vee = n$ on the decorated cyclic nodes, and $h_i^\vee = 1$ for the specified unpaired interval tensors. This is evaluation of the indicated background slots of the Bianchi source; there is no inverse of the full singular pairing. With $\delta_i = 1$, the cyclic values are $(12, 0)$ and $(15, 0)$. For the $m = 2, 1$ intervals they are $(3, 2)$ and $(2, 2)$. The decorated cyclic examples can have the same total area and distinct R projections. The formula in this physical specialization is not a rule for reinterpreting the gauge-free $(2, 0)$ product. The next step is to isolate precisely what the radical does to charges and to periods.

Configuration	Genus	$(\widehat{\kappa}_R, \widehat{\kappa}_P)$	Diagonal	Chs.
Gauge-free I_3 base	1	n/a	$(2, 2, 2)$	8
Gauge-free I_2 base	1	n/a	$(2, 2)$	5, 8
I_3 base, split I_4	1	$(12, 0)$	$(2, 2, 2)$	8, 9
I_3 base, split I_5	1	$(15, 0)$	$(2, 2, 2)$	8, 9
Interval $m = 2$	0	$(3, 2)$	$(1, 2, 1)$	8, 9, 10
Interval $m = 1$	0	$(2, 2)$	$(1, 1)$	8, 9, 10

Table XV.11.4: Full-fiber comparisons. The genus is that of the nearby full fiber. Each row has a primitive all-ones radical and a reference area of ten; the genus and background slots require more than that null charge.

XV.11.5 Charge lattices and retained scales

If two strings have the same relative charge, must they have the same tension? A relative charge is an equivalence class. A wrapped brane instead measures the area of a specified curve class in a specified metric. We can compare the two measurements on the full-fiber geometries of the previous section.

First distinguish three operations on the pairing. Restricting to a subset of a basis takes the principal block A; the kept generators still represent the original strict curves. A blowdown can replace those curves by numerical pullbacks that are orthogonal to the

removed ones. For a single removed curve of pairing $d_0 > 0$, these pullbacks give

$$\Omega_{\text{restriction}} = A, \qquad \Omega_{\text{blowdown}} = A - bb^{\mathsf{T}}/d_0. \tag{XV.11.41}$$

This second interpretation uses a geometric map. In (XV.11.31) it takes [2] to [1] by an integral total transform; in (XV.11.24) the transfer is rational. Neither is a quotient by a null vector. For a quotient we start with a degenerate pairing on a full integral lattice L, and identify charges differing by its primitive radical δ. For the all-ones δ of the full-fiber fixtures, the quotient map and its representative with last component zero are

$$\pi(q) = (q_1 - q_r, \dots, q_{r-1} - q_r), \qquad q - q_r\delta = (\pi(q), 0), \qquad L/\mathbb{Z}\delta \simeq \mathbb{Z}^{r-1}. \tag{XV.11.42}$$

The pairing descends because $\Omega\delta = 0$. The matrix on the chosen representatives is a principal block, but the map on charges is subtraction, not deletion. For example the I_3 block is $\left(\begin{smallmatrix} 2 & -1 \\ -1 & 2 \end{smallmatrix}\right)$, whereas the $m = 2$ interval block is $\left(\begin{smallmatrix} 1 & -1 \\ -1 & 2 \end{smallmatrix}\right)$. Writing Ω_{rel} for the descended pairing, the relation can be checked as a matrix identity,

$$\Omega = \pi^{\mathsf{T}}\Omega_{\text{rel}}\pi, \qquad \Omega_{\text{rel}} = \big(\Omega_{ij}\big)_{i,j<r}. \tag{XV.11.43}$$

The quotient introduces no new geometry. A source can evaluate as an ordinary covector on the quotient only if it annihilates δ. The null Bianchi projections of (XV.11.40) were instead evaluations on δ itself.

Now let $a_i = \int_{C_i} J$ be positive areas and τ_3 the D3 tension factor in fixed microscopic units. In the Einstein-frame calibration the period is linear on charges, and for a calibrated effective wrapped string

$$T(q) = \tau_3 q^{\mathsf{T}} a, \qquad T(q+\delta) - T(q) = \tau_3 \delta^{\mathsf{T}} a, \qquad (q+\delta)^{\mathsf{T}}\Omega(q+\delta) = q^{\mathsf{T}}\Omega q. \tag{XV.11.44}$$

For a signed charge this formula computes its signed period, and does not establish a BPS state. For an effective sum the period comparison is meaningful even without an isolated one-particle or one-string representative. At $a = (2, 3, 5)$, take $q = (1, 2, 3)$ and $q + \delta = (2, 3, 4)$. Both have relative coordinates $(-2, -1)$ and I_3 norm 6; their calibrated period values in units of τ_3 are 23 and 33. Thus the absolute tension does not descend to the quotient. In Figure XV.11.5 the two absolute lifts differ by exactly one full fiber.

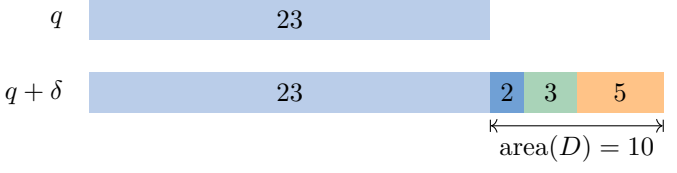


Figure XV.11.5: Two lifts of the same I_3 relative charge have a period difference $2 + 3 + 5 = 10$ at the specified reference areas. The three colored segments added in the lower bar represent one copy of each compact component.

A fourth operation is a limit of periods in the original geometry. At fixed $\delta^{\mathsf{T}}a$ the allowed relative variations satisfy $\delta^{\mathsf{T}}da = 0$. The actual periods need not annihilate δ; indeed that would kill the full-fiber tension. For the $m = 2$ interval compare the paths

$$(\epsilon, 2\epsilon, 10 - 3\epsilon), \quad 0 < \epsilon < 10/3, \qquad (\epsilon, 2\epsilon, L), \quad L \to \infty \text{ before } \epsilon \to 0^+. \tag{XV.11.45}$$

On the first path the left neighborhood shrinks while the right period approaches ten and the full-fiber period stays ten. On the second the right end is opened before the left neighborhood shrinks, so the full-fiber period diverges. The left pairing and left incidence can be the same in both comparisons. Only the latter path removes the right finite scale in this way, and the isolated local interpretation still requires its own physical conditions. Scaling all three periods uniformly to zero would instead remove the positive little string scale.

To see that a positive period split can come from a geometric class, use the marked section o of the I_2 surface and its exceptional component C_1. Then $o \cdot (C_0, C_1) = (1, 0)$, $C_1 \cdot (C_0, C_1) = (2, -2)$, and a relative reference class gives

$$(10[o] - 4[C_1]) \cdot (C_0, C_1) = (10, 0) - 4(2, -2) = (2, 8). \tag{XV.11.46}$$

This is the chosen relative chamber calculation, not a claim about the entire ample cone of a compactification. The same geometry supplies the section marks needed when these strings are compared on a circle.

XV.11.6 Circle comparison and inverse selection

What can be compared when one threefold has two sectioned elliptic projections? We will compare the marks and the absolute masses of the primitive charges in one common five-dimensional frame. To identify the two six-dimensional constructions we must still remember which surface is the base in each projection.

Let E be the smooth cubic $y_E^2 = x_E^3 - x_E$, and let $S \to D$ be the elliptic surface of Section XV.11.4, first with an I_3 central fiber. Write o_E, o_S for the points at infinity in their respective fibers. The two actual maps and sections of $X = E \times S$ are

$$p_A(e, s) = s, \qquad s_A(s) = (o_E, s), \tag{XV.11.47}$$

$$p_B(e, s) = (e, t(s)), \qquad s_B(e, t) = (e, o_S(t)). \tag{XV.11.48}$$

Thus A has elliptic fiber E and base S; B has elliptic fiber S_t and base $E \times D$. The full compact base fiber of A is S_t, and that of B is E. Changing the projection is not an exchange automorphism of the two elliptic curves. In particular one family varies with t and the other does not.

Choose the compact curves $F_E = E \times \{s_*\}$ with s_* away from the central fiber, and $c_i = \{e_*\} \times C_i$, where C_0 is the proper transform and C_1, C_2 are exceptional. Put $F_S = c_0 + c_1 + c_2$. The section divisors Z_A, Z_B evaluate only on F_E, c_0, respectively, with value one. The exceptional divisors $D_i = E \times C_i$ have degree zero on F_E and evaluate on each c_j by $C_i \cdot C_j$. The matrices in the original basis and in the marked basis (F_E, F_S, c_1, c_2) are therefore

$$K_3 = \begin{pmatrix} 1 & 0 & 0 & 0 \\ 0 & 1 & 0 & 0 \\ 0 & 1 & -2 & 1 \\ 0 & 1 & 1 & -2 \end{pmatrix}, \qquad P = \begin{pmatrix} 1 & 0 & 0 & 0 \\ 0 & 1 & 0 & 0 \\ 0 & 1 & 1 & 0 \\ 0 & 1 & 0 & 1 \end{pmatrix}. \tag{XV.11.49}$$

$$K_3P = \mathbf{1}_2 \oplus \begin{pmatrix} -2 & 1 \\ 1 & -2 \end{pmatrix}. \tag{XV.11.50}$$

The change is unimodular since $\det P = 1$. For I_2 the same construction yields a block $[-2]$, using the two intersections of C_0, C_1. Thus the indices of the marked evaluation images are 3 and 2, respectively. They are indices for the given generators and divisors, not statements about saturation in the full homology or the global gauge group. In fact, for $u_i = D_i \cdot q$, the finite block of (XV.11.50) gives

$$(\beta_1, \beta_2) = -\tfrac{1}{3}(2u_1 + u_2, u_1 + 2u_2). \tag{XV.11.51}$$

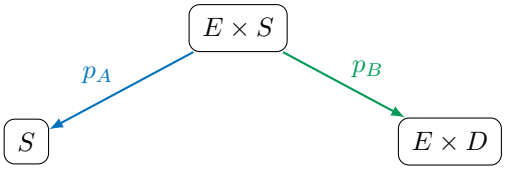
For instance $(0, 0, 1, 0)$ is an integral evaluation vector, but its last two marked coordinates would be $(-2/3, -1/3)$. It is outside the integral marked image in this example.

Take the changed class $(d, b_0, b_1, b_2) = (1, 4, 2, 7)$ in the original basis. The coefficients of F_S and F_E in the marked basis control the primitive full-fiber legs; subtracting b_0 from the other two b_i keeps the relative charges. The ordinary circle dictionary gives

$$(n_A, w_A, \beta_1, \beta_2) = (1, 4, -2, 3), \tag{XV.11.52}$$

$$(n_B, w_B, \beta_1, \beta_2) = (4, 1, -2, 3), \qquad K_3 q = (1, 4, 7, -8)^{\mathsf{T}}. \tag{XV.11.53}$$

The relative entries do not exchange. They are coefficients after subtracting a full fiber, so a negative entry does not contradict effectiveness of the original class. Neither the markings nor the exchange alone determine a mixed-charge BPS mass. Figure XV.11.6 shows which geometric charge supplies each primitive leg.



F_E: KK F_S: winding $\qquad$ F_S: KK F_E: winding

Figure XV.11.6: In the two projections of the same product, F_E is the momentum fiber for A and the wrapped base fiber for B, and F_S does the reverse. The map changes which surface is retained. The simple relative charges are marked separately in (XV.11.53).

In a common external metric let $m_E, m_S > 0$ be the two pure wrapped M2 masses. Using circumference $2\pi R$, the two pure momentum and winding relations imply

$$R_A = 1/m_E, \qquad R_B = 1/m_S, \qquad 2\pi T = m_E m_S, \tag{XV.11.54}$$

$$2\pi R_A T = m_S, \qquad 2\pi R_B T = m_E. \tag{XV.11.55}$$

These equalities use the ordinary adiabatic M/F interpretation and a controlled common finite-circle chamber. At $(m_E, m_S) = (3/2, 10)$ one gets $(R_A, R_B) = (2/3, 1/10)$ and

$2\pi T = 15$. If the external metric is rescaled by $ds_I = \lambda_I ds_{\text{common}}$, invariance of the worldline and worldsheet actions gives

$$m_{I,\text{native}} = m_{\text{common}}/\lambda_I, \qquad T_{I,\text{native}} = T/\lambda_I^2, \qquad R_{I,\text{native}} = \lambda_I R_I. \tag{XV.11.56}$$

For $(\lambda_A, \lambda_B) = (2, 3)$, native radii are $4/3, 3/10$ and native $2\pi T$ values are $15/4, 5/3$. A pure $n_A = 2$ leg has common mass 3, read as $3/2$ in A's units and 1 in B's. A pure unit winding leg of A has common mass 10, read as 5 and $10/3$. Comparing the unconverted native numbers would misdiagnose the same two legs.

The absolute and relative data can now be varied independently in the specified reference comparison. In the chosen M2 mass units the simple gaps come from c_1, c_2, and the affine gap comes from c_0. With a_i the corresponding periods in that frame and $A_S = \sum_i a_i$, one obtains

$$(M_1, M_2; M_0) = \frac{m_S}{A_S}(a_1, a_2; a_0), \qquad A_S = 10, \quad (3, 5; 2) \longrightarrow (4, 5; 1). \tag{XV.11.57}$$

The arrow changes the areas from $(2, 3, 5)$ to $(1, 4, 5)$, without changing (XV.11.54). Changing only the area of E so that $m_E = 5/2$ instead leaves the first set of gaps fixed but changes R_A to $2/5$ and $2\pi T$ to 25. The product comparison keeps the two six-dimensional parents distinct; the different base pairings in Table XV.11.5 make this explicit.

Projection	Base fiber	Index	Diagonal	Chs.
I_3 product, A	S_t	3	$(2, 2, 2)$	8, 10
I_3 product, B	E	3	(0)	8, 10
I_2 product, A	S_t	2	$(2, 2)$	8, 10
I_2 product, B	E	2	(0)	8, 10

Table XV.11.5: The two projections for each product. The displayed index is that of the common marked evaluation image. B has a single compact base class of square zero.

A rational change of coordinates is a weaker input than two sectioned maps. In the alternate interval chart from Chapter 10, put $x = \sigma\tau^3$, $s = X/(\sigma^2\tau)$ and $y = \tau^2 Y/\sigma^2$ on the common dense open of the old coordinates (σ, τ, X, Y). With $t = \tau$ and $x = \sigma\tau^3$, the forward relation $Y = t^{-8}x^2 y$ in (F.3) of Bhardwaj et al. (2015) gives $y = \sigma^{-2}\tau^2 Y$; the printed inverse (F.10) has only one power of τ. Substitution into the original equation yields $y^2 = x^3 + Ax^2 + Bx$, where

$$A = \tau(s^3 - 3s\tau^2 + \tau^3), \qquad B = \psi^m \tau^8. \tag{XV.11.58}$$

Translating the cubic gives $f = B - A^2/3$, $g = 2A^3/27 - AB/3$. At the literal center of the proposed ordinary base blowup put $s = 1, \tau = \epsilon, \psi = \epsilon\eta$. The leading orders of A, B are $1, 8 + m$; thus the orders of f, g are $(2, 3)$ for both tested powers. Canonical division gives

$$\left(\operatorname{ord}_\epsilon \frac{f}{\epsilon^4}, \operatorname{ord}_\epsilon \frac{g}{\epsilon^6}\right) = (-2, -3). \tag{XV.11.59}$$

The poles exclude the literal ordinary crepant procedure at that center. They do not exclude other birational models, establish a general obstruction, or disprove a heterotic duality. Here the rational map on a dense open supplies no second resolved projection.

Finally suppose we start from an output rather than a geometry. Separate four questions: a finite tensor effective description, a definite contraction candidate, a fixed-scale little string candidate, and a finite-circle comparison. First ask whether an actual ordinary geometry, marked charges, and the relevant background have been supplied. Then ask for the specific physical ingredients. For instance a finite tensor description needs realized positive periods and the charged and anomaly data. A contraction candidate needs an existing definite surface configuration and a realized contraction path. A fixed-scale question instead needs an effective primitive full fiber, the semidefinite pairing of corank one, and a positive fixed absolute tension. For either UV interpretation the decoupling path, normalizable isolated sector, and the corresponding physical dictionary must still be supplied. The circle comparison needs actual marked projections, a common controlled chamber at finite circle, matched units and charges, and the sourced dictionary.

For the I_3 example suppose the finite positive full-fiber tension and radical have been supplied but normalizability has not. The LST question remains open on that evidence. If the full fiber is instead taken to zero, its tension explicitly contradicts the fixed-positive-scale condition; a different question may still be meaningful. If the supplied data are the exact I_4/I_6 geometry, positive realized periods and charged anomaly data in an admissible background, the finite tensor requirements are filled even when no circle comparison has been specified. An unproved second projection is missing evidence for the circle question, not a failure of the finite-tensor requirements. These decisions test supplied hypotheses. Filling a list of conditions does not independently verify their truth, construct a missing geometry, or establish a UV completion. In the exercises, a premise that is unknown and a premise contradicted by the stated path must be treated differently.

Exercises

Use exact rational numbers. For Exercises 1–4, give the specified numerical and labeled answers. Use `benchmark/tasks.json` for the JSON fields and `benchmark/PROTOCOL.md` for submission. All written arguments are human assessed. The questions below change one ingredient at a time.

1. Keep the two-node pairing and a full bifundamental, and propose defining dimensions $(5, 8)$. For this matter ansatz, find the two conditional external fundamental multiplicities. Then keep the old external multiplicities $(3, 6)$ instead, and give the four residual coefficients ordered as (q_1, q_2, ps_1, ps_2). Is the resulting quartic test a construction of the changed geometry? Identify the coefficient and ordinary-locus tests still needed, and contrast with (XV.11.5)–(XV.11.7).

2. In the E_7 source calculation put $s_L = -3d, s_R = 5d$. Submit the d^2 coefficients of the pulled-back $s_L s_R$ terms, in the order removed and retained. Submit the coefficient triples in order (c, p, d) of the two shifted neighboring sources. Give the

corresponding mixed d^2 coefficients for the unshifted source with the coarsened pairing and with the raw principal block. Explain why the correct coarsened result does not define an integral lattice of dynamical tensors.

3. Use the $m = 2$ interval at the positive periods $(3, 4, 6)$ and the two effective charge vectors $(2, 1, 4), (4, 3, 6)$ in left-to-right order. Compute both relative coordinate vectors, their common squared pairing, the two absolute period values, and their difference in units of τ_3. Explain why deleting the last coordinate differs from taking the quotient.

4. In the I_3 product take original curve coefficients $(3, 5, 1, 9)$. Give the A and B vectors in the order (momentum, winding, two relative coefficients), and the evaluation vector in the order (Z_A, Z_B, D_1, D_2). For an independent proposed evaluation $(2, 7, 2, 0)$, solve for the marked coordinates over $\mathbb{Q}$ and decide if the evaluation is in the integral marked image. Explain why this test does not determine the saturation of the displayed generators in full homology.

5. For each of the following premise cards, identify the construction question affected and say whether the premise is missing or contradicted. (i) An effective primitive full fiber has fixed positive period, but normalizability of the local modes is unknown. (ii) A path scales every compact period to zero. (iii) A literal alternate chart is known birationally, but a second resolved projection has not been constructed. Can (iii) by itself exclude a finite tensor effective description supported by separate data? Explain what a completed list of supplied hypotheses establishes.

Status and sources

§1. Finite gauge data. The retained pairing, Cox lift and disk orders are [MATH]; the charged dictionary is [GEO-E]; the stale gauge and source comparison is [ANOM]. See Morrison and Taylor (2011), arXiv:1106.3563v3, §2.3 (2.26), §3.2 (3.23), (3.28), and §3.3 (3.58), (3.61); Katz et al. (2011), arXiv:1106.3854v1, Table 1, §5 and Appendix A; and Ohmori, Shimizu, Tachikawa, and Yonekura (2014), arXiv:1408.5572v2, §2.1 and Appendix A. The coefficient and trace comparisons use Chapters 1–4 at their named ordinary loci. The calculations use the Weierstrass convention $\Delta_{\text{book}} = 4f^3 + 27g^2$ and the integral anomaly trace conventions of Chapter 3.

§2. Contractions and periods. The fan, compact periods and surface contraction criterion are [MATH]; the separate ordinary contraction interpretations are [DEC] at the stated scope. See Heckman et al. (2013), arXiv:1312.5746v3, §2–3.1, §4.1 (4.9)–(4.10), and Fig. 1, and Bhardwaj et al. (2015), arXiv:1511.05565v3, §3. The analytic contraction and the dynamical isolation assumption are distinct. The actual compact period chamber and product come from Chapter 5.

§3. Conformal matter and source transfer. The regular and coarsened fans, strict and total transforms are [MATH]; the ordinary branch dictionary is [GEO-E], and the paired source comparison is [ANOM]. See Del Zotto, Heckman, et al. (2014),

arXiv:1407.6359v3, §2 (2.2), (2.3), (2.5), (2.6), and Chapters 5–7. Ohmori, Shimizu, Tachikawa, and Yonekura (2014), v2, §3.3.1 (3.26)–(3.33) and §3.3.2 (3.34)–(3.38), gives the source transfer and normalization in the stated cases. The rational E_7 fan is an additional explicit geometric calculation. The E-string comparison uses Ohmori, Shimizu, and Tachikawa (2014), arXiv:1404.3887v2, (1.1)–(1.5), (2.26), §3.2–3.3, and the isolated small-instanton interpretation and free sectors of Chapter 7.

§4. Affine and interval fibers. The central fibers and strict curve geometry are [MATH] within Chapters 8–9. The ordinary rigid physical interpretation ([DEC]) and Bianchi specialization ([ANOM]) use Bhardwaj et al. (2015), v3, §3.1.2, §4.1–4.2, and Appendix F (F.1), and Del Zotto and Ohmori (2020), arXiv:2009.03489v3, §3 (3.3)–(3.6), Table 1, and specifically §4.3 (4.7)–(4.8) for the decorated cyclic physical specialization. The selected E_8 square ([ANOM]) uses Apruzzi et al. (2017), Appendix A.2.1 (A.26)–(A.31), printed pp. 48–49 (PDF pp. 49–50), and Ohmori, Shimizu, and Tachikawa (2014), v2, §3.2–3.3. These are not full LST anomalies or proofs of bulk isolation.

§5. Charges and periods. The integral quotient and period tests are [MATH] on the stated classes; tension ([GEO-E]) uses the ordinary calibrated dictionary of Chapters 2 and 8 and Bhardwaj et al. (2015), v3, §2 (2.1)–(2.7), §3 (3.1)–(3.7), and the opening of §5. The absolute period is evaluated before the quotient, in the calibrated Einstein-frame units of the preceding chapters.

§6. Circle and inverse questions. The marked evaluation, charge comparison, literal chart and hypothesis tests are [MATH] within the displayed objects, with the ordinary finite-circle interpretation ([DEC]) inherited at its stated scope. See Bhardwaj et al. (2015), v3, §4.1, §9 opening and Appendix F (F.2)–(F.8) and (F.9)–(F.12), with the power in (F.10) fixed by (F.3); Seiberg (1997), arXiv:hep-th/9705221v2, §2.1 (2.1)–(2.4); Schwarz (1995), arXiv:hep-th/9508143v5, §4 (25)–(32); and Vafa (1996), arXiv:hep-th/9602022v1, §2–4. Chapter 10 fixes the native and common units. The comparison uses the ordinary torus calculation and the qualified adiabatic fiberwise interpretation only in their respective substeps. No new dynamical equivalence follows from the comparison.

References

Apruzzi, F., J. J. Heckman, and T. Rudelius (2017). “Green–Schwarz automorphisms and 6D SCFTs”. In: arXiv: 1707.06242.

Bhardwaj, L. et al. (2015). “F-theory and the classification of little strings”. In: arXiv: 1511.05565.

Del Zotto, M., J. J. Heckman, et al. (2014). “6d conformal matter”. In: arXiv: 1407.6359.

Del Zotto, M. and K. Ohmori (2020). “2-Group symmetries of 6d little string theories and T-duality”. In: arXiv: 2009.03489.

Heckman, J. J., D. R. Morrison, and C. Vafa (2013). “On the classification of 6D SCFTs and generalized ADE orbifolds”. In: arXiv: 1312.5746.

Katz, S. et al. (2011). “Tate’s algorithm and F-theory”. In: arXiv: 1106.3854.

Morrison, D. R. and W. Taylor (2011). “Matter and singularities in F-theory models on elliptic Calabi–Yau threefolds”. In: arXiv: 1106.3563.

Ohmori, K., H. Shimizu, and Y. Tachikawa (2014). “Anomaly polynomial of E-string theories”. In: arXiv: 1404.3887.
Ohmori, K., H. Shimizu, Y. Tachikawa, and K. Yonekura (2014). “Anomaly polynomial of general 6d SCFTs”. In: arXiv: 1408.5572.
Schwarz, J. H. (1995). “The power of M-theory”. In: arXiv: hep-th/9508143.
Seiberg, N. (1997). “New theories in six dimensions and matrix description of M-theory on T^5 and $T^5/\mathbb{Z}_2$”. In: arXiv: hep-th/9705221.
Vafa, C. (1996). “Evidence for F-theory”. In: arXiv: hep-th/9602022.